Dissertation zur Erlangung des akademischen Grades
eines Doktors der Ingenieurwissenschaften (Dr.-Ing.)
im Fachbereich Elektrotechnik/Informatik
der Universität Kassel

Hybrid Power System Modelling-Simulation and Energy Management Unit Development

A Dissertation
in Candidacy for the Degree of
Doctor in Engineering (Dr. Eng.)

FB 16 Elektrische Energieversorgungssysteme
Elektrotechnik/Informatik
Universität Kassel

By

M.Sc. Eng. Rajesh Saiju

From Panauti, Nepal

1. **Supervisor: Prof. Dr. -Ing. Siegfried Heier**
2. **Supervisor: Prof. Dr. –Ing. habil. Peter Zacharias**

Dissertation Day: 19.12.2008

Declaration / Erklärung

I herewith certify that I performed this thesis independently, without any disallowed assistance and I did not use others than the aid in this thesis. I marked all places, which are literally or in a general manner taken out of the published or unpublished books or articles. No part of this thesis has been previously submitted in support of an application for any other degree or qualification in this or in any other university.

Hiermit versichere ich, daß ich die vorliegende Dissertation selbständig und ohne unerlaubte Hilfe angefertigt und andere als die in der Dissertation angegebenen Hilfsmittel nicht benutzt habe. Alle Stellen, die wörtlich oder sinngemäß aus veröffentlichten oder unveröffentlichten Schriften entnommen sind, habe ich als solche kenntlich gemacht. Kein Teil dieser Arbeit ist in einem anderen Promotions- oder Habilitationsverfahren verwendet worden.

Kassel,20.04.2008

Acknowledgements

The delivered thesis has been achieved during my work as a scientific researcher in the department of Electrical Energy Supply System [IEE, EVS] in the Electrical and Communication branch of University of Kassel. This researched work was partially financed by SMA Technologie AG, Kassel.

My ambition to achieve a doctor degree in electrical engineering could not have been a part of successful story in my life without the support of the Prof. Dr.–Ing. Siegfried Heier, director of the research section “wind energy technology” and initiator of the project “Hybrid Power System model development” who not only supervised but also encouraged and bolstered me throughout my research work. So my special thanks goes to him.

I am grateful and highly indebted to Prof. Dr.-Ing. Peter Zacharias, the director of the department of IEE, EVS and president of ISET, for his interest in my work and his support the thesis as the second supervisor.

Additionally, I wish to thank Prof. Dr.–Ing. Bernd Weidemann, the director of electrical machines department, for his valuable technical suggestion regarding electrical machines. At the same time, I am grateful to scientific researcher Dipl.–Ing. Aziz Azhari for his technical support.

The complete research work was carried out in the department of IEE, EVS. My special thanks go to colleagues Mr. Bernhard Siano, Mr. Volker Berge and Dipl. –Ing. Bernd Gruß for their support and help with electrical machines measurements, electronics circuit developments etc.

Furthermore, I would like to thank all the colleagues of IEE, EVS and students who supported me through their project works. Especially, I would like to thank to Ms. Anja Clark-Carina, Dipl.-Ing. Werner Döring and Dipl.–Ing. Abdelbahi Tamzarti.

Finally, I would like to thank my mother Sita, father Vijay, brothers and sisters who gave me courage and support to achieve this work. Consequently my great word of thank goes to my wife Mandira for her support and patience during complete work and our son Raymond for his motivating moments.

Last but not least, I would like to thank Oma Helga Walter and Opa Werner Walter from Soest.

Abstract

The globally accepted concept for providing electricity to remote areas around the world, where still more than two billion people live, is to develop an autonomous Hybrid Power System [HPS] consisting of locally available renewable energy sources. Up to now, many PV-Diesel-Battery HPS have been installed.

The control system applied in the existing HPS is complicated, less reliable and costly because of the use of battery bank as the energy storage unit. The battery is costly, complex in monitoring and difficult to manage because of its limited lifetime in remote areas. This research work is focused on the development of a completely new HPS in which a water reservoir is introduced as an energy storage unit. This concept is explored keeping in the mind that such a system might be highly suitable for the hilly areas of developing countries like Nepal where small rivers are available, the sun shines most of the time and micro hydro technology has been exploited.

The proposed HPS consists of a synchronous generator, which forms the state variables of an isolated grid, frequency and voltage. Other renewable energy sources such as a photovoltaic system and wind turbine generator are integrated together to utilise more renewable energy. Beside that, a diesel genset is connected to make system reliable.

The different energy converters including the battery bank are simulated and to verify the validity, comparisons are made between simulation results and measurement. As more systems with different characteristics are integrated together, the complexity in the control mechanism increases. This complex integration process is carried out first in the powerful software Matlab/Simulink. The complete program is tested with different loading conditions and meteorological conditions.

The aim of this research work is to develop a modular expandable energy management unit based upon priority basis renewable energy utilisation. Technically, it is based upon the grid frequency measurement in the sense that the frequency of the grid is a mirror of the grid in terms of the power-load equilibrium. It is the natural behaviour of the grid that the deviation of the frequency from its reference value occurs if the power-load status changes. Based upon this frequency deviation, which predetermines the connected load in the grid, online state variables, the meteorological data and the reservoir conditions, the Energy Management Unit [EMU] generates an optimal energy dispatch pattern for different energy converters as reference power by governing the energy management guidelines, which guarantee the continuous supply as well as minimise the fuel consumption.

Furthermore, this research work is oriented to develop a compact, reliable, easily replaceable and economically viable EMU following the Simulink based HPS simulation model. For this purpose, microcontroller MSP430 based hardware is developed in which different sensors, display system, and a user-interfacing keyboard are integrated. On the software side the energy management code written in computer language C is loaded to run the complete HPS.

1 Introduction

It is now a globally accepted reality that electrical energy is fundamental for social and economic development. Unfortunately still one third of the worlds population lives in developing and threshold countries and have no access to electricity [1]. It has been estimated that the world population will reach 8 billion by 2020 [2]. The statistic shows that the population growth is mostly in developing countries where most of the people live in remote, rural areas. The extension of utility grid is complicated and expensive due to geographical, economical and social barriers. Up to now, mostly diesel gensets are used for rural electrification. This is not a good solution because the fuel and maintenance cost are expensive and it is also not environment friendly. In such circumstances, an alternative is to use locally available renewable energy sources (e.g. PV, wind, hydro etc) and implement modular, expandable and task-oriented system concepts that guarantee cost-effective and sustainable resources of energy, especially for remote and rural areas [kleinkauf-94]. At the world engineering convention in 2000, it has been mentioned that the energy needed will be provided, distributed, and consumed in a suitable way. Keeping this promise in mind, many decentralised HPS have been installed worldwide.

1.1 Structure of Hybrid Power System

Many different types of HPS architecture have been practiced. The possible different architectures are shown in fig. 1.1 [2]. Each system has its own advantages and disadvantages. The choice of the layout for particular location depends upon geographical, economical and technical factors. The centralised AC-bus architecture has been chosen for this research work because of its suitability for the target area ,Nepal. Besides that, as mentioned above, the HPS, which is going to be investigated, consists of a micro hydro power plant as the main component in terms of an isolated grid formation. Another import change is the use of a water reservoir as the energy storage unit. Up to now, a battery bank has been used as the energy storage unit. The disadvantages associated with the battery system will be totally eliminated. The detail layout of the targeted system will be explained in chapter 7.

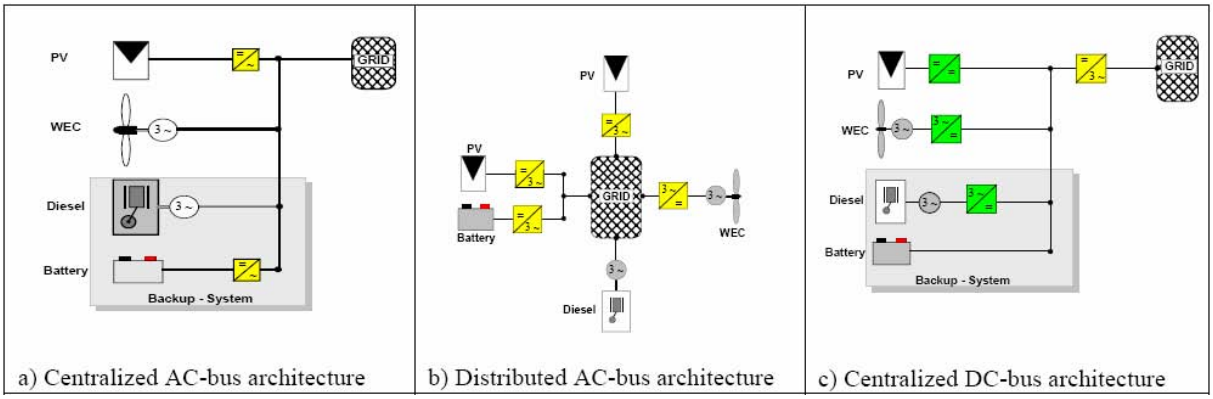

Fig. 1.1: Different architecture of hybrid power systems

1.2 Problem formulation

Nepal, a small landlocked mountainous country situated between India and China is well known for the Himalaya maintains and water resources. Due to the continuous flow of huge rivers from the Himalayas through hilly areas, there is tremendous hydropower potential. Many feasibility studies have shown that there is a total capacity of 85000 MW of hydropower potential and of this 45000 MW is considered to be economically suitable. But due to the economical, technical and social problems only around 800 MW of electricity is currently being generated. Due to the complex geography, low population density distribution in many rural areas and additional reasons the grid extension is quite expensive. Most of the people living in remote areas are to be integrated into the mainstream to ensure sustainable development. Many programmes are running through INGO and governmental efforts regarding sustainable energy supply. Up to July 2005, 8816.6 kW of micro hydro unit have been installed through out Nepal [3].
Most of the installed micro hydro power plants consist of an electronic load controller [ELC] to control the frequency. This means that micro hydro runs always at full load due to the lack of a mechanical governor. It is clear that in rural areas the difference between peak load and base load is quite high. To cover the peak load, a larger unit needs to be installed which in turn the system costly. Beside the peak time, the system runs at partial load.
Another problem is that for areas where very small rivers are available but load demand is high, a micro hydro system only can not fulfil the total demand. This research work is focused on these problems. The aim is to build cost effective HPS using micro hydro as the main unit. Due to meteorological conditions, the best solution is to integrate PV and micro hydro systems. A PV system alone can not fulfil the demand all the time. If only a PV system is used, then it must be considered that the larger PV module array and the battery facility should be applied to collect enough solar power [4]. Further more during the rainy season, the power production from PV system decreases and the power from micro hydro increases. It can be said that PV and micro hydro systems are weather dependant and each has its weak point. On the other hand, these two systems have their own unique advantages which off set the weak points of the other systems. By hybridising these two power systems it is possible to form a stabilised power system. To cope with the changes in the load, water flow, irradiation etc, a water reservoir is essential.

1.3 Research objective and methodology

As mentioned above, a research work is focused on the development of a HPS, its optimal control structure, simulation model and micro-controller based energy management unit.

Objectives

1. Modelling of different HPS individual energy conversion systems
2. Formation of micro hydro based HPS in which PV system, water reservoir and diesel genset are integrated.

3. Development of cost effective, compact and optimal energy management unit using micro-controller
4. Economical analysis of such a complete system for developing countries

1.4 Methodology

The aim of this research work is achieved based on the methodology shown in fig. 1.2.

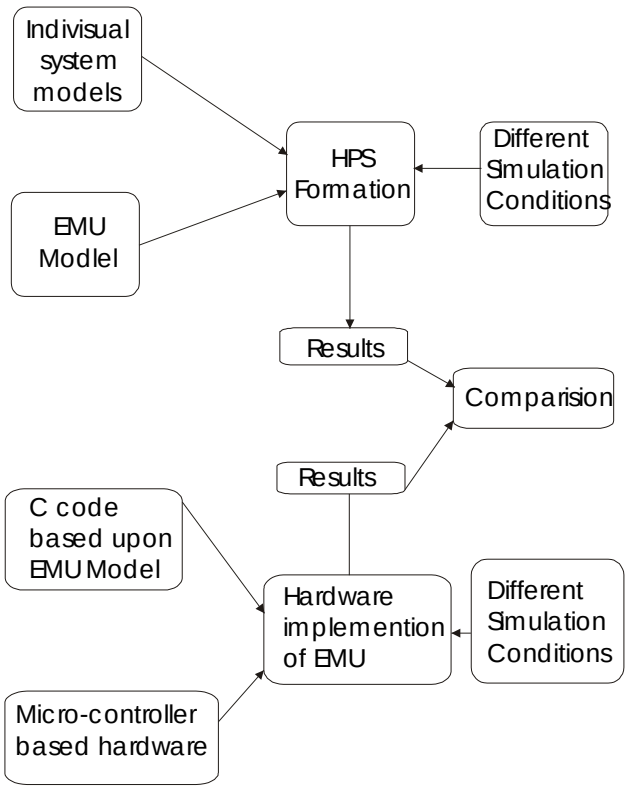

Fig. 1.2: The methodology of the research work

1.5 Work structure

This thesis is structured as follows!

In chapter 2 the stability of a conventional grid and an isolated grid consisting of renewable energy sources, in terms of voltage and frequency are briefly described.

The aim of chapter 3 is to provide a general overview of Nepal, the availability of electricity and development of power systems based on renewable energy sources.

Chapter 4 is very important in this research work because that all energy converters of HPS –micro hydro power plant consisting of synchronous generator with reservoir, PV system, wind turbine generator consisting of an induction generator, battery system and diesel genset are technically described. They are modelled based upon mathematical equations. The behaviour of all mentioned energy converters are explained in detail.

The core of chapter 5 is the integration process of different simulated energy converter models to form the HPS. The newly developed control strategy to find out the optimal energy dispatch pattern based upon the online inputs obtained from environment, reservoir and grid frequency are described in detail. The development platform is the Matlab/Simulink software. The developed HPS has been tested with different meteorological conditions, varied amount of water in the river which allows the turn-on and turn-off behaviour of the diesel genset to be observed. The achievement of power balance in the isolated grid (i.e. maintaining the frequency and voltage) are described.

In chapter 6 the validity of different energy converters are verified by making comparisons between the simulation results and experimental results.

Chapter 7 explains the development of a hardware based energy management unit. The hardware is developed in such a way that it behaves in the same manner as the Simulink based energy management unit. The different components used in the hardware system, their characteristics, the applied flow chart algorithm, the used software and the sensors to measure irradiation, temperature, water level etc are described in detail. The functionality of the developed EMU is tested with different conditions.

In chapter 8 the cost-benefit analysis for the proposed HPS for Nepal has been conducted. The component costs, labour cost, transportation cost etc all are used based on the Nepali market.

The chapter 9 describes the conclusions of this thesis, its practical application and further work.

2 Stability of conventional and renewable electricity supply

An infinite grid is formed by many power plants consisting of interconnected synchronous generators. The grid variables, frequency and voltage, are to be kept within permeable limits. The variation in these variables determines the grid quality [4]. The characteristics of a conventional large grid and an isolated grid formed by renewable energy sources may be quite different in terms of voltage and frequency stability. In this chapter the level of stability of the above-mentioned grids will be explored.

2.1 Power system stability and control

Power system stability indicates the ability of an electric power system to regain a state of operating equilibrium after being subjected to a physical disturbance, with most of the system variables bounded so that system integrity is preserved [1]. The stability can only be achieved if the faulty section of the grid (loads or generators) is disconnected without affecting the other generators. In other words, the stability is the equilibrium between the mechanical torque and electrical torque. A large power system is a highly non-linear system because it operates with changing conditions like load, generator powers, topology and operating parameters
When system parameters change, for example through the disconnection or connection of a large load or disconnection of a large generator, the power system must reach a new equilibrium state to remain stable. This is achieved by automatic controls and human operators. If after a disturbance, the system cannot return to normal condition, then it has become an unstable system. This means the system will result in a run-away or shut down situation.
The stable system can be represented as shown in fig. 2.1.

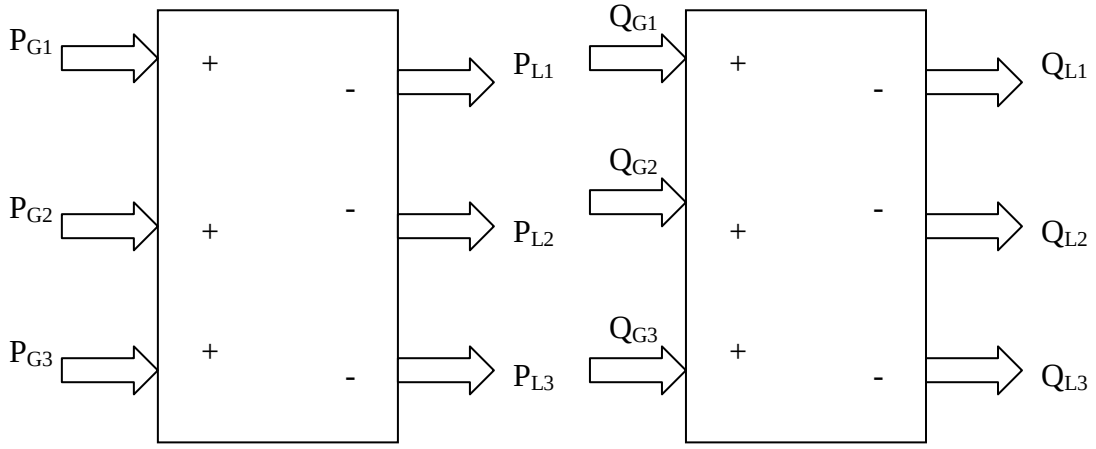

Fig. 2.1: The active and reactive power balance in a grid

2.1.1 Frequency stability

The entire grid, where many synchronous generators and many loads are connected at many different points can be considered to be one large electromechanical entity [2], [3] as shown in fig 2.1. To achieve the desired frequency at all conditions, the power production from the different generators must always match to the connected loads. Generally the three following situations may occur

1. $\Sigma P_{gen} > \Sigma P_{sink}$
2. $\Sigma P_{gen} = \Sigma P_{sink}$
3. $\Sigma P_{gen} < \Sigma P_{sink}$

The relation between P_{gen}, P_{sink} and mechanical rotation or frequency is expressed as

$$\sum P_{gen} - \sum P_{\sin ks} = \frac{d(K.E.)}{dt} = \frac{d}{dt}\sum J_i \Omega_i^2 \qquad (2.1)$$

Where

P_{gen}	=	total generated power at that instant
P_{sinks}	=	total connected load at that instant
J_i	=	moment of inertia of the total system
Ω_i	=	angular speed of the grid

This physical behaviour is not dependent upon the types of connected machines and loads [2].
In other terms, the angular speed can be expressed as

$$\Omega_i = \frac{1}{J_i}\int (T_m - T_e)dt \qquad (2.2)$$

The above equation can be converted into a model as shown in fig. 2.2.

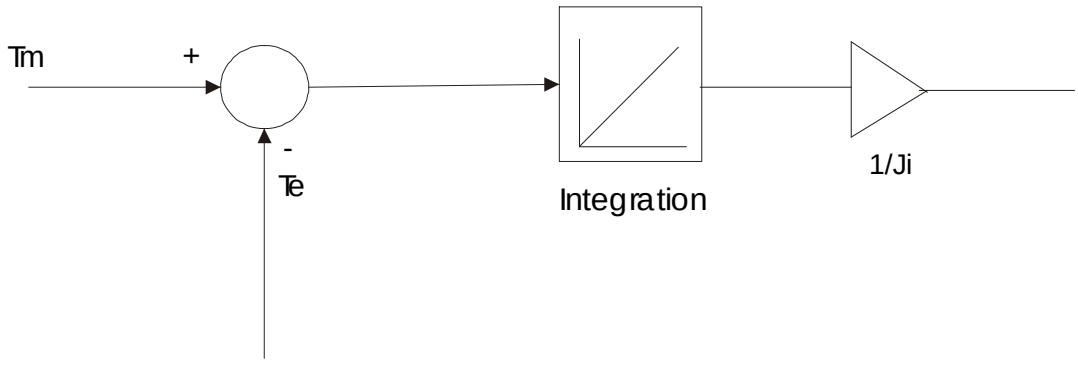

Fig. 2.2: The dynamics of the rotating machine

The behaviour of the angular speed Ω_i with respect to time is shown in fig 2.3.

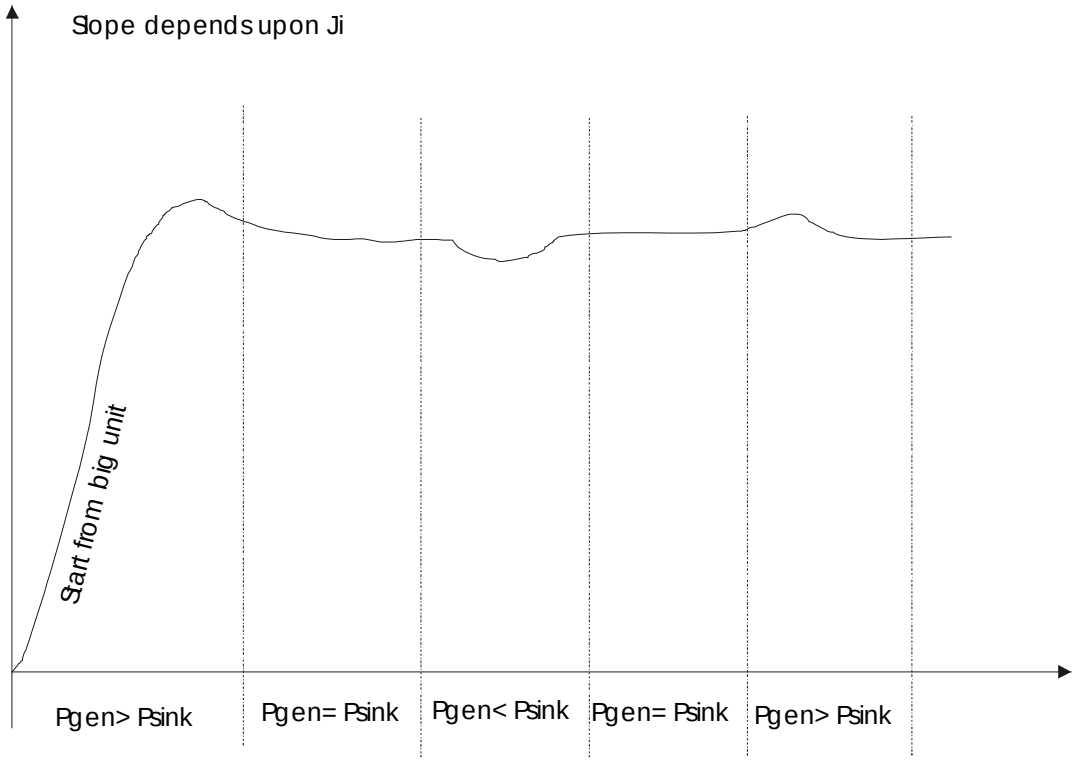

Fig. 2.3: The behaviour of the frequency with respect to the change in load

Since the system is started at no load, the angular speed increases slowly. The time taken by the system to reach the nominal speed depends upon the moment of inertia of the first grid-forming unit. The grid is formed by a single large unit and, additional units are synchronised with it.
When $P_{gen} > P_{sink}$, the rotational speed of the synchronous machine in the system increases, thus an increment in the frequency occurrs. For this condition, the power generation is to be decreased until $P_{gen} = P_{sink}$ has been reached. Similarly if the frequency decreases due to $P_{gen} < P_{sink}$, the power generation has to be increased. In the grid, power generation management is done by the central power management through a SCADA system.

2.1.2 Voltage stability

Analogously, the regulation of the AC voltage of the power system is a matter of maintaining an equilibrium between the source and sink reactive power (VARs) in the system [2]. In the grid, most of the loads are inductive in nature like induction motors, wind turbines with asynchronous generators, transformers and distribution lines. They consume the reactive power. On the other hand power factor correction capacitors are sources of reactive power. Synchronous generators can be either sink or source. As compared to active power and active load relation where energy storage is possible in rotating mass during imbalance, in the case of reactive source and sink, storage is not possible. This means the loads consume whatever reactive power is produced.

Mathematically

$$\sum Q_{gen}(V_{ac}) - \sum Q_{\sin ks}(V_{ac}) = 0 \qquad (2.3)$$

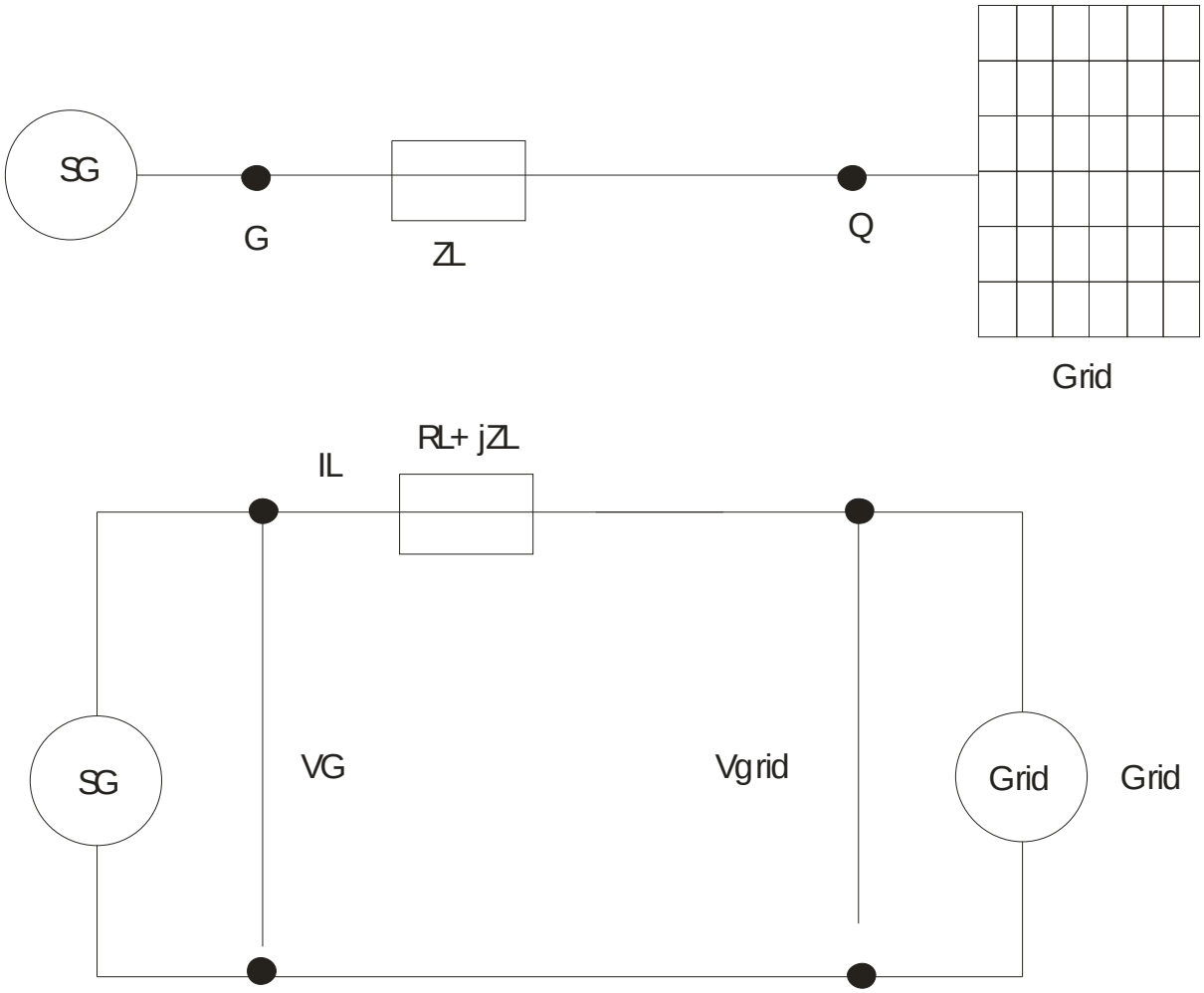

Fig. 2.4: Example of a grid to determine the voltage change

Where

Q_{gen} = reactive power (kVAR)

V_{ac} = AC bus voltage (kV)

The above equation shows that if $Q_{gen} > Q_{sink}$, voltage increases from the reference value and vice versa. To achieve constant voltage, Q_{gen} has to be matched to the Q_{sink} demanded by the load.
A generator connected to the grid can be represented as shown in fig. 2.4.

Once the synchronous generator is synchronised, the terminal voltage will be the same as the grid voltage. After that a single synchronous machine can not change the grid voltage. The flow of reactive power is controlled by changing the excitation. This means the synchronous generator can be run in either over excitation or under

excitation mode. The voltage difference between the grid and generator V can be resolved into direct axis voltage difference ΔV_d and quadratic axis voltage difference ΔV_q.
These voltage drops can be represented as

$$\frac{\Delta V_d}{V_{grid}} = \left(I_G.R_L - I_G.X_L\right) = \frac{1}{V^2_{grid}}\left(P_G.R_L + Q_G.X_L\right) \tag{2.4}$$

$$\frac{\Delta V_q}{V_{grid}} = \left(I_G.R_L + I_G.X_L\right) = \frac{1}{V^2_{grid}}\left(P_G.R_L - Q_G.X_L\right) \tag{2.5}$$

From the above equation, it is clear that the voltage at the common coupling point (PCC) depends upon from active power flow and reactive power balance. In the case of high voltage lines where R/X ratio is approximately 0.1, the voltage difference is mainly determined by the reactive power [3]. In case of medium and low voltage grid, active power plays an important role.

Voltage stability can be defined as the ability of the power system to maintain nominal voltage at all buses in the power system under normal operating conditions and after being subjected to a disturbance [1]. If voltage instability occurs, the grid voltage at some section increases or decreases progressively, loads will be disconnected. Finally the complete system may collapse. Voltage instability may occur due to more current flowing through the transmission lines than they are rated for. This causes additional voltage drops at the receiving end. Another cause may be reactive power limitation of some connected generators.

2.2 Contribution of wind farms in grid stability

In a conventional grid, the capacitor banks or FACTS devices like STATCOM etc are used to provide the demand reactive power by the load system. Due to the rapid development in power electronics components, control system (hard- software) and wind turbine technology; an application of wind turbine generators [WTG] is possible to support the grid during voltage dips. The variable speed complete decoupled wind farm(s) can provide the controllable reactive power to the grid. The possible contribution in regards to the voltage stability during heavy load connection is determined by modelling the existing wind farm(s) in Software Matlab-Simulink-Simpower. In this study, wind farm(s) are used to compensate the voltage dips instead of FACTS devices. Due to continuous feeding of active power by the wind farms and also regulation of output voltage at the terminals of the WTG, the experiments show that wind farms can contribute to boost grid voltage up to some extend [4].
The formation of wind farms is briefly described here. The wind farm(s) system distribution at the point of common coupling [PCC] is shown in fig 2.5. Total three wind farms of capacities 9, 11 and 9 MW are integrated into the medium (20 kV) voltage grid. Each wind farm consists of E66 1.8 MW wind turbines. This wind turbine is directly connected to Enercon ring type generator. Output power of the

generator is converted to DC then inverted again to AC and finally transformed up to 20 kV. Using NA2XS2Y 3x1x300 mm^2 cables, each wind farm is connected at PCC. The high voltage grid has a P_{sc} of 2 GVA and a voltage level of 110 kV. Using two sets of 110/20 kV step down transformers of rating 31.5 MVA, the PCC is formed where wind farms and loads are connected.

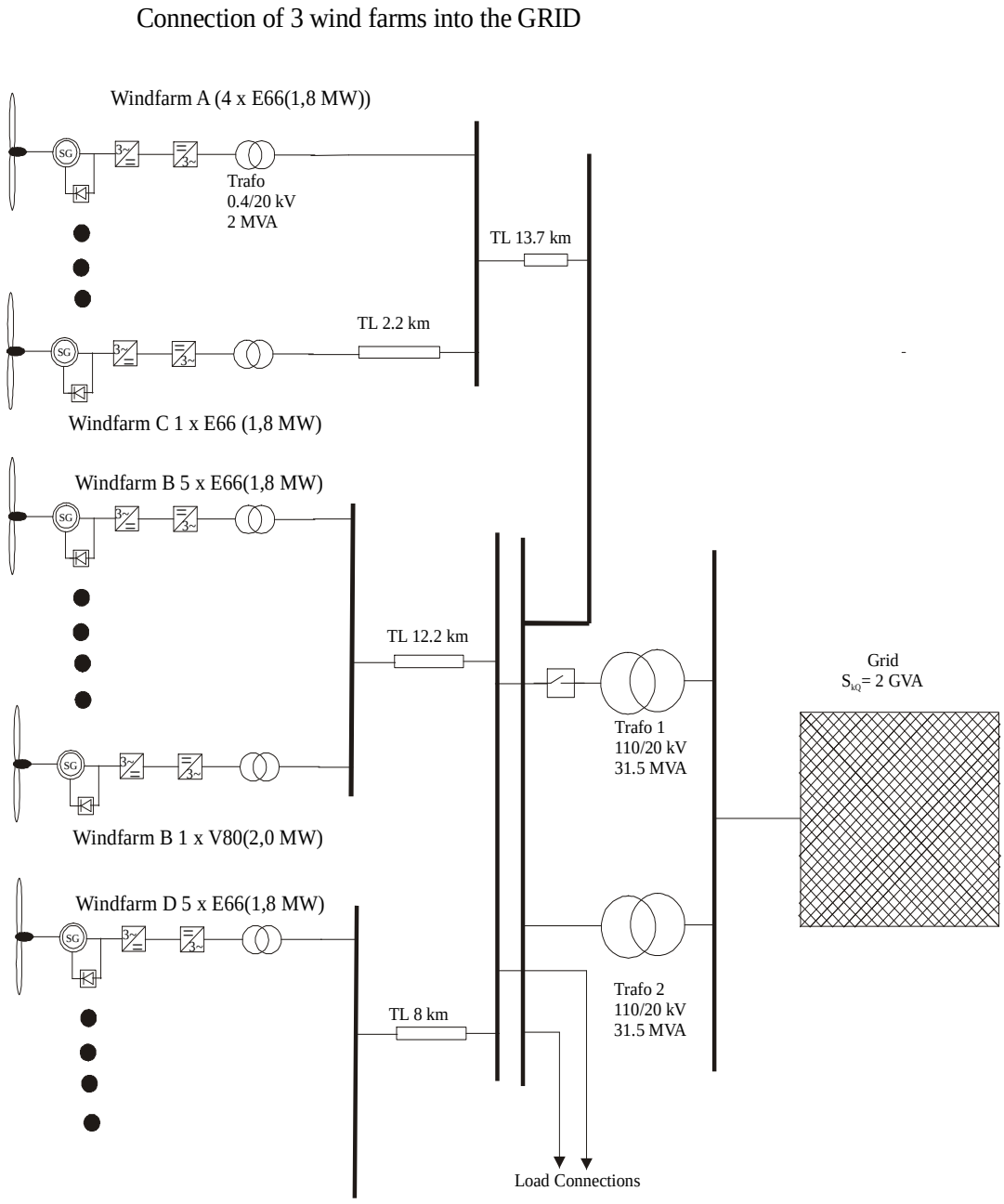

Fig. 2.5: Schematic connection diagram of the wind farms into low side grid

Result obtained in this investigation show that a wind farm of 9 MW capacity can boost the voltage of medium size 20 kV grid of 200 MVA, from 0.5 to 2.6 percent [4] in different loading conditions. It explores the possibility that WTG can be used as DGFACTS tool to control the voltage of the grid during voltage dips or rise.

2.2.1 Grid control

As explained above, grid parameters ,voltage and frequency, are to be kept very close to nominal value. The UCTE recommends 5 steps load disconnection plans to keep frequency stable [3].

Table 2.1: The 5 step plan of UCTE for load disconnection

Grid frequency (f_{grid})	Action
< 49.8 Hz	Alarming all the personals, Activation of all not yet operated power plants
< 49.0 Hz	Disconnection of 10-15% of load with delay
< 48.7 Hz	Disconnection of further 10-15% of load with delay
< 48.4 Hz	Disconnection of further 15-20% of load with delay
< 47.5 Hz	Disconnection of the power from the grid

2.3 Stability in isolated grid formed by HPS

The basic principle of a grid stability is similar for an isolated grid with respect to the grid, but control possibilities, available time constant, deviation from nominal values are not same. In the case of a normal grid, many synchronous generators, capacitor banks maintain the state variables. In the case of an isolated grid formed by the HPS where first priority is the utilisation of renewable energy, there may be only one unit, which regulates the voltage and frequency. In this work as mentioned above, the synchronous generator connected to the water turbine is an only one unit to maintain voltage and frequency.

2.3.1 Primary control

The water turbine driven synchronous generator builds the grid variables. As shown in fig 2.6, the water from a river passes to the water turbine through a water reservoir. It indicates that the water reservoir works as the energy storage unit. It makes the system more reliable in the sense that the balance between power generator and power sink is maintained by the water storing or using. The task of frequency control is achieved through a mechanical governor associated in the water turbine. As shown in fig 2.6, the amount of water flow to produce demand power is controlled using only one water valve.

2.3.2 Secondary control

A hybrid power system consisting of a PV system and a micro hydro may not always be able to supply the demanded power because of meteorological conditions like insufficient irradiation or no irradiation and less water flow than required. In such condition, a secondary back up power supplier is required. A diesel genset is used as the back up system. It supports the grid to maintain a nominal frequency by providing the required active power.

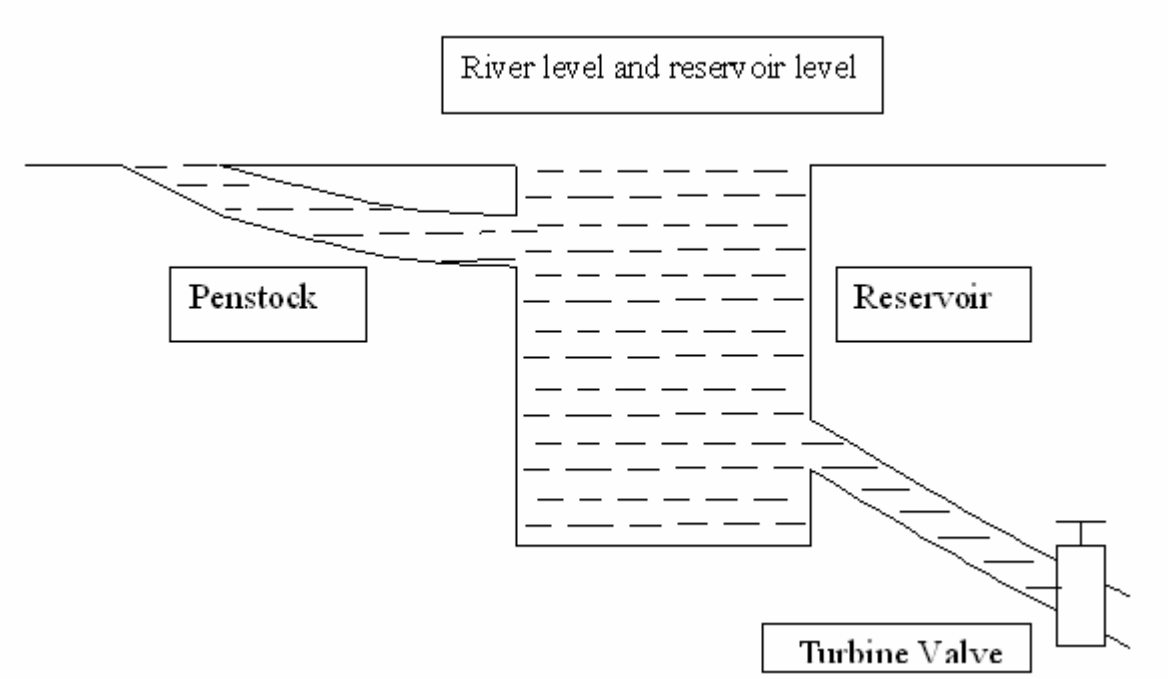

Fig. 2.6: Arrangement of a water reservoir, penstock pipes and a turbine valve

2.3.3 Weather dependency of renewable energy sources

Renewable energy sources like PV system and WTG are meteorological dependent electrical power generators. For example the power production from PV system and WTG depend upon irradiation and wind velocity respectively.
A primary energy fluctuation makes problem on mechanical and electrical components on one hand, on the other hand fluctuations in electrical outputs like, power, voltage, current, flickers [3]. In the case of micro hydro without a reservoir water flow in a river determines the available power. An addition of a reservoir eliminates this problem.

The PV system produces direct current electrical power. An integration of a PV system into the gird formed by the micro hydro must be done through the inverters. Now-a-days the sunny boy inverters produced by a world leading company SMA Regelsystem are widely used for such application. The SMA-sunny boy inverters have following characteristics.

- Maximum power production through integrated MPP Tracker
- Production of sinus forming voltage output
- Production of pure active power (cos =1)
- Self grid failure detection and disconnection by ENS system
- Efficiency optimisation through variable frequency

3 Electricity Supply in Nepal

3.1 Introduction of Nepal

Nepal is a small landlocked developing country situated between India and China in south Asia. Total population of Nepal is approximately 30 million. It is one of the least developed countries in the world with approximately 42% of the population living below a poverty line. Agriculture provides a livelihood for over 80% of the population and accounts 40% of the Gross National Product [GNP]. Over 85% of the total population lives in rural areas of the country [1].

Fig. 3.1: The map of the Nepal and its neighbouring countries

Beside its poverty, Nepal has a lot of natural resources and potential to develop itself. It is well known in the world as the top of the world because of its Himalaya ranges. The Mount Everest (8848 m), the highest peak of the world, is in Nepal. The 8 highest mountains out of 10 are situated in Nepal. Due to high mountains in north and plain region in south, huge rivers flow from north to south with enormous hydro potential. Natural beauty is another face of Nepal. It has many different cultures, languages, hills, rivers, plain areas, which make it very beautiful area for tourism.

3.1.1 Geography

Nepal is situated in south Asia and extends from 26 to 30th northern latitude and 80 to 8 eastern degree of longitude. It covers a surface area of 147,181 km^2 in which 4,000 km^2 is inland water. The country has been divided into three regions namely Himalaya, central country [Hill] and the Terei [Plain area] as shown in fig. 3.2.

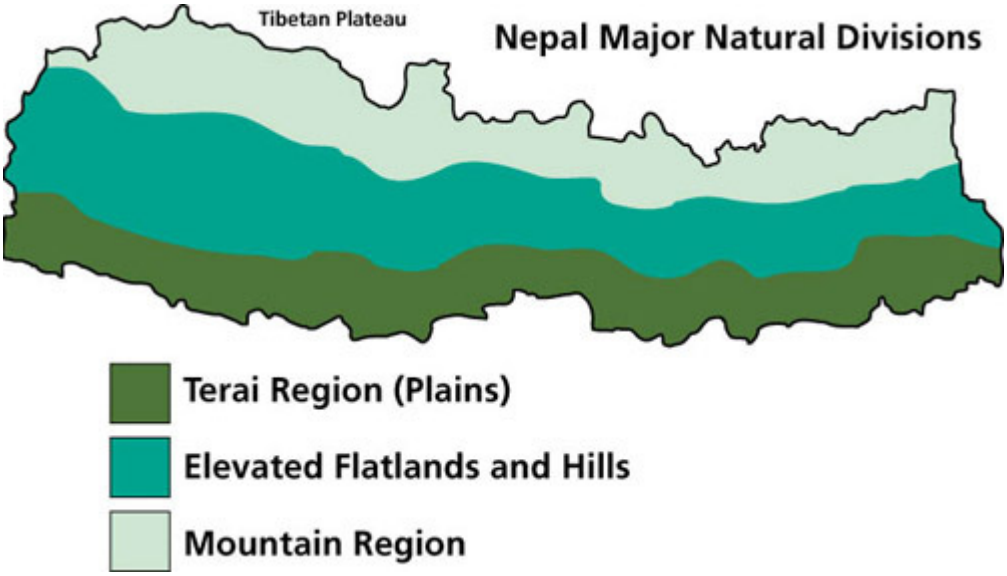

Fig. 3.2 The different regions of Nepal

The Himalaya covers around 35% of the total country area and it has west to east going high mountain belt [5]. It is the main source of rivers in the country. Above 3000 m area has been categorised as high latitude area. Less than eight percent of the population of Nepal live in this region.

The central country covers around 42% of the total land. It consists of many hills, valleys and the capital of the country Kathmandu. Young hills, many rivers, complex geography make it difficult for entire infrastructure development.

The Terai is the plain area of Nepal which extends from west to east in the narrow strip fashion with averages only 20 km in width and occupies 23% of land. The height of the Terai region starts from 60 m to 150 m above sea level. This region of the country is very important from agricultural side. Over sixty percent of grains are grown in this area that constitutes seventy percent of the arable land for the country.

3.1.2 Climate

Nepal's weather is generally predictable and pleasant. There are four climatic seasons: March-May (Spring), June-August (Summer), September- November (Autumn) and December-February (Winter). About 80% rain falls during Mansoon period (the end of June to the middle of September). So the remaining period is dry. Spring and autumn are the most pleasant seasons. In summer, temperatures range from 28^0C to 40^0C in the Terai. In winter temperature falls to freezing with a high level snowfall in the mountains. Due to low temperature and high irradiations, high water flow in the big rivers, Nepal has very good potential for renewable energy. In hilly regions, temperature varies from 2^0C to 30^0C. On average, the sun shines 6.8 hours per day i.e. 2482 hours per year with the intensity of solar radiation ranging from 3.6 to 5.9 kWh/m^2-day [2].

3.1.3 Economy

Agriculture is the main economic activity of Nepal. More than 80% of the population is involved and 37% of GDP provided by agriculture. Besides that the tourism and hydro power are other important economic sources of the country.

3.2 Electricity availability in Nepal

Due to its unique geography, it has an enormous capacity of hydropower development. It is estimated that Nepal has more that 6000 rivers, whose total length is 45000 km. From these rivers, 85000 MW electrical power can be generated, in which 45000 MW is economic. Up to now 25 hydropower plants have been constructed and total installed capacity is 609 MW which is just 0.73% of total capacity [2], [3]. Out of the total electric power, about 91 percent comes from hydroelectric plants, the remaining 9 percent from diesel plants. About 40% of the population has benefited from electricity by 2002. This 40% is reported to include 33% from national grid and 7% from alternative energy [2].

Fig. 3.3: 132 kV transmission, 800 km long running parallel to Indian border, connects big cities across the country [4]

Even though the huge potential, an increasing demand of electricity (8%)with the growth of industry and the use of electrical appliances, due to the complex geography, a poor economic infrastructure, the lack of technology, the political instability a progress in hydropower development is very slow. The neighbouring country India is a big market for the electricity export. In future, if India agrees to buy electric power from Nepal, it will be golden opportunity for both countries to develop infrastructures. Many international companies are showing interest to invest in the sector of hydropower. The Khimti-I hydropower plant [60 MW] is the first "BOOT" based

private sector invested project. It produces 350 GWh of energy per year. The total electrical power production in Nepal is 1755 GWh per year.

3.3 Renewable energy in Nepal

It is a well-established concept that the development of a nation can be scaled by the amount of energy consumption per person per year. Even though Nepal has hugh hydropower potential, still very less energy has been explored. Most of the population are living without electricity in rural areas. In such circumstances, the traditional energy (fuelwood, agricultural residues, and animal dung) contributes most in total energy consumption. In 2002 it covered around 85.27% of the total energy consumption. Similarly the commercial energy provided 14.24% and the renewable energy provided only 0.48% [2].
The use of biomass (fuelwood and other petroleum products) is not a good solution to meet the daily energy requirement. This is neither sustainable nor desirable from the environmental considerations as well as from the prospective of the effort to improve the quality of life (CES 2000). The centralised electricity supply seems not to be relevant because of the complex geography, a high cost of transmission lines and imported oil. As mentioned above, the suitable climatic conditions, scattered population density etc provide suitable background for a decentralised energy system based upon the renewable energy.

Many national and international organisations are involved in Nepal to develop the sustainable energy programs [6].

Table 3.1 Multi-lateral/Bi-lateral programmes and their role in micro-hydro development in Nepal

SN	Programme	Support from	Major Areas of Work
1	ESAP	DANIDA, Norwegian Govt./Nepal Govt.	Supporting micro-hydro, solar PV, ICS, etc. MGSP of AEPC/ESAP manages the Micro-hydro Components
2	REDP	UNDP, The World Bank/ Nepal Govt.	Implementation of micro-hydro and other renewable energy
3	SHPP	GTZ	Study and R&D in small hydro including micro-hydro
4	TRPAP	UNDP/Department of National Parks and Wildlife Conservation of Nepal Govt.	Supporting micro-hydro and other renewable energy installations in second programme districts
5	GEF/SGP	UNDP	Energy including micro-hydro, environment, facilitation for funding

6	CSP	DFID	Support community development programmes including micro-hydro (in Mugu, Kailali, Dailekh, Jajarkot)

3.3.1 Micro hydropower

It has been already mentioned that Nepal has many small rivers which are very suitable for micro hydro power plant development. The first small hydro power plant (500 kW) namely “Pharping” was constructed in A.D. 1911. After that it took many years to construct second and third projects “Sundari Jal” and “Panauti” in 1936 and 1965 respectively. At this moment, micro hydro technology is well developed in Nepal. All over the country micro hydro power plants have been constructed and sustainable environmental friendly electrical energy is fed to decentralised grid. The total micro hydro based electricity generation in Nepal is up to 2003 was 14000 kW from 2065 micro hydro plants [4].

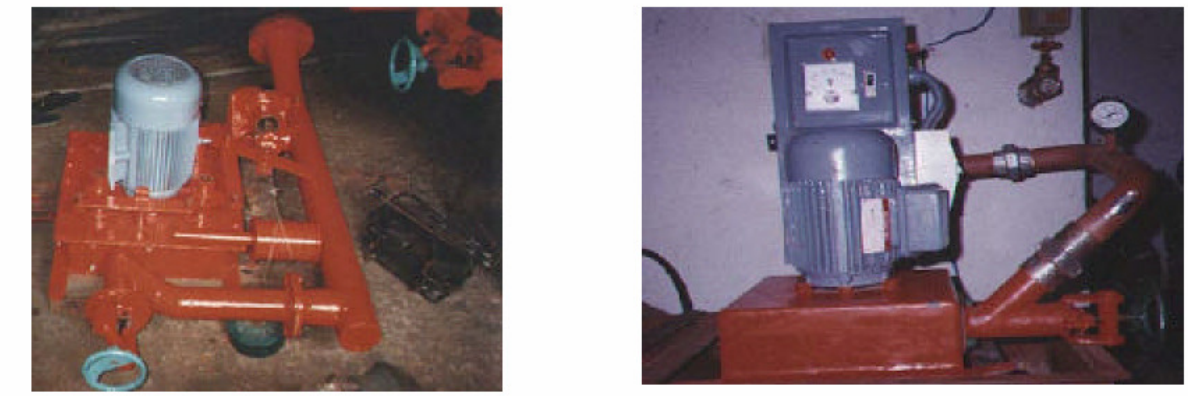

Fig. 3.4: Examples of small peltric set turbines used in Nepal

3.3.2 Solar energy

The history of electricity generation from photovoltaic cells in Nepal is not long. The first PV based rural electrification project was implemented in 1988/89 with the French government support. Due to many international doners likes Danida, Norad, Jaika, GTZ etc the PV application is exponentially increasing. After first successful Solar Home System [SHS] demonstration project in 1993, where 36 Wp SHSs were installed in 67 households in “Pulimerang”, the PV system became very popular for small isolated household application. Nepal government and international organisations provide technical and financial support to the communities, villages and private households. SHS is available in 10 Wp, 18Wp, 36 Wp and 50 Wp.

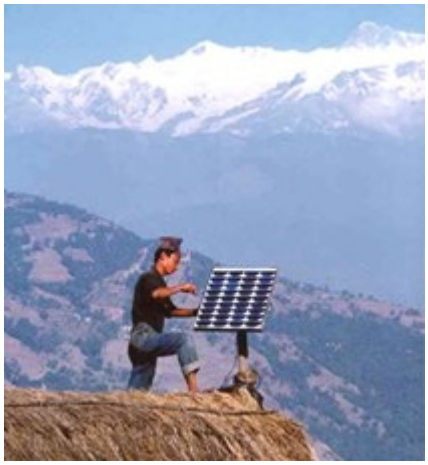

Fig. 3.5: An example of a solar home system in Nepal

Due to suitable meteorological conditions, the PV based electricity generation potential is huge. It is estimated that about 2500 kWp of a PV power is currently being used in public and private sectors (telecommunication, utility supply, stand along water supply, traffic, aviation etc) [2].

3.3.3 Wind power

Wind is still one of non-harnessed energy sources in Nepal. Its countrywide potential has not been assessed yet. Many studies have indicated that there is only some potential for power generation from wind. Due to variations in topographical and meteorological conditions, it is difficult to generalize the wind condition in Nepal. The wind energy generation is favourable in Tansen of Palpa, Lomangthang of Mustang and Khumbu regions of Nepal. Climate records of Nepal during 1976-1984 show that the maximum wind speed recorded was 19.5 m/s in Jumla and Thakmarpha with the average wind speed of approximately 4.1m/s to 5.0m/s. The Nepal government conducted first feasibility study to find out the wind energy potential in 1985. In 1992, a wind survey was carried out by Dangrid in a 12 km long corridor from Kagbeni to Chusang and found that 200 MW of wind power could be generated. The estimated energy was 500 GWh. The study was financed by UNDP [2], [5].

In 1989, two 10 kW wind turbines were installed from Cresswell Engineering for a rural electrification programme near Kagbeni in Mustang district. These turbines worked only for two months. The reason of unsuccessful was a higher than expected average wind speed as predicated from the wind speed survey.

Many organisations like AEPC, ITDG, RECAST etc are still working in the field of wind energy. Nevertheless some private companies are installing wind turbines. Power Tech Nepal (P) Ltd installed a hybrid wind and solar energy system at the Panorama Hotel in Dhulikhel (30 km from Kathmandu along the road to Tibet) which supplies electricity during times of load shedding.

4 Simulation models for HPS

4.1 Micro Hydro Power Plant

In developing, hilly countries where small rivers are available, a micro hydro power plant [MHPP] is a possible environment friendly solution for the rural electrification. The MHPP constructed at the remote area is capable to supply the electrical power to local consumers through an isolated transmission line. It is possible to construct the MHPP with or without a water reservoir [WR]. A disadvantage of the MHPP without WR is that the water is not utilised in its full capacity and the generator runs always in full load condition without delivering active power. In the case of Nepal, most of the MHPP have been constructed without WR. For this research work, WR is included as an important part of the complete system. As mentioned above the MHPP plays the main role to stabilise the isolated grid, WR functions as an energy storage unit, which will be capable to deliver or store the energy in the form of water volume. The symbolic representation is shown in fig. 4.1.

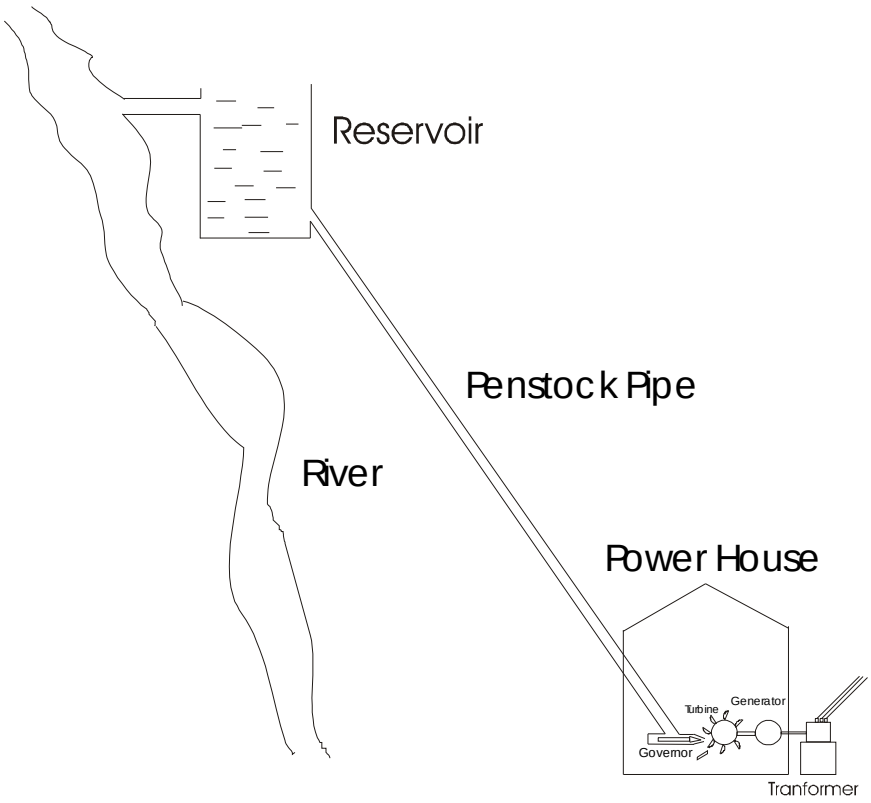

Fig. 4.1: The symbolic representation of a MHPP

4.1.1 Components

A technical design of the MHPP consists of three different engineering aspects [1], [2]. It consists of civil, mechanical and electrical components. These are mentioned below.

Important components of these three categories are explained in detail with Simulink model and simulation results.

4.1.1.1 Civil Components

Intake
Weir
Settling basin
Headrace
Forebay
Penstock
Powerhouse building
Tailrace
Stop-logs
Reservoir

4.1.1.2 Mechanical Components

Trash rack
Penstock pipe
Expansion joints
Valves
Turbines
Drive system
Water governor

4.1.1.3 Electrical components

Generator
Automatic Voltage Regulator [AVR]
Control and Protection System
Earthing System
Transmission Network

4.1.2 Important Components

4.1.2.1 Generator

A generator is the main unit which converts mechanical energy associated with water into electrical energy. Two types of generators (synchronous and asynchronous) can be used. Depending upon the size of a machine, types of a load to be fed, other energy sources later to be integrated, a generator is to be chosen. Normally induction generators are chosen for a small MHPP due to its low cost. Synchronous generator

should be chosen if reactive loads like induction motors are to be supplied and the total installed capacity is more that 10 kW. The generator general guidelines for selecting the phase and type of the generator are shown in table 4.1 [1].

Table 4.1: Generator general guidelines for selection

Capacity	Up to 10 kW	10 to 15 kW	Above 15 kW
Type of generator	Synchronous or induction	Synchronous or induction	Synchronous
Phase	Single- or three-phase	Single- or three-phase	Three-phase only

The size of the generator can be chosen based on the factors shown in table 4.2 [1].

Table 4.2: Generator size confirmation factors

Maximum ambient Temperature (^oC)	20	25	30	35	40	45	50	55
A Temperature factor	1.10	1.08	1.06	1.03	1.00	0.96	0.92	0.88
Altitudes (m)	1000	1250	1500	1750	2000	2250	2500	2750
B_1 Altitude factor	1.00	0.98	0.96	0.945	0.93	0.915	0.90	0.88
Altitudes (m)	3000	3250	3500	3750	4000	4250	4500	
B2 Altitude factor	0.86	0.845	0.83	0.815	0.8	0.785	0.77	
C ELC correction Factor								0.83
D Power factor	When load is only light bulbs (resistive load)							1.0
	When load includes tube light and other inductive loads							0.8

After finding out the parameters based upon the location from the above table, the generator formula for the size calculation is expressed as [1]

$$kVA = \frac{Installed\_capacity\_in\_kW}{ABCD} \qquad (4.2)$$

The factor C can be omitted if a mechanical governor is used. A safety factor of around 30% should be added in above calculated value to allow following conditions:

a) The output of a turbine could be higher than expected.
b) If large motors (> 10% of the generator size) are supplied by a generator, the generator should be able to bear the heavy starting current.
c) In case of ELC, the generator runs always at full load.

Further important points to be considered are

1. Brushless self-excited, self-regulated generators are preferable due to less maintenance work.

2. AVR of the generator must regulate the voltage to margin fluctuations of +, -5% when it moves from no load to full load.
3. The largest motor to be started or the total motor load in an isolated grid at any time must not exceed 35% for a synchronous generator.
4. A soft-start mechanism is recommended for the motor loads.

4.1.2.2 Turbine

The energy (kinetic and potential) associated with water is converted into mechanical energy through a water turbine. The mostly used types of a turbine in a MHPP are cross-flow and Pelton turbines. The size and type of the turbine for a particular site depend upon the net head and the design flow. Pelton turbines are suitable for the site where ratio of head to flow is high. If there is more flow and low head is available the cross-flow turbine is suitable. The selection of turbine type should be based on the cost effectiveness and the technical limitations as explained below.

1. If the net head (H_{net}) exceeds 50 m, a cross-flow turbine is not a preferred option, especially for the output power below 20 kW. The cross-flow turbine commonly manufactured nowadays in Nepal is the T12 model; whose maximum upper head is 50 m. The improved T15 design can be successfully used for heads of 65–80 m. As a rule, a runner width should not be less then 15 to 20% of the diameter or otherwise it causes decrement in efficiency.
   The power available from all type of turbines can be expressed as follows [1].

$$P_e = {}_t {}_g Q g H_{net} \qquad (4.3)$$

where

P_e	Nominal electrical power	W
$_t$	Efficiency of turbine	
$_g$	Efficiency of generator	
Q	Design flow	m^3/s
g	Acceleration due to gravity	m/s^2
H_{net}	Net head	m

- Pelton 5-30 kW: 70-80%
- Pelton above 30 kW: 75-85%
- Cross-flow 5-30: 60-70%
- Cross-flow above 30 kW: 65-78%

One important parameter is that the speed up ratio should not exceed 1:3 (turbine: generator). For example, if the generator RPM is 1500, the turbine RPM should not be more than 500 RPM. For a cross-flow turbine, depending on the head and the runner diameter, the upper limit for RPM is between 100 (runner diameter 300 mm) and 1500 RPM (runner diameter 200 mm). For the T12 cross-flow turbine, the RPM is calculated using the equation 4.4. When selecting a certain type for a site, its

suitability in terms of flow and rotational speed (at a given net head) shall be considered as follows [1]:

$$n = \frac{n_g \sqrt{H_{net}}}{Dt_t} \qquad (4.4)$$

Where

D_t	Runner diameter	m
n	Rotational speed	rpm
n_g	Efficiency of generator	
H_{net}	Net heat	m

For Pelton turbine, RPM should be equal to the generator as far as possible so that the turbine and generator can be directly coupled and a belt drive is avoided. The suitable RPM for a Pelton is determined by the head and the runner pitch circle (pcd). The generator formula is given below [1].

$$n = \frac{60 k_u \sqrt{2gH_{net}}}{D} \qquad (4.5)$$

Where

D	Pitch circle diameter	m
n	Rotational speed	rpm
k	0.45-0.49	Permitted range 0 0.38-0.56, which results in an efficiency loss of less than 5%; this is suitable for directly coupled units only)
H_{net}	Net heat	m

The efficiencies at the rated output to be used in a feasibility study are as follows:

- Pelton 5-30 kW: 70-80%
- Pelton above 30 kW: 75-85%
- Cross-flow 5-30: 60-70%
- Cross-flow above 30 kW: 65-78%

The specific speed (n_q) is a parameter, which can be used to choose the type of turbine. It is calculated as follows [1]

$$n_q = \frac{n\sqrt{Q}}{H_{net}^{3/4}} \qquad (4.6.)$$

A decision regarding the turbine type should be based on the ranges of specific speeds (n_q) presented in table 4.3.

Table 4.3: The relation between turbine type and specific speed

Turbine type	n_q Ranges
Single-jet Pelton	3-9
Double-jet Pelton	9-12
Triple-jet Pelton	12-15
Cross-flow	9-22

4.1.2.3 Penstock

A penstock pipe conveys water under pressure from the forebay to the turbine. Mild steel and HDPE pipes are widely used as penstocks for MHPP schemes in Nepal. The penstock alignment should be chosen such that the significant head can be gained at a short distance but it should still be possible to lay the penstock pipe. The number of bends should be kept to a minimum so that the number of anchor blocks and head loss can be minimised. For an exposed (i.e. above-ground) penstock alignment, a clear cover of 300 mm between the pipe and the ground should be provided to facilitate maintenance and minimise corrosion.

The selection of the diameter should be based on the following formula.
The initial diameter is calculated based on the following empirical formula [1]:

$$D = 41Q^{0.38} \qquad (4.7)$$

Where

D	Internal diameter of pipe	mm
Q	Design flow	Lt/s

This formula is suitable for the pipe length less than 100 m.
An alternative formula can be used to determine pipe diameter [1]

$$D_{opt} = 0.5H - \left(\frac{1}{7}\right)\left(\frac{P_{hydro}}{H}\right)^{3/7} \qquad (4.8)$$

$$P_{hydro} = QgH$$

Where

D_{opt}	Optimal diameter of pipe	cm
P_{hydro}	Available power	kW
H	Appropriate net head	m
Q	Design flow	m^3/s
g	Acceleration due to gravity	m/s^2
	Density of water	kg/m^3

After calculating the diameter, the total head loss of the pipe is also to be considered. It should not be more than 10% of the gross head.

4.1.2.4 Transmission and distribution system

1. Transmission lines can be buried or suspended overhead on poles. Overhead lines are common as they are less expensive and easier to install. Overhead lines are also easy to repair and maintain. However, when houses are densely located or heavy snowfall is expected during winters, underground transmission lines may be preferred. If properly installed and protected, they require little maintenance.
2. The design of transmission and distribution lines should be such that a voltage drop at any distribution line end is limited to 10% of the nominal value.
3. The maximum transmission line-to-line voltage level permitted in isolated system is 11 kV. Transformers should be at least 20-25% over-sized than the existing demand and keeping load extensions in the future.
4. ACSR conductors are generally used for overhead transmission lines in MHPP schemes. Arial bundled cables (ABC) may also be used for overhead lines if poles are expensive. ACSR conductors are available in various sizes and designations. Their properties are presented in table 4.4 [1].

Table 4.4: Sizes and designation of ACSR conductors used in MHPP

Name	Current rating in still air (A)	Resistance (Ω/km)	Inductive reactance at 50 Hz and 50 cm spacing (Ω/km)	Approximate Weight (kg/km)
Squirrel	76	1.374	0.355	80
Gopher	85	1.098	0.349	106
Weasel	95	0.9116	0.345	128
Rabbit	135	0.5449	0.335	214
Otter	185	0.3434	0.328	339
Dog	205	0.2745	0.315	394

4.1.3 Mathematical model of the MHPP

Based on the block diagram, a mathematical model is developed as shown in fig 4.2. WR is constructed in such a way that the maximum water level in WR is same as the water level in the river. An advantage is that water flow into WR is automatically controlled by a mechanical governor. Water from the river flows on the top of WR and into the turbine through the governor from the bottom. The mechanically connected synchronous generator [SG] produces electrical power, which is transmitted to the isolated grid through a step of transformer. The most important component of the model is SG, which is modelled as a grid former. It means the generator receives active and reactive loads (P_L, Q_L) as inputs and gives state variables, frequency and voltage, (f_{grid}, V_{grid}) as the outputs. The stability of an isolated grid is maintained

through controlled units associated with SG at changing load profile. The complete model is shown in fig. 4.2.

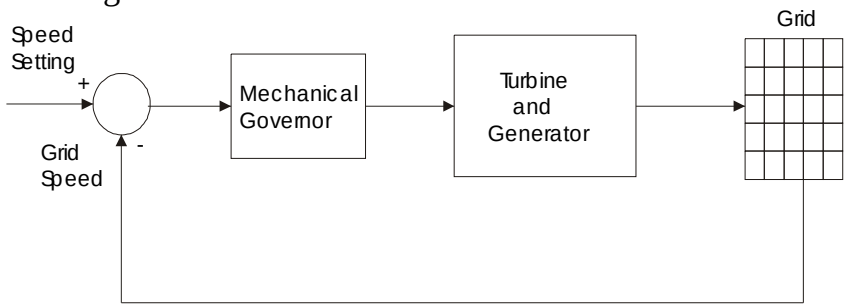

Fig. 4.2: Block diagram of micro hydro power plant

The simulated MHPP has following data

Table 4.5: Data of the simulated MHPP

Parameter	Description	Value
P_e	Nominal electrical power	7.5 kW
H_{net}	Appropriate net head	15 m
Q	Design flow	0.09 m^3/s
Generator	Synchronous	
Voltage Regulator	Automatic voltage regulator	
Frequency regulator	Mechanical	
Energy storage	Water reservoir	

The complete model is shown in fig 4.3.

4.1.3.1 Water turbine

The mechanical power available from the turbine has been formulated above. In this equation, the only one possible controllable variable is Q. which is controlled to maintain the power from the turbine.

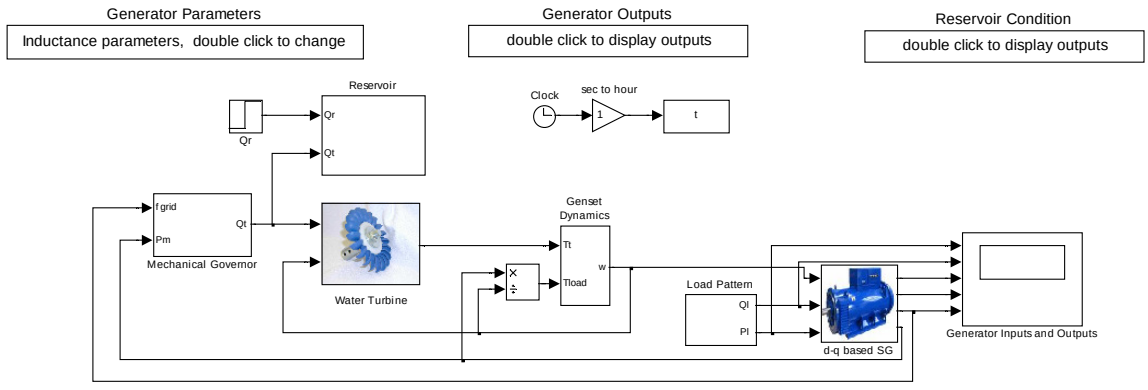

Fig. 4.3: The complete simulation model of MHPP

4.1.3.2 Synchronous generator

The SG is directly connected to the water turbine. Variable inputs for the generator, which determine the frequency and the voltage, are mechanical torque from the turbine and field current (I_f) from a dc voltage source. A separately excited SG is versatile

because it is possible to operate in all four quadratures. It means the SG can absorb or deliver active and reactive power to maintain grid stability as per reference. The model is developed based on the two-axis theory.

The two-axis (dq) model of SG is expressed by following equations [3], [4].

Power equations

$$\begin{aligned} P_L &= \sqrt{3} V_L I_L \cos \\ Q_L &= \sqrt{3} V_L I_L \sin \end{aligned} \qquad (4.9)$$

Current equations

$$\begin{aligned} I_q &= I_L \cos(\quad + \Delta) \\ I_d &= I_L \sin(\quad + \Delta) \end{aligned} \qquad (4.10)$$

Flux equations

$$\begin{aligned} {}_q &= I_q L q \\ {}_d &= I_d L_d - I_f . L_{fd} \end{aligned} \qquad (4.11)$$

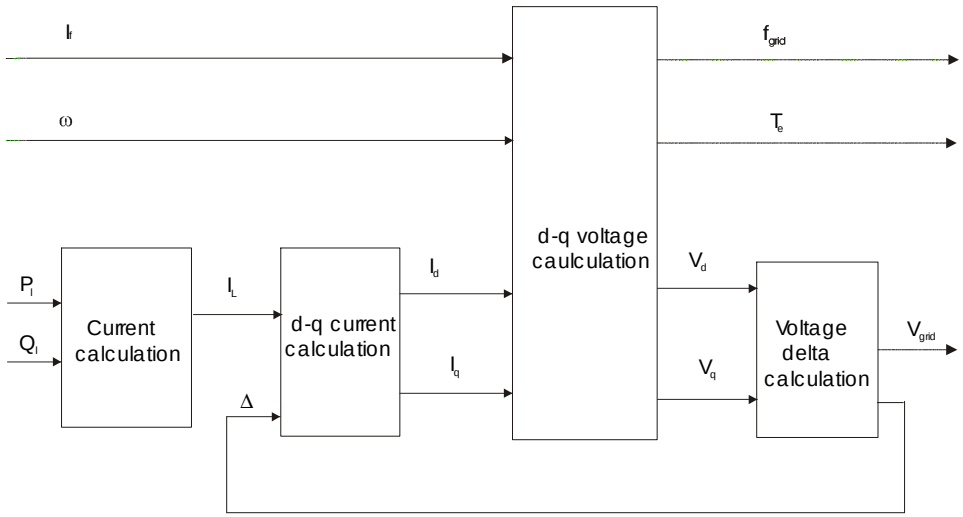

Fig. 4.4: The block diagram representation of the synchronous generator

Voltage equations

$$\begin{aligned} V_q &= -\Omega p \quad {}_d - I_q R_s - \frac{d \quad {}_q}{dt} \\ V_d &= \Omega p \quad {}_q - I_d R_s - \frac{d \quad {}_d}{dt} \\ V &= \sqrt{V_d{}^2 + V_q{}^2} \\ \Delta &= \tan^{-1}\left(\frac{V_d}{V_q}\right) \end{aligned} \qquad (4.12)$$

Swing equation

$$\Omega = \frac{1}{J}\int (T_t - T_e)dt \qquad (4.13)$$

Based upon equations from 4.9 to 4.13, a model is developed as shown in fig. 4.4. The electrodynamics response of the SG is very fast as compared to the water turbine so the transient parts in SG voltage equations can be omitted [3].

4.1.3.3 Mechanical governor

A function of a mechanical governor is to maintain the speed of the synchronous generator respectively the frequency of the grid. The variable parameter is the water flow Q_t that is controlled by changing needle position in the nozzle. A block diagram is shown in fig. 4.5 [6], [11].

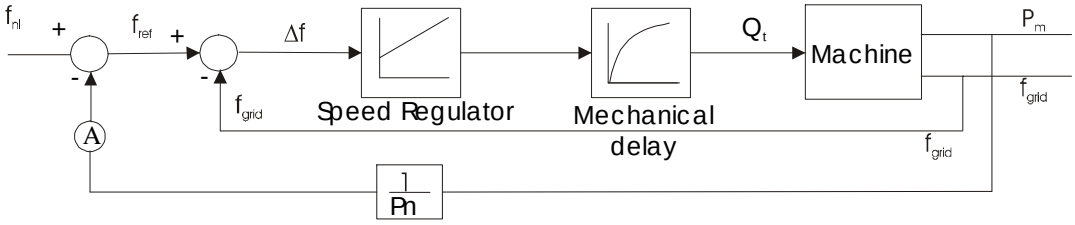

Fig. 4.5: The mathematical model of mechanical governor

By using active power-droop characteristics (factor A) the frequency of the system can be adjusted as per requirement [11]. For this simulation model, A is adjusted such that, the frequency decreases up to 48 Hz at full load and increases up to 52 Hz at no load condition. The system behaviour from no load to full load test is shown in fig. 4.6.

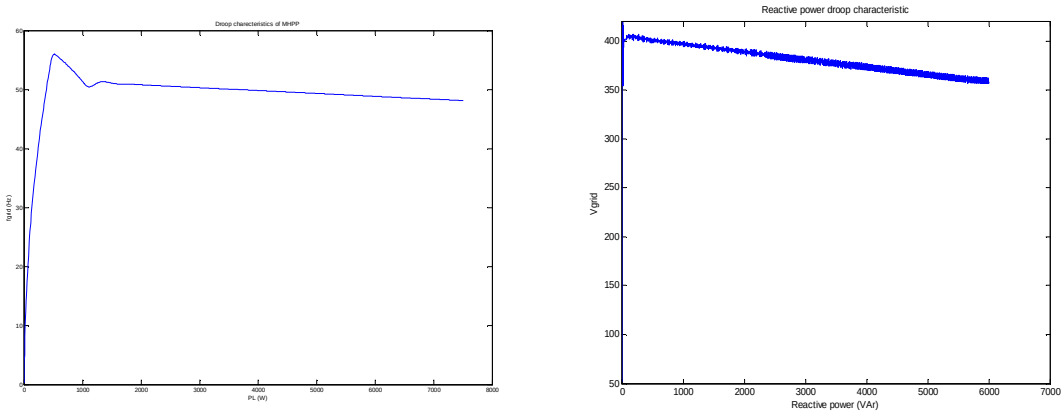

Fig. 4.6: Frequency and voltage droop characteristics of the SG control system

4.1.3.4 Automatic Voltage Regulator [AVR]

AVR is an electronic device, which is mounted near to SG, and its function is to control the terminal voltage of SG as per reference value in the changing load scenario. Most of the time, it consists of P or PI controller, which controls the field current depending upon the voltage difference between the reference and the actual voltage. Besides the electronic behaviour, a delay may occur to adjust the voltage due to a mechanical adjustment. As, in the case of the mechanical government, the droop

characteristics can be adjusted by changing the reactive power droop factor B [6], [11]. In case of an isolated grid, up to 10 % voltage drop at full reactive load is allowed.

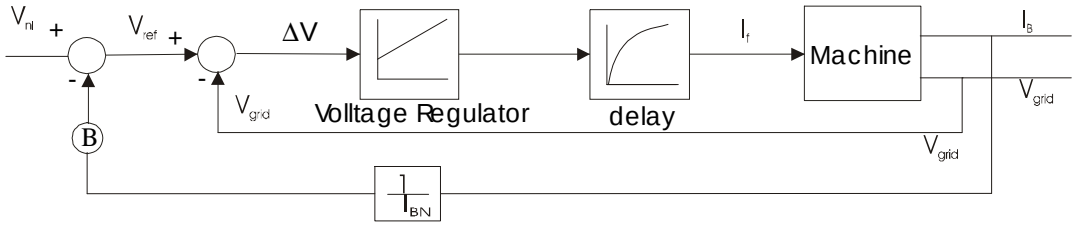

Fig. 4.7: Inside view of automatic voltage regulator

4.1.3.5 Reservoir

The main energy storage unit of the MHPP is a water reservoir. The volume of the reservoir is determined in such a way that the full amount of water can produce nominal power for six hours. The deviation of f_{grid} from f_{ref} (may be positive or negative) determines whether water is stored or drawn in/from WR. Data of WR are given below

Nominal water flow	=	0.09 m^3/s
Water volume required to full load for 6 hours	=	0.09*6*60*60
	=	1944 m^3
Height of the reservoir	=	5 m
Area of the reservoir	=	389 m^2
Length and breadth of the reservoir	=	19.5 m

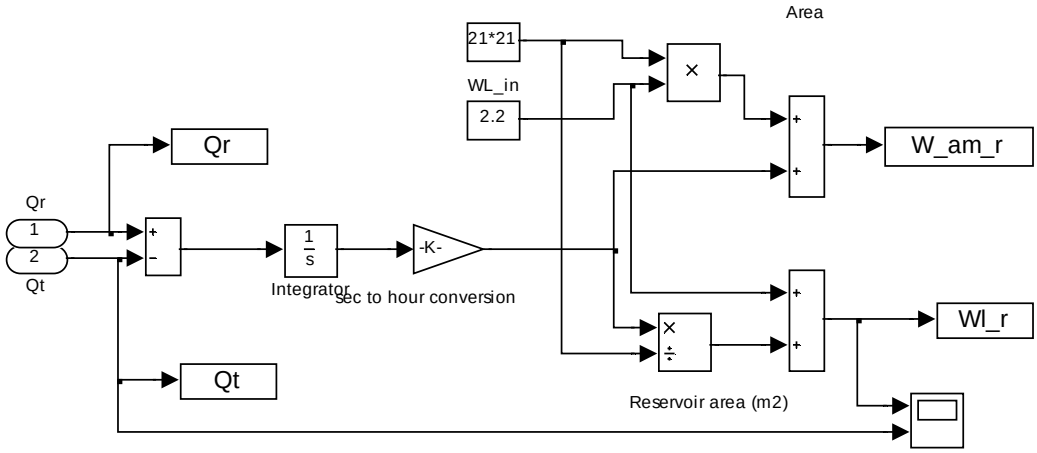

Fig. 4.8: The calculation of the water level and volume in the reservoir

The water level and volume in the reservoir is calculated in the Simulink model which is shown in fig 4.8.

4.1.4 Experiments

At the beginning, the machine is brought in motion without connecting the load and the speed of the generator increases slowly. The mechanical governor maintains the nominal speed. After that field voltage is applied so that the generator produces nominal voltage at the nominal speed. After achieving the nominal voltage and frequency, the load can be connected.

The simulation is carried out in second time unit. To observe the behaviour of the water storage in the reservoir, the model must be simulated for many hours, which is very time consuming. To tackle this problem, the second is converted into hours by multiplying by suitable factor.

4.1.4.1 No load to full load test

The frequency and voltage response of the SG are tested through no load to full load test. At the same time the water status in WR is also observed. As mentioned above SG is modelled as grid former so P and Q are given as inputs to SG. The simulation is carried out for 20 seconds, which corresponds to 4.5 hours.

Generator status

Fig 4.9 shows the generator status. The first and second graph shows P_L and Q_L. The generator is started with no load condition. After achieving nominal voltage and frequency, at 1.1 hour P_L increases to the half of its full load, correspondingly Q_L increases to full load at 1.6 hours. The third graph shows the current produced by SG. The current increases from 0 to 6 A at cos = 1.0 and as cos decreases to 0.8, SG produces nominal current of 14.5 A.

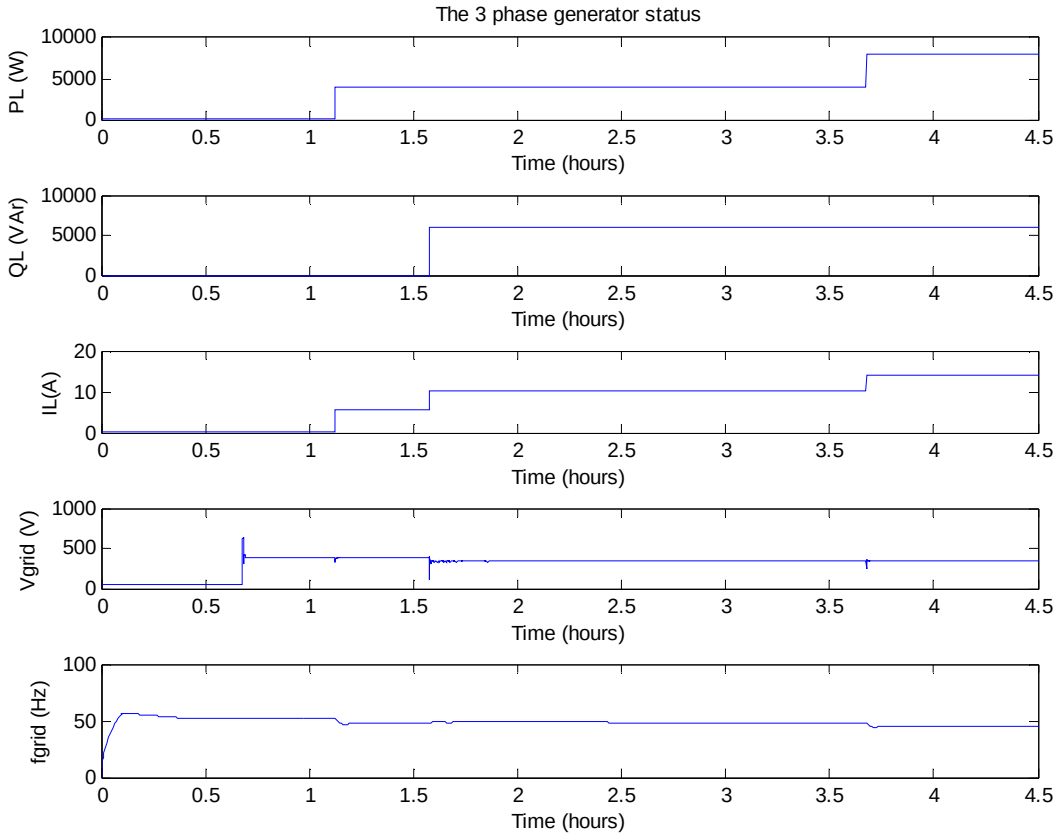

Fig. 4.9: The generator status during load changing from no load to full load

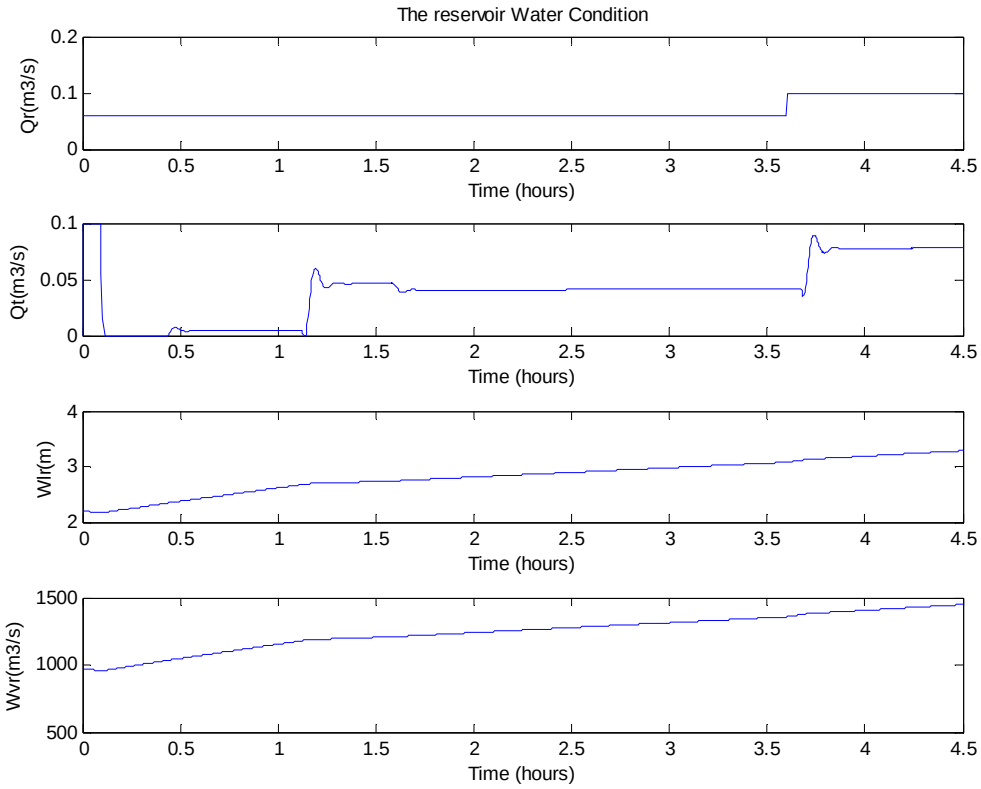

Fig. 4.10: The reservoir status during load changing from no load to full load

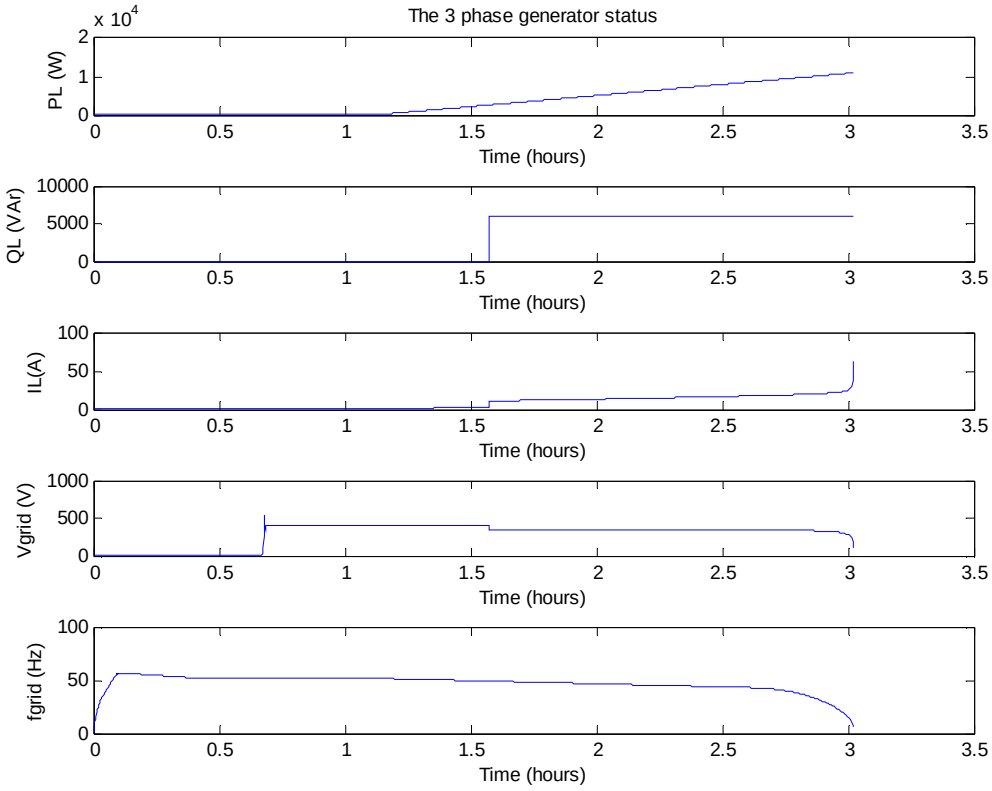

Fig. 4.11: The generator status during load changing from no load to over load

The grid variables V_{grid} and f_{grid} are shown in the fourth and the fifth graphs. At no load condition, SG produces 400 volt line to line. At full load conditions with cos = 0.8 voltage decreases to 380 volt (around 5%). As P_L or Q_L changes transient effect can be observed. The frequency of the SG increases slowly and goes up to 55 Hz and decreases slowly. At some time no load frequency of 52 Hz is maintained. As the active load jumps to the full load the frequency decreases up to 46 Hz, after transient behaviour, the frequency is maintained at 48 Hz (4% droop) . By changing the P and I parameters of voltage and frequency controllers, the response characteristics of the controllers can be adjusted.

4.1.4.2 Over Load Test

This experiment shows that the system can not maintain the frequency and voltage, if the load is increased above nominal load. It is shown in fig. 4.11. The first graph shows the load increment in ramp fashion. When the load crosses 8 kW, the frequency goes down slowly and the system finally collapses.

4.2 PV System

Photovoltaic cells produce DC electricity directly when they are exposed to the sunlight. A photovoltaic cell is technically a P-N junction made up by the silicon. An ideal photovoltaic cell can produce 0.82 V at no load condition [7]. It indicates that many such cells are to be connected parallel to get suitable operating voltage. Cells are connected together and placed in the supportive material covered by the glass layer and known as module. In market different types of the modules are available with respect to the open circuit voltage (Voc) and the power. Some modules are rated up to 100 W_p [8]. Different types of PV modules are shown in fig. 4.12.

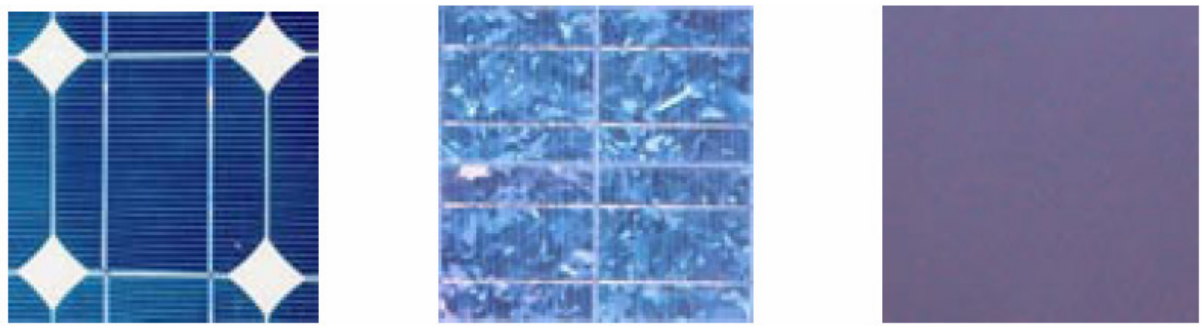

Fig. 4.12: Different types of PV modules available in the market

There are lots of advantages associated with the PV system. They are as follows

1. Environmentally sound performance-cleanest technology available
2. Low maintenance and long life time
3. Free accessibility of sun irradiation

Besides many advantages, the key deficiency is the poor economic performance. A high initial investment cost for the system makes it the least preferred choice as compared to other energy sources.

4.2.1 Market trend

Applications of a PV system in different fields of electrical energy supply system (decentralised or grid connected) is rapidly increasing due to the advancement in technology as well as the reduction of cost for per kWh. Fig. 4.13 shows a trend of PV system installed capacity. While in 1990, the use of PV system was only on the stand along system in remote areas, but at the end of the decade PV systems were used to build small-decentralised grid connected systems [SGCS]. Now MW range PV plants have been connected into the existing central grid.
The cost of the PV system is the most important factor for future implementation in remote areas of developing countries. Fig. 4.13 shows that cost trend of 3 kWp system in Austria, Germany, Japan, the Nederland, USA, and Switzerland. It shows that the prices decreased consequently and tended to stabilise around 7$ /Wp in 2001. From this trend it can be predicted that the cost will be decreased in future too.

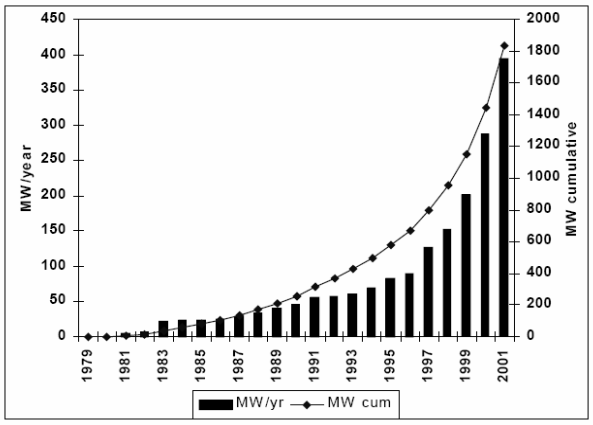

Fig. 4.13: Development of PV market worldwide 1978- 2002[9]

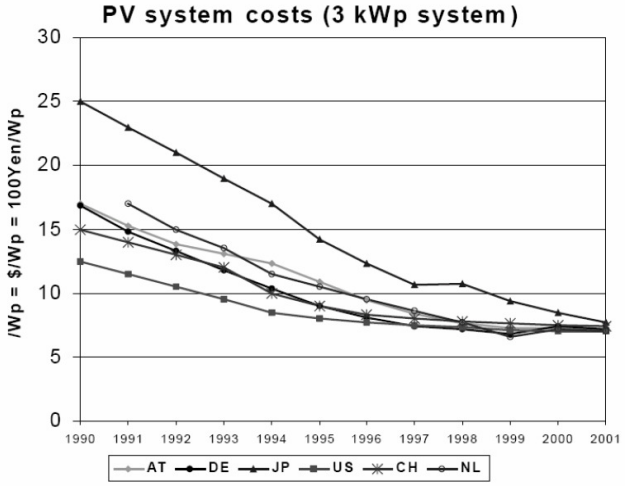

Fig. 4.14: Decrement of PV price in different countries from 1990 to 2001[9]

4.2.2 Mathematical Expression

As mentioned above a PV cell is a PN junction, which is shown in fig. 4.15. Physical parameters of such a cell can be mathematically expressed using an ideal equivalent circuit of the cell shown in fig. 4.16.

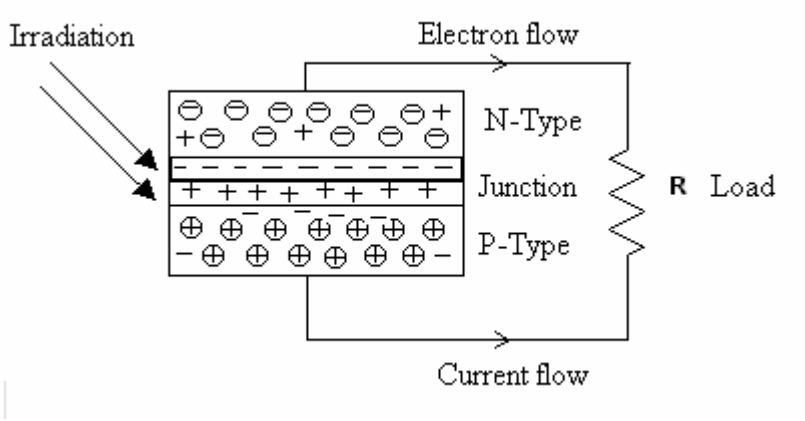

Fig. 4.15: P-N junction of a photovoltaic cell

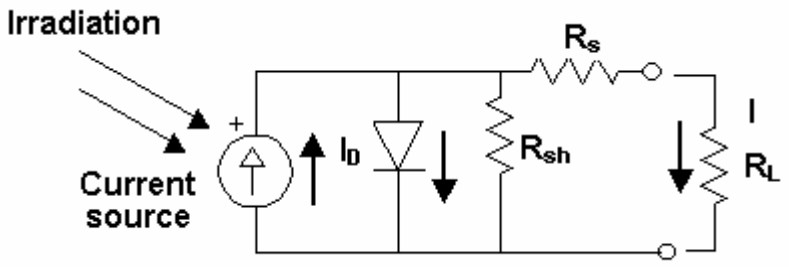

Fig. 4.16: Signal diode equivalent circuit of PV cell

The current produced by the PV cell I_{ph} is not totally delivered into the load because of a connection of the diode parallel to the cell. The current available from the PV cell to the load is expressed as

$$I_{pv} = I_{ph} - I_D \tag{4.14}$$

Where the photo current and the current flowing into the diode are given by following equation

$$I_{ph} = e_0 \int_0^{\infty} \frac{E\ d}{h}. \tag{4.15}$$

$$I_D = I_0 \left[\exp\left(\frac{e_0 V_L}{K T_c} \right) - 1 \right]. \tag{4.16}$$

By replacing the value of I_D into (2.1.5), the final expression for PV current can be expressed as

$$I_{pv} = I_{ph} - I_0\left[\exp\left(\frac{e_0 V_L}{KT_c}\right) - 1\right] \tag{4.17}$$

Important variables of the PV cell are short circuit current (I_{sc}) and open circuit voltage (V_{oc}). The short circuit current is the current produced by the PV cell when its terminals are short-circuited. In this condition, I_D is small compared to I_{pv} so it can be neglected. The short circuit current is expressed as

$$I_{sc} = I_{pv} = I_{ph} \tag{4.18}$$

The voltage across the terminals at no load condition is called the open circuit voltage (V_{oc}). An expression for it can be obtained by replacing I_{pv} with zero as follows

$$V_{oc} = \frac{KT_c}{e_0}\left[\exp\left(\frac{I_{ph}}{I_D}\right) + 1\right]. \tag{4.19}$$

The power production from the PV cell is a product of the current flowing into the load and the voltage across the load. At the short circuit condition, the current is maximum but the voltage is zero so no power is produced. Similarly at the open circuit condition, the voltage is maximum and the current is zero, so no power is produced. At one point, the PV cell delivers maximum power, which is known as the maximum power point (MPP). At the MPP the current and the voltage are approximately given by

$$V_{mpp} = (0.75 - 0.9)V_{oc} \tag{4.20}$$

$$I_{mpp} \approx (0.85 - 0.95)I_{sc}$$

Based upon the above equations the relation between the voltage and the current for variable irradiation / constant temperature and constant irradiation / variable temperature are shown in fig 4.17.

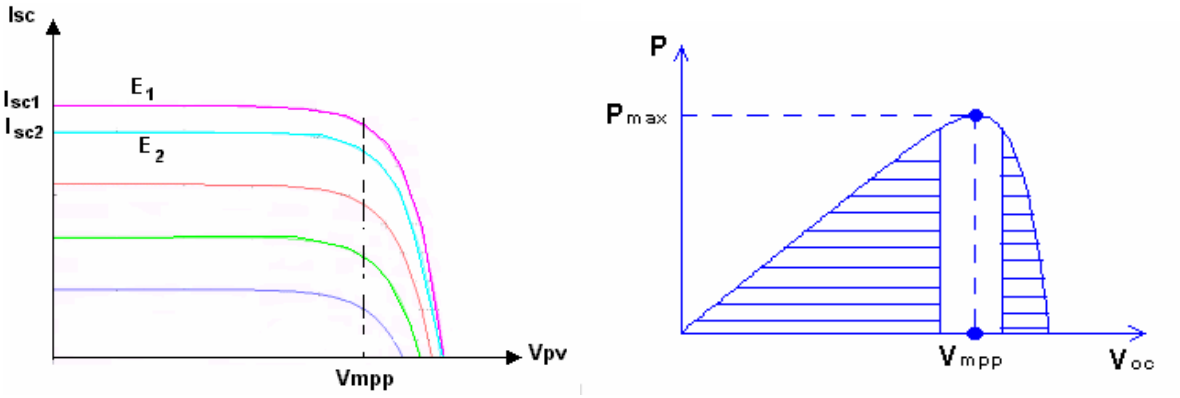

Fig. 4.17: Characteristics of PV cell at variable irradiation and constant temperature

Fig. 4.17 (left) shows that the short circuit current decreases when the irradiation decreases and the open circuit voltage decreases as the temperature increases.
The relation between the power and the voltage is shown in fig. 4.17 (right) for a particular irradiation and temperature. This figure clearly shows that the power production from PV module can be controlled by changing the PV cell voltage.

4.2.3 System configuration

An integration of the power section in the PV system to the control section is very important. The control section determines the way of the power controlling in the PV system. The power demand in an isolated grid may not always to be the maximum available power. So, simply a MPP tracker can not be used. The system configuration is shown in fig 4.18 [24]. The PV module is connected to the grid or the isolated grid through the power electronic block (for example sunny boy inverter). In the control section, three controllers are used to inject the demanded power from the PV system into the grid. As shown, the voltage and the current of the PV module are measured and the actual power is calculated.

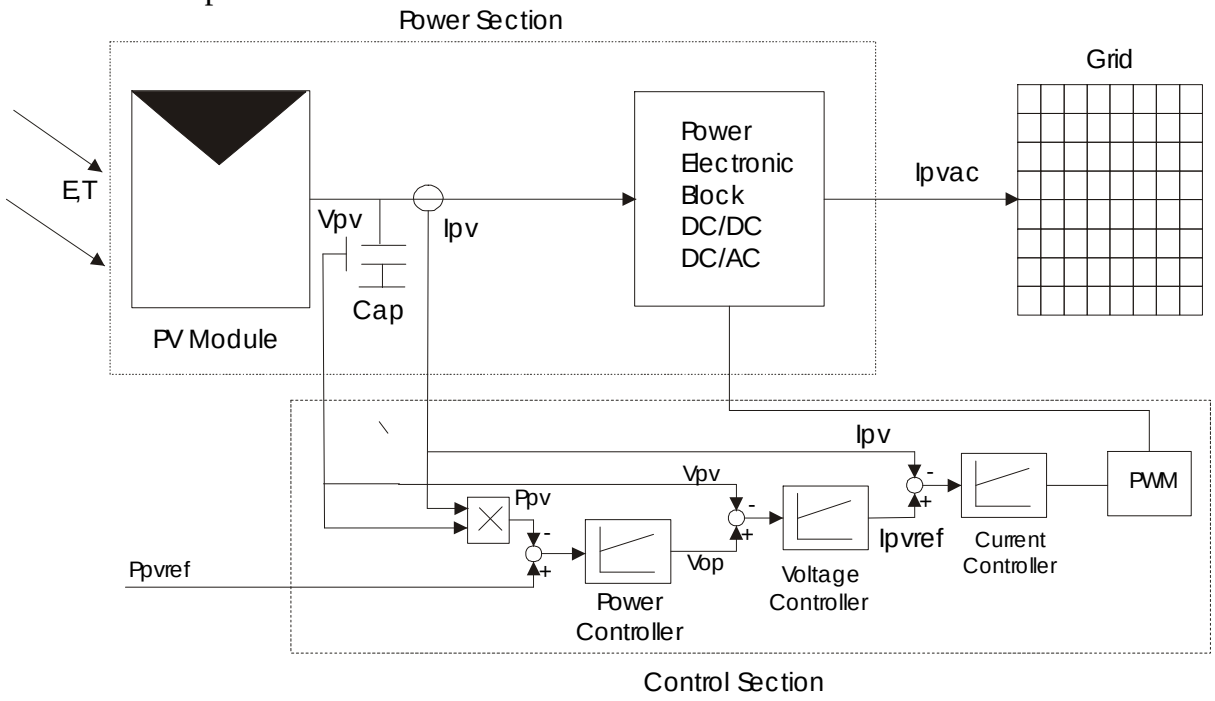

Fig. 4.18: The system configuration of the PV system connected into a grid

This power is compared with the reference power, using a power controller the optimal voltage V_{op} is determined. Next attempt is to find out the reference current I_{pvref}. It is done by comparing the optimal voltage and actual voltage V_{pv} of the PV module. Finally this reference current is compared with actual current I_{pv} and the output is used to generator PWM signal, which controls the current flow from the PV system into the grid. The terminal voltage of the inverter is guided by the grid voltage, which is constant so by controlling the current, the power is controlled as defined.

4.2.4 PV System Model

The first view of the model is shown in fig 4.19. It consists of an environmental block from where irradiation and temperature inputs can be fed. For a simplification of

modelling, the environmental temperature is used directly as junction temperature. The thermal model can be found in [3].

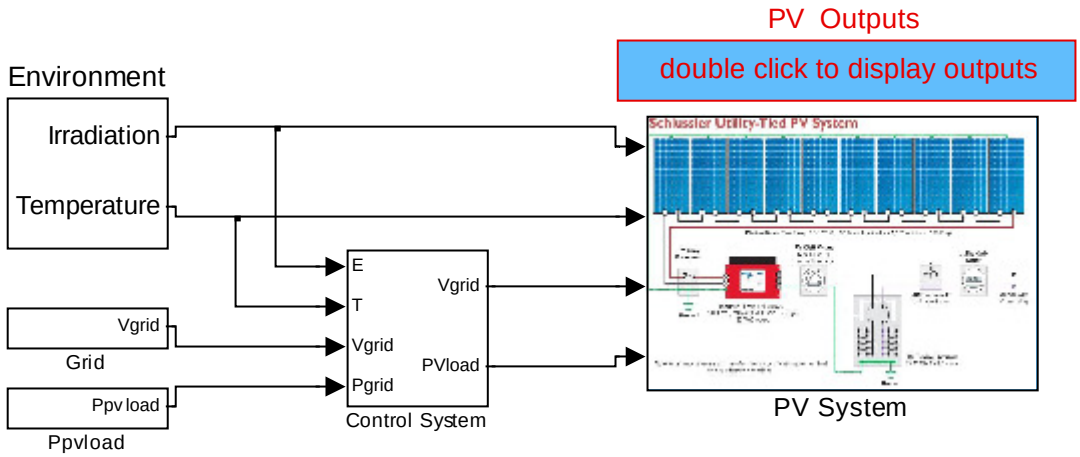

Fig. 4.19: The model of PV system developed in Simulink

Its function is to disconnect the PV system from the grid, if the grid voltage drastically changes from its normal values. At the same time, if the reference load is more that its actual capacity based upon actual meteorological condition, the PV system is loaded with its actual capacity.

The inside view of the PV system is shown in fig 4.20 and it is based upon the system configuration shown in fig 4.18. In this model, PV module is connected with existing grid, technically, it means the inverter gets the voltage from the grid, and it gets also the optimal reference voltage from the voltage controller. The inverter controls the current flow in such a way that the reference power is delivered by the PV model. A detail modelling of the inverter system has been avoided here to simplify the model. A better understanding can be gained from the works [10].

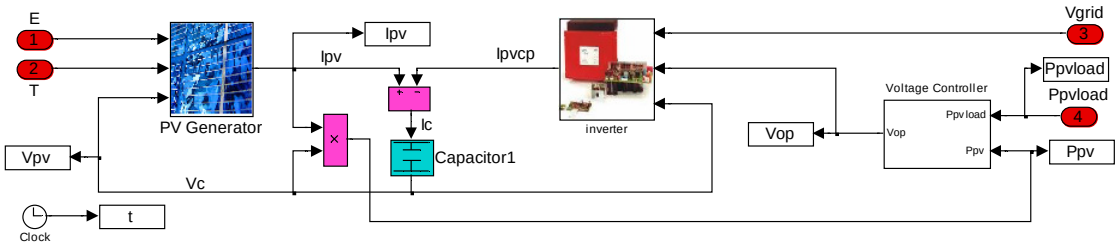

Fig. 4.20: Inside view of the PV system

The main focusing component is the PV module. The modelling of the PV module is based upon the Standard Test Conditions [STC] because the nominal power of PV module is rated on the STC. The variation in voltage, current and power from the module is calculated based upon these parameters at the STC. Following five equations (4.21- 24.25) describe the PV module.

$$I_{sc-new} = I_{sc-stc}\left[\frac{E_{new}}{E_{stc}}\right]\left[1 + A\left(T_{new} - T_{stc}\right)\right] \tag{4.21}$$

$$V_{oc-new} = V_{oc-stc}\left[1 + B\left(T_{new} - T_{stc}\right)\right] \tag{4.22}$$

$$= \frac{V_{mpp} - V_{oc}}{V_{oc} * \log\left(1 - \frac{I_{mpp}}{I_{sc}}\right)} \tag{4.23}$$

$$I_o = \left(I_{sc} - I_{mpp}\right) * \exp\left(\frac{-V_{mpp}}{* V_{oc}}\right) \tag{4.24}$$

$$I_{pv} = I_{sc-new} - I_o\left[\exp\left(\frac{V_{pv}}{* V_{oc-new}}\right) - 1\right] \tag{4.25}$$

$$P_{pv} = I_{pv} V_{pv} \tag{4.26}$$

Another important component from the point of modelling is the voltage stabilising capacitor. The voltage across the capacitor or the PV module is expressed as

$$V_{pv} = \frac{1}{C}\int \left(I_{pv} - I_{pvcp}\right) dt \tag{4.27}$$

Where, C is the capacitance in Faraday.

4.2.5 Experiments

4.2.5.1 Characteristics test

The PV system is simulated to obtain its basic characteristics at the variable irradiation and constant temperature. At one particular irradiation for example 300 W/m^2, the voltage of the module is changed from V_{oc} to zero volt [short circuit]. The behaviour of the module is shown in fig. 4.21. Initially no current flows, and as the voltage slowly decreases, the current slowly increases. It reaches to maximum value and remains constant up to the short circuit point. Similar behaviour can be observed for other irradiations.

In lower graph, it can be clear observed that PV module produces its maximum power at one particular voltage, which is the MPP. From this experiment, it can be said that the irradiation has more effect on the current but not on the voltage. The behaviour of the module is very close to a real module.

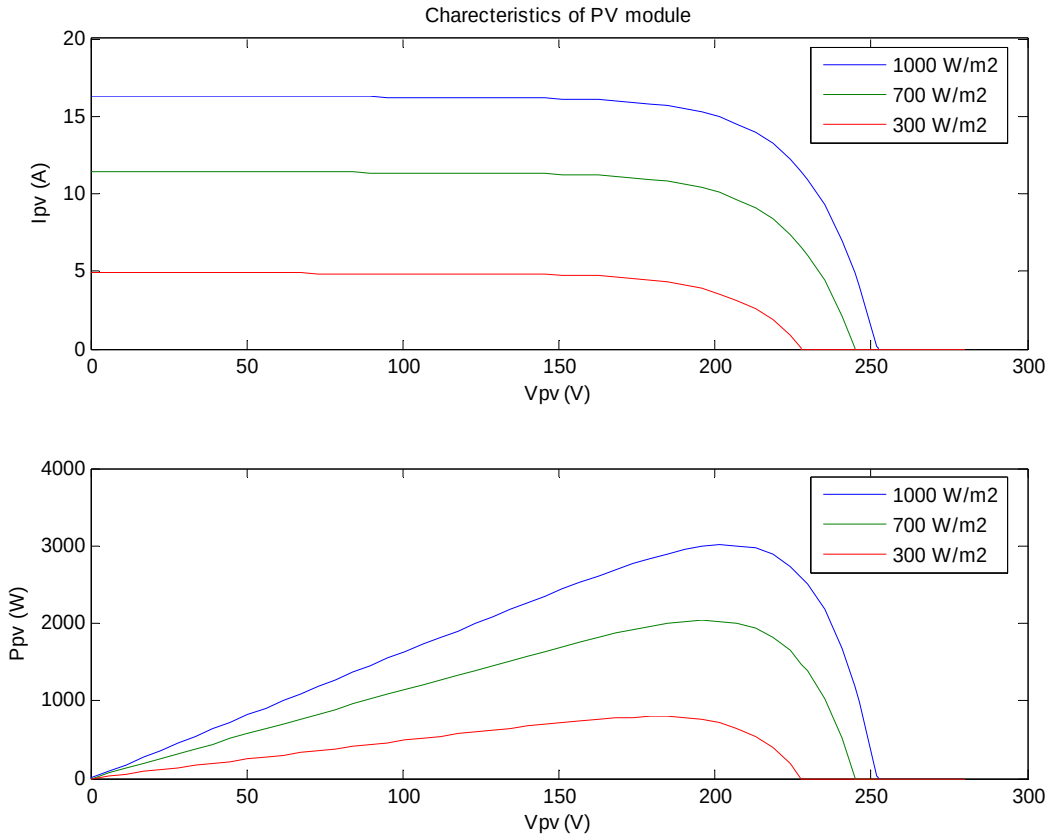

Fig. 4.21: PV cell characteristics with variable irradiation with constant temperature

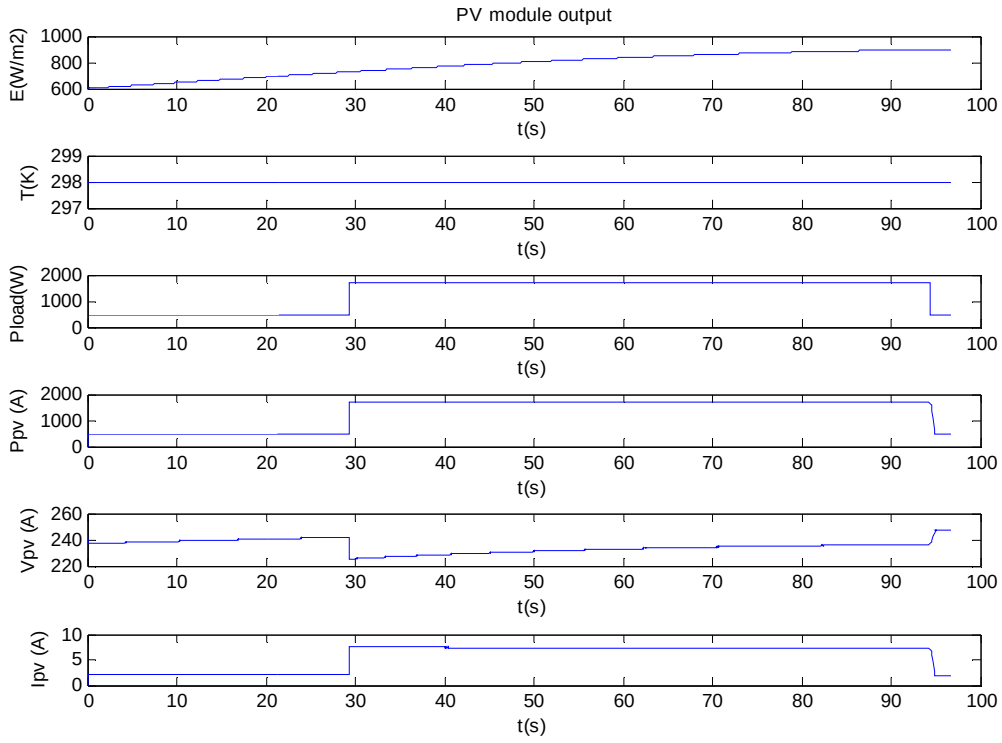

Fig. 4.22: PV system behaviour during variable irradiation with step load increment

4.2.5.2 Power control test

This test is carried out to confirm whether the complete system can control the power of the PV system as per the reference value. The system behaviour is shown in fig. 4.22. A ramp irradiation with constant temperature is fed into the system as inputs, which are shown in the first and second graph. The third graph shows the reference power. Initially the system is loaded with 500 W up to 29 sec and it jumps to 1800 W. Finally it decreases to 500 W at 95 sec. The fourth graph shows the power production from the PV system. It shows that the power production is just same as to the reference. In increasing irradiation and constant reference, the power control is achieved by changing the PV voltage between the open circuit voltage to the MPP voltage. It can be observed in the forth graph. The fifth graph shows the PV current.

4.3 Wind Turbine Generator

In changing energy scenario, the importance of renewable energy is increasing day by day. Due to the technological advancement and the low investment cost as compared to other sources, a popularity of WTG is increasing. A wind turbine in range from 1 to 100 kW is taken as a small wind turbine [23]. As compared to MW range WTG, small WTG are simple in design and construction. A stall-controlled algorithm has been implemented in such system. It is possible to use a synchronous or an asynchronous generator to produce electrical power. The choice depends upon the nature of a load that has to be delivered. If the grid is available, an asynchronous generator is a good choice. If the grid is to be formed by it, or it has to deliver the reactive power, a synchronous generator should be chosen. A possible interconnection of WTG with an available grid is shown in fig 4.23.

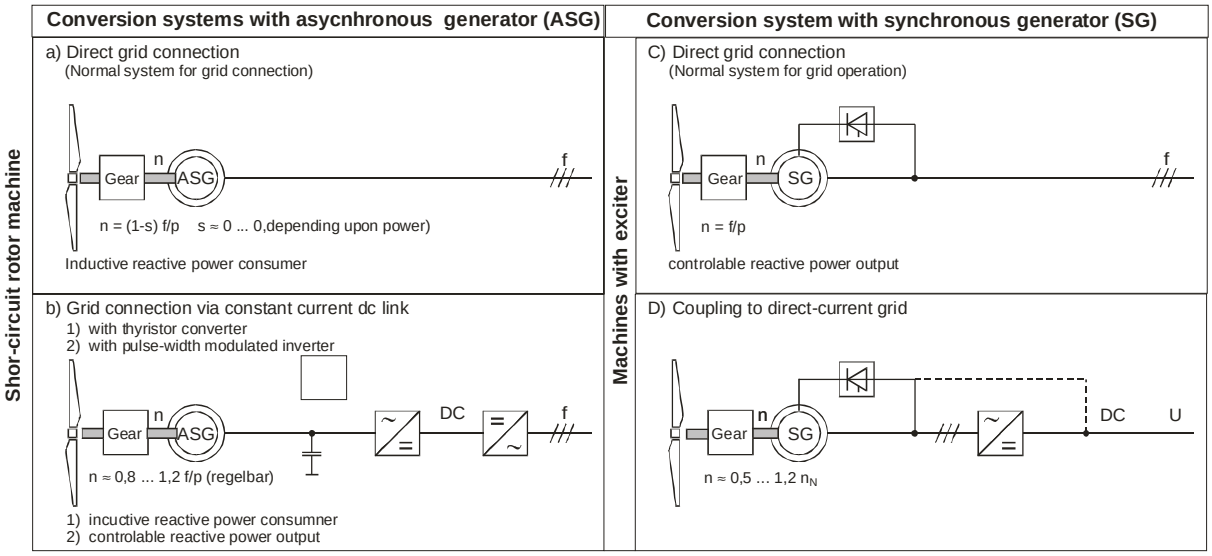

Fig. 4.23: Systems for converting mechanical energy into electrical energy [4]

As mentioned above, the PV system and the WTG support the grid formed by the MHPP. In such a circumstance, the first configuration, which is also known as the Danish concept, is the suitable one. The reason for this is the application of an induction machine, which has advantages, like on the one hand its low cost, robust construction and on the other hand, capability of feeding the active power into the grid

without getting the reactive power from any separate source. It means an induction machine draws the reactive power from the available grid and delivers the active power into the grid, if the machine is driven by external torque. Fixed blades of the wind turbine provide the mechanical torque to produce the electrical power. The step up gear is used to match the speed of the generator to the grid frequency. The investigated generator is a pole changeable one. This provision is kept to achieve more power in different velocity ranges.

4.3.1 Control system

As compared to other energy sources like gas or steam, hydro or diesel, in which the power production can be controlled as per demanded by end consumers. In contrast, the primary energy source in WTG is not controllable. A delivery of the energy can be affected by changes in wind velocity regardless of the demand of end user [11]. In the case of WTG, the control is possible in only one direction. This means it is possible to decrease the power from WTG or control at some level if the power available is more than the demand. If the WTG is connected to the strong grid, it is possible to inject nominal power to grid at all the time. In the case of a small isolated grid, the power might be reduced. Different types of control mechanism have been applied in WTG. They are

1. Pitch control
2. Passive stall control
3. Active stall control

Among above three methods, the second one is suitable for the small WTG. In this control mechanism, the rotor blades are fixed mounted and the power is maintained at a nominal value by applying aerodynamics characteristics of the rotor blades.

4.3.2 Wind Turbine Generator Model

As mentioned above, the WTG is connected into the grid formed by the MHPP. The WTG provides the active power if the wind velocity increases above the cut_in velocity. The technical data for the modelled WTG is given below in table 4.6 [25].

Technical data

Table 4.6: Technical data of simulated wind turbine generator model

Cut in wind velocity (V_{wcut_in})	3 m/s
Cut off wind velocity (V_{wcut_off})	25 m/s
Nominal velocity (V_{wnom})	12 m/s
Nominal power (P_{nom})	5000 W
Blade diameter (2R)	5.1 m
Nominal voltage (V_{nom})	(400/230 V)
Nominal frequency (f_{nom})	50 Hz

The system is modelled based on the connection method as shown in fig. 4.23 (a). It consists of a wind turbine, a 3-phase asynchronous generator, a wind system, a control mechanism as shown in fig 4.24. The operation behaviour of the model is tested by connecting and disconnecting it with the available grid at the changing wind speed.

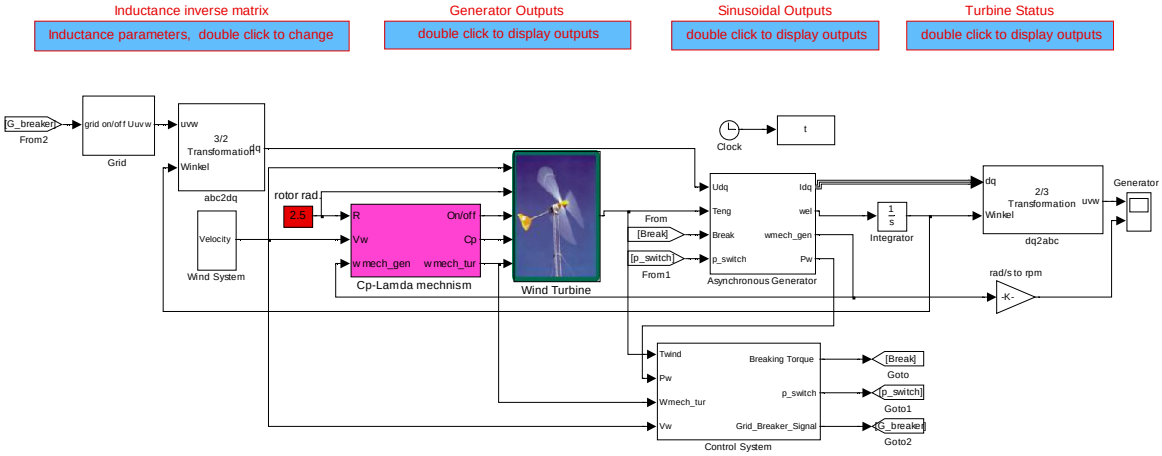

Fig. 4.24: The model of asynchronous generator rigidly connected to the grid

4.3.2.1 Wind Turbine

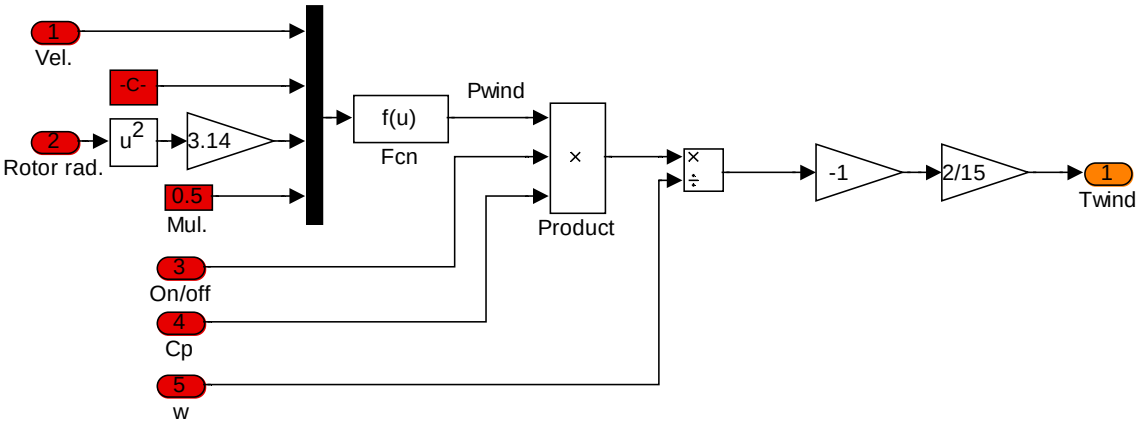

Fig. 4.25: The inside view of the mechanical governor

The model of the wind turbine is shown in fig. 4.25. The maximum power available from WTG is given by

$$P_{wind} = \frac{1}{2} AC_p V^3 \tag{4.28}$$

And the torque produced by the turbine is given by dividing the rotor power by its angular velocity.

$$T_{wind} = \frac{1}{2\Omega} AC_p V^3 \tag{4.29}$$

Due to the application of step up gear, the speed of the generator increases but the torque available at the generator shaft decreases with the same ratio. The torque available at the generator shaft is given by

$$T_g = \frac{1}{n}\frac{1}{2\Omega} AC_p V^3 \qquad (4.30)$$

The torque is multiplied by -1 to run the asynchronous machine in generator mode.

4.3.2.2 Cp- Mechanism

A C_p- mechanism represents the aerodynamics behaviour of the rotor blades. In this model, a look up table is used to characterise it. It is used to determine C_p of the wind turbine. The C_p of the wind turbine is function of the pitch angle and . In the case of the considered turbine, the blades are fixed. Then is expressed by (4.31)

$$= \frac{\Omega R}{V} \qquad (4.31)$$

Where

Ω is angular velocity (rad/s), R is radius of the wind turbine (m) and V is the wind velocity (m/s). Fig 4.26 shows the C_p- mechanism model.

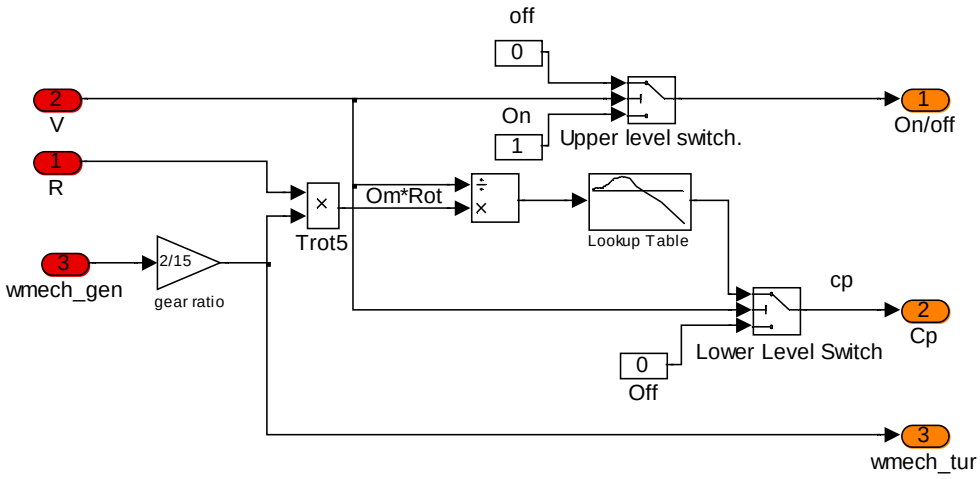

Fig. 4.26: The inside view of C_p- mechanism model mode

4.3.2.3 Control block

Small WTGs are designed to achieve 20% of the turbine nominal output at 50 to 70% of the nominal speed. This means that the small WTG can produce favourable power at lower wind velocity range. At higher velocity, it can produce the nominal power only if WTG rotates at the nominal speed. The system can function as the variable-speed WTG with a frequency converter but only with two fixed speeds. This principle can be implemented either by connecting additional generator or by a pole changing generator.

The control guidelines to operate the WTG in favourable conditions are mentioned below. To avoid a high frequency of changeovers on the borderline between a low wind velocity and a high wind speed, the overlap is provided between two operating conditions. The changeover hysteresis applied in this model is shown in fig 4.27.

Control Strategies

1. Connect the turbine in available grid
    a. $V_{cut\_off} >= V_w >= V_{cut\_in}$ if
    b. $T_{wind} > 0$
    c. $W_{mech\_tur} > 17.7$ rad/s
2. Breaking
    a. $V_w > V_{cut\_off}$
3. Pole changing
    a. $P_{wind} > 1200$ W -> from 6 to 4 pole
    b. $P_{wind} > 800$ W -> from 4 to 6 pole

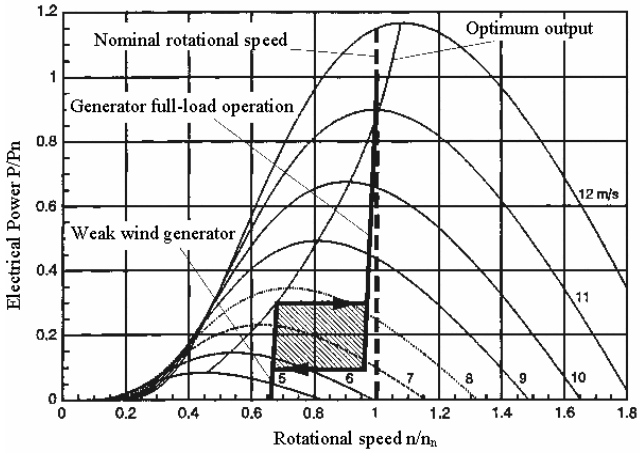

Fig. 4.27: Group of turbine characteristics for output as a function of rotational speed, with wind speed being a parameter, and the working range of weak wind and a full-load generator [11].

The above-mentioned control guidelines are implemented in Simulink as shown in fig 4.28.

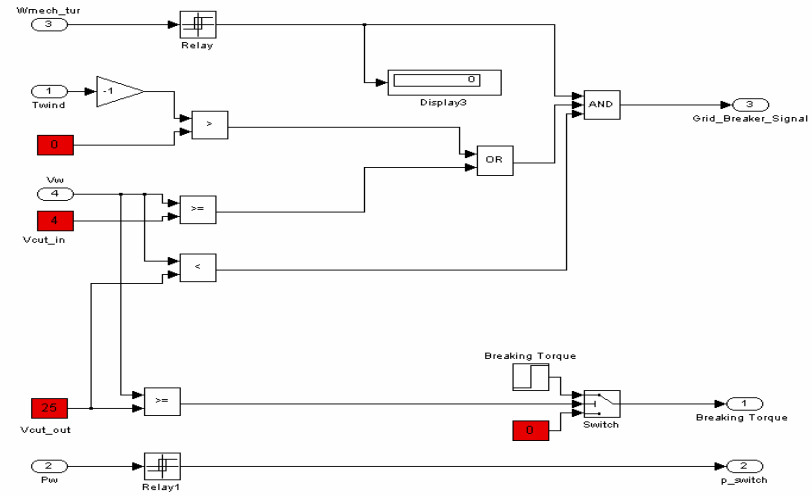

Fig. 4.28: A control system of the wind turbine model

4.3.2.4 Asynchronous generator

Asynchronous machines are mostly used as motors in industrial application. Due to its robust and simple construction, maintenance free long term operation, such machines have been found suitable to use as generator in small hydropower plants or in diesel genset sets to operate in isolated form or in wind turbines rigidly connected to a grid.

Technically an asynchronous generator is different from a synchronous generator because the asynchronous generator has no field winding. Instead of a field winding, the rotor consists of a number of copper or aluminium bars which are connected electrically by aluminium end rings (Squirrel cage induction generator).

Fig. 4.29: The simplified view of squirrel cage rotor

In fig 4.29, it can be observed that the rotor is provided with an "iron" core, using a stack of thin insulated steel laminations, with holes punched for the conducting aluminium bars. The rotor is placed in the middle of the stator, which in this case, once again, is a 4-pole stator, which is directly connected to the three phases of the electrical grid.
When the stator is connected to an electrical grid, a rotating magnetic field is produced in the air gap. Due to the induction phenomenon, a very strong current is induced in the rotor bars (very low resistance due to the short circuit) and produced its own magnetic field. These two magnetic fields interlocked each other and the rotor rotates with speed slightly below the synchronous speed. It is the motor action of the asynchronous generator. If the rotor is rotated by an external torque above the synchronous speed, the electrical power is supplied into the electric grid. The machine can be mathematically expressed by following equations [12].

The stator voltage equations

$$V_{d1} = R_1 I_{d1} + \frac{d}{dt}\psi_{d1} - \Omega_1 \psi_{q1}$$
$$V_{q1} = R_1 I_{d1} + \frac{d}{dt}\psi_{d1} + \Omega_1 \psi_{d1} \qquad (4.32)$$

$$0 = R'_2 I'_{d2} + \frac{d}{dt}\psi'_{d2}$$
$$0 = R'_2 I'_{q2} + \frac{d}{dt}\psi'_{q2} \qquad (4.33)$$

The above equations show the relation between voltages, currents and fluxes. The rotor is short circuited in cage induction generator.

$$\begin{aligned} {}_{d1} &= L_1 I_{d1} + L_h I'_{d2} \\ {}_{d1} &= L_1 I_{q1} + L_h I'_{q2} \end{aligned} \qquad (4.34)$$

$$\begin{aligned} {}'_{d2} &= L'_2 I'_{d2} + L_h I_{d1} \\ {}'_{q2} &= L'_2 I'_{q2} + L_h I_{q1} \end{aligned} \qquad (4.35)$$

The above two groups of equations give the relation between fluxes and inductances.

The electrical torque produced by a generator is given by

$$T_{el} = p.\left({}'_{q2}.I'_{d2} - {}'_{d2}.I'_{q2} \right) \qquad (4.36)$$

Relations between fluxes and inductances are expressed in matrix form to simplify the modelling.

$$\begin{bmatrix} {}_{d1} \\ {}_{q1} \\ {}'_{d2} \\ {}'_{q2} \end{bmatrix} = \begin{bmatrix} L_1 & 0 & L_h & 0 \\ 0 & L_1 & 0 & L_h \\ L_h & 0 & L'_2 & 0 \\ 0 & L_h & 0 & L'_2 \end{bmatrix} * \begin{bmatrix} I_{d1} \\ I_{q1} \\ I'_{d2} \\ I'_{q2} \end{bmatrix} \qquad (4.37)$$

The above equations are based on the d-q axis representation. The model receives 3-phase voltage as input and it provides 2-phase current as output. The inputs and outputs are to be transformed from 3 to 2 and 2 to 3 phase (inverse) using power invariance transformation equations as given below.

$$\begin{bmatrix} V_d \\ V_q \\ V_0 \end{bmatrix} = [T_{ZW}] \begin{bmatrix} V_u \\ V_v \\ V_w \end{bmatrix} \qquad (4.38)$$

$$[T_{ZW}] = \begin{bmatrix} \cos A & \cos\left(A - \frac{2}{3}\right) & \cos\left(A - \frac{2}{3}\right) \\ -\sin A & -\sin\left(A - \frac{2}{3}\right) & -\sin\left(A - \frac{2}{3}\right) \\ \frac{1}{\sqrt{2}} & \frac{1}{\sqrt{2}} & \frac{1}{\sqrt{2}} \end{bmatrix} \qquad (4.39)$$

Where

A is relative angle between stator and rotor quantities.

4.3.3 Experiments

4.3.3.1 Turbine Status

The wind turbine model is tested with variable wind pattern consisting of different wind phases like above and below cut_in, above and below cut_off, nominal, below nominal velocity etc. The first graph of fig 4.30shows the wind velocity pattern. As the simulation is started, the wind velocity is 0 m/s. The second graph shows the angular velocity of wind turbine. At 5 sec, as the velocity crosses to the cut_in level, the wind turbine starts to rotate and speed goes slowly up. As the speed reaches just above 1000 rpm, the turbine is connected to the grid and the generator runs in slightly above 1500 rpm with 4 poles due to the high wind speed. At 24 sec, as the velocity decreases to low range, the pole is changed from 4 to 6 and generator runs with 1000 rpm and delivers partial load (1 kW). As the velocity goes down below cut_out, the braking system works and the speed goes slowly down. The third graph shows the torque production from wind turbine.

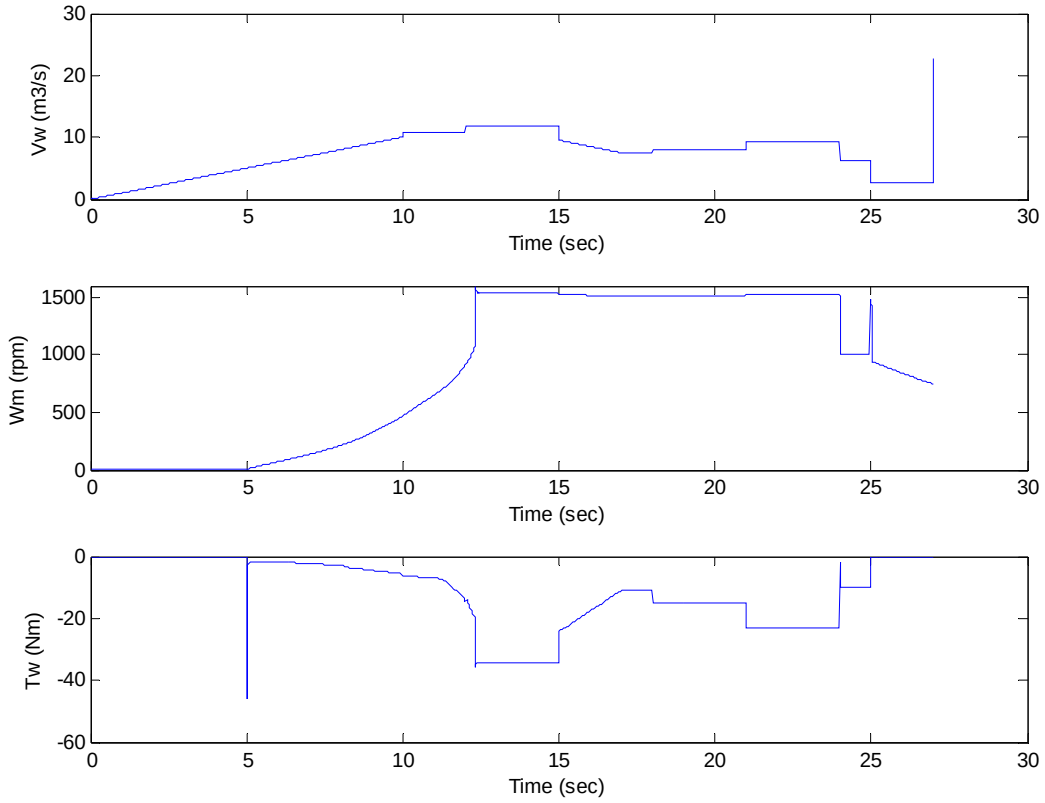

Fig. 4.30: The behaviour of the wind turbine in different wind velocity

4.3.3.2 The generator status

Fig 4.31 shows the generator status. The first graph shows the current delivered by the generator. As the grid circuit breaker is connected, initially the asynchronous generator draws heavy current around 5-6 times of the nominal current for few milliseconds. After that, it delivers the full load current of 10.5 A. The current production varies as per the wind velocity.

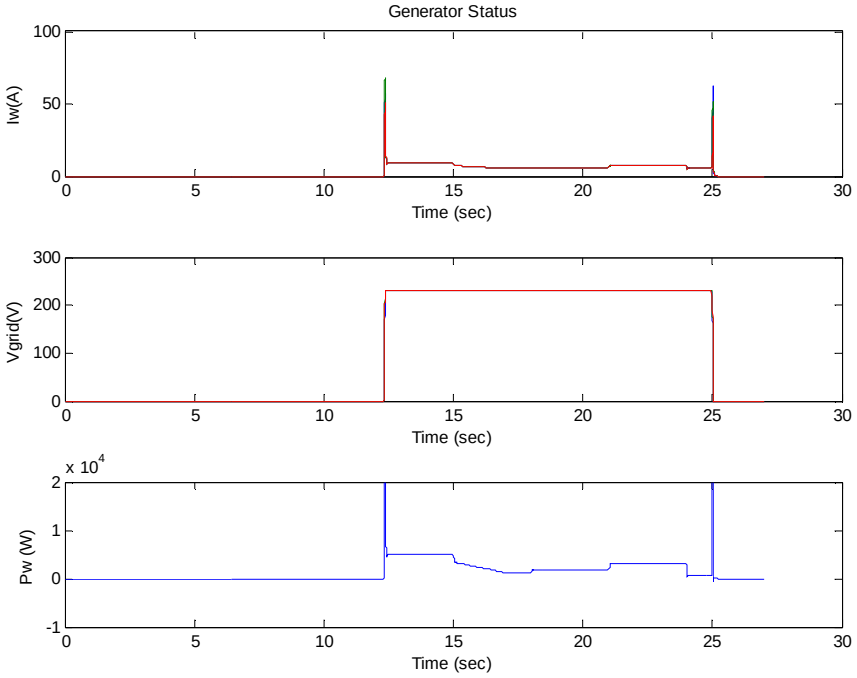

Fig. 4.31: RMS values of current, voltage and power

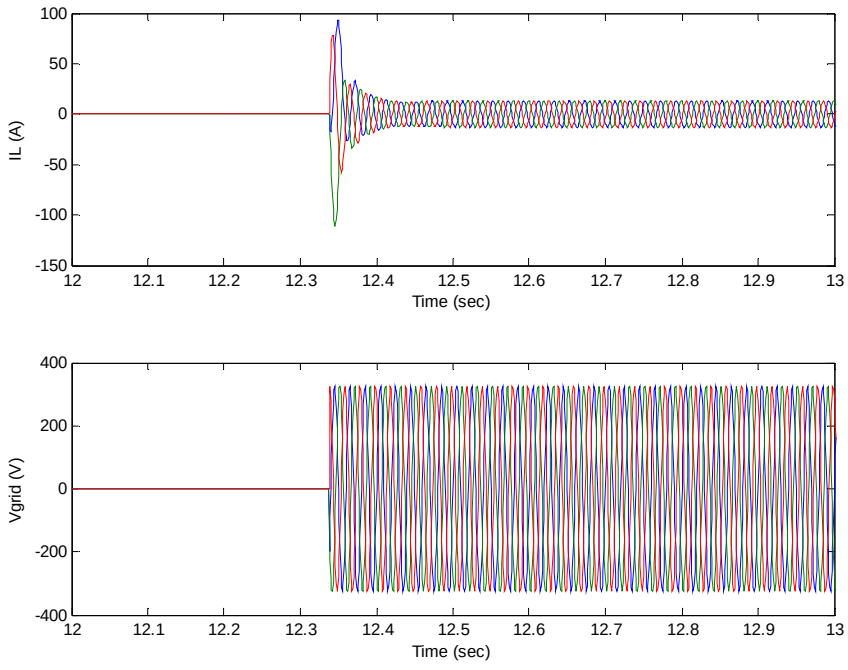

Fig. 4.32: The three phase sinusoidal current and voltage in close form

change in the velocity. At 25 sec, the generator is disconnected due to the low velocity. The second graph shows the voltage pattern of the generator. The third graph shows the power production from WTG. Fig 4.32 shows the transient behaviour of the asynchronous generator in sinusoidal form during the connection to the grid.

4.4 Battery System

Battery is a device, which is widely used in almost all electrical systems, where the energy supply or storage is required. It is an electrochemical device. It means the form of energy changes from electrical to chemical and vice versa. Energy can be stored or consumed from the battery. The concept of electrical energy supply system is changing towards a decentralised system. The decentralised system is possible through HPSs. HPSs consist of different energy sources and supply energy to an isolated load. In HPSs, the battery plays very important role, in other words it is the heart of the system. For example the operating voltage of PV module is determined by the battery voltage, turn off/on of diesel genset is determined by the battery soc/voltage. That's why a battery model that is to be used in such a system must be formulated in such a way that it governs non-linear, complex behaviour. Different types of the battery modelling have been approached. The complexity in the battery model depends upon the field where it should be implemented.

4.4.1 Equivalent Circuit

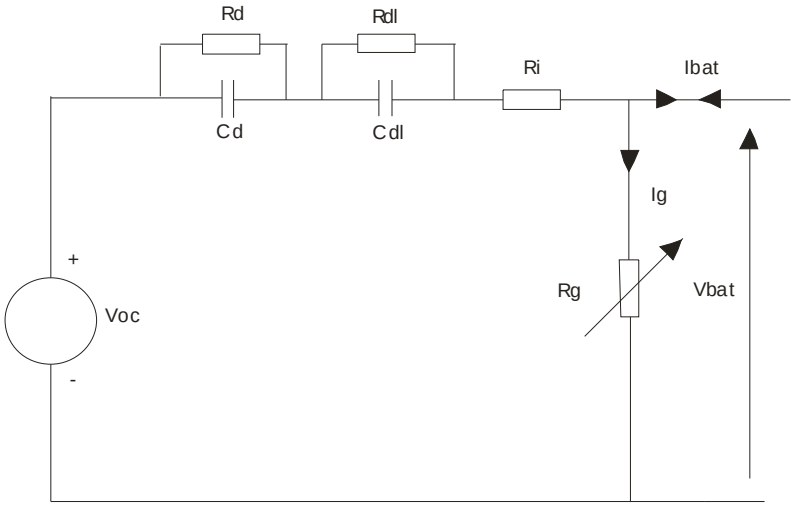

Fig. 4.33: Equivalent circuit diagram of the battery model

Where

V_{oc} Open circuit (internal) voltage
R_i Internal resistance
C_{dl} Double layer capacitance
R_{dl} Double layer resistance
I_{bat} Battery current
C_d Diffusion capacitance
R_d Diffusion resistance
R_g Gassing resistance
V_{bat} Battery voltage

When a battery is charged or discharged, the current flows through the internal resistance and capacitors. It causes the ohmic drop and generates heat. At the same time, the electrolyte is polarised and causes the voltage drop, which is known as an overvoltage. As a result, the battery voltage will be different from its equilibrium voltage. This difference is called a polarisation. Mathematically polarisation is sum of two parts

Polarisation = overvoltage + ohmic voltage drop

The equivalent circuit of a battery cell is shown in fig. 4.33 [13], [26].

4.4.1.1 Internal Resistance (R_i)

The internal resistance of a battery depends upon SOC. It remains nearly constant up to 90% of SOC after that it increases exponentially. It is an important parameter because as this parameter will be higher, during charging or discharging process, the ohmic drop will be more or losses will be more. The charging and discharging behaviour of the battery is not same because the internal resistance of the chemical substances are not same. It is also not an ohmic resistance so its value depends on the applied method.

4.4.1.2 Double layer capacitance (C_{dl})

Electrical double-layer capacitors are based on an operating principle of the electric double-layer that is formed at the interface between activated metallic surfaces (electrodes) and an electrolyte. The principle behind the capacitor is shown in fig 4.34. The electrodes are used in the solid form, and the electrolyte is in liquid form. When these materials come in contact with each other, positive and negative poles are distributed relative to each other over an extremely short distance. Such a phenomenon is known as an electrical double-layer. When an external electric field is applied, the electrical double-layer is formed in the vicinity of the electrolyte surface and the electrolyte fluid surface.

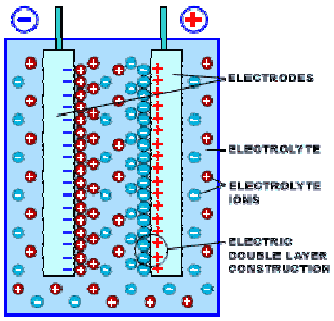

Fig. 4.34: General phenomenon of a double layer capacitance

The physical behaviour of a double layer capacitance can be more precisely cascaded RC network. Such a complicated structure is required only to model electrochemical capacitors.

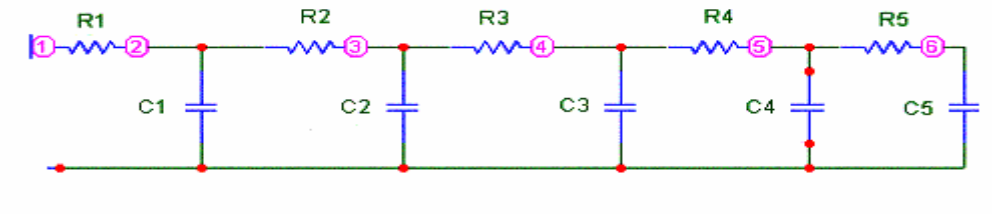

Fig. 4.35: Schematic diagram of a double layer capacitance

A single capacitance and resistance model of an electrochemical capacitor can be used in many applications like battery modelling. For the targeted battery also a parallel RC circuit has been used. During a charging process, the double layer capacitance also charges exponentially. The time constant of RC circuit depends upon the surface area of the electrode, type of electrode, electrolyte etc. The voltage across this capacitor also contributes on the terminal voltage of the battery. The voltage across the double layer capacitor also discharges during discharging process. The time constant, which is proportional to the capacity of the battery, lies in the range of ms. In this model, the parameters R and C can be changed as per requirement.

4.4.1.3 Diffusion Capacitance (C_d)

The diffusion process can be defined as the movement of chemical species (ions or molecules) under the influence of concentration difference. The species will move from the high concentration area to the low concentration area till the concentration is uniform in the whole phase. Diffusion in solutions is the most important phenomenon in electrochemistry, but diffusion will occur also in gases and solids. The rate of diffusion (diffusional flux) is proportional to the gradient of the concentration in the solution, with the proportionality constant called the "diffusion coefficient."

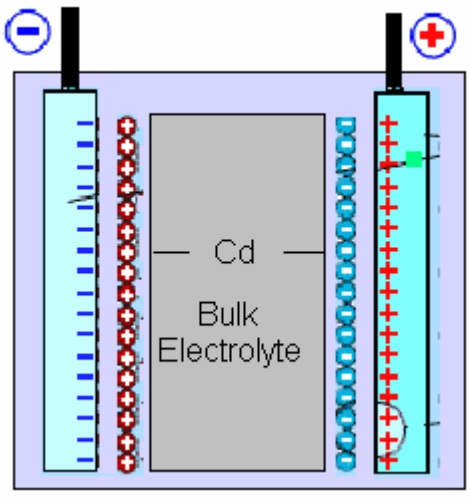

Fig. 4.36: Diffusion capacitance in the battery

In the case of the battery, the electrolyte solution can be divided into three distinct parts: the bulk solution and the two diffusion layers at the surface of the electrodes as shown in fig 4.36. The concentration of the bulk solution can be assumed as uniform. The species transport in this layer occurs only through convection, while the mass

transport in the diffusion layer is possible only through diffusion. The two diffusion layers carry opposite charges (negative and positive). The bulk electrolyte behaves like as dielectric. It means the combination of three layers produce capacitance effect that is known as diffusion capacitance. The time constant of the RC circuit due to the diffusion capacitance is much larger as compare to the double layer capacitance. It is in a range of hours.

4.4.2 Gas effect

During an energy conversion process in the battery, not only the main reaction takes place but side reactions also. If the battery is charged faster than its nominal charge rate, the battery is heated more in consequences hydrogen and oxygen gases are produced in the positive and negative plates respectively [14]. The cause of the gassing is that when the battery is charged faster, the energy conversion process can not be faster than its capacity so side reactions take place. The gassing phenomenon occurs even though the battery is charged by nominal rate. When the terminal voltage of the battery crosses the onset voltage (also known as gassing voltage) the gassing process starts inside the battery. In electrical term, gassing phenomenon can be represented by the current known as the gassing current. As shown in fig 4.37 when the battery is charged, the internal voltage increases correspondingly and the terminal voltage too. The onset voltage can be compared to the forward bias voltage of a diode. If the voltage across the diode crosses this value, the gas current flows through the R_g. With respect to the time, the gas resistance decreases exponentially and the gas current increases exponentially. This means the main reaction current (I_{mr}), which converts the electrical energy to the chemical energy, decreases correspondingly. Finally complete charging current becomes the gassing current. In this stage, further increment in the internal voltage is not possible.

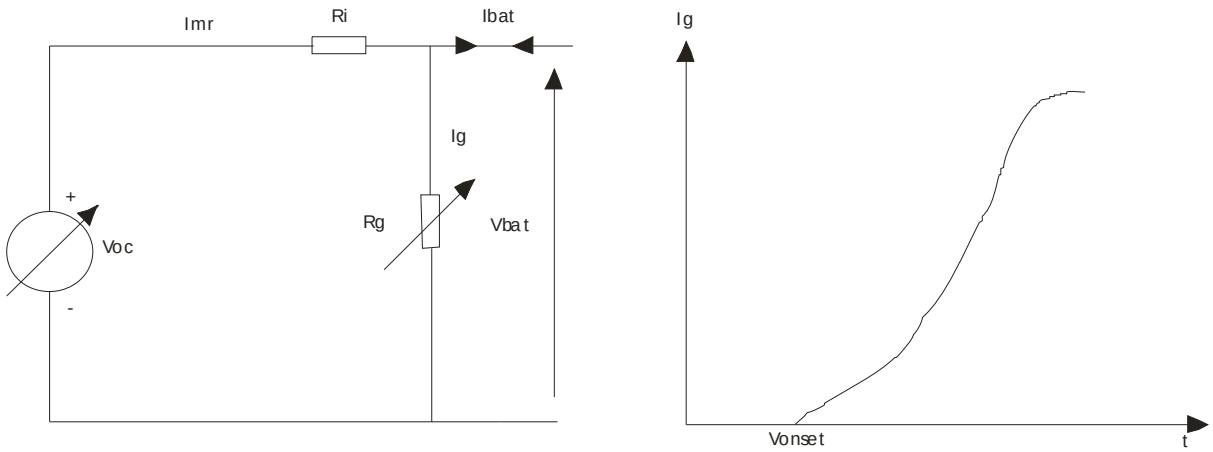

Fig. 4.37: A schematic diagram of the gassing effect in the battery

4.4.3 Different approaches for the battery modelling

Simple model as a storage device: In such a model, the battery is treated only as an energy storage device with certain efficiency. Such model may be sufficient for many applications, but it has many disadvantages. Many terms of the battery, which are

critical for combined functionality, are not taken in account. States of charge, terminal voltage, gas evolution, water losses etc are not considered. These terms are critical to charge, discharge or disconnection of the battery. The only advantage is that the model is simple. For a power balance analysis, such model may be useful.

In the second approach the battery terminal voltage is determined on the base of the battery current (which may be positive or negative) or on the state of charge. This approach is more complex as compared to the first one. The battery is treated as a resistance that varies with SOC of the battery. The changing behaviour of the resistance is different during charging and discharging process. It is due to the fact that different chemical reactions. The variation in the resistance depends upon type and the capacity of the battery. Such model is possible to use in HPSs up to some level because the terms, which are important for the combined functionality, are determined. But such model has its one limit. It treats the battery as a homogenous physical device; while in reality the battery behaviour is non-linear due to many side reactions like electrolyte stratification and ageing.

The Shepherd model is perhaps the best known and most often used battery model. The model describes the electrochemical behaviour of the battery directly in terms of voltage and current. It is often used in conjunction with the Peukert equation to obtain the battery voltage and state of charge. The terminal voltage of the battery is calculated as follows [15]

$$E_t = E_o - R_i * I - K_i \frac{Q}{(Q - f)} \qquad (4.40).$$

Where

- E_t = battery terminal voltage [volts]
- E_o = open circuit voltage of a battery cell when fully charged [volts]
- R_i = internal (ohmic) resistance of the battery [ohms]
- K_i = polarization resistance [Ohms]
- Q = battery capacity [ampere-hour]
- I = instantaneous current [amps]
- f = integral of I*dTIME/Qo = accumulated ampere-hours divided by full battery capacity.

The fractional state of a charge is then found via Peukert equation. It states a relationship between the discharge current and the ,constant current, discharge time. It says the possible discharging time decreases with increasing discharging current. The expression is given by [16]

$$I^n * T_i = Cons\tan t \qquad (4.41)$$

Where

- I = discharge current [amp]
- n = battery constant (n=1.35 for typical lead-acid batteries)
- T_i = time to discharge at current I [seconds]

The advantage of this model is its simplicity and it consists of not many equations. The disadvantage is that it does not consider other parameters, which play also important role during the battery operation. For example, the variation in internal resistance with respect to SOC has not been considered.

4.4.4 Battery model

To simulate, test, verify and implement a HPS, still a more complicated model is required which takes into account of complex parameters inside the battery. In this study, a complex mathematical model is developed which is going to be interfaced into real HPS. A critical sensitive output of the battery is the terminal voltage which has a great influence on the complete control phenomena in terms of connection and disconnection of the energy sources and the loads.To predict the best possible voltage from the battery model, all the parameters and phenomena, which affect the terminal voltage, are to be considered. Such parameters are like a diffusion capacitance, a double capacitance, the gassing effect, and the internal resistance.

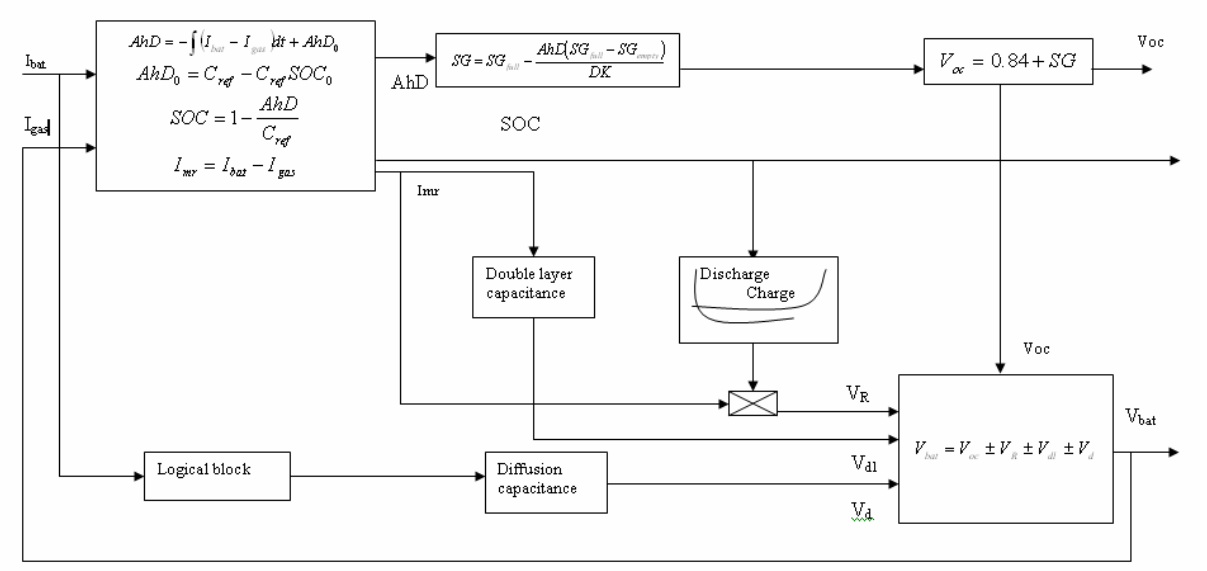

Fig. 4.38: A general block diagram of the battery model

The developed model is the universal one in a sense that it could be used for any type and capacity of a battery. The only important thing to keep in mind is the parameter suitability.

4.4.5 Model description

The relation between the voltage and the current during an operation phase of a battery can be described using the available mathematical relations and some curve fitting techniques. To describe the voltage as much as possible close to the real battery, a previously explained important phenomenon, which occurs in the battery, is to be considered. Based on requirements of this model, the model has been developed using Simulink and Simpower block sets available in Matlab software. The first look of the model is shown in fig 4.39.

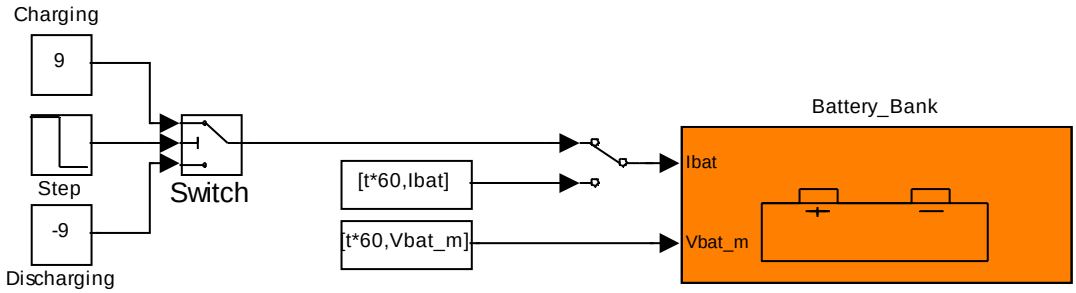

Fig. 4.39: the battery model developed in Simulink

The sub block in the main battery model is shown in fig 4.40 and each block will be explained with the parameter, their functions, possible values and effects on the complete battery behaviour.

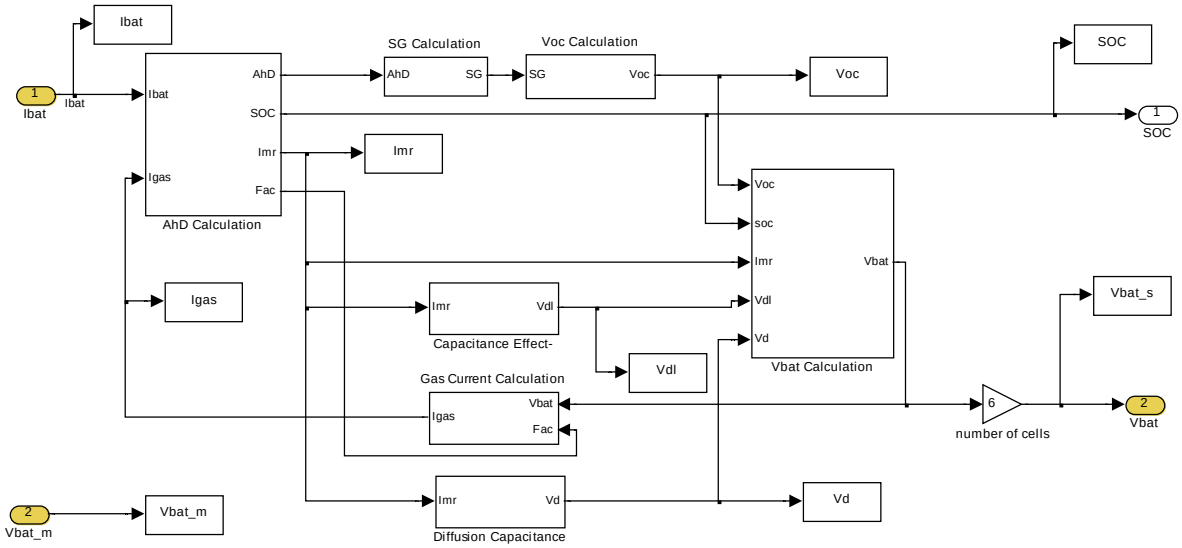

Fig. 4.40: The inside view of the battery model developed in Simulink

Following blocks are available inside the battery model.

AhD, SOC calculation block
SG Calculation block
Double layer capacitance block

Gassing current block
Diffusion capacitance block
Internal resistance and terminal voltage block

4.4.5.1 AhD, SOC calculation block

SOC of a battery is very important parameter because the internal resistance as well as the internal voltage of the battery depend on it. The determination of SOC must be accurate as much as possible. SOC of the battery can be defined as a ratio of the ampere-hour remaining in the battery to the total ampere-hour of the battery.

$$SOC = \frac{AhR}{Ah_{nom}} \qquad (4.42)$$

$AhR=Ah_{nom}-AhD$

Where Ah_{nom} is total capacity of the battery and AhR is Ah remaining in the battery. Further more it can be calculated as

$$AhR=Ah_{nom}-AhD \qquad (4.43)$$

Where, AhD is the number of Ah that would have to be discharged from fully charged battery to bring it to its current state. Finally in this model SOC is calculated by as follows

$$SOC = 1 - \frac{AhD}{Ah_{nom}} \qquad (4.44)$$

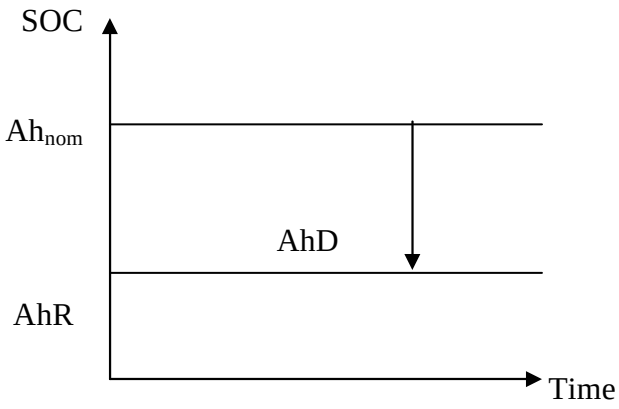

Fig. 4.41: Different terms of battery Ah

So in this model AhD is calculated as follows [14] [17]

$$AhD = -\int I_{mr}\left(I_{bat} - I_{gas}\right)dt + AhD_0 \qquad (4.45)$$

$$I_{mr} = I_{bat} - I_{gas} \tag{4.46}$$

In the above equation, important parameters are $I_{mr,}$ I_{bat}, I_{gas} and AhD_0.
where

I_{mr}	It is the main reaction current, which converts electrical energy into chemical energy.
I_{bat}	It is the battery current in Ampere. This current may be positive or negative. If the battery is charged, it is positive and if battery is discharged, it is negative.
I_{gas}	It is the gassing current of the battery, which flows due to the gassing phenomenon. The gassing current flows only during the charging process. Its maximum value can be equal to I_{bat}.
AhD_0	It is AhD at the beginning of the simulation.

It is calculated as follows [14]

$$AhD_0 = Ah_{nom} - Ah_{nom} SOC_0 \tag{4.47}$$

The parameters Ah_{nom} and SOC_0 should be given during simulation time as per requirement. Based on the above mathematical expressions, the Simulink block is created and shown in fig 4.42.

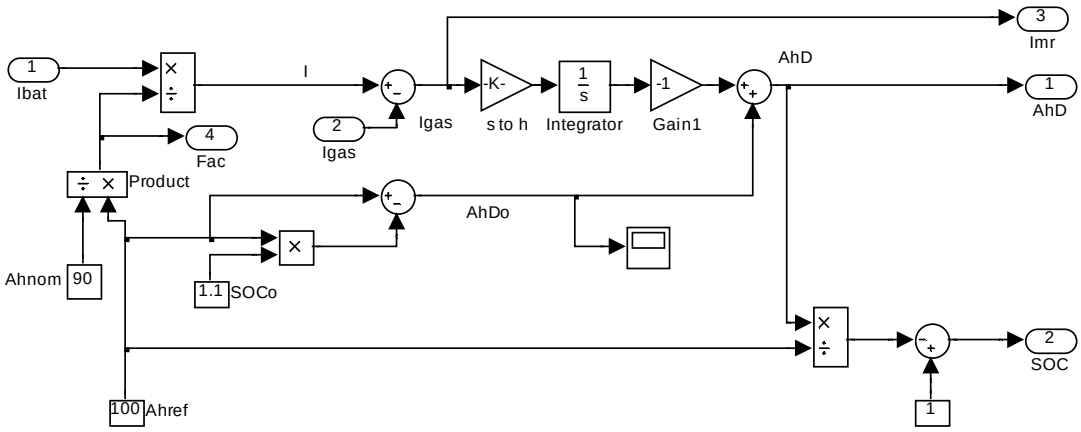

Fig. 4.42: The inside view of AhD and SOC calculation

In the above block, the battery current I_{bat} should be normalised as per the reference battery capacity by dividing through the normalisation factor. In this model, the capacity of the reference battery is taken as targeted battery. The gas current is subtracted from the battery current to get the main reaction current. The first gain factor is to match the simulation time in sec. The output of the integrator is added with AhD_0 to get final AhD. Using this AhD, SOC is calculated. As per requirement, the capacity of the battery and the reference battery can be changed.

4.4.5.2 SG (Specific Gravity) calculation block

The internal voltage (V_{oc}) of a battery depends upon the specific gravity of an electrolyte. It is necessary to determine SG from the parameters available from the previous block. The SG of the electrolyte is a reflection of SOC. As SOC increases, V_{oc} increases and vice versa. In other term, the SG of the electrolyte can be interconnected with AhD by the following equation [17].

$$SG = SG_{full} - \frac{AhD\left(SG_{full} - SG_{empty}\right)}{DK} \tag{4.48}$$

Where

SG_{full}	It is the specific gravity of the electrolyte when the battery is fully charged. This value can be found from manufacturer data sheet. Its value lies between 1.24 to1.28 g/cm^3 .
SG_{empty}	It is the specific gravity of the electrolyte when the battery is completely discharged. This value can be found from manufacturer data sheet. Its value lies between 1.0 to 1.1 g/cm^3.
DK	It is a fit parameter corresponding to the discharge capacity of the reference cell at an infinitesimal discharge current (i.e. the capacity of an active material in the cell) in Ah.

The most important term in the battery model is the calculation of the internal voltage. From previous blocks the required parameters are determined to calculate Voc. A mathematical formulation is as follows [13]

$$V_{oc} = 0.84 + \left(SG\right) \tag{4.49}$$

From this equation, it is clear that V_{oc} depends upon SG of the electrolyte.

4.4.5.3 Gassing current block

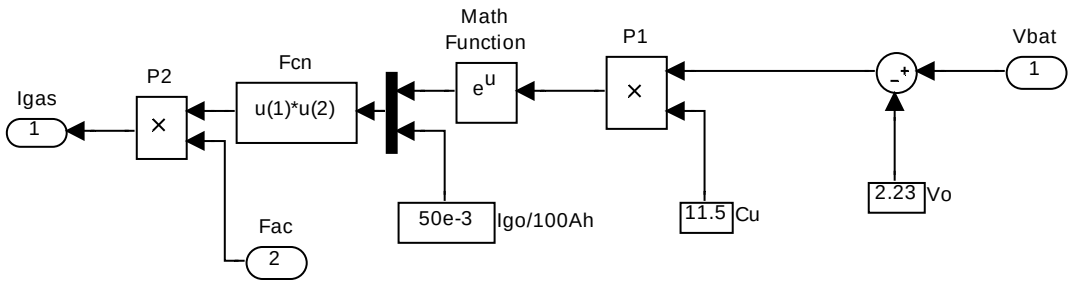

Fig. 4.43: The inside view of the gassing current calculation block

The mathematical expression of the gassing current is given below [14]

$$I_{gas} = I_{go} - \exp(C_u * (V_{bat} - 2.23)) \tag{4.50}$$

where I_{go} is the gassing current at the no load condition and C_u is the voltage dependent constant. The value of I_{go} can be taken around 30 to 70mA/100Ah. Correspondingly, the value of C_u lies between 11-12/V [3].

These values are around approximation. For this model, these two parameters have been chosen in such a way that the simulation model gives satisfactory results.

4.4.5.4 Double layer capacitance block

This block has been formulated using components from Simpower package. The output from this block has been interfaced with the Simulink blocks.

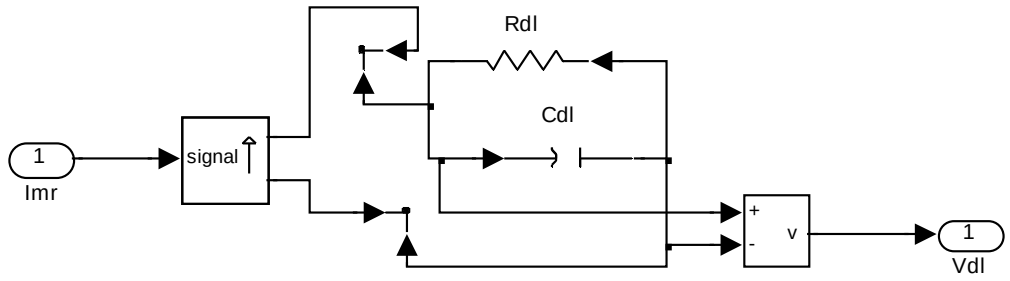

Fig. 4.44: The inside view of double layer capacitance block

In this block, I_{mr} is fed as an input and the voltage across the double layer capacitor is taken as an output. The values of the RC component is chosen in such a way that the time constant lies within the ms range.

4.4.5.5 Diffusion Capacitance block

With the help of this block, it has been tried to bring the effect of the diffusion capacitance inside the battery model. This block is also prepared from Simpower tools. The difference from previous block is that the time constant of RC component is much higher in the range of hours.

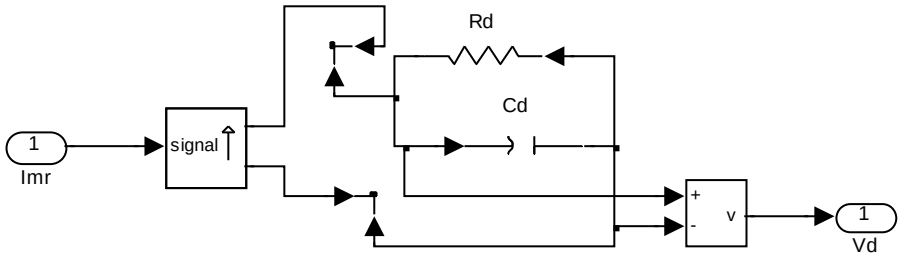

Fig. 4.45: Inside view of diffusion capacitance block

The modelling of diffusion capacitance is done similar to that of the double layer capacitance.

4.4.5.6 Internal resistance and terminal voltage block

The internal resistance during the charging and the discharging process is a function of SOC, type of electrolyte and the electrodes. The main factor for determining R_i is the SOC. In this block, two look up tables are separately used for the charging and the discharging process. In this block, the main reaction current is fed as input. Two dead zone blocks are used to identify the current whether charging or discharging. It is important to use exact look up table. For the look up tables which receive SOC as the input and provide R_i as the output in milliohm. The milliohm resistance is converted to ohm to calculate the voltage drop across it. Now all the voltage drops are added to V_{oc} to determine the terminal voltage of the battery.

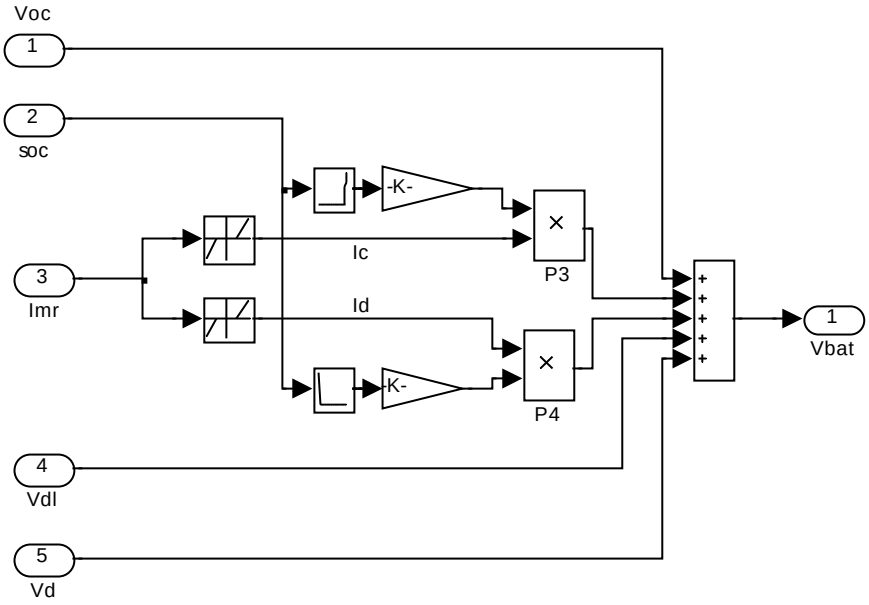

Fig. 4.46: The inside view of terminal voltage calculation block

4.4.6 Experiments

4.4.6.1 General Test

The model is first simulated with the full load charging and discharging current to analyse the general charging and discharging behaviour of the model. The nominal charging and discharging current of the battery is 9 A. This means the battery should be charged or discharged for 10 hours from SOC = 0 to SOC = 1 respectively. The initial value of SOC_0 is to 0.2 and simulation time is set to 3600*17 sec (17 hours). The battery is charged up to 12 hours and after that the battery is discharged using a switch. The important parameters of the battery model are captured and shown in fig 5.15.

The first graph shows the SOC of the battery. As the simulation is started, the SOC increases from SOC_0 with a constant slope because the charging current of 9 A is maintained through out the charging process. At the time of $3.6*10^4$ sec (10 hours), the

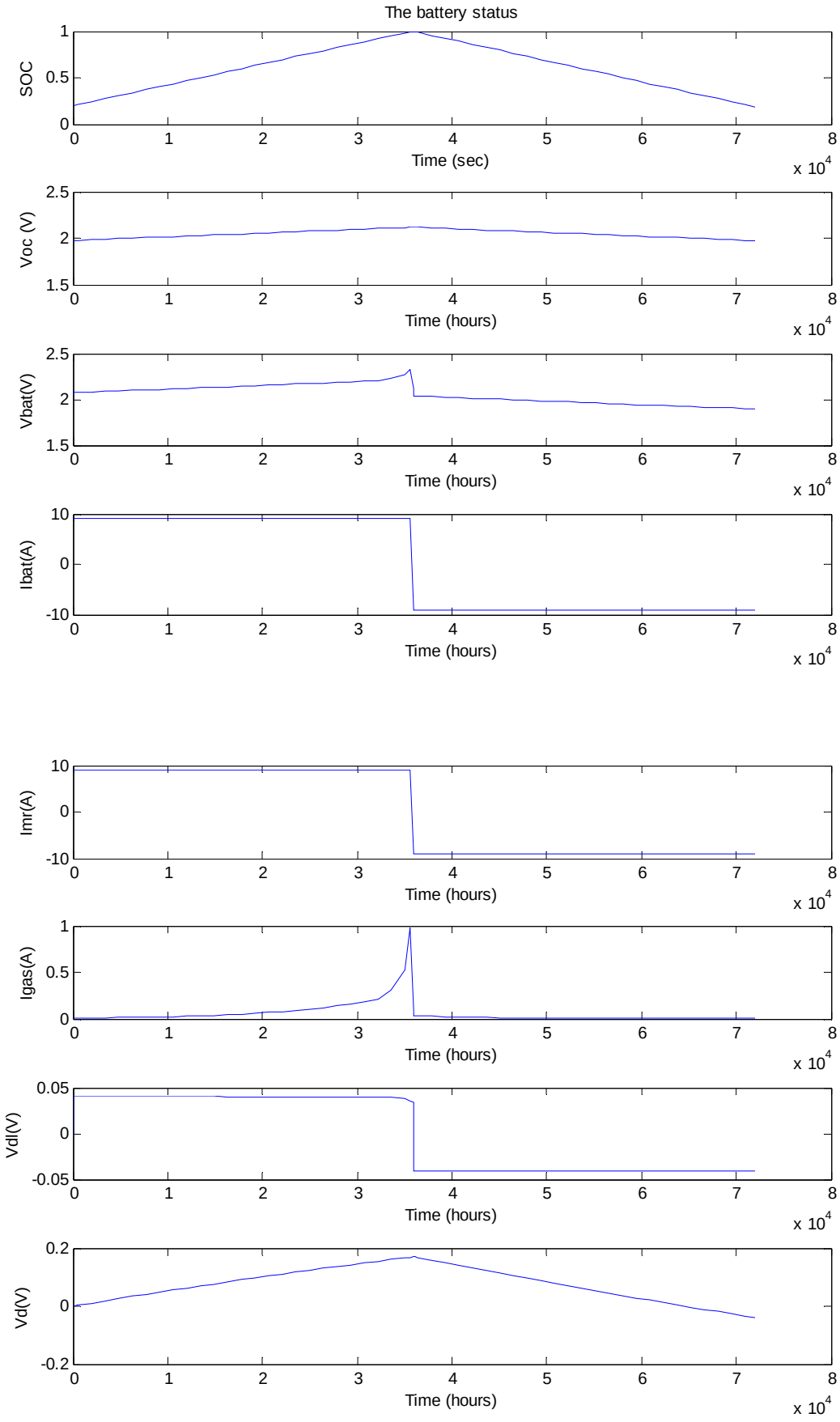

Fig. 4.47: General performance of the battery model

battery is fully charged or SOC becomes 1. After that the polarity of the battery current is changed from + to – and the battery is discharged. The SOC starts to decrease with a constant slope. The second graph shows the behaviour of the internal voltage. It is a function of the SOC so the pattern is similar to it. The third graph shows the terminal voltage of the battery. As mentioned above, it is a contribution from overvoltages and the voltage across the internal resistance. It can be observed that the terminal voltage increases suddenly from the initial no load voltage of 2.0 to 2.1 volt; it is due to a contribution from the double layer capacitance, which has a very less time constant. After that its value increases with the constant slope. As SOC reaches around 90%, the internal resistance (charging) increases so correspondingly the resistance drop increases. It causes the sharp bending in the voltage curve from 90 to 100% of SOC. As the polarity of the current is changed, V_{bat} goes down suddenly because the positive resistance drop becomes negative and also the overvoltage becomes zero. Due to the diffusion process, V_{bat} decreases slowly with a constant discharging current. This curve shows that the behaviour of the developed model is close to the real battery.

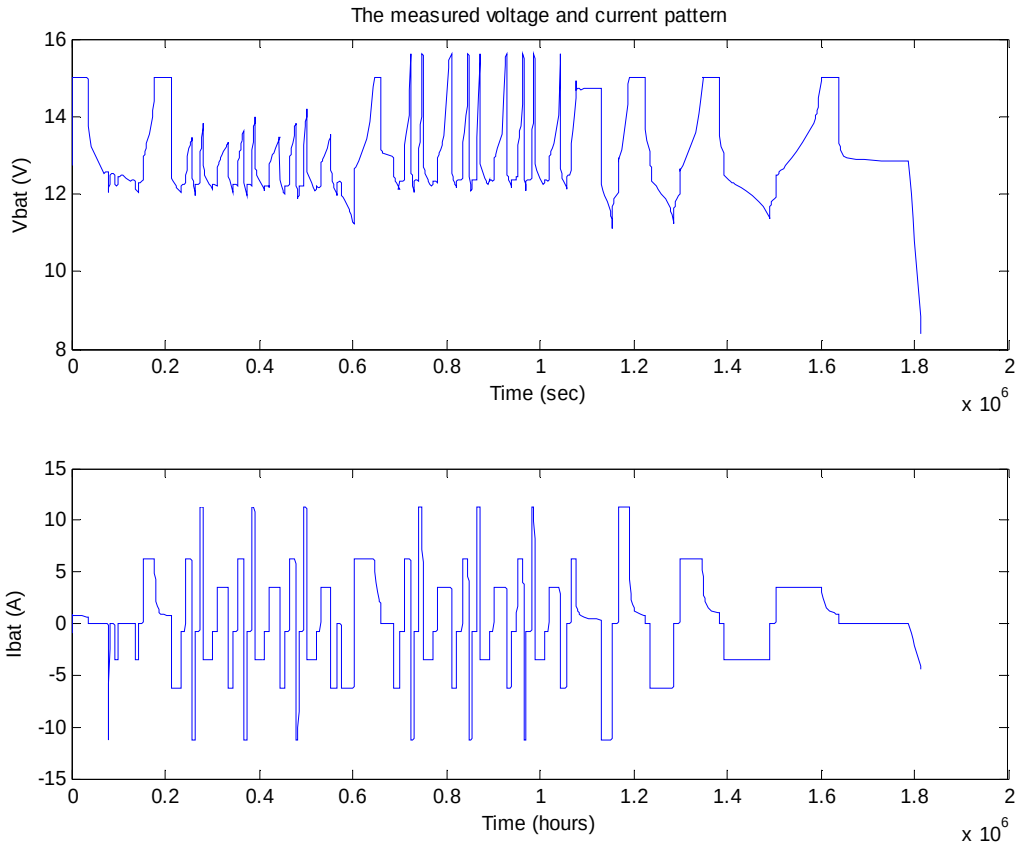

Fig. 4.48*: The measured current and voltage pattern*

The fourth graph shows the input current pattern applied to the battery model. Using the automatic switch, the polarity of the current is changed.

The fifth and sixth curves show the I_{mr} and I_{gas} patterns. Up to the point, when V_{bat} is lower than its onset voltage, I_{mr} is nearly equal to the charging current or I_{gas} is very low. As SOC increases from 90 %, V_{bat} increases rapidly so the gassing increases rapidly and I_{mr} decreases correspondingly. During the discharging period, there is no

gassing effect. The seventh graph shows that the overvoltage due to the double layer capacitance. It can be observed that it is the function of RC parameters and I_{mr}. Due to lower time constant, the charging and discharging behaviour vary in a range of ms. During the constant charging current, this voltage also remains constant. As gassing starts, the overvoltage decreases correspondingly. The eighth graph shows the overvoltage due to the diffusion capacitance. Due to the very high time constant, the voltage change during charging and discharging process is very slow.

4.5 Diesel Generator set

A Diesel genset consisting of an engine connected with a generator produces electrical power by consuming the fossil fuel. The engine (Otto or diesel) and the generator (synchronous, asynchronous) used in the genset may have different type of characters. In this chapter some technical characteristics of the diesel genset and its mathematical model are presented.

Fig 4.49 shows a cylinder of a diesel engine. The process of generation of mechanical power by combusting the fuel is a complex process. This process is not a relevant and important topic for this work. The most important subject is the fuel system and consumption during the diesel genset operation.

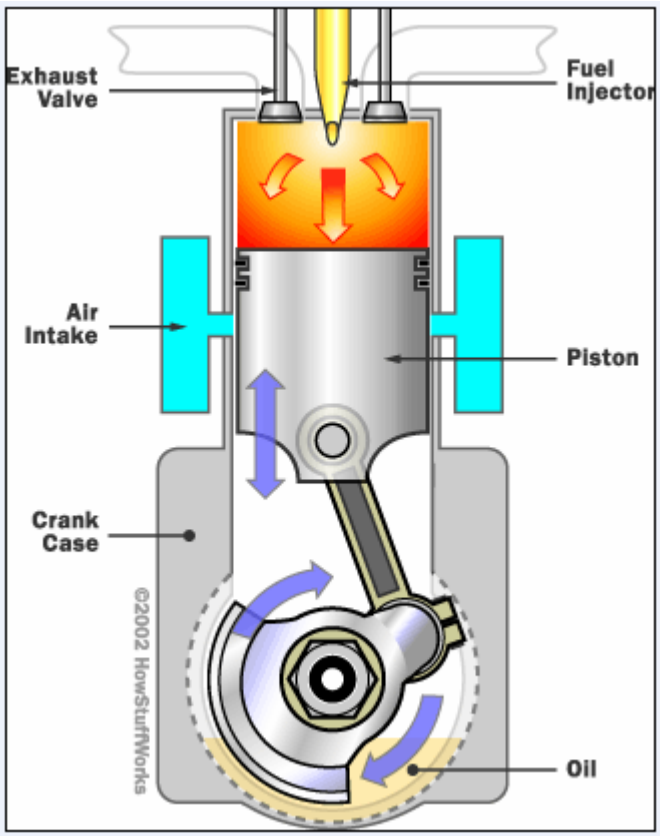

Fig. 4.49: The inside view of a cylinder of a diesel

The most important parts of the diesel engine are

1. Fuel injector
2. Exhaust Valve

3. Air Intake
4. Piston
5. Crankcase
6. Oil

4.5.1 Fuel System

The fuel stored inside the fuel tank is supplied to the engine through the fuel injector, which is kept just above the cylinder. The principles and functions of the fuel systems are complex and their details are classified as top secret of the manufactures. For simplification, it is assumed that the fuel injector consists of a nozzle, which makes to and fro motion inside the inlet valve. The amount of fuel injecting inside the cylinder is a function of the opening of inlet valve respectively the movement of the nozzle. The important parameter to control the amount of fuel is the air-fuel mixture ratio parameter . The is maintained at 1 (or >1) in stochiometic combustion i.e. the mixture with minimum air supply that theoretically could lead to complete combustion. It is easily achieved in diesel engines because as compared to petrol engines, there is no throttle valve control system. This means that there is always sufficient amount of air available to make the complete combustion.
On the other hand, the fuel consumption of the diesel engine normally depends upon the load, construction and machine type. The fuel efficiency drastically decreases in partial load and above 90% load the diesel genset delivers the best efficiency. Its efficiency varies from 20 to 37%. So, it is always recommended by the manufacturer to load the genset fully. The fuel efficiency of the diesel genset is expressed as follows [14]:

$$_{D} = \frac{P_d}{Q_{LV} m_f} \qquad (4.51)$$

Where
P_d = Power generated by the diesel genset (kW)
H_g = the rate of fuel consumption (l/hr)
Q_{LV} = the low heat value of the fuel (kWh/l)

The fuel consumed by the diesel genset can be calculated based on an empirical formula provided by a diesel genset manufacturer [18].

For 10 kW diesel genset and 10 kW load

m_{f_load} = 10 kW * 1/3 l/kWh = 3.33 l/h

m_{f_noload} = 0.15 * 10 kW * 1/3 l/kWh = 0.45 l/h

Total fuel consumption, m_f = $m_{f\_load} + m_{f\_noload}$
= 3.33 l/h + 0.45 l/h
= 3.75 l/h

Similarly,
For 10 kW diesel genset and 2 kW load

m_{f_load} = 2 kW * 1/3 l/kWh = 0.66 l/h
m_{f_noload} = 0.15 * 10 kW * 1/3 l/kWh = 0.5 l/h
Total fuel consumption, mf = m_{f_load} + m_{f_noload}
= 0.66 l/h + 0.5 l/h
= 1.32 l/h

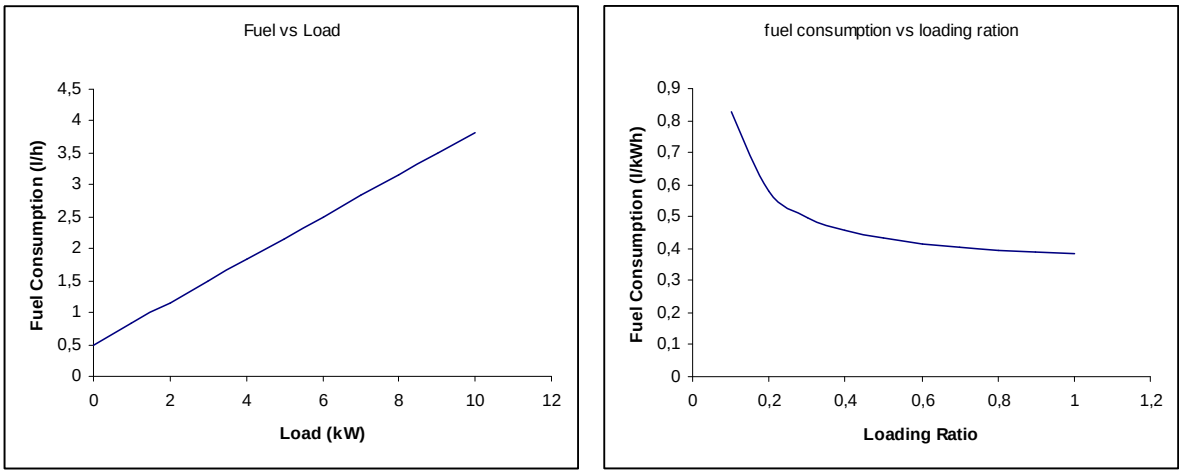

Fig. 4.50: Relation between fuel consumption and loading ratio

The above mentioned two examples show that the diesel genset consumes 35 % of full load fuel consumption when the machine is loaded at 20%. At no load condition, it consumes around 15% of full load fuel consumption [18]. Based upon above formula, the fuel consumption verses the load and loading ratio are plotted and shown in fig. 4.50. Second graph clearly indicates that the fuel consumption per kWh reduces as the loading ratio increases.

4.5.2 Auto-start

Most of the diesel gensets available in market consist of auto-start function. An auto-start function works with an electric-starting system. The electric-starting system consists of a battery, a cranking motor with a solenoid switch, a master switch and complementary cables as shown in fig. 4.51.

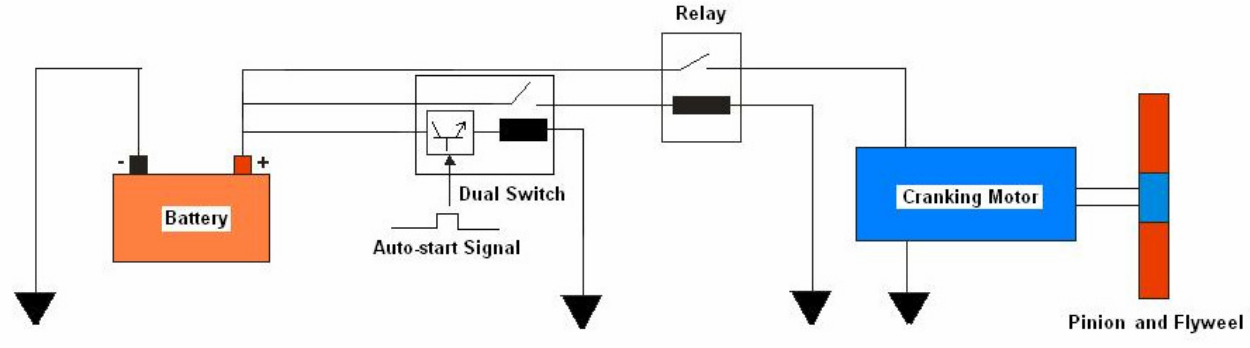

Fig. 4.51: The auto-start circuit of a diesel engine

As the auto-start signal goes high, the cranking motor receives direct current from the battery and converts it to mechanical energy (rotary motion). The mechanical energy is

transmitted from the armature in the cranking motor to the pinion and onto the flywheel ring gear, causing the crankshaft to rotate. Once the piston is pushed toward TDC, the fuel is injected. After 1-2 cycles the engine starts and the cranking motor is disconnected.

4.5.3 Frequency and voltage control concept

In small diesel gensets (<= 10 kW), mostly mechanical governors are used to control the speed of the diesel engine and correspondingly frequency of the generator. The speed control may be an isochronous or a variable speed mode. In the case of the isochronous, the speed of the diesel genset is maintained constant at no to full load variation. Another possibility is the variable speed. This means the diesel genset can be operated in different speed ranges for example 1800 rpm for 60 Hz and 1500 rpm for 50 Hz. In the case of the variable speed operation, the speed droop concept is applied. The deviation in the frequency may be up to 5%. Another possibility is an electronic speed controller, which is more expensive and more accurate. The accuracy band lies within 0.3 Hz [19].
The terminal voltage of the diesel genset is controlled by different control concepts. In a diesel genset with a synchronous generator, mostly an automatic voltage regulator (AVR) has been used. In such genset only the speed is controlled. The electronic voltage controller is a very fast and accurate. In the diesel gensets with asynchronous generators, the voltage is controlled by variable capacitors. Mostly no voltage controller is used in such gensets. Manufactures mention the voltage deviation band from no load to full load. In market, the decoupled system is also available. This means the diesel genset is decoupled from the grid which makes it possible to operate the isolated grid in preferred voltage and frequency band.
Permanent magnet [PM] generators are also available in market. The PM generators are expensive but due to high efficiency they are used by some manufactures. In the PM generators, there is no possibility to control the voltage by direct means as in electrically excited generators so the possibility is to use cylco-converters or inverters.
For the HPS, which will be investigated later using the Matlab/Simulink software, the diesel genset consisting of an asynchronous machine is used because an isolated grid is formed by the MHPP.

4.5.4 The model of diesel genset connected into the grid

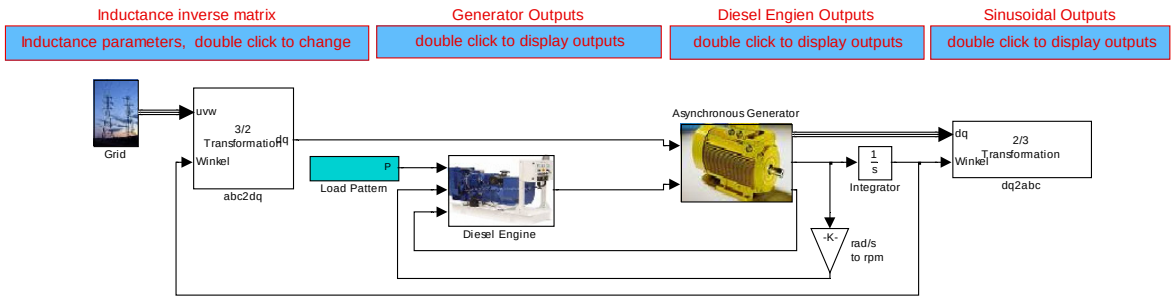

Fig. 4.52: The model of asynchronous generator rigidly connected to the grid

The overall model of a diesel genset consisting of an asynchronous generator as mechanical to electrical power converter is shown in fig 6.4. This model consists of a diesel engine, an asynchronous generator, 3 to 2 and 2 to 3 phase transformation blocks, load pattern block and the grid. The generator terminals are connected to the available grid system. As the genset is connected, initially machine runs as a motor and as the machine achieves negative slip, the machine works as the generator. By setting the reference power at load pattern, the power generation from the genset can be controlled. As per reference value, the mechanical governor adjusts the fuel flow so that the required mechanical torque is produced. The model can be investigated as the motor or the generator. Simply negative torque as input to the machine makes it the generator. The torque produced by the diesel engine is given by equation 4.52 [20]:

$$T_d = \frac{H_g h_{it}}{4}\left(\frac{C_f m_f}{ne}\right)\frac{V_e}{4} P_{fme} \qquad (4.52)$$

Where

T_d = engine torque (Nm)
H_g = gross heating value of the fuel (kJ/kg)
h_{it} = indicated thermal efficiency
C_f = units conversion factor
m_f = fuel consumption rate (kg/h)
n_e = engine speed (rpm)
V_e = engine displacement (L)
P_{fme} = friction mean effective pressure (kPa)

The fuel consumption can be converted from kg/h to l/h by multiplying it with the factor 1.117 (0.850 kg/L). The targeted diesel engine can get up to 6 l/h fuel which is around 20% more than its nominal capacity. It means the diesel genset can be overloaded by 20%. The mathematical equations of the asynchronous generator have been explained in the wind turbine section.

4.5.5 Experiments

4.5.5.1 No Load Test

This test is carried out to analyse the no load behaviour of the diesel genset. In fig 4.53 the first graph shows the reference power. The second graph shows the power produced by the generator. As the switch is closed, initially the machine works as motor (positive slip) and draws very high initial starting (inrush) power. The third graph shows the grid voltage or terminal voltage. The fourth graph shows the current pattern. Nearly after 500 ms, the inrush current decreases to no load current (5.37 A), which is exactly same to the measured data. The above behaviour clearly shows that the model of asynchronous generator represents the real machine characteristics.

4.5.5.2 No Load to Full Load Test

Now the diesel engine is connected to drive the asynchronous machine so that the system works as generator. As the diesel engine is started, no load is applied up to 3

seconds and suddenly full load (9000 W) is applied. The performance of the diesel genset is shown in figures 4.55, 4.56 and 4.57.

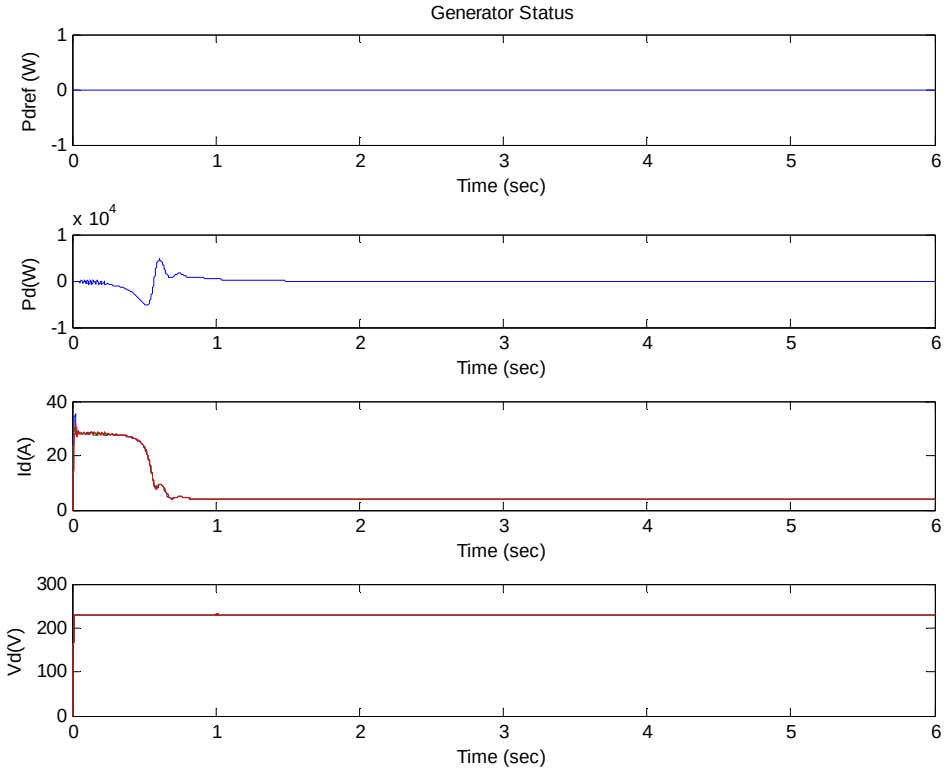

Fig. 4.53: The behaviour of the generator during no load condition

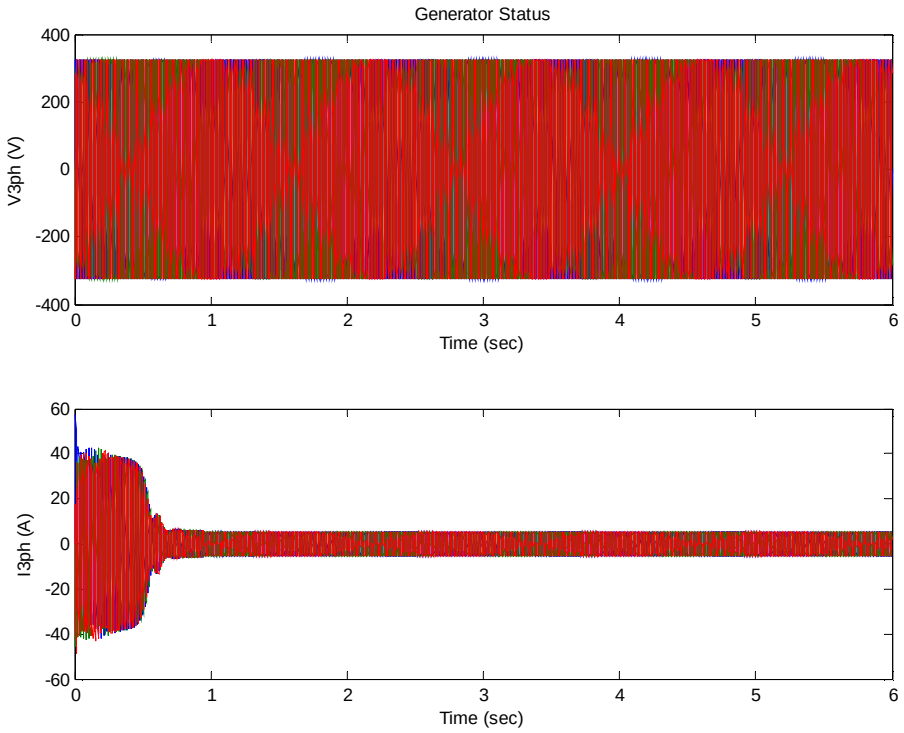

Fig. 4.54: The three phase sinusoidal current during no load condition

Electrical behaviour

The first graph in fig 4.57 shows the reference load applied to the governor control system. Initially no load is applied and the diesel genset is started. At 3 sec, full load is applied. The second graph shows the response of the generator. As the genset is connected, initially the machine draws power from the grid and starts to build up the speed. The motoring action goes on until the speed crosses the no load speed (nearly about 500 ms). At 3 sec, as reference power increases suddenly to full scale, the generator also just increases its production simultaneously. The delay is due to the governor character. The third graph shows the current pattern. At the beginning of the simulation, the machine draws very high inrush current as explained above. After that the generator draws no load current (magnetisation current). At 3 sec, the current goes up to around 16 Amp to meet the reference demand. The fourth graph shows the grid voltage pattern.

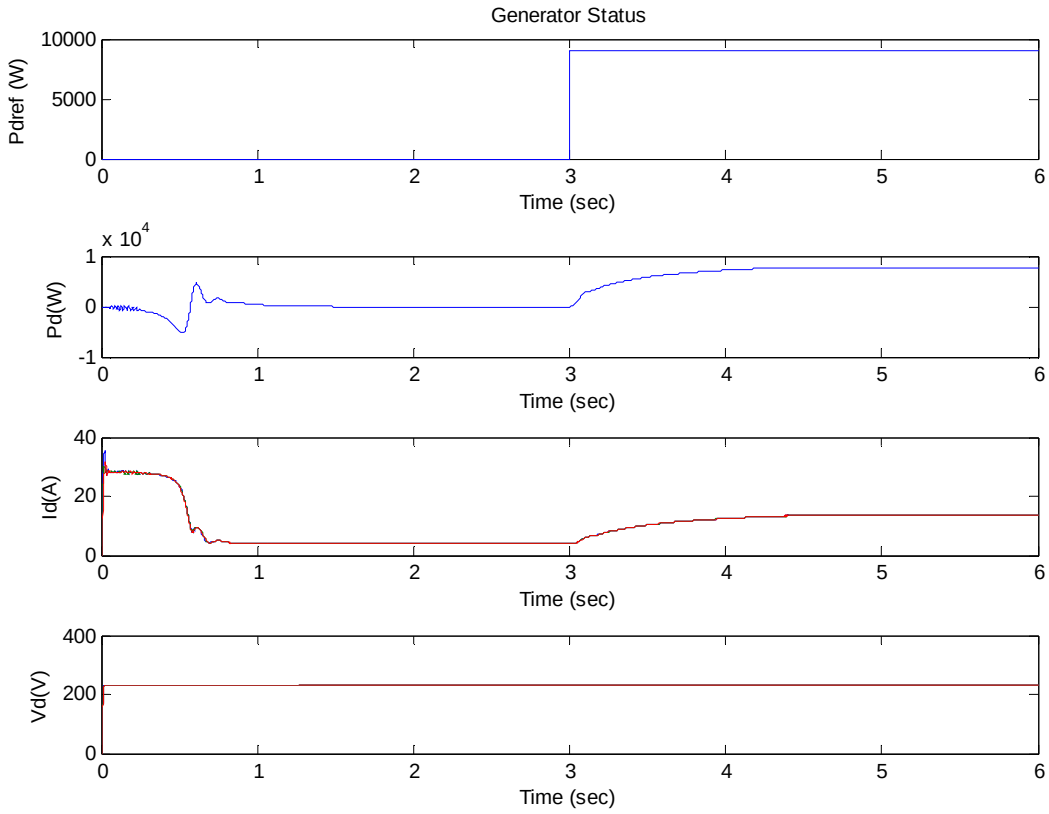

Fig. 4.55: Behaviour of the generator during no load to full load condition

Diesel Engine Behaviour

In fig 4.57 the first graph shows the fuel consumption by the diesel engine. As the genset is started, initially the amount of fuel consumption increases rapidly to accelerate the genset. When the speed of the diesel genset reaches to the no load speed, the governor starts to reduce the fuel amount. The load applied is up to 3 sec is zero so the fuel consumption is just to compensate the no load losses. At no load condition, it consumes around 0.5 l/h fuel. At 3 sec, as full load is applied, fuel consumption increases slowly up to 5 l/h. The second graph shows the torque production from

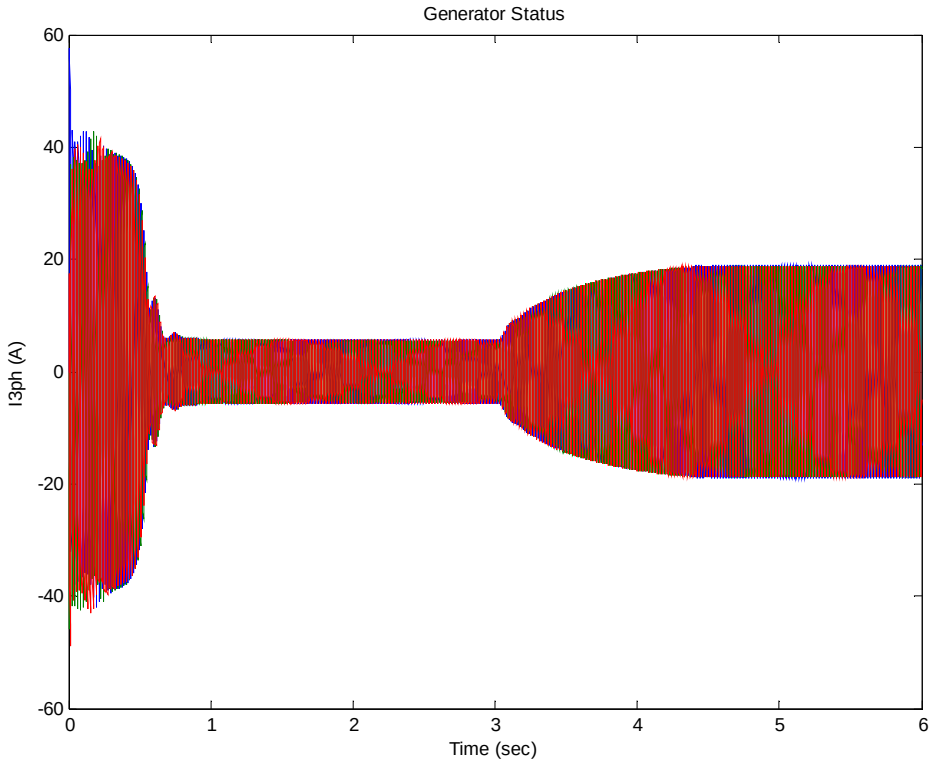

Fig. 4.56: Three phase sinusoidal current during no load to full load condition

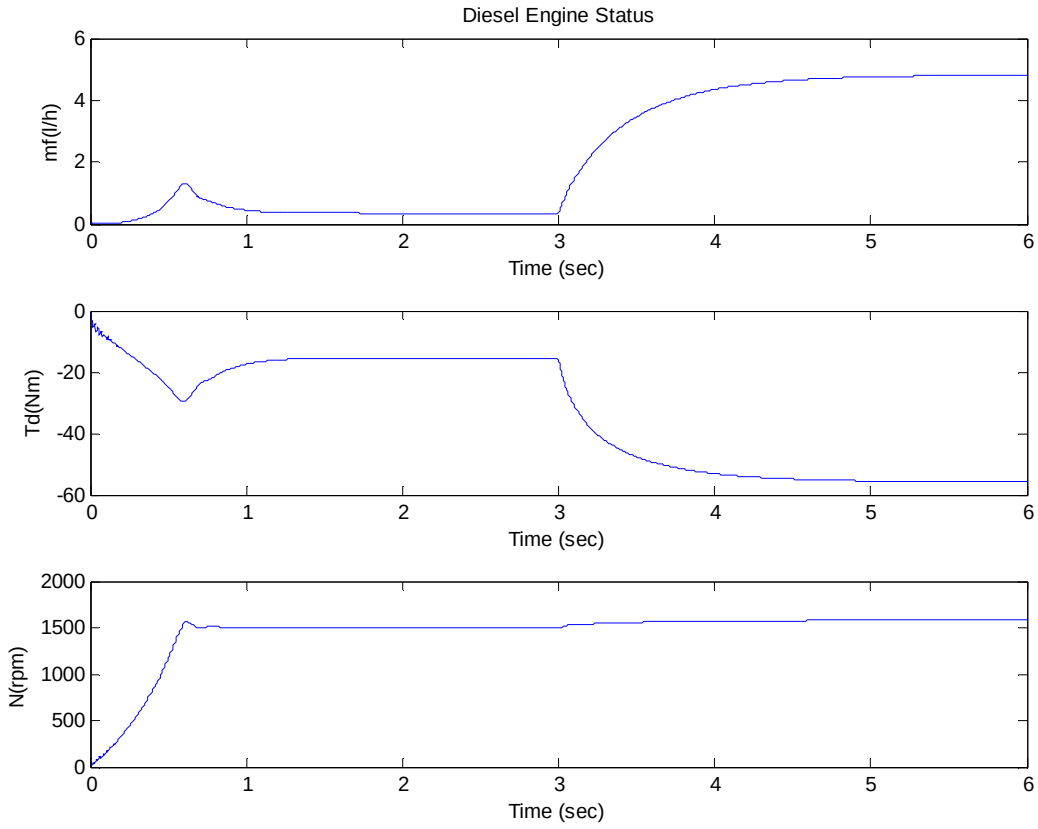

Fig. 4.57: Behaviour of the diesel engine during no load to full load condition

diesel engine. The torque is just a function of the fuel consumption. It follows the same pattern as the fuel consumption. The third graph shows the mechanical speed of the diesel engine. The speed starts to increase from 0 rpm and reaches to no load speed at around 500 ms. This time is a function of the governor parameters and the moment of inertia of complete system. The diesel engine runs in this speed up to 3 sec. It means the slip is zero. At 3 sec, the speed increases to 1537 rpm and the slip is -2.4%.

4.5.6 Isolated grid operation

If the diesel genset consists of an asynchronous generator has to supply the electrical power to an isolated grid, then the power supply system becomes complex. The operation point at generator mode (s < 0, n > n1) lies on the lower half circle in the complex circle diagram. As mentioned above, the asynchronous generator requires reactive power to magnetise its stator windings. Without supplying of the reactive power from an external source, the asynchronous generator can not produce the terminal voltage or simply it can not generate the electrical power. The solution to this problem is to connect a capacitor or capacitor bank at the terminals of the asynchronous generator. A need of the lagging reactive power of the asynchronous generator is compensated by the leading reactive power coming from the capacitor.

The asynchronous generator in the isolated operation can be formed as shown in fig. 4.58. To run the machine at no load condition and to get no load voltage, the asynchronous generator demands no load magnetisation current. This current should be supplied by an external capacitor. Each asynchronous machine has its one magnetisation curve [21].

$$I_c = I \tag{4.53}$$

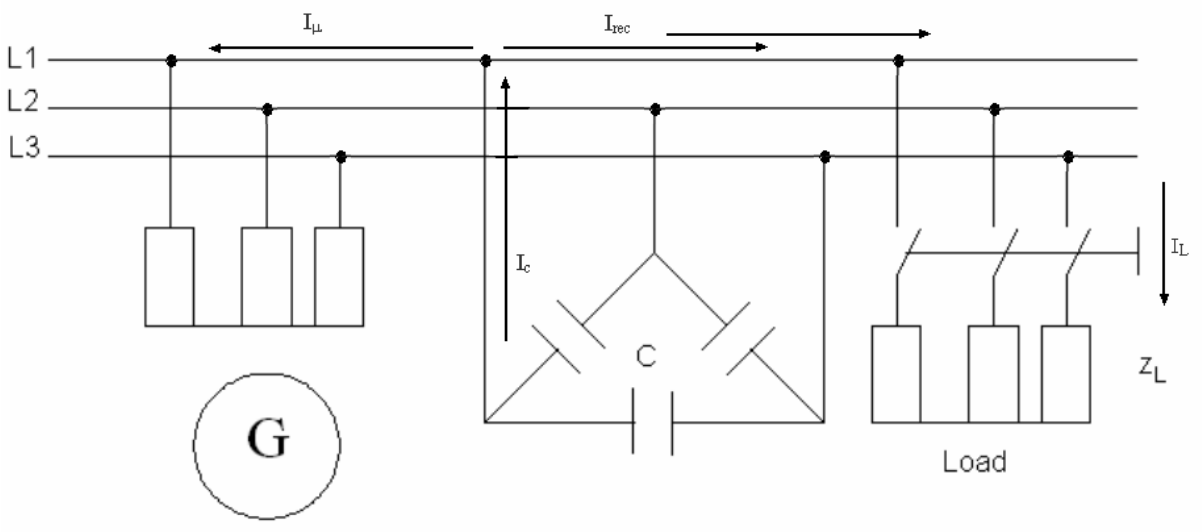

Fig. 4.58: Switching arrangement of asynchronous generator with capacitors and load

Fig. 4.59 shows the no load behaviour $V = f(I\ )$ of the asynchronous machine with connected capacitor slope $V = \frac{I_c}{\Omega C} V_0$.

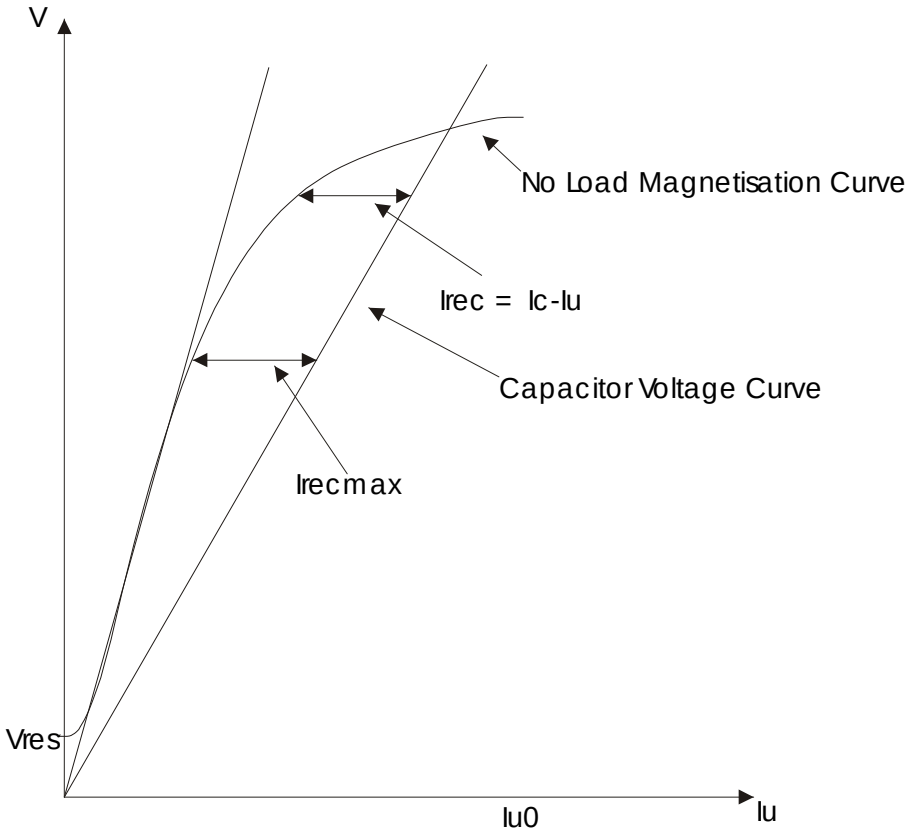

Fig. 4.59: No load behaviour of asynchronous machine and capacitor voltage slope

As the rotor is rotated by an external mechanical power, a resonance field is developed between the external capacitor and the main inductance of the asynchronous machine. The voltage builds slowly up and the stable point is achieved where two curves intersect each other.
To produce the no load voltage V_0, the minimum required capacitor can be calculated as follows [22]

$$I_c = V_0 . j\Omega C = -I \quad = \frac{V_0}{j\Omega L_h} \tag{4.54}$$

$$C = \frac{1}{\Omega^2 L_h} = \frac{1}{(2\ f)^2 L_h} \tag{4.55}$$

If the connected capacitor is small, the initial slope of the capacitor voltage will be bigger than the slope of the magnetisation curve, then it is not possible to get operating point or the machine will not be able to produce the voltage.

As the machine is loaded, the asynchronous machine demands extra lagging reactive power. This extra requirement of the reactive power must be fulfilled by the capacitor.

Even though only resistive load is connected, due to internal inductances of the machine, load current lags behind voltage or inductive current flows. Now the current that must be supplied from the capacitor is the sum of the magnetisation current and reactive load current.

$$I_c = I \quad + I_{rec} \tag{4.56}$$

By ignoring the stator resistance and the reactive load current for pure reactive load at constant frequency can be calculated as follows

$$\frac{I_{act}}{I_{rec}} = \frac{R_2^{'}}{sX_k} \tag{4.57}$$

During the resistive loading, the terminal voltage goes down slowly. At nominal load, the generator produces nominal voltage. If the load further increases with constant capacitor, the terminal voltage goes down and machine loses its residual magnetism. In such a case, the machine must be first magnetised by external battery. If the inductive load is connected, the reactive power demand will be still more and bigger capacitor is required.

4.5.7 The model of diesel genset in the isolated operation

The model has been developed using the equations mentioned above and a look up table, which gives the magnetisation curve (magnetising current vs no load voltage) of the asynchronous generator. Beside that this model consists of 3 to 2 phase and 2 phase to 3 phase transformation blocks, reactive current block, load pattern block as in previous model.

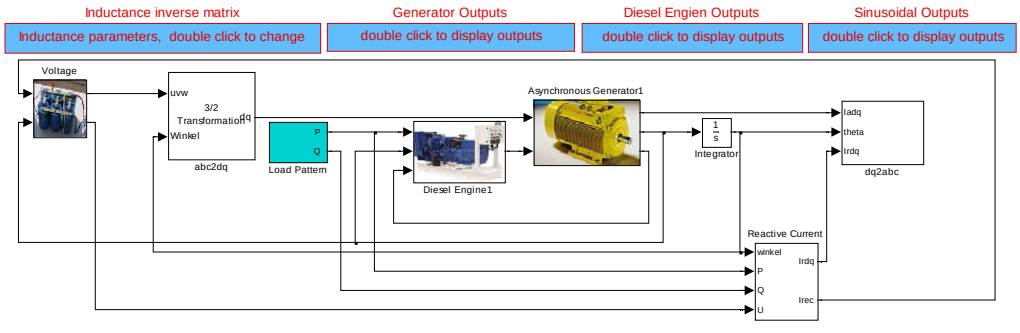

Fig. 4.60: Complete Simulink lookout of the asynchronous machine model in the isolated operation

Load pattern block

It is possible to load the generator in different fashion to analyse its different behaviour. The apparent power S can be applied to the machine in ramp or step fashion. Power factor (pf) of the load can be given in Matlab file so that desired inductive or capacitive load can be connected.

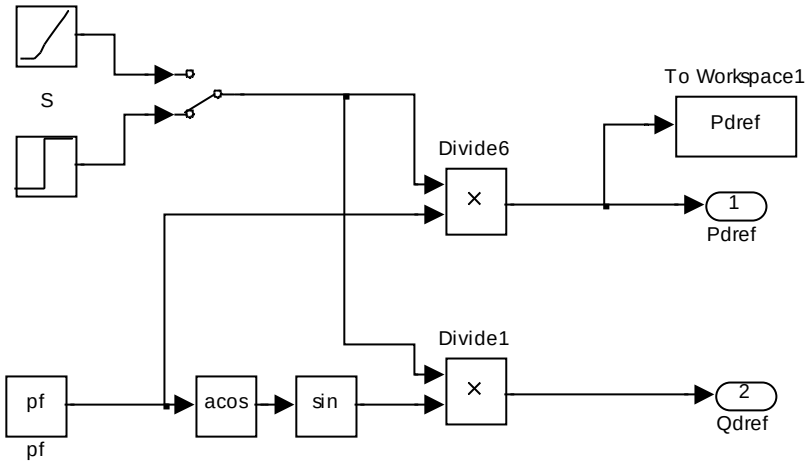

Fig. 4.61: The inside view of the load pattern block

Voltage calculation block

The asynchronous generator model is same as in the grid connected one. The machine must work in the isolated mode so the voltage calculation block is required. This block represents the magnetisation phenomenon of the machine. The block is shown in fig 4.62. It is possible to connect different amount of capacitances as per demand of the load. The look up table gives the rms voltage and is converted to 3 phase sinusoidal voltages. The connected capacitor provides the capacitive current. If the resistive load is applied, simply this capacitive current will be equal to the magnetising current. PT1 transfer function is used to represent machine circuit (inductive-resistive-capacitive).

Reactive current calculation

Even though the generator is loaded with resistive load, it requires capacitive current (the electrical machines are inductive in nature). The required capacitive power is around 20% of nominal load. The second look up table is used to define the reactive current during resistive load. If the generator is inductively loaded, the inductive current flows and that must be compensated. The total required capacitive current is sum of two currents. This inductive current is also transformed into dq form. The block is shown in fig 4.63.

4.5.8 Experiments

4.5.8.1 Ramp active load increment

With constant capacitor (capacitor required to run the machine at no load condition), the nature of the modelled asynchronous generator can be compared with theoretical behaviour. As the active load is increased slowly, correspondingly the terminal voltage goes down and at one point, the terminal voltage collapses. To investigate this behaviour, the active load is increased in the ramp fashion. In fig 4.64, the first graph

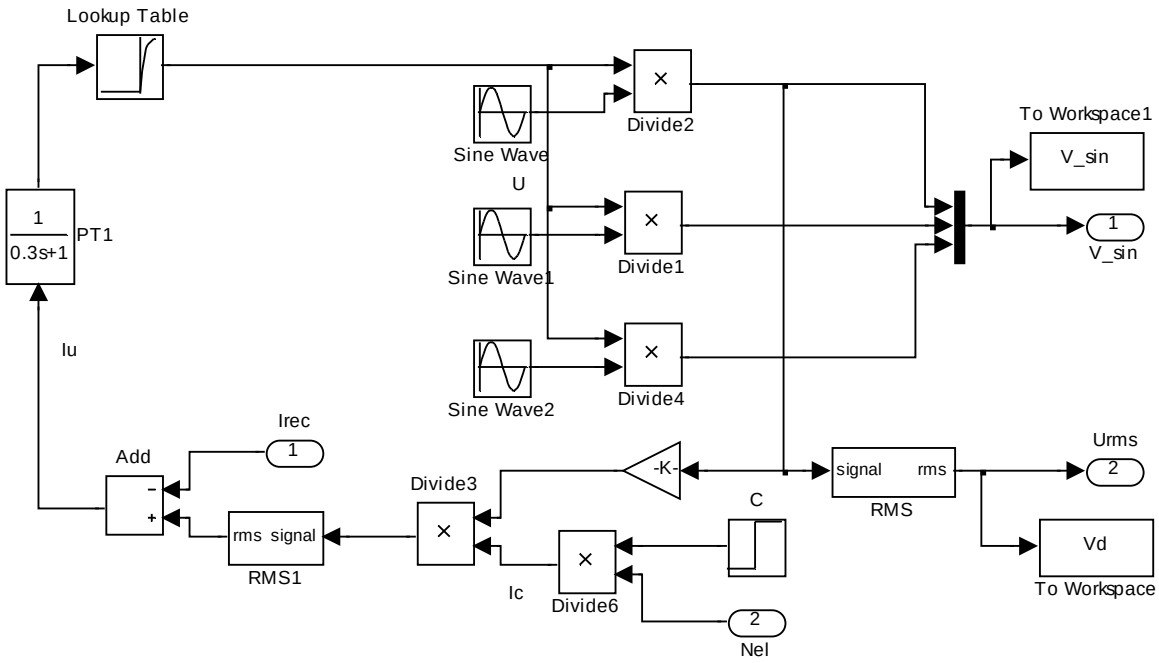

Fig. 4.62: Simulink inside view of the voltage calculation block

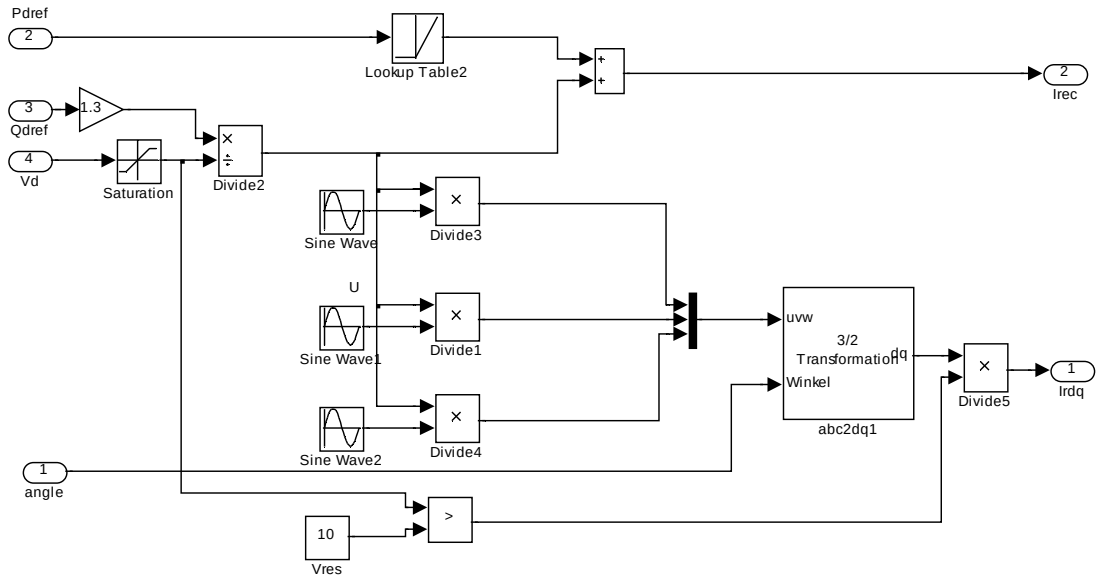

Fig. 4.63: Simulink inside view of the reactive current calculation block

shows the reference active load. At 3 sec, the load increases with 1100 W/s. This means the nominal load is applied at around 11 sec. The second graph shows the produced power by the generator. As the load is applied, some transient behaviour due to friction could be observed for few ms. After that, the power follows the reference point. At nearly 9 sec, the system collapses. The third graph shows the terminal voltage. It increases very slowly from the residual voltage. As the speed crosses the threshold point (1200 rpm), it increases rapidly and achieves its nominal value at around 3.5 sec. Due to the increment of the load in ramp function, it decreases

correspondingly and as the load crosses its nominal value, it starts to decreases rapidly and collapses. The fig 4.65 shows the current and voltages in three phase sinusoidal form.

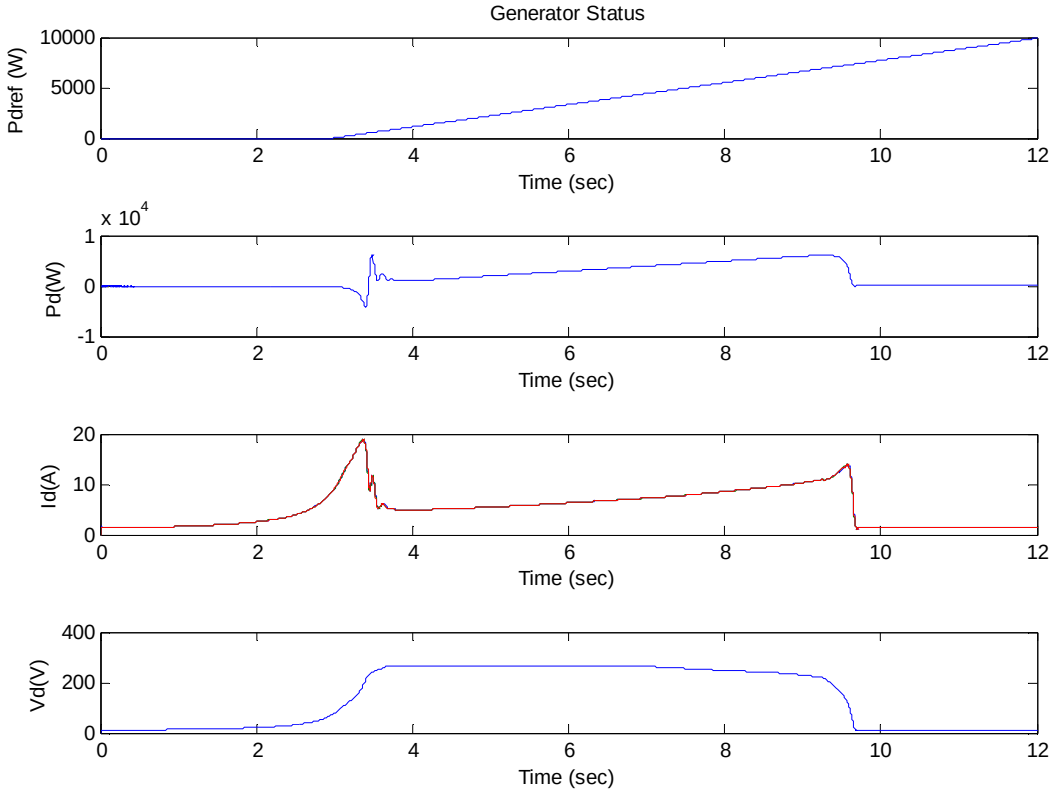

Fig. 4.64: Generator behaviour during ramp load condition

4.5.8.2 Sudden load change with constant capacitor

Generator Behaviour

In fig 4.64, the first graph shows the reference power of the diesel genset. Up to 6 sec the generator has no load. At 6 sec, the system is loaded with full load. The second graph shows the system response. Up to 6 sec, there is no power production from the generator. At 6 sec, the generator starts to produce power and follows the set point. It can be observed that the power production reaches nearly to the reference point within 700 ms. But due to the insufficient reactive current compensation, the system voltage collapses. The third graph shows the current flowing in the generator. Up to nearly 3 sec, only no load or magnetisation current (I_c) flows and as the voltage increases due to the increment in the speed, the increment in current occurs. As the full load is applied, the current increases up to 18 amps. The fourth graph shows the terminal voltage. Up to 2.5 sec, the terminal voltage reaches to no load voltage, after that the decrement in the voltage can be observed due to the sudden application of load.

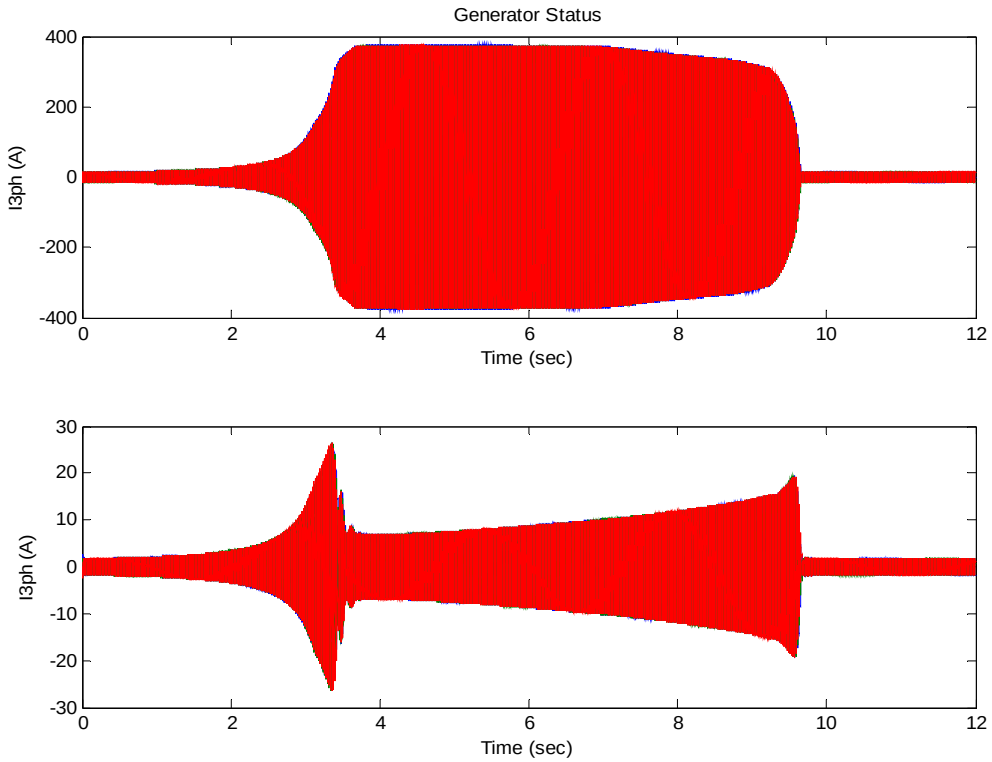

Fig. 4.65: Three phase sinusoidal current and voltage during ramp load condition

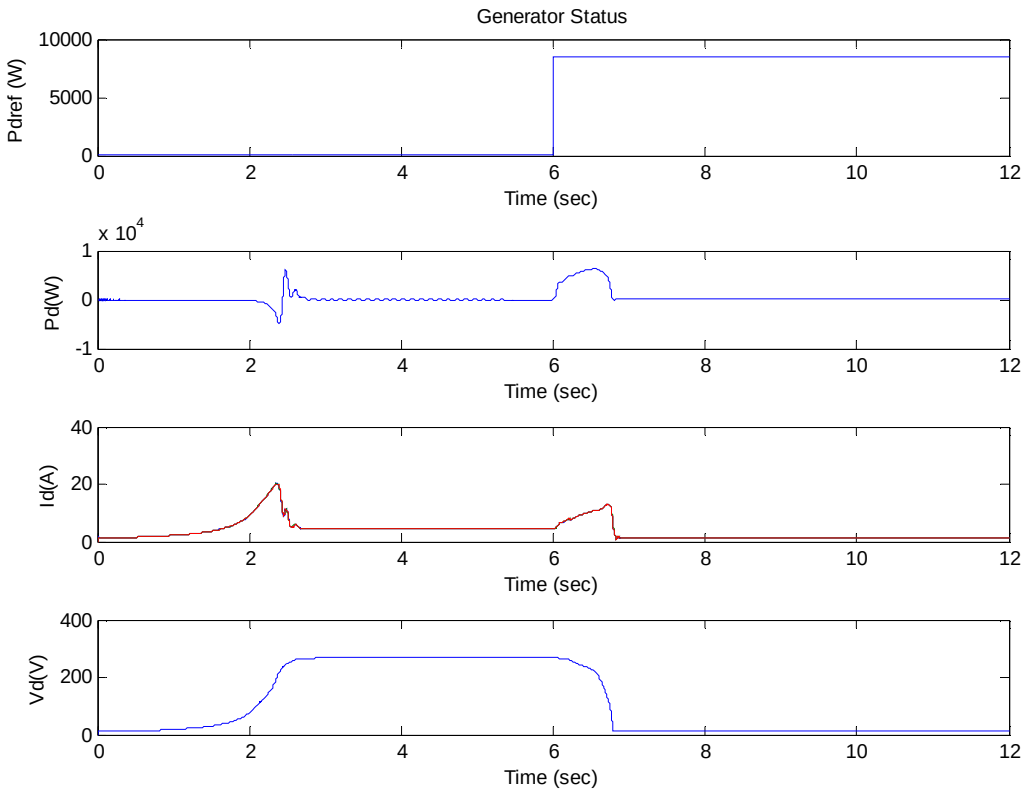

Fig. 4.66: Generator behaviour during sudden full load application at constant capacitance

4.5.8.3 The voltage establishment through the capacitor increment

This experiment is carried out to show that the generator voltage can be maintained as per requirement in the isolated operation by increasing the amount of the capacitance connected across it. As shown above, if more capacitive current is not provided the terminal voltage collapses. How fast the extra capacitor is to be connected, it depends on machine parameters. For pure resistive load, the delay time can be up to 500 ms (for this model). The fourth graph in fig 4.67 shows the voltage pattern. The voltage goes down, and as extra capacitor is connected, it goes up again to the nominal level.

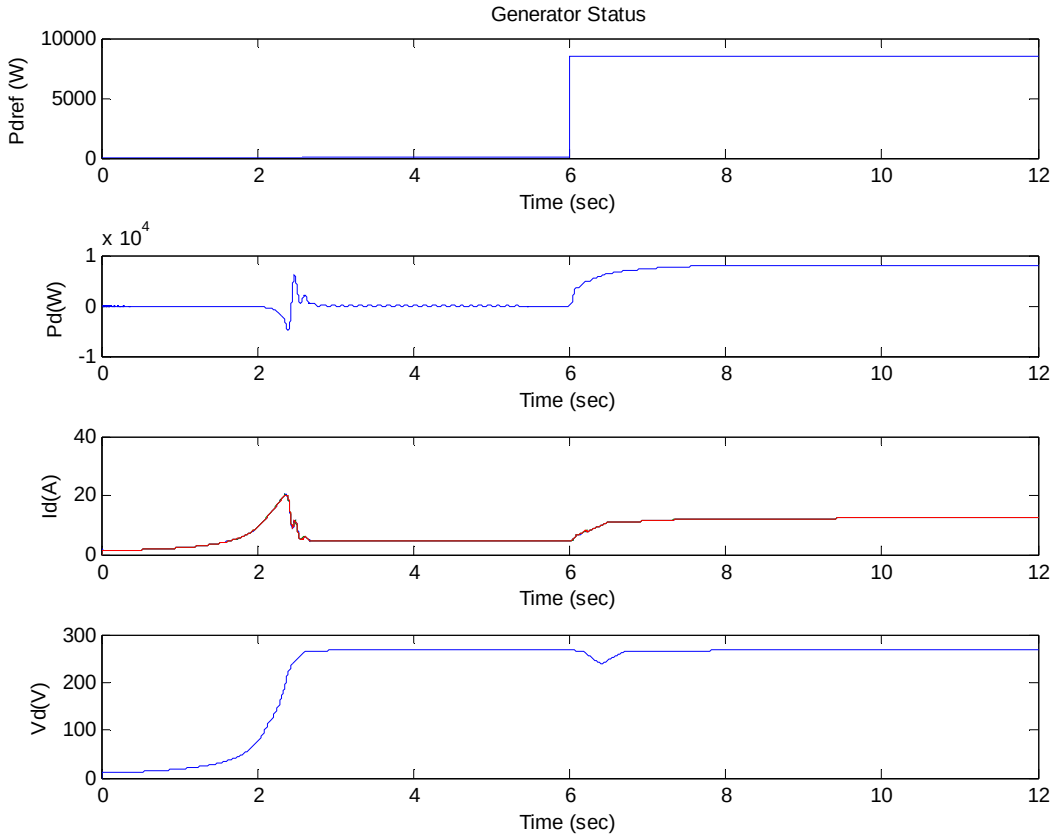

Fig. 4.67: Generator behaviour during sudden full load application at variable capacitance

5 HPS- Integration Process

The synchronous generator driven by the water turbine forms the isolated grid. Variable load is connected in the grid formed by it. The stability of the gird depends on the balance between the active power – active load and reactive power – reactive load. The grid collapses if the connected load is more than available power [1].

5.1 Structure

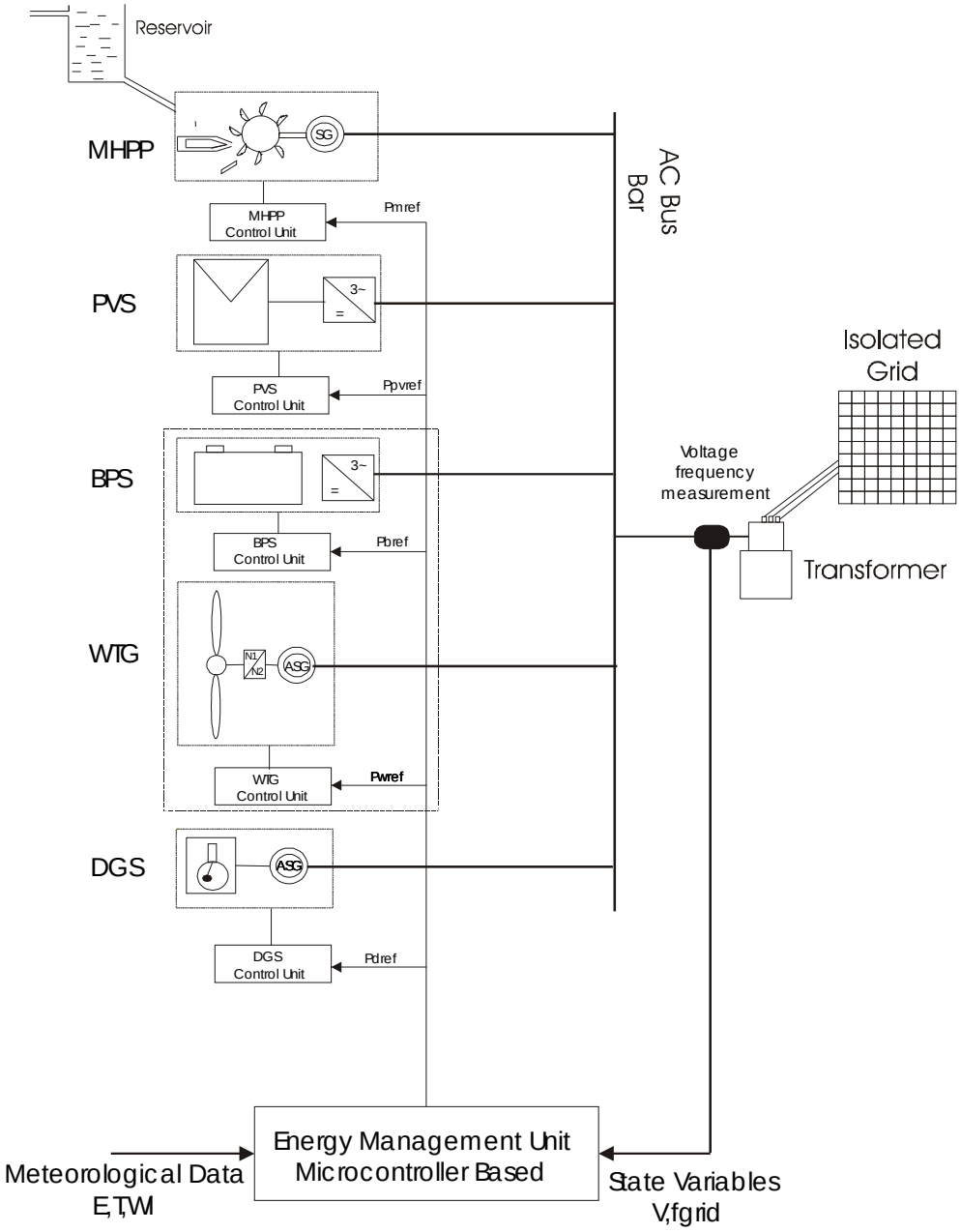

Fig. 5.1: The possible layout of the Hybrid Power System

The power from SG is determined by the water level in reservoir. To secure the stability of the grid in full load condition all the time, different energy sources can be integrated. Such system is known as Hybrid Power System [HPS]. HPS may be

centralised DC bus system or centralised AC bus system or decentralised AC bus system or mixed system [2]. For this research work, a centralised AC system is chosen because of suitability in the target location (Nepal).
The possible HPS structure layout is shown in fig. 5.1. Renewable energy sources, PV system and wind turbine generator [WTG] are connected into the common AC bus formed by MHPP. The battery bank is also connected at same bus via a bidirectional inverter. Diesel genset is used as a back up system. The most of the HPS, which exists, consists of the battery bank as an energy storage unit. In this research work, instead of the battery bank, the reservoir is used for the energy storage purpose. In case of Nepal, PV system is more suitable because of the favourable meteorological conditions. In such circumstances, the targeted HPS is simplified from fig. 5.1 to fig 5.2 as shown below.

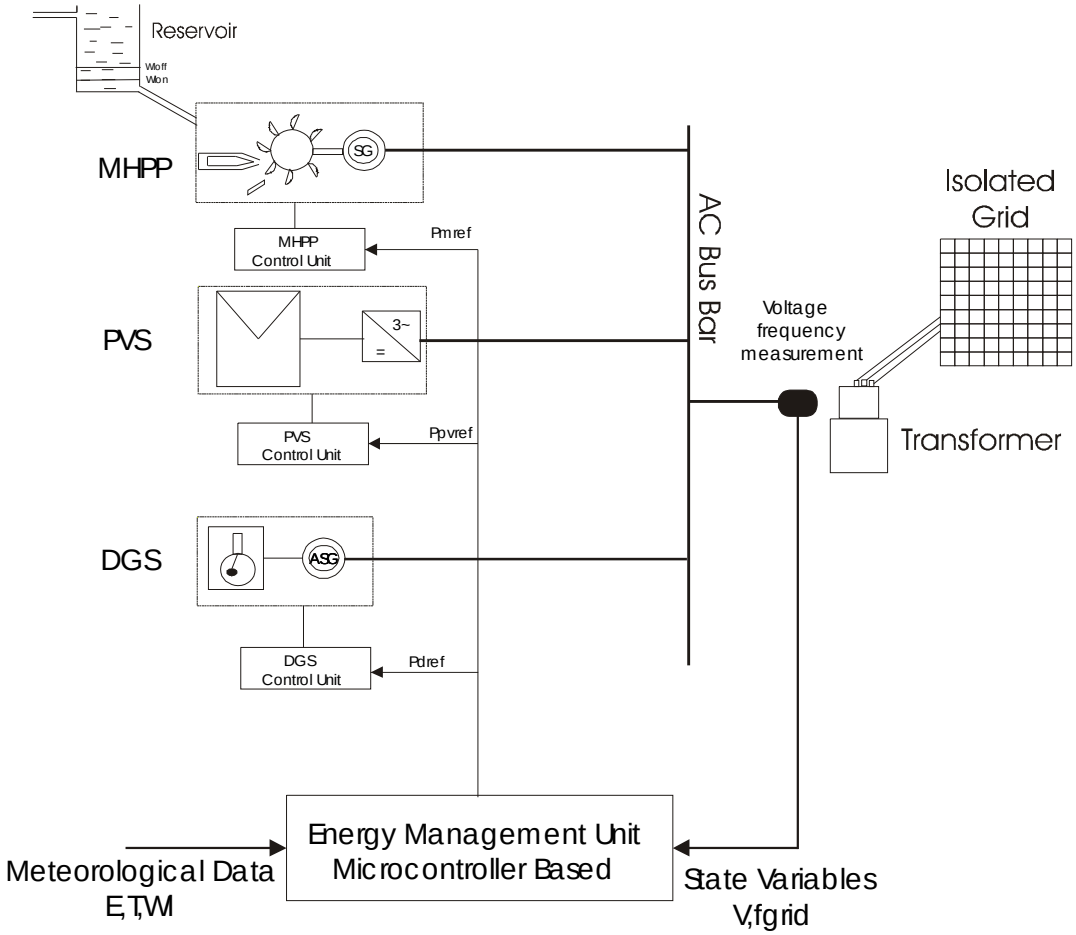

Fig. 5.2: The target layout of the Hybrid Power System

5.2 Control system of HPS

The overall control system must guarantee the smooth operation at variable load and environmental conditions. Environmental conditions represent the parameters – irradiation, temperature and water level in the reservoir. These parameters must be input for the control system. Beside that the grid frequency, which is the reflection of the grid must be fed back to the control system. Based upon such available variable parameters, the control system commands HPS to fulfil the load requirement with the priorities mentioned below [3], [4].

Priority

1	Use of the maximum power available from PV system
2	Use of the power available from MHPP
3	Use of the power from the diesel genset

An integration of more energy systems with different operating characteristics makes the control system more complex. To operate the system at the best economical, technical aspect, the control system is divided into different levels based upon its working level. The control levels are shown in fig 5.3.

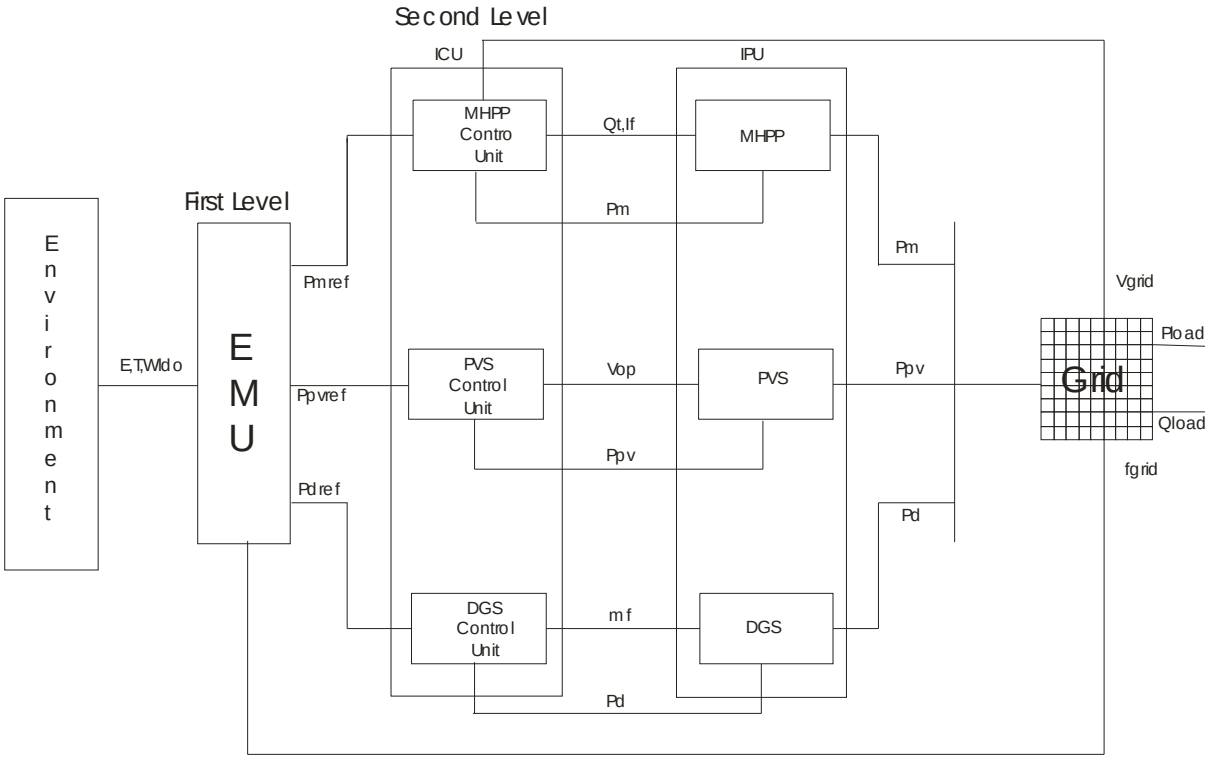

Fig. 5.3: The control level structure of the targeted HPS

5.2.1 Energy Management Unit [EMU]

EMU is the heart of the control system so it is the first level strategy in the control system. By using different sensors, the meteorological data (E, T), and water level in the reservoir are measured. The data are fed into EMU, to calculate the maximum available power from MHPP and PV system. Another important parameter is the grid frequency that reflects the load connected in the grid. EMU determines the reference powers for Individual Power Unit [IPU] by governing the priority levels mentioned above and consequently maintaining the grid quality.

5.2.2 Individual Control Units [ICU]

The reference powers supplied by EMU are to be produced by each IPU to fulfil the grid requirement. The task of ICU is to control IPU such that they produce the power

as per the reference values given by EMU. ICU for different energy systems are tabulated in table 6.1.

Table 6.1: Different energy systems and respective control units

IPU	ICU	Inputs	Outputs
MHPP	Mechanical governor Automatic voltage regulator	P_{mref} V_{ref}	Q_t I_f
PV System	MPP tracker	P_{pvref}	V_{op}
Diesel Genset	Mechanical governor	P_{dref}	m_f

5.3 Simulation Model

The individual power units are integrated together on the common AC bus bar to form HPS. A model consisting of different sub systems as mentioned above is developed in Matlab/Simulation and shown in fig. 5.4.

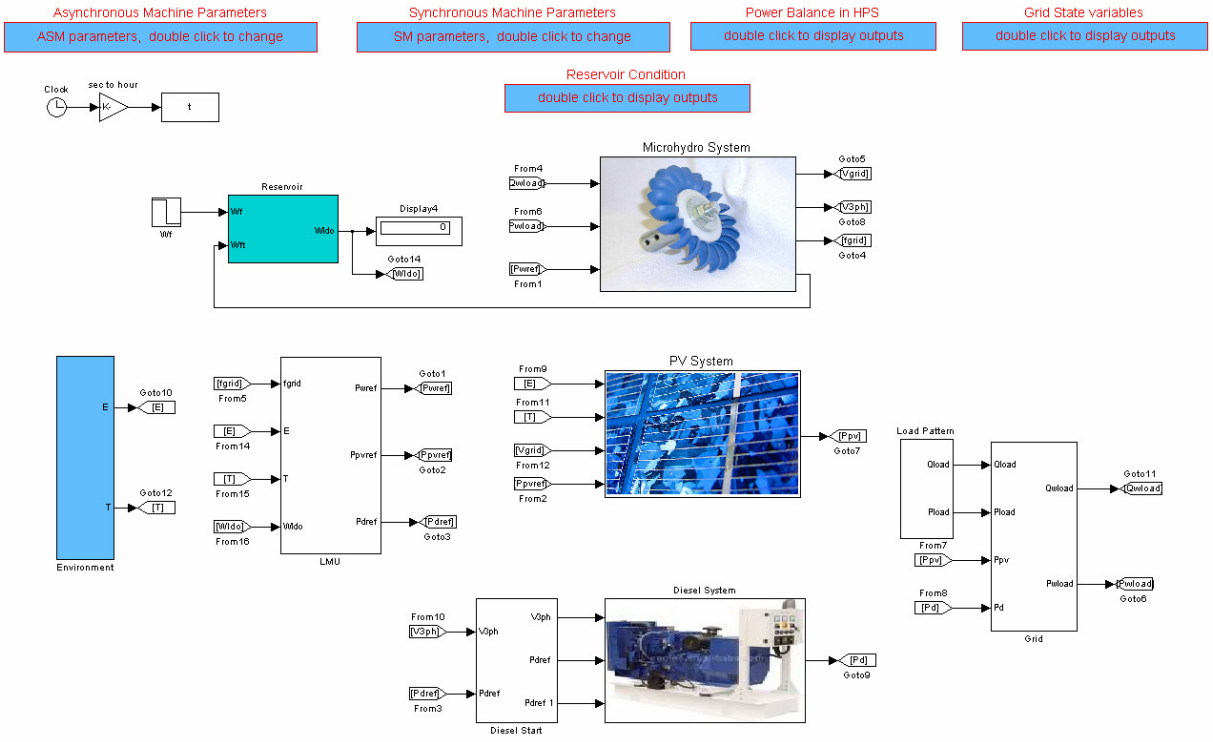

Fig. 5.4: The complete mathematical model of the targeted HPS in Simulink

At the top of the model, small blue rectangles are available. These blocks are used to get machine parameters from the source code written in Matlab files. At the same time, these blocks are also used to plot the simulation results in Matlab workshop. At the left hand side, an environment block is available where meteorological patterns can be stored. It provides E, T for EMU. Next block is EMU. At the middle, three IPUs

MHPP, PV system and DGS are kept. The most right block is the grid, where the load patterns can be fed as the input to HPS.

5.3.1 Control strategy

MHPP is the main unit of the system because it builds up the grid variables and other units are grid-supporting units. In that sense, the operation of MHPP is to be guaranteed at all the time. The size of PV system is chosen in such a way that it covers at least the base load of the grid load. Depending upon the load profile, water flow, cost etc the actual size is defined. At daytime when the sun shines the power from the PV system is injected into the grid and the water is stored. DGS will be started only if the water level in WR goes down to the lower level. To avoid the high frequency of DGS turn on and off, two levels are created in WR. The turn on and off processes are controlled by a hysterisis loop on the water level [5].

5.3.2 Function of EMU

The principle of load sharing is based upon the determination of a virtual load in the grid through the grid frequency and instantaneous meteorological and WR conditions. The philosophy of EMU is shown in fig. 5.5.

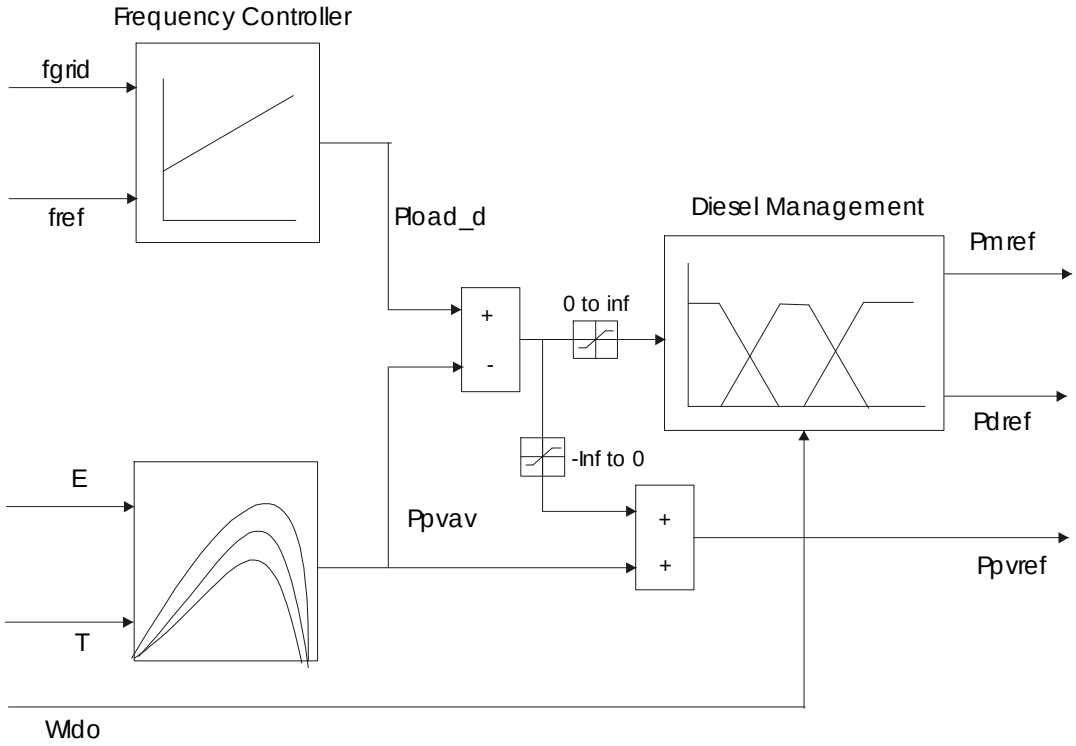

Fig. 5.5: The load shearing policy of the energy management unit

A PI controller, determines P_{load_d} by using the error between f_{ref} and f_{grid} The maximum available power from PV system is determined using E,T values. The difference between P_{load_d} and P_{pvref} is determined and assigned as the error power [3].

$$P_{error} = P_{load\_d} - P_{pvref} \qquad (5.1)$$

The meaning of P_{error} is pointed out in the table.

P_{error}	Meaning
+ve	PV power is not sufficient.
-ve	Surplus power is available.

If $P_{error} < 0$, it indicates that the PV system can produce more power than the load in the grid. This surplus power can not be stored so the power from the PV system must be reduced. If $P_{error} > 0$, it indicates that the power from the PV system is not sufficient, this power will be provided by MHPP if the water level is above the upper level in WR as shown in fig. 5.6.

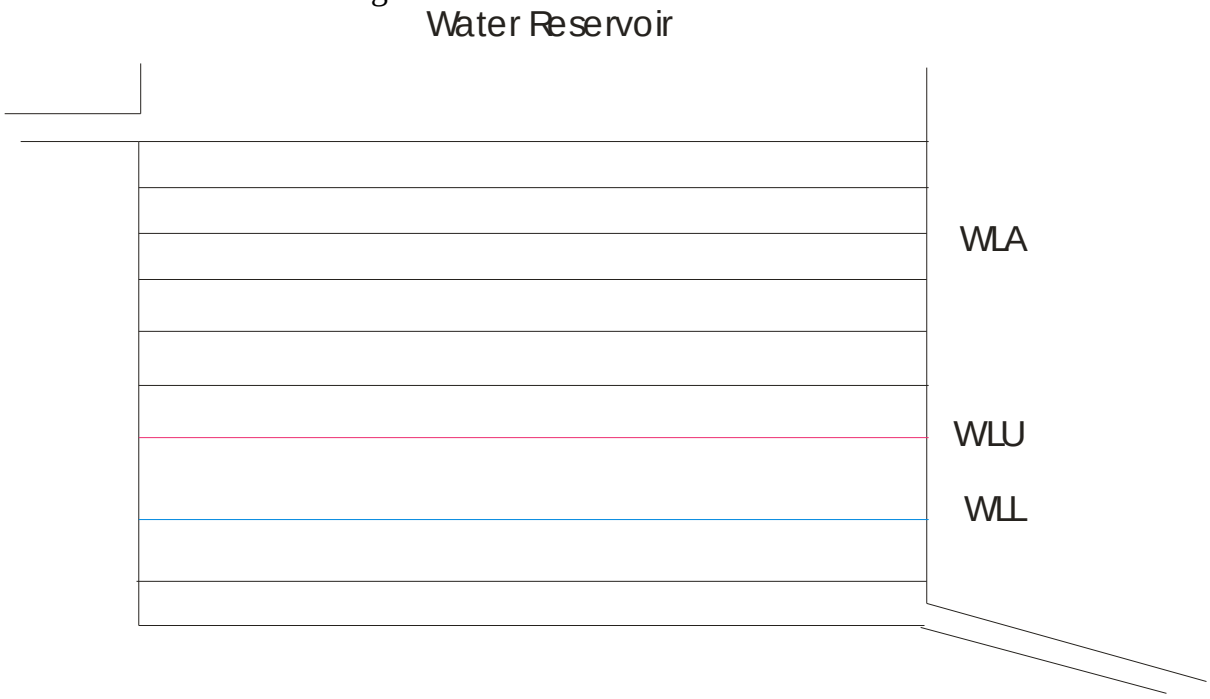

Fig. 5.6: The important levels in the water reservoir

The MHPP can support the full load if WLA is greater than WLU. As the back up system, DGS supports the grid by providing the active power at any time when EMU sends the command. If WLA decreases and becomes equal to WLL, the sensor provides $W_{ldo} = 1$ to EMU and EMU generates a signal to turn on DGS. The reference power for DGS P_{dref} increases slowly in the ramp fashion. The slope of the P_{dref} can be set by the operator. Correspondingly P_{mref} decreases with the same slope so that the sum will be always constant. The transient process of DGS turn on and off is shown in fig 5.7.

The slope turn on strategy has been developed to avoid possible grid instability due to sudden heavy load change in IPU. MHPP is loaded with $P_{mrefmin}$ to run SG continuously. At this time, MHPP provides reactive power to the grid and to the induction generator used in DGS.

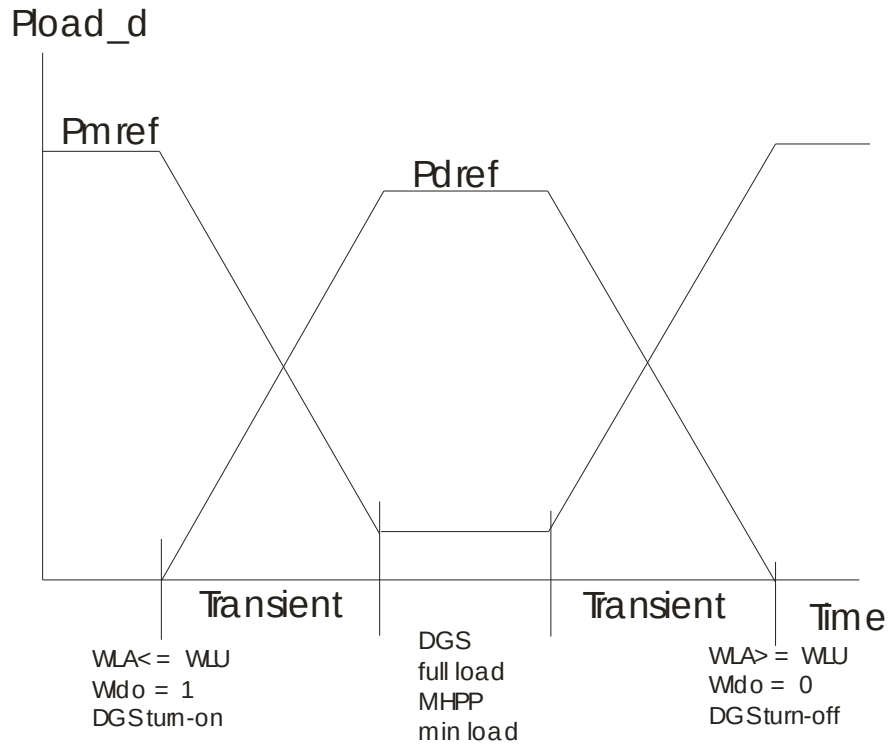

Fig. 5.7: Transient processes of the diesel genset turn on and off

5.4 *Experiments*

5.4.1 Integration of PV system with MHPP

The maximum power available from the PV system is utilised to reduce the amount of water drawn by the water turbine so that the water could be stored at daytime. Fig. 5.8 shows the contribution from the PV system in the power-shearing scenario. The first graph shows an applied load pattern. Initially SG is loaded with 1 kW and load is increased to full load of 7.5 kW step by step. The second graph shows the determined load by EMU through the frequency error. Initially due to high +ve difference between f_{ref} and f_{grid}, P_{load_d} is set maximum so that SG achieves the nominal frequency quickly. The third graph shows the power production from MHPP. It follows the load pattern. As the PV system starts to produce power (the fourth graph), the power production from MHPP starts to decrease in the same fashion. The last graph shows the condition of diesel genset.

Fig. 5.9 shows the power balance in the HPS together. It can be observed that the deviation between the power produced and the determined power increases with respect to increment in the load. It is due to the droop characteristics set at MHPP. Fig. 5.10 shows the state variables of the grid the frequency and the voltage respectively. The frequency decreases from around 52 Hz at no load to 48 Hz at full load. In the voltage pattern, the effect of the load changes can be observed. As the full load is applied, the voltage goes down but AVR brings back the voltage to the set point. The deviation in the frequency and voltage from the no load to the full load can be adjusted by setting the control parameters [5].

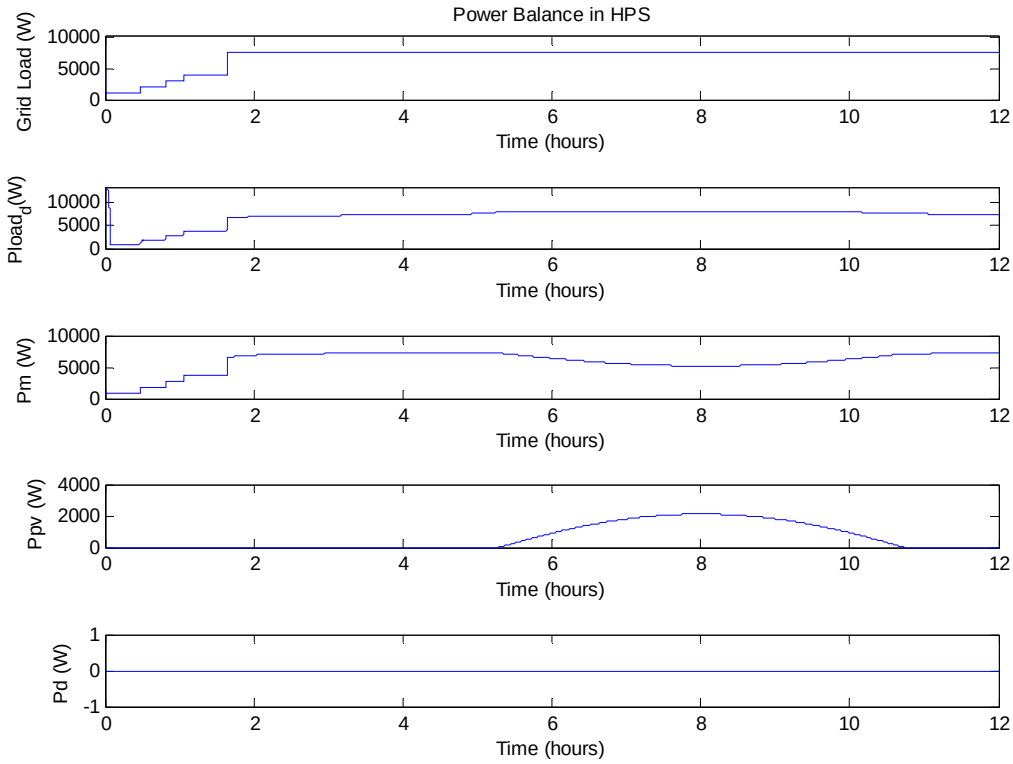

Fig. 5.8: The power balance in HPS during integration of PV system

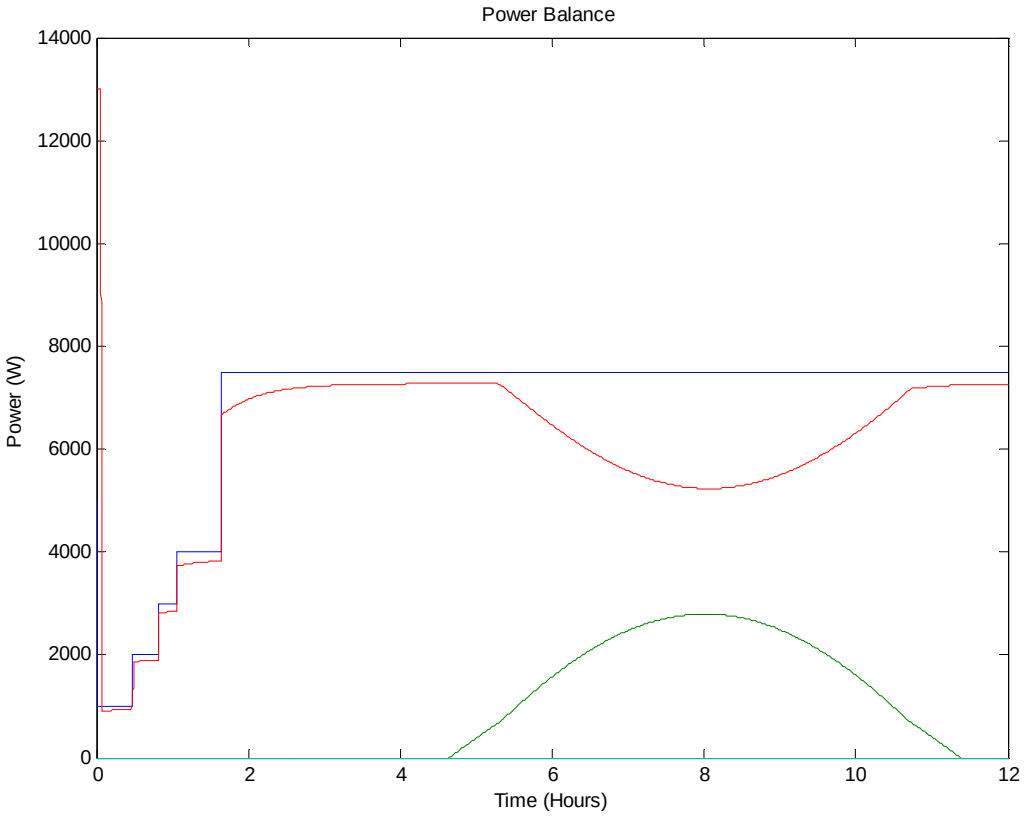

Fig. 5.9: The power balance (close look up) in HPS during integration of PV system

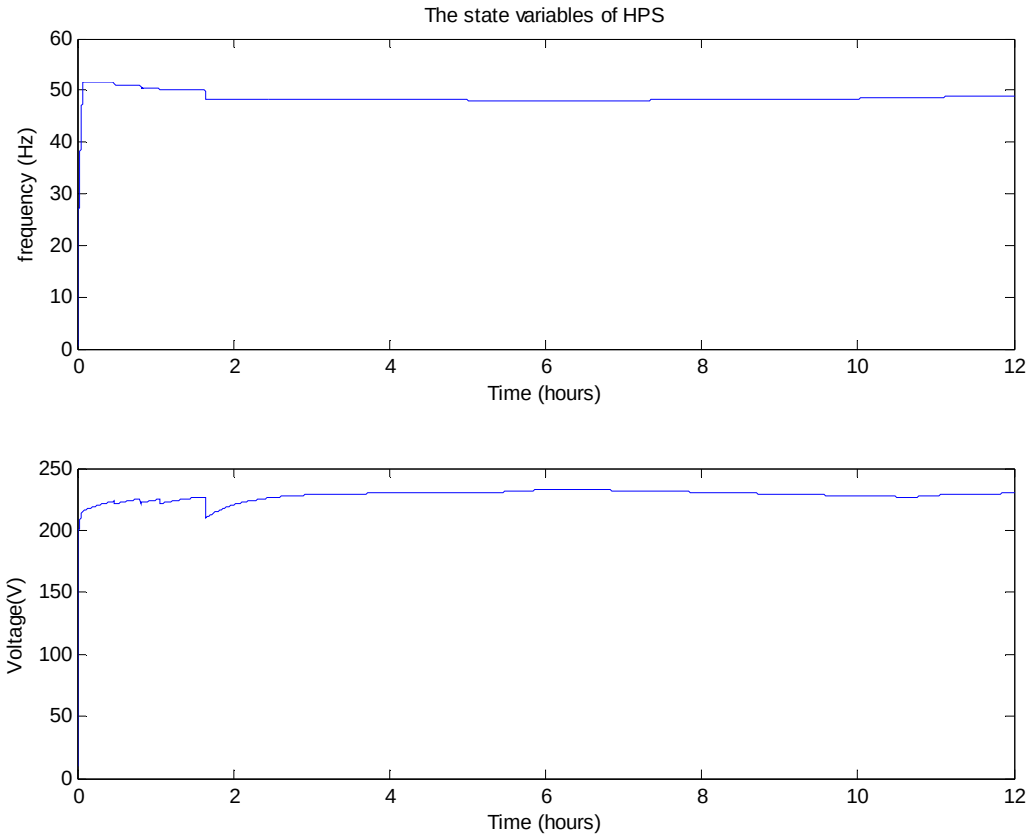

Fig. 5.10: The state variables of HPS during integration of PV system

5.4.2 Diesel genset turn_on and _off

This experiment is carried out to test the behaviour of HPS during turn on and turn off of the diesel genset. Initially 1 kW load is applied to bring the grid frequency quickly to the reference value. After some time the load is increased to the full load. The water flow into WR is changed time to time as shown in the first graph of fig. 7.11 to meet DGS turn-on condition. As the water level in WR goes below to 1 m (WLL) at around 6 hours, DGS is started and the power increases with the slope defined by the user at LMU. The parallel effect is observed on the power production from MHPP. P_m decreases with the same slope such that the sum is always very near to the grid load. After some time, MHPP runs at the minimum load to feed only the reactive power to the grid and the diesel genset. The water flow is increased to meet DGS turn off condition. As the water level reaches to 2 m (WLU), the power from DGS reduces slowly and it is turned.

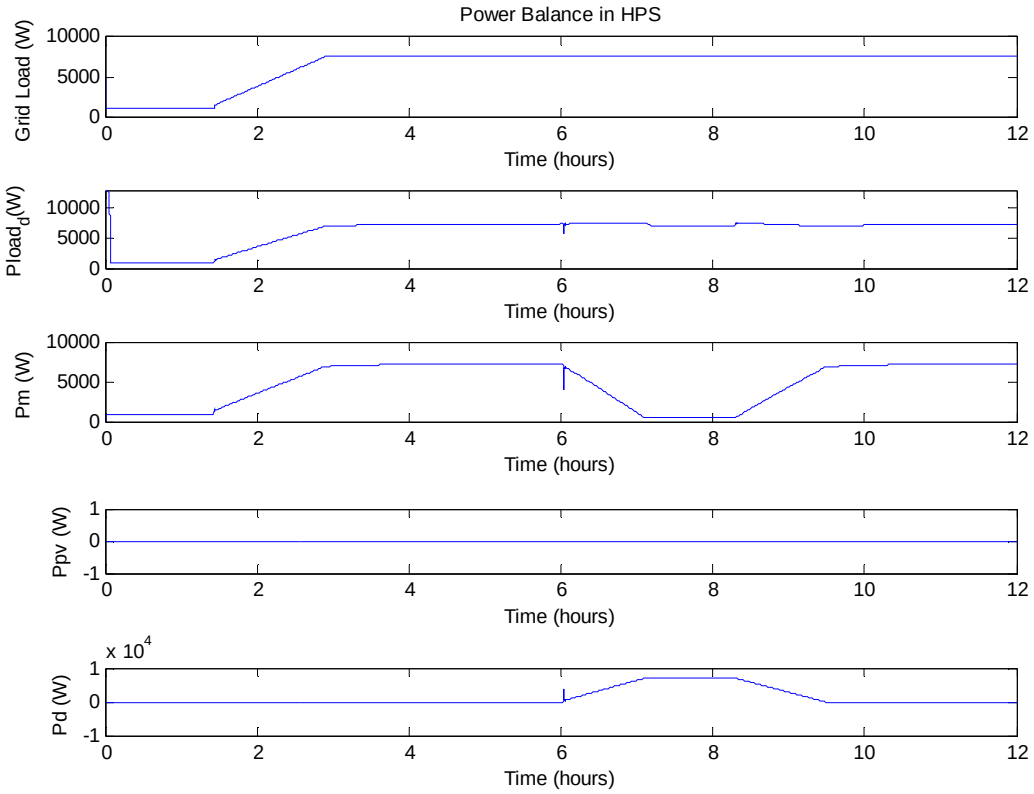

Fig. 5.11: The state variables of HPS during integration of PV system

5.4.3 Complete operation

The interaction between different systems and the stability of HPS during variable load and meteorological conditions are to be tested to confirm the functionality of the control strategy. This test is carried out in such a way that all the IPU come into operation to support MHPP. The behaviour is shown in the fig 5.12. The applied load pattern is developed to represent 24 hours load in a remote area where peak load occurs at the evening time nearly for 4- 5 hours. Beside that only the base load is connected. During a complete day, power factor of 0.8 is maintained. The first graph represents the load pattern. 3 kW of base load is applied. Around 12 pm the load increases gradually and it reaches to the peak load of 7.5 kW at 17 pm.
The second graph shows the grid power determined by EMU. Based upon this power EMU determines, optimal reference powers for IPU maintaining the control criteria mentioned inside. The third graph shows the power production from MHPP. The deviation in P_m from P_{load_d} can be observed which is due to the power contribution from the PV system and DGS. Fig. 5.13 shows the power balance in HPS together. The stability of the isolated grid is in the sense of state variables is shown in fig 5.14. The grid frequency is maintained at around 50 Hz during base load of 3 kW. As the load increases, correspondingly the frequency decreases. The similar behaviour can be observed in the voltage pattern.

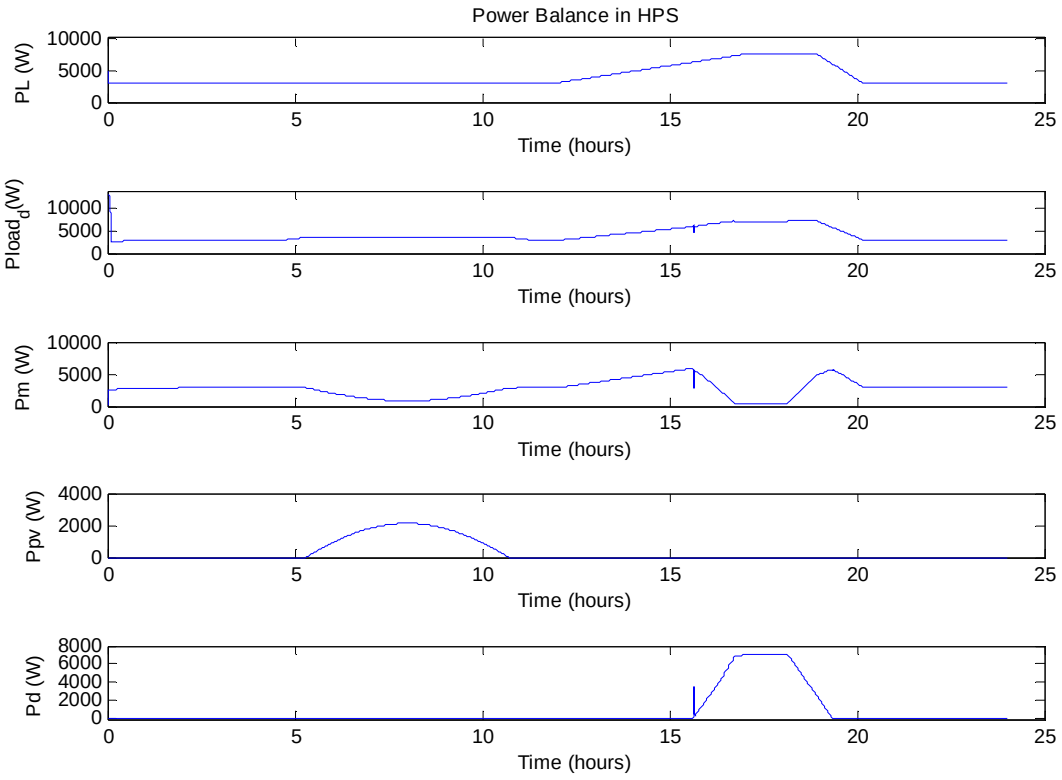

Fig. 5.12: Power balance in HPS during integration of PV system and diesel genset

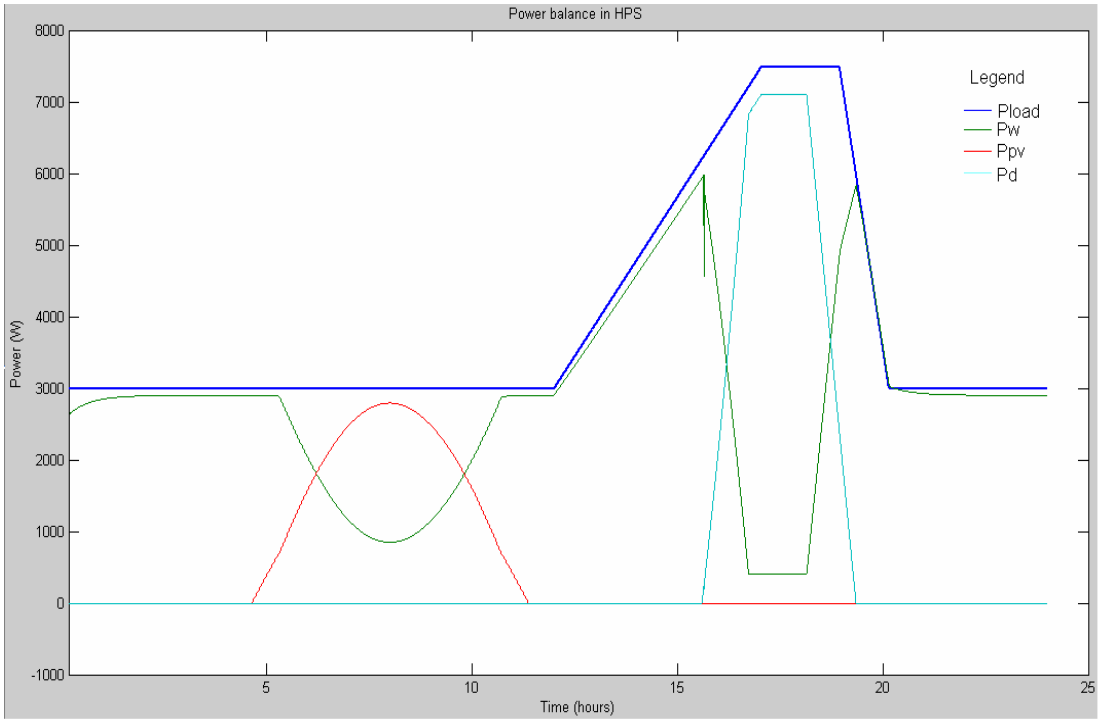

Fig. 5.13: Power balance (close look up) during integration of PV system and diesel genset

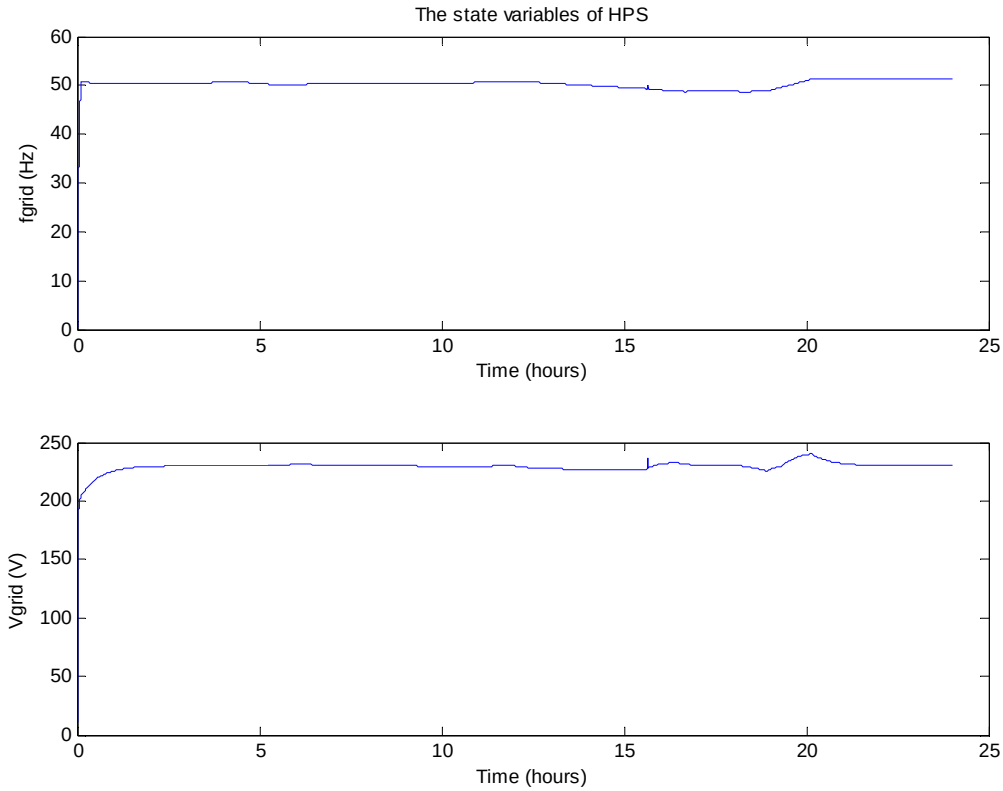

Fig. 5.14: The state variables of HPS during integration of PV system and diesel genset

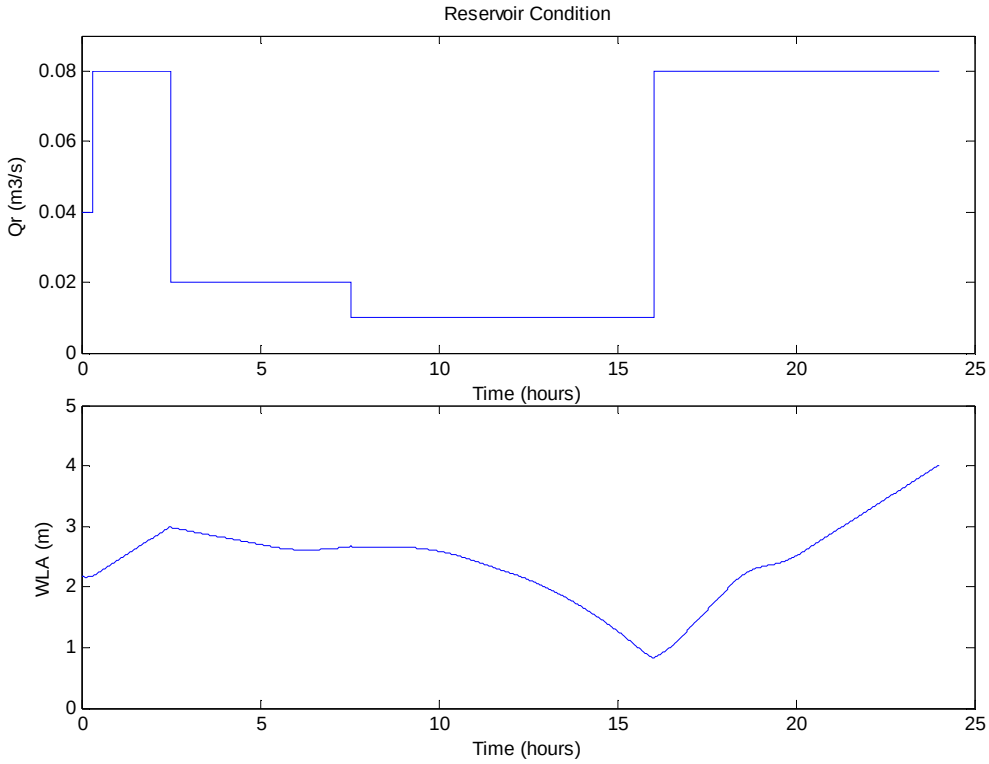

Fig. 5.15*: The reservoir condition during integration of PV system and diesel genset*

6 Comparison between measurement-simulation

The behaviour of individual models, which have been explained above and have been used to form the target HPS, can be verified through the measurements. To get the parameters and to find the characteristics behaviour of the components like PV module, synchronous generator, asynchronous machines some measurements were done in the lab as well as data sheets available from the manufacturers were used.

6.1 Synchronous generator parameter determination

The important parameters of the SG necessary to make a model have been determined by carrying out the experiments like open circuit test and circuit test [1], [2]. The data of SG is shown below.

Fig. 6.1: The nameplate of the synchronous machine used for the parameter determination

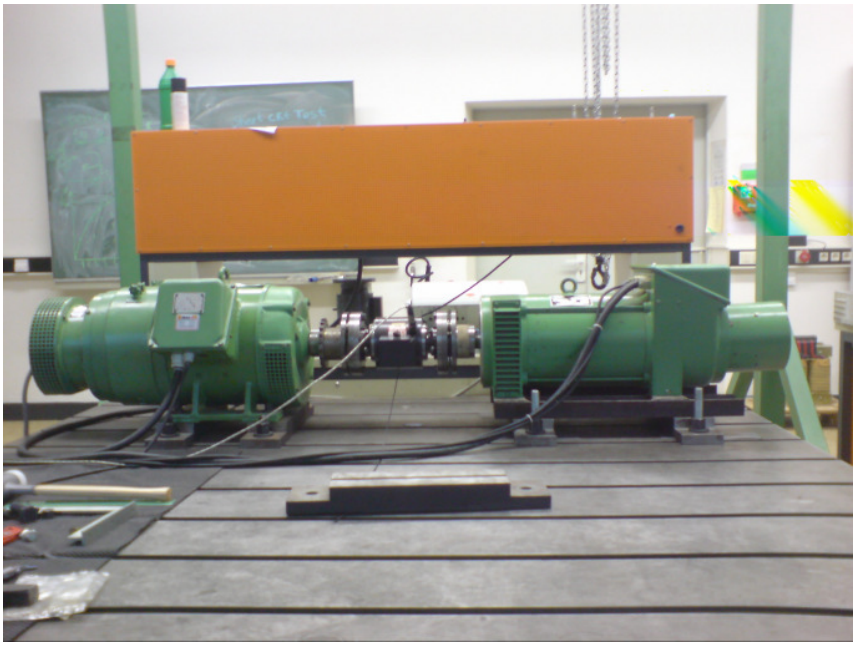

Fig. 6.2:Arrangement of DC motor and SG to determine the generator parameters

Open circuit test

The open circuit test is carried out to determine the effect of field current on the terminal voltage at no load condition. The test is carried out as shown in fig. 6.3. The result is tabled below.

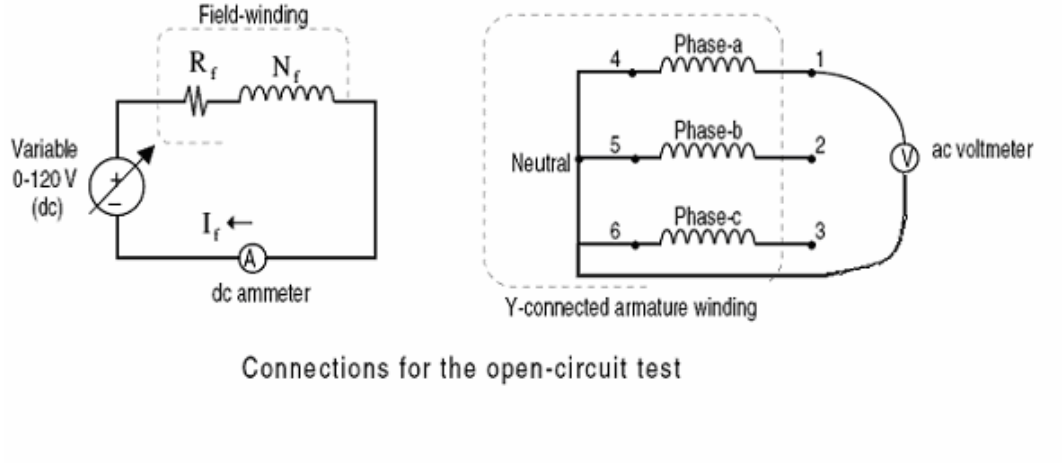

Fig. 6.3: Connection arrangement for the open circuit test

I_f (A)	1	2	3	3.5	5
V_{ph}(V)	59.2	154.3	202.5	232.5	251

6.1.2 Short circuit test

The short circuit test is carried out to find the behaviour of current in relation to the field current when all the terminals of SG are short-circuited as shown in fig. 6.4.

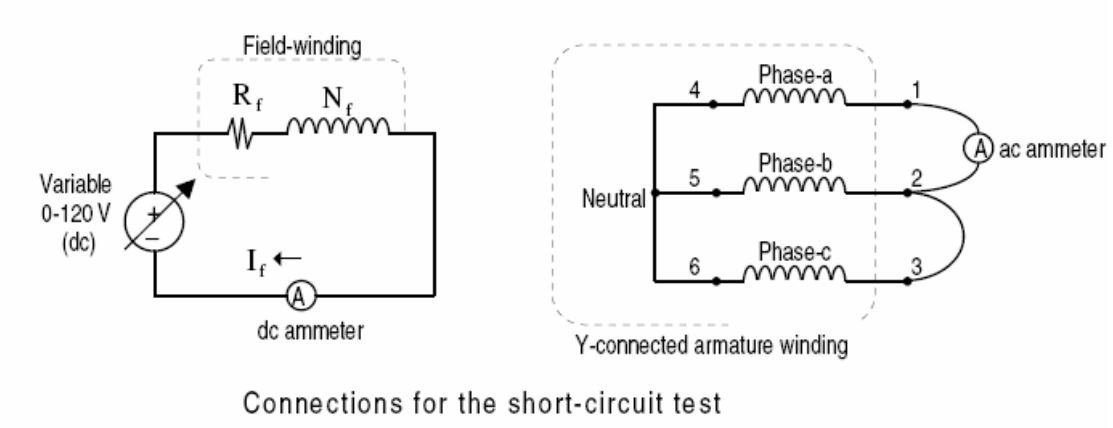

Fig. 6.4: Connection arrangement for the short circuit test

The result of this test is tabulated below.

I_f (A)	1.5	2.0	3.0	3.5
I_{sc}(A)	6.6	10.5	13.0	14.3

To determine the parameters, both curves are converted in per unit and plotted together in one graph which in shown in fig 6.5.
The nominal values are

$$V_{ph(n)} = 230[v]$$
$$I_{line(n)} = 14.4[A]$$
$$I_{f(n)} = 10.5[A]$$

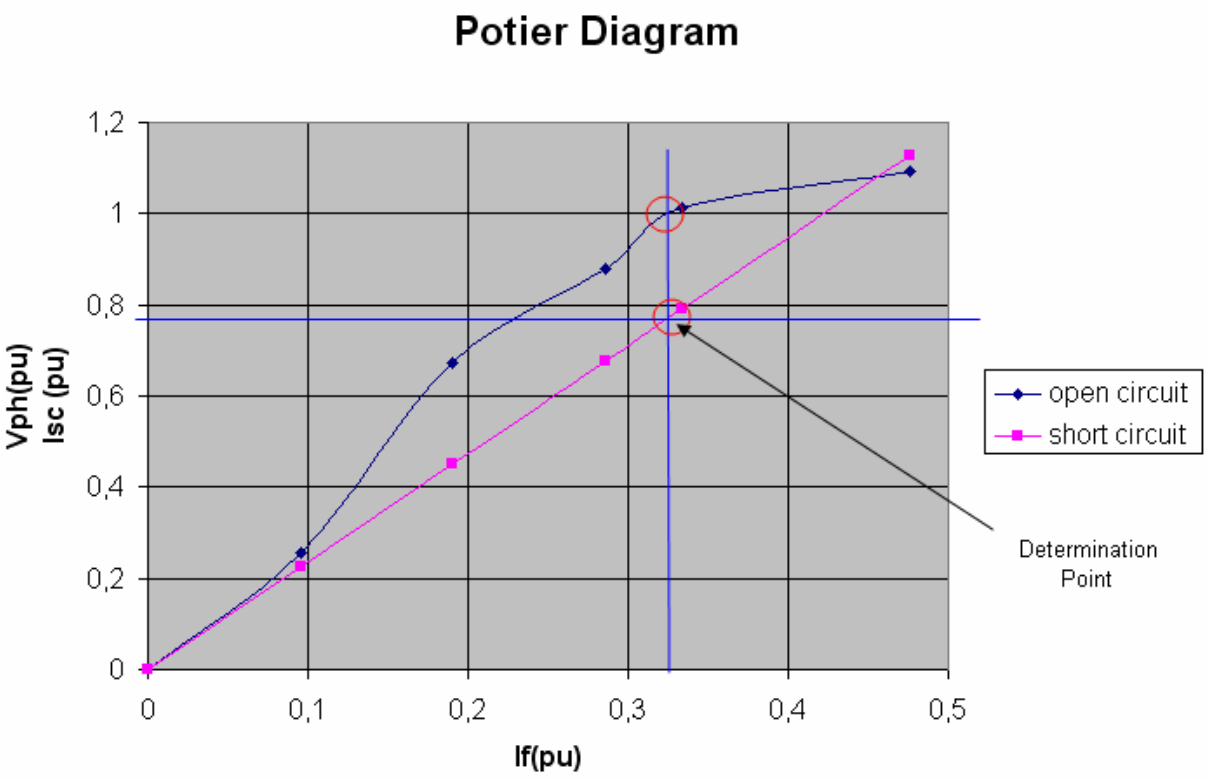

Fig. 6.5: Construction of pu open and short circuit diagram based upon the measured data

From the diagram, the synchronous d – axis reactance (X_d) is calculated as below

$$Z_d = \frac{V_{sN}}{I_{sc}} = \frac{230}{11.5} = 20[\Omega]$$
$$X_d = \sqrt{Z_s^2 - R_s^2} = \sqrt{20^2 - 1.05^2} = 19.97[\Omega]$$

The synchronous q-axis reactance can be calculated as

$$X_q = 0.65 X_d = 12.96[\Omega]$$

The stator resistance is measured directly by a multimeter. The measurement are given below

R_{12}	R_{23}	R_{31}	R_{ave}	R_s=0.5Rave
2.2	2.1	2	2.1	1.05

The field resistance (R_f)
It is measured by supplying the dc current to the field winding.

$$R_f = \frac{V_{DC}}{I_{DC}} = \frac{0.973}{0.277} = 3.5[\Omega]$$

6.2 Asynchronous machine

The behaviour of an asynchronous machine used in DGS and the wind turbine generator can be verified by comparing the current patterns between the measurements and model when the generator is connected to the available grid. The comparison is shown in fig. 6.6 where first figure is the current pattern from the simulation model and second figure is the current pattern from measurement. Both patterns show that at the beginning the machine draws very higher current (~ 25 A), which is around 5 times of no load current in case of 6 poles. After the 4th cycles, the current decreases to the no load current, which is around 5 A in both cases.

(a) simulated behaviour

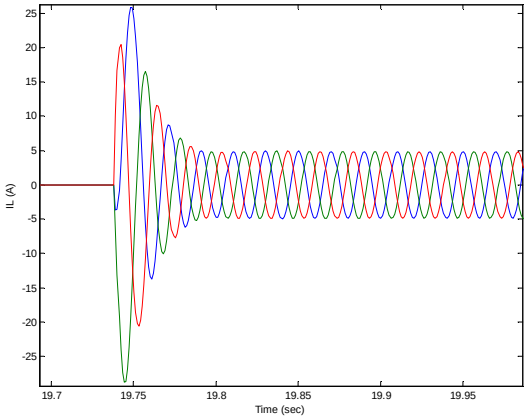

(b) measured behaviour

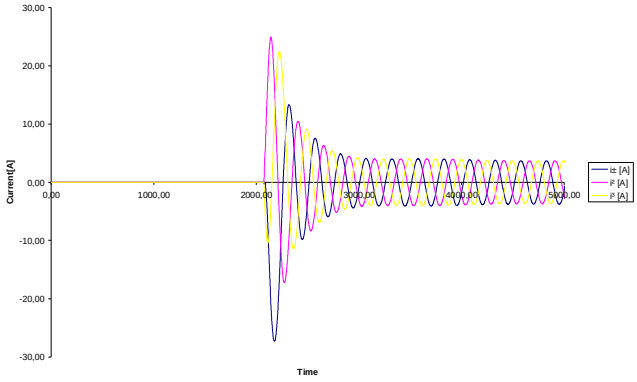

Fig. 6.6: Comparison of (a) simulated and (b) measured current pattern during connection of ASM

6.3 PV System

The characteristic behaviour of PV module obtained from the simulation model is varied by the measurement. A monocrystal PV module of 10 W_P is used to measure the characteristics. It is shown in fig 6.8.
STC parameters of above module

$E(Wm^{-2})$	T(K)	AM	$P(W_p)$	I_{SC}(A)	V_{OC}(V)	V_{mpp}(V)	I_{mpp}(A)
1000	298	1.5	10	0.62	21.5	16.9	0.6

The power production from the PV module depends upon the meteorological conditions (E and T) and the module voltage. In this experiment, the relation between P and V at different irradiation levels were measured. During the measurement, it has been observed that temperature of the PV module increased from initial temperature

298 K to 313 K when the load was changed from no load to full load. To compare the behaviour closely, a slope is used to change the temperature similarly as in the real measurement.

Fig. 6.7: The 10 W_P PV module used to determine the characteristics

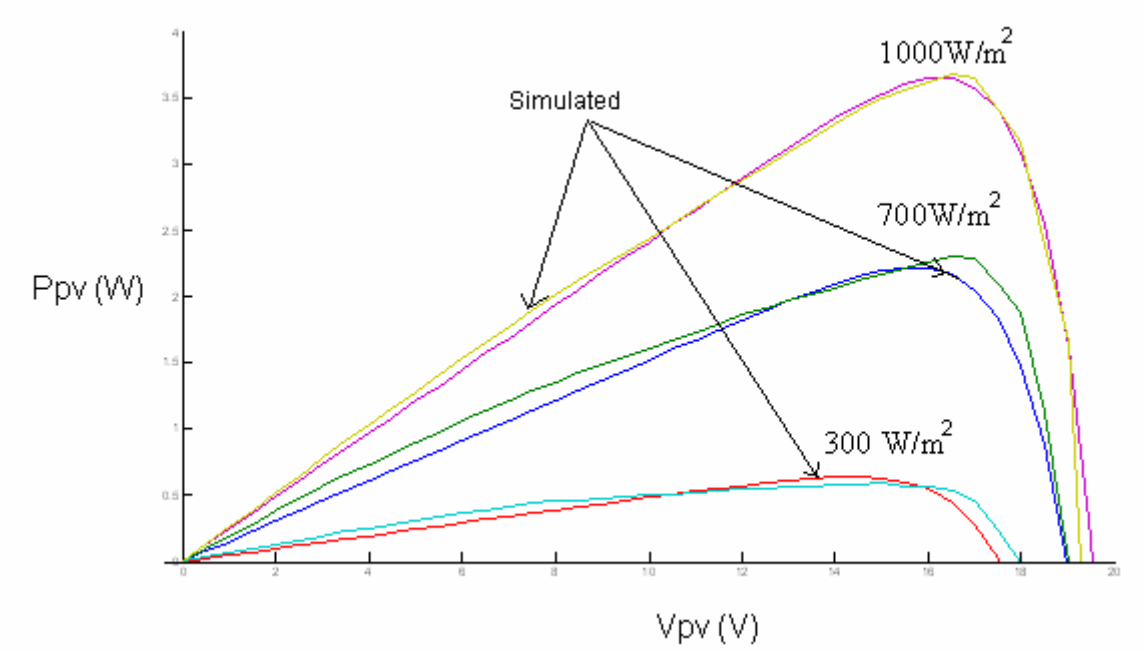

Fig. 6.8: Comparison of PV model characteristics between measurements and simulations

6.4 Battery Model

After simulating the battery model with normal charging and discharging current pattern, it is important to validate the performance. It is done through simulating the model with a real current and voltage data. A battery of 90 Ah, 12-voltage battery had been tested for nearly 3 weeks of time. During the testing phase, the current and

voltage data had been measured in time interval of 1 minute. So the model is also parameterised to 90 Ah, 12 volt real battery. The real data of current and voltage available in excel file is imported to Simulink file.

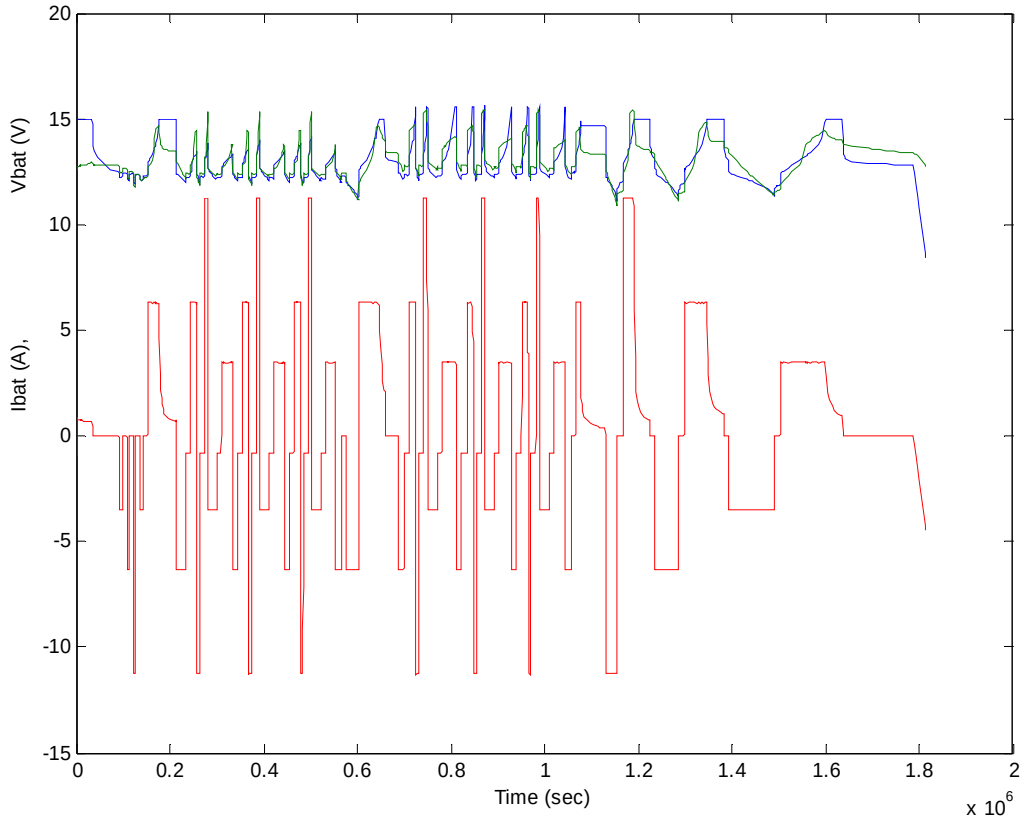

Fig. 6.9: The comparison between measured (green) and simulation (blue) voltage patterns

The above fig 6.9 shows that the comparison between the voltage patterns obtained from simulation and measurement. In this figure, three curves have been shown. The first and second curves, which are much closed to each other, are the voltage curves where the blue colour curve represents the measured voltage pattern and the green colour represent the simulated pattern. The third curve represents the measured current. The reason behind this type of current pattern is that the battery is charged and discharged every time with same among of Ah but with different charging and discharging rates. From the voltage curves it can be observed that the simulation voltage pattern is close to real one. Even though the current is changed suddenly, the voltage pattern changed with some curve, which is due to an effect of the diffusion capacitance, with higher time constant.

7 Microcontroller based EMU development

In this chapter, a hardware system is implemented based upon the Simulink model. A simple, compact, reliable and easily replaceable EMU is developed using a low power microcontroller and computer language C. The hardware EMU consists of a microcontroller MSP430F449 as the main unit, which receives the on-line data from outside, processes based upon program, supplies output to outside components. The EMU is implemented in two steps. First one, the microcontroller is integrated with a keyboard and a display unit. The inputs are given through the keyboard and outputs are displayed in the LCD display. Second one, some sensors are used to capture outside online data like irradiation, temperature, water level, frequency etc.

7.1 Microcontroller MSP430F449

MSP430F449 from the Texas instruments is a digital signal processor, which has been constructed, based on “von-Neumann-Architecture”. This processor has 16 bit RISC and it is designed for low power operation which is also known as ultra low-power-mc. Because of such a low power consumption, this microcontroller is an optimal solution for long-term operation with batteries. The short abbreviation MSP comes from “Mixed Signal Processor” and it can process analog and digital signal.
To achieve the energy efficient operation, six different modes are available in MSP430Fxx family microcontrollers and they are controlled by an intelligent management. By such an intelligent system, the microcontroller is brought to slip mode when it is not in operation. In this mode, it is possible to save up to 90% of energy with only one battery; it is possible to operate up to 10 years.

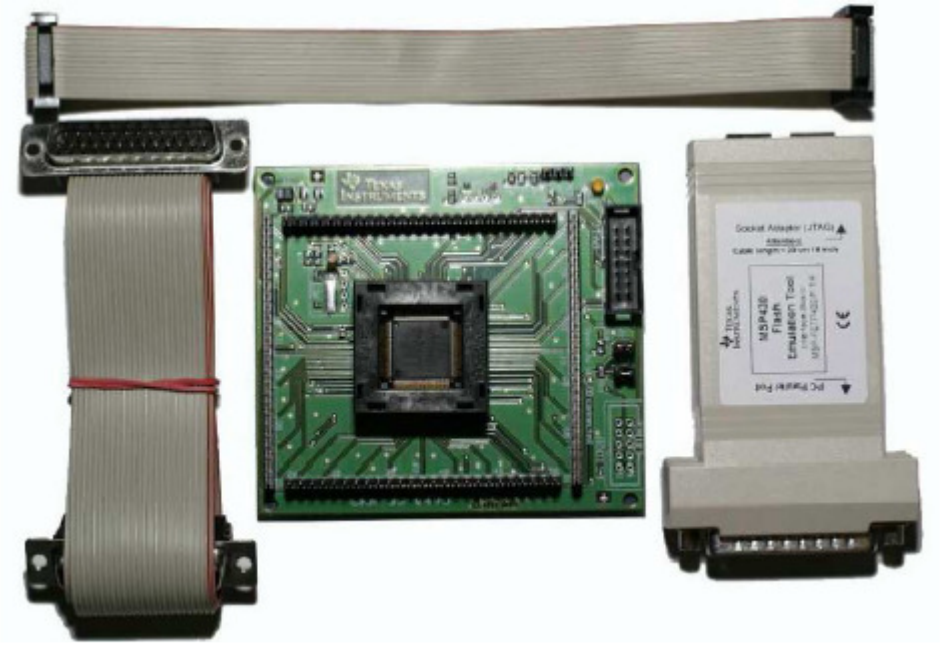

Fig. 7.1: The microcontroller MSP430F449 with its emulator

The six operation modes are

- Active mode
- Low Power Mode 0 (LPM0)

- Low Power Mode 1 (LPM1)
- Low Power Mode 2 (LPM2)
- Low Power Mode 3 (LPM3)
- Low Power Mode 4 (LPM4)

From above six modes, the four important modes are active mode, LPM0, LPM3, and LPM4. The meaning of these modes is briefly described.

Active mode: CPU is active.
LPM0: CPU is in sleep mode but peripheral units are active.
LPM3: Operation mode battery applications, peripheral units, which work on ACLK, are active and the rest is in, sleep mode.
LPM4: only interrupts are active; all other units are in sleep mode.

7.1.1 CPU Architecture

The CPU of MSP430 has been made as 16 Bit CPU. It consists of 16 16-Bit registers, in which four are reserved as special registers. They are program counter, stack pointer, status register and constant generator. Others are general purpose registers. The register structure is shown in fig. 7.2.

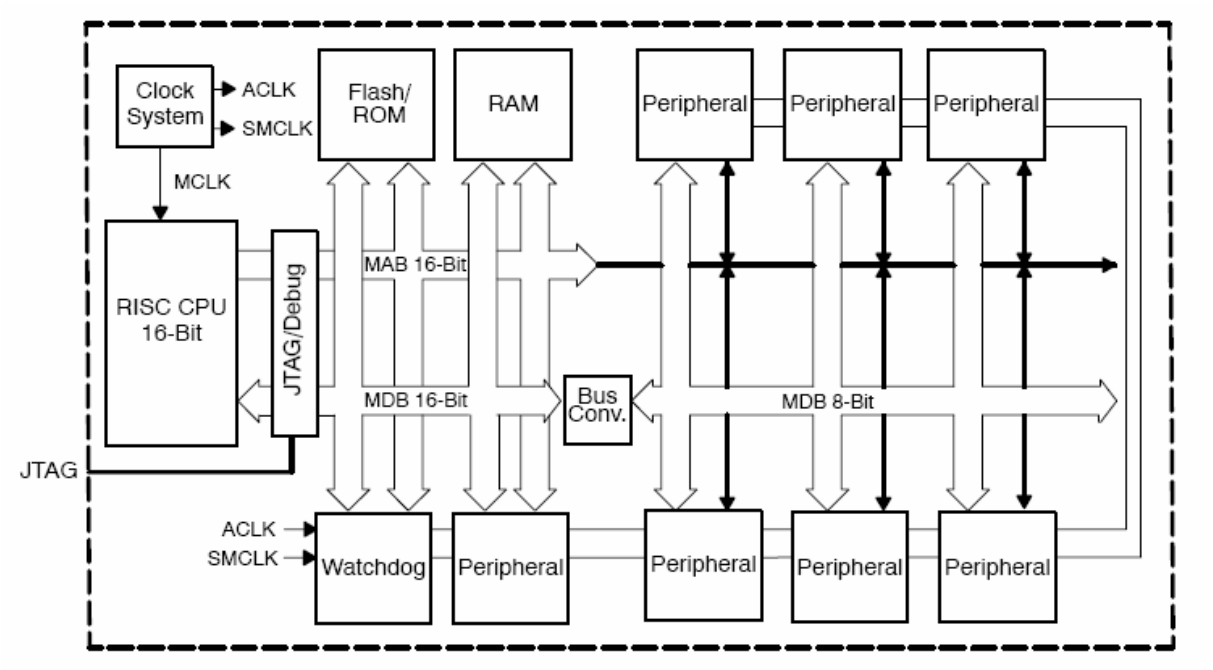

Fig.7.2: Internal structure of MSP430F449

Key features of MSP430x4xx family includes

- Ultralow-power architecture extends battery llife
  - 0.1 mA RAM retention
  - 0.8 mA real-time clock mode
  - 250 mA/MPS active
- High – performance analog ideal for precision measurement
  - 12-bit or 10 bit ADC – 200 ksps, temperature sensor, V_{ref}

- 12-bit dual DAC
- Comparator-gated timers for measurement
- Supply voltage supervisor

- 16-bit RISC CPU enables new applications at a fraction of the code size
  - Large register file eliminates working file bottleneck
  - Compact core design reduces power consumptions and cost
  - Optimised for modern high-level programming
  - Only 27 core instructions and seven addressing modes
  - Extensive vectored-interrupt capability
  - In-system programmable Flash permits flexible code changes, field upgrades and data logging

Fig MSP430 architecture

7.1.2 Address Space

The MSP430 consists of 64 kB internal flash memory. Using 16-bit address bus, 65534 (64KB) memory cells can be addressed. The memory cells are 8 bit in size and possible to address byte wise. The flash memory had two sections. First one is n-segment main memory and second one is data memory A & B. Both types of memory sections can be individually deleted. The memory structure is shown in fig. 7.3.

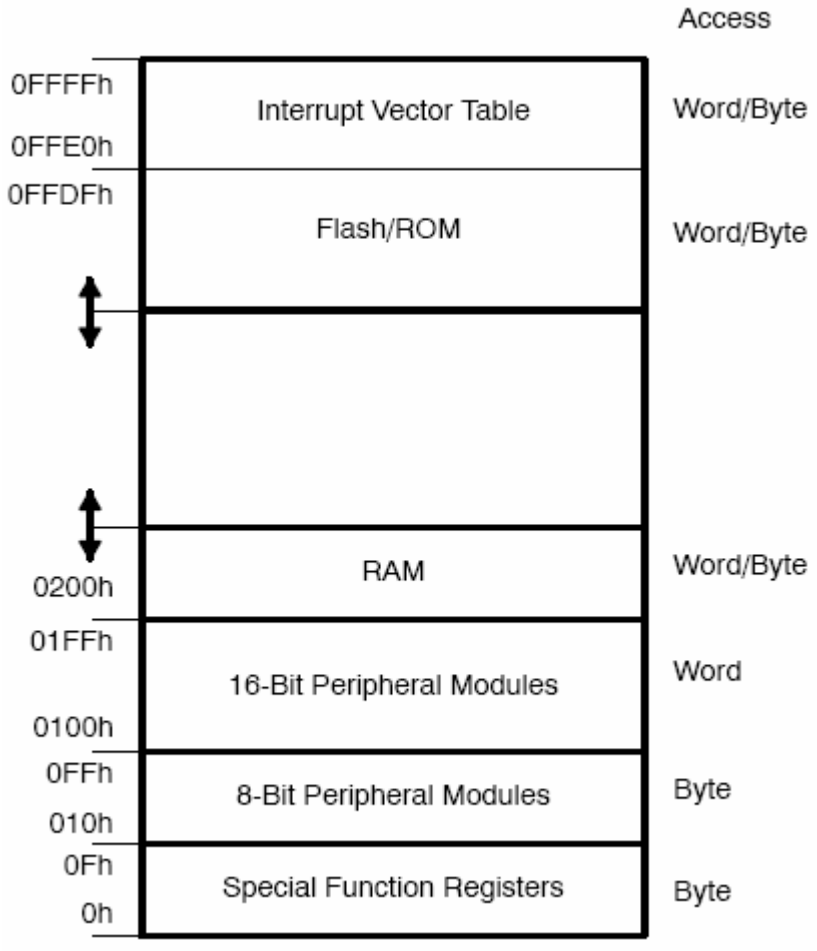

Fig.7.3: The address space of the MSP430F449

7.1.3 On-chip peripheral units

The MSP430 family has different types of peripheral units and interfacing is different from one version to another.

1. Clock generator
2. SVS (supply voltage supervisor)
3. Hardware multiplier
4. DMA controller
5. Digital I/0
6. Watchdog Timer
7. USART peripheral interface
8. ADC, DAC
9. LCD controller
10. Timer

Clock generator

The MSP430 family consists of the frequency locked loop (FLL+) hardware, which supports low system cost and ultralow power consumptions. Three different types of clock sources LFXT1,DCO and XT2 oscillator can be connected to the MSP to produce low to high frequencies (ACLK, MCLK, SMCLK) where

- ACLK: auxiliary clock: ACLK is produced by LFXT1CLK source. It is 32 kHZ used for individual peripheral modules.
- MCLK: Master clock: it is produced by LFXT1CLK or DCOCKL and it can be divided by 1,2,4 or 8 within the FLL block. MCLK is used by CPU and system.
- SMCLK: sub-main clock: sub-main clock: it is also produced by XT2CLK or DCO and used by individual peripheral modules.

SVS (Supply Voltage Supervisor)

It is used to monitor the Avcc supply voltage so that the malfunctioning of software execution can be avoided.

Hardware multiplier
The hardware multiplier is a peripheral and not a part of MSP430 CPU. It can multiply with or without 8 bit/16 bit numbers and provides result in 32 bit.

DMA controller
It can transfer data from one memory address to another without intervening CPU. For example, the DMA controller can move data from ADC12 to DAC12.

Digital I/0
The MSP430F449 has 6 digital I/O ports, in which port 1 and port 2 have interrupt capability. Each port has 8 I/O pins. Every I/O pin is individually configurable for input or output direction and each I/O pin can be individually read or written.

Watchdog-Timer
The primary function of the waterdog timer module is to perform a controlled system restart if a software problem occurs. It the selected time interval expires, a system reset is generated. It can be achieved by hardware or software.

USART Peripheral Interface
The MSP430 has two universal synchronous/asynchronous receive/transmit (USART) ports which supports communications with UART, SPI and I^2C peripheral units.

ADC12 and DAC12
The MSP430F449 consists of 12 bit analog to digital and 12 digital to analog converter. Port 6 can be used for ADC purpose.

LCD-Controller
The MSP430F449 controller has an internal LCD driver. It can directly drives LCD display by creating the ac segment and common voltage signals automatically. The MSP430 LCD controller can support static, 2-Mux, 3-Mux and 4-Mux LCDS. The available pins are S0 to S38 for LCD or 7 segment display connection.

7.1.4 Pin configuration

The pins are the most important part of the processor because they stabilize the communication between external world and processor possible. Six communication ports (P1-P6) are available and each port has 8 pins. The reason of grouping for 8 pins as port is that the control functions or signals can be directly stored in a 8 bit register. To achieve the economic and compact processor, the ports are designed with main function and extra function. The desired function can be configured by SEL register. Normally the ports are used as I/O pins (PxSEL=0x00). By selecting '1', the second function of the pin is chosen. It is also possible to configure pin as an input or output. The command PxDIR = 0x00 makes all pins as output. If a particular pin is to be configured as input, for example pin 0, PxDIR=0x01. Another important command is PxIN = 0xFF or PxIN = 0x00.This command enables the related pins to receive data. A particular pin can be chosen, for example pin 3P3IN=0x03.
To receive and transmit data, two registers are built in MSP430. The IN-register of individual ports receives input signal and the OUT-register provides output signal (data). It can give 3.3V as logic high and can receive max 3.8 V.
Table 7.1 shows once again the complete control register with their functions.

Table 7.1: The configuration of pin for different purpose

Control Register	Function	Bit=0 (not used)	Bit=1(used)
PxIN	Input	Low-Level at input	High-Level at input
PxOUT	Output	Low-Level at output	High-Level at output
PxDIR	Direction	Pin as input	Pin as output
DxIFG	Interrupt Indicator	No interrupt	Interrupt
PxIE	Interrupt possibility	Pin is not allowed for	Pin is allowed for

		interrupt service	interrupt service
PxIES		Interrupt at Low/High-change	Interrupt at High /Low-change
PxSEL	Module selection	Port selected	Module selected

7.1.5 Power supply for MSP430F449

The microcontroller MSP430 family works on 3.3V. To get the accurate 3.3V, 230V AC voltage is stepped down to 12 V DC and a voltage regular LM1117T is used. The power supply circuit is shown in fig. 7.4.

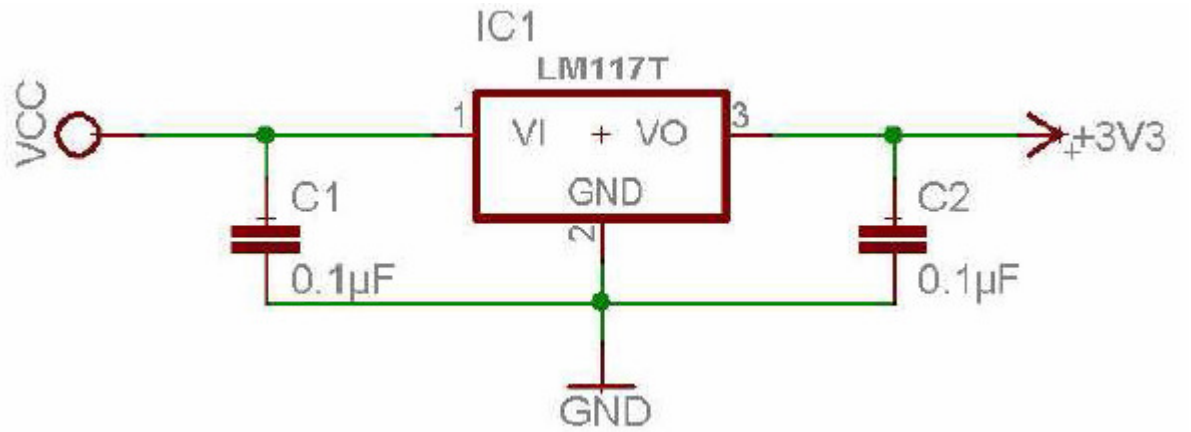

Fig.7.4: The schematic diagram of 3.3 V supply for the MSP430F449

7.2 Point –Matrix LCD Display

It is necessary to display the desire results properly to know the actions taken by the microcontroller and to know the outputs. For this purpose, a 4x20 LCD- display unit is used. This display unit has own controller, which controls the individual matrixes. Even though the manufacturers are different, LCD displays have moistly same pin configuration.

The display "LCD204B LFD" from Reichelt (www.reichelt.de) has HD44780 compatibleJS0076B controller to control display. It consists of fix characters known as as ASCII table in internal ROM. It is also possible to generate user-defined characters. This unit has total 14 lines, in which 11 lines are signal lines and rest are control lines.

The important features are

- 4 bit or 8 bit transmission
- ROM for 80 characters
- Internal reset
- 2xKS0076b controller
- Display format for 5x7 points of 5x10 point

The interface between the LCD display and microcontroller is shown in fig 7.6. Pins 16.17 and 31,32 are reserved for background light adjustment and have not been connected here. The LCD display works on 5 V so the voltage regulator 7805 is used. The microcontroller transmits data with 3.3 V as logic high, which is not suitable for LCD display. It means this 3.3 V signal must be converters into 5 V. It is done through unidirectional driver IC-SN74LS244 (octal buffer, line driver).

Table 7.2: the pin configuration of the LCD display

Pin NO.	Symbol	Level	Description
1, 17	VSS	0V	Ground
2, 18	VDD	5.0V	Supply voltage for logic
3, 19	VO	---	Input voltage for LCD
4, 20	RS	H/L	H : Data signal, L : Instruction signal
5, 21	R/W	H/L	H : Read mode, L : Write mode
6, 22	E	H, H → L	Enable signal for KS0076
7, 23	DB0	H/L	Data bit 0
8, 24	DB1	H/L	Data bit 1
9, 25	DB2	H/L	Data bit 2
10, 26	DB3	H/L	Data bit 3
11, 27	DB4	H/L	Data bit 4
12, 28	DB5	H/L	Data bit 5
13, 29	DB6	H/L	Data bit 6
14, 30	DB7	H/L	Data bit 7
15, 31	A	---	Back light anode
16, 32	K	---	Back light cathode

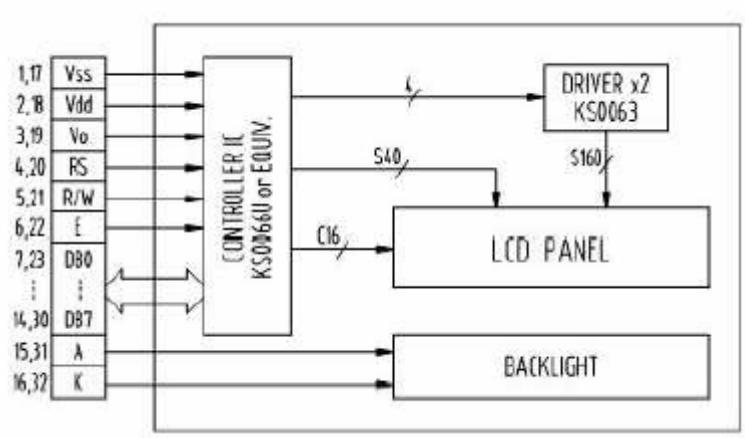

Fig.7.5: The pin configuration of LCD display

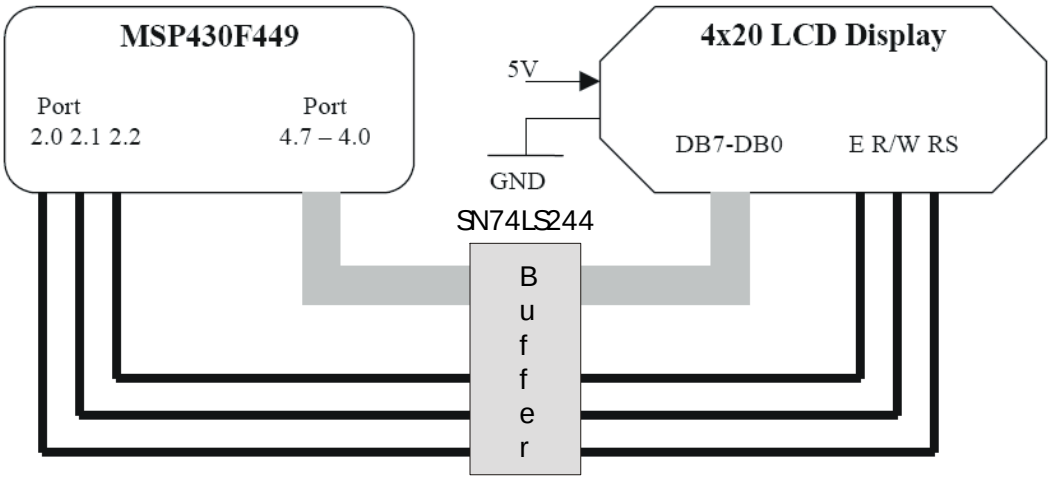

Fig.7.6: The interfacing of the LCD display with the MSP430F449

Table 7.3: the address map of the LCD display

Characters	1	2	3	4	5	6	7	8	9	10	11	12	13	14	15	16	17	18	19	20
First line (H)	00	01	02	03	04	05	06	07	08	09	0A	0B	0C	0D	0E	0F	10	11	12	13
Second line (H)	40	41	42	43	44	45	46	47	48	49	4A	4B	4C	4D	4E	4F	50	51	52	53
Third line (H)	14	15	16	17	18	19	1A	1B	1C	1D	1E	1F	20	21	22	23	24	25	26	27
Fourth line (H)	54	55	56	57	58	59	5A	5B	5C	5D	5E	5F	60	61	62	63	64	65	66	67

7.3 4x4 matrix keyboard

A simple 4x4 matrix keyboard is constructed to feed inputs to the microcontroller. It consists of the switches, which have been connected, in matrix form. One complete port of the microcontroller has been used to connect the keyboard. The schematic arrangement of keyboard is shown in fig 7.7. The keyboard is connected into port 3 in which 4 lines are set as outputs and 4 lines as input. C code is used to find out the pressed key. The 12 kΩ registers are used to reduce disturbance voltages. The pins of the microcontroller are very sensitive. The keyboard has numerical numbers from ‘0 to 9’, characters (-/+), point (.) curser moving right and left, OK and Del.

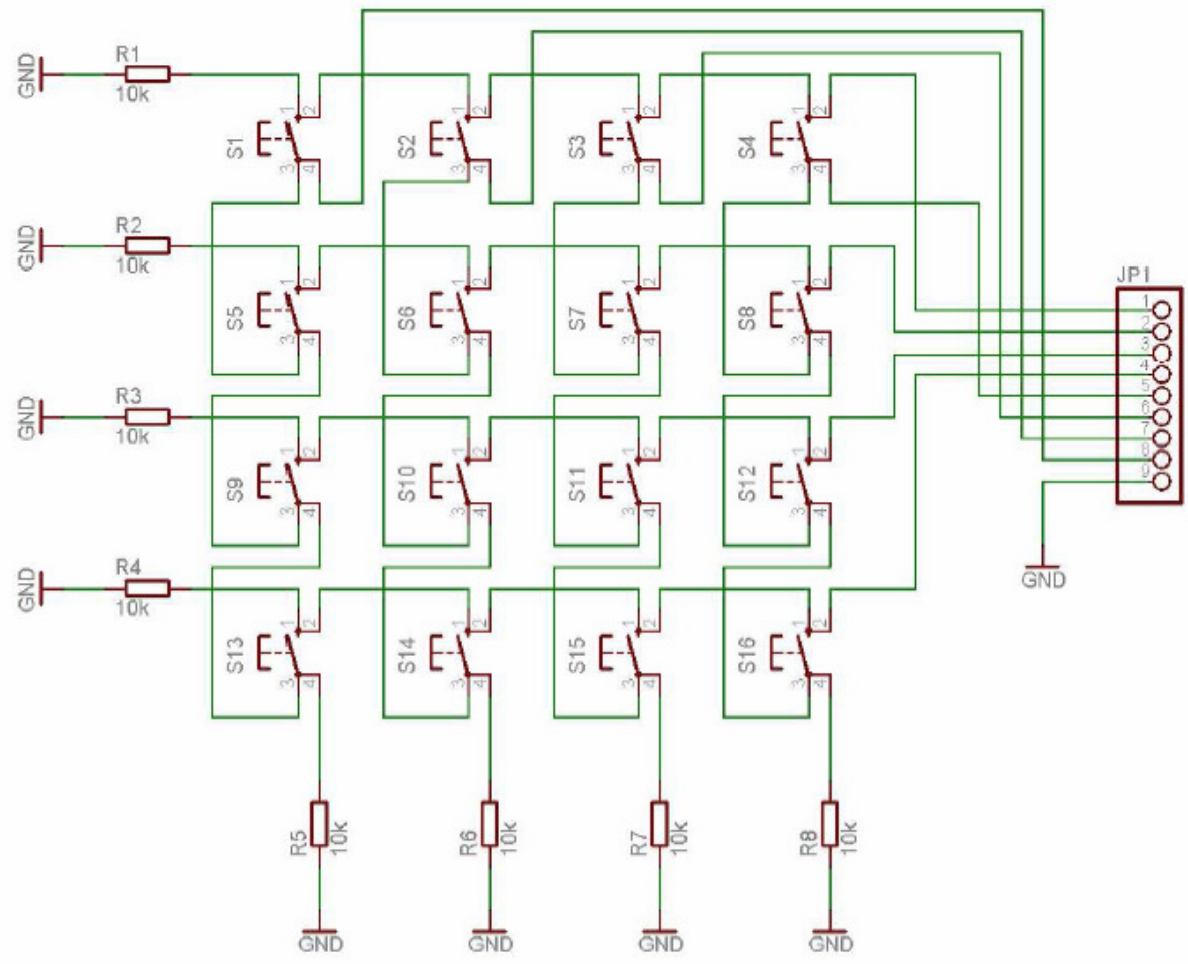

Fig.7.7: The schematic connection of switches to form 4x4 matrix keyboard

7.4 Software simulation in hardware level (embedded system)

Most of the microcontrollers are programmed with the computer language 'C'. If the program is small, not complex and small size memory is available, assembly language can be used. By using C language, the program is more understandable and easy to write. It is a structural and modular language. Further advantages of C are development speed, reliability and reuse capability. It is possible to structure main program in many small functions. The interfacing between the microcontroller MSP430x family and the computer is done through development software from IAR embedded workbench (http://www.iar.com). This software can easily be used in Microsoft windows.

7.4.1 C code for PV module

The power available from the PV module is determined continuously to manage the optimal energy dispatch. As explained above irradiation and temperature play main role in the PV power contribution. As in Simulink, C code for PV module is written based upon STC. Using two sensors, E and T are captured (measured) and supplied to the microcontroller. The C-code written for PV module calculates available power from PV module. To test the behaviour of C code, first it is run only in 'C' compiler with variable E and T. The C code is given in appendix.

7.4.2 Energy Management Unit in microcontroller

As mentioned above the functionality of EMP is tested in two ways. The behaviour of EMP is first tested by providing inputs like load in the isolated grid and available power from PV system through KB. In second option, further hardware is integrated with microcontroller to capture variable variables.

Keyboard option
In this option, EMP consists of many functions like keyboard, display, energy management code. In this program all the possible events in the HPS has been written, like changing PV power, diesel on, diesel off sequences etc. All C codes for keyboard, display and energy management are given in appendix.

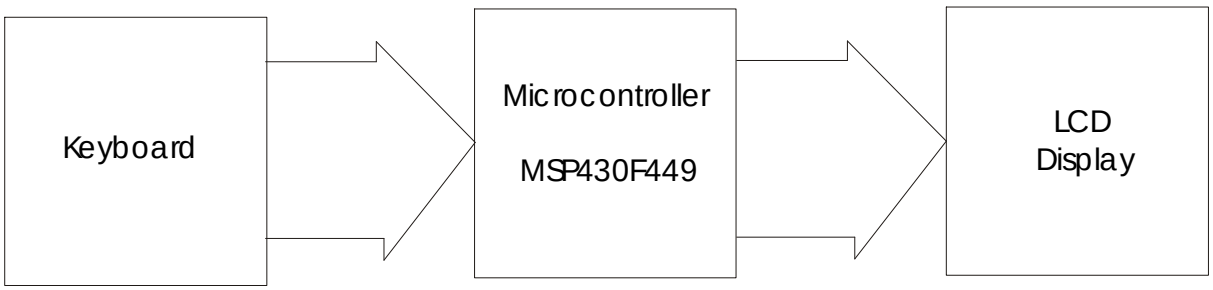

Fig.7.8: The architecture of EMU with the keyboard

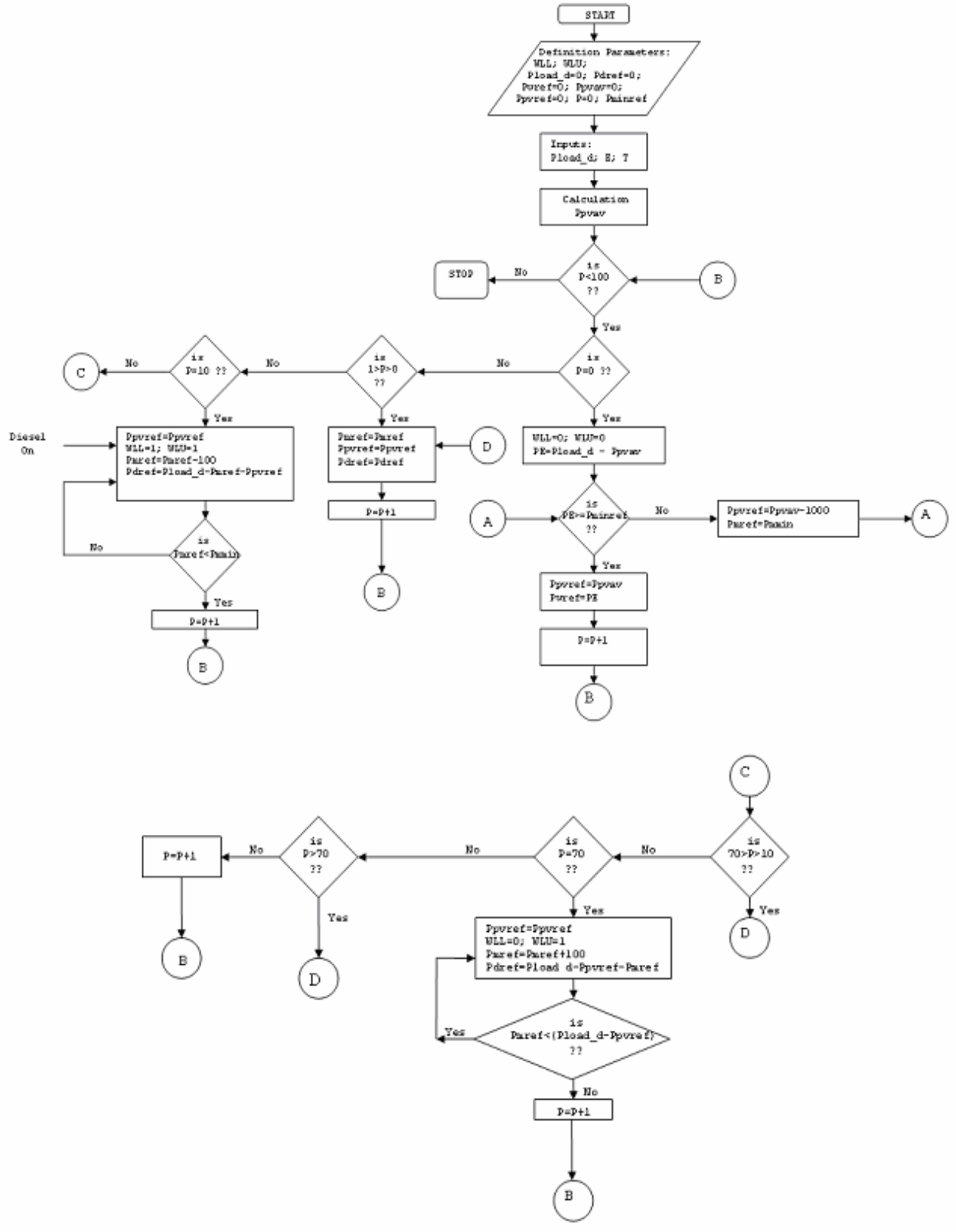

Fig.7.9: Flow chart diagram of the keyboard option EMU

Flow chart

The complete program runs in a loop, the number of loops is user-defined number. As the program runs initially all variables are initialise to zero. The program requests the P_{load}, which is to be given the keyboard. When $P_{load} > 0$ program goes to loop. At the beginning, when $0 >= P < 100$, DGS is off, $P_{pvav}=0$ so $P_{mref} = P_e = P_{load}$. At the end of the program, P is increased by 1 and at the beginning P is checked. When P is equal to 10, the diesel genset is turned on and P_{mref} is reduced in steps which is user defined number. This decrement is done until $P_{mref} <= P_{mmin}$. The diesel genset is kept on at this stage unit P < When P is equal to 50, the diesel turn off signal is generated and P_{mref} is increased in step fashion, correspondingly P_{dref} is decreased. This process occurs until P_{dref} becomes 0. If somewhere P_e is less then P_{mmin}, P_{pvref} is reduced in used defined step.

Result

The power balance in the system is maintained by the software code downloaded in the microcontroller. The reference powers generated for different energy systems at the constant load of 7000 W are shown in fig.7.10.

As the simulation is started, the reference power from the PV system is increased in sinusoidal function from the point A to the point B. Because of power availability from the PV system, the reference power for the MHPP is reduced in same function such that the sum of two reference powers remains always same as to the load. At point C, the diesel turn-on signal is generated so the reference power for DGS is increased is slowly in a ramp function; the effect on the MHPP is that its reference power decreased with same slope. At point D, the reference power of MHPP reaches to minimum and it remains in this level until the diesel turn-off signal is generated. The reference power for the diesel genset is reduced slowly in the ramp function. At the point F, the diesel genset is completely shut down.

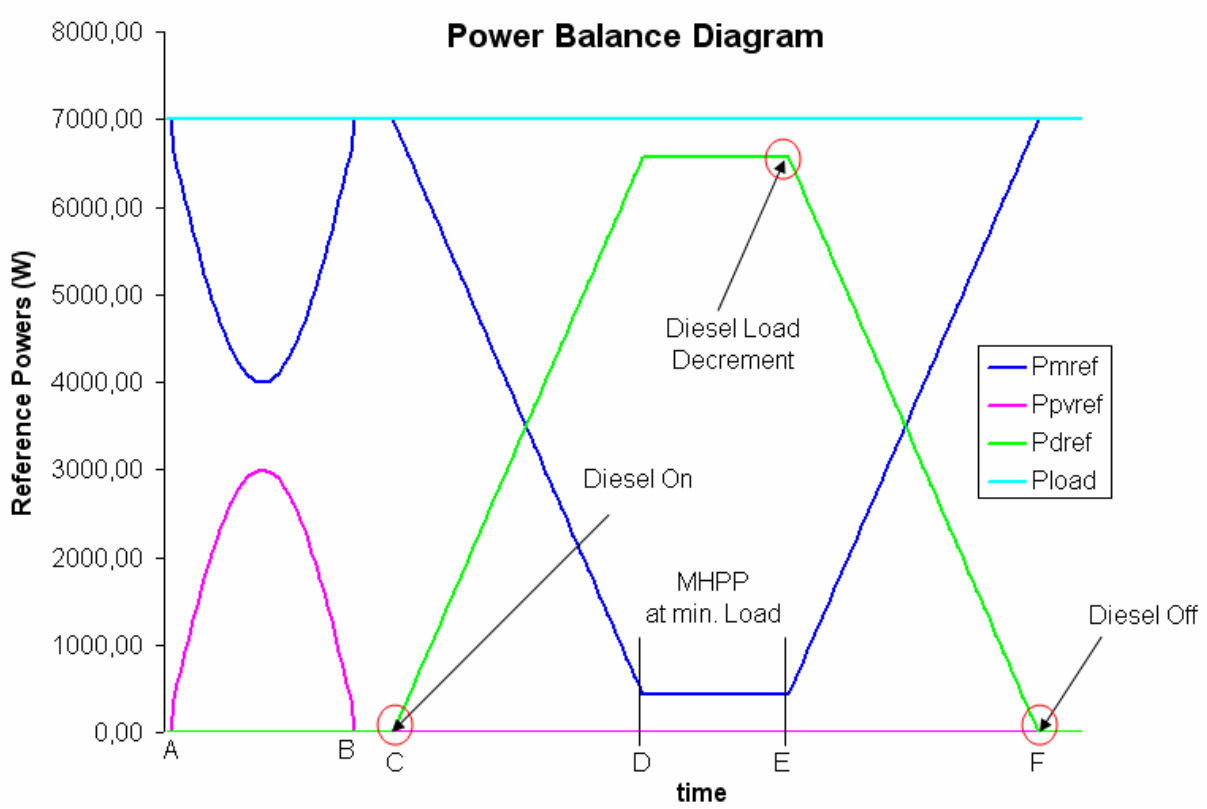

Fig.7.10: The power balance in the system

Sensor integration with microcontroller

In this option, the sensors are used instead of the keyboard to capture the external inputs. For example, the load in the grid is given as the voltage signal through potentiometer. The inputs E and T are captured by a photocell and temperature sensor. As mentioned above, the microcontroller has internal ADC. These signals are analog voltage. Using ADC, they are converted into equivalent digital voltages and further converted into appropriate values. For example, ADC provides 4095 decimal value if input is 2.5 V (in case of internal voltage reference). If this signal is to be used as the available power from the PV system, it is necessary to multiply by 0.73 so that maximum available power will be 3000W. An op-amp based circuit is developed to get signal from the water reservoir. Simply two wires are used as sensors. The interconnection of these sensors with microcontroller is shown in fig. 7.11. The detailed scheme is give in appendix.

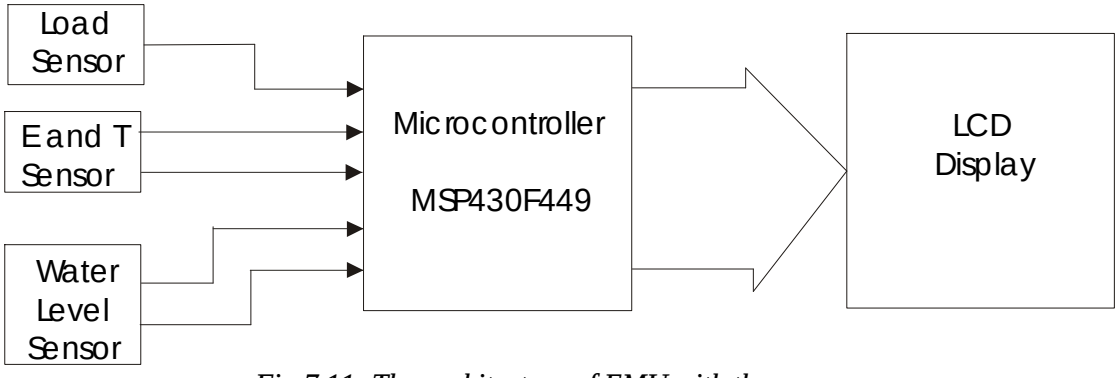

Fig.7.11: The architecture of EMU with the sensors

8 Cost-Benefit Analysis –HPS for Nepal

The question of economy plays a very important role in the utilisation of renewable energy sources. This is the main negative factor which most of the time tries to stop its application [1]. Even though economically HPS may be expensive than conventional system, it is very important to promote such system in rural areas of the developing countries like Nepal. In this chapter, the total cost to develop such HPS-Project, its kWh cost, its benefit to the society will be analysed.

The implementation of a project starts from the feasibility study to commissioning. Many steps are to be carried out to make a project successful so that it starts to deliver power to community. Every step in the implementation requires investment. Such steps may be

1. Feasibility study
2. Design
3. Transportation
4. Civil construction
5. Equipments
6. Installation
7. Commission

After commissioning the project, new cost comes in the calculation that is the operation and maintenance cost of the project. The total investment cost is not only the investment cost but the sum of the investment cost and O&M cost.

The cost-benefit cost analysis has two parts – financial analysis and economic analysis. According to the Asian Development Bank [ADB], “for a project to be economically viable, it must be both financially and economically efficient. If a project is not financially sustainable, the economic benefit will be not released. Financial analysis and economic analysis are therefore two sides of the same coin and complementary” [2]. These two analyses can be separately expressed as follows.

8.1 Financial analysis

A financial analysis is usually undertaken in order to evaluate the cost and benefit brought about by the project to a person or business [3]. It indicates that the financial analysis is only related to the investor or business group who invests and confirms all investment needs and the revenue return from the project though out the life of the project [4].

8.2 Economic Analysis

An economic analysis is undertaken in order to access the overall impact of the projects on the economic welfare of the citizens of the country. Thus, the scope of the economic analysis is larger than the financial analysis as it assesses a project in the context of the national economy [2]. In such circumstances, the private groups may not be interested. The subsidies for its promotion is required, the donors are to be motivated.
In contest of Nepal, most of the micro hydro projects are supported by the government subsidises, international donors, community contributions. In such conditions, only financial analysis will be considered. The total investment cost required to develop such a project and its revenue return for defined life time is first interest for the investors, governmental organisation, INGO and communities so that they can confirm the net subsidy required at the beginning of the project.

8.3 HPS Project – MHPP, PV System, Diesel Genset

As explained above in chapter, the HPS consists of MHPP with a reservoir, PV system and diesel genset. Each system has many components. To make the cost-benefit analysis, all components are to be listed out. Transportation, labour costs etc are to be determined.
The cost analysis can be made by considering the capital interest or without it. Here first option is taken because the investment is done through the development agencies and the investments are done for social development instead of the profit.
In general the total cost of the project can be formulated as follows

$$Invest_{total} = A_o + \sum_{i}^{n} A_i \qquad (8.1)$$

Where

$Invest_{total}$	=	total investment cost
A_o	=	Investment cost
A_i	=	O&M cost for each year

So yearly total cost is given by

$$Invest_{year} = \frac{Invest_{total}}{n} \qquad (8.2)$$

If every year E_y energy is produced from the system, the cost for unit electricity energy is given by

$$E_c = \frac{Inverst_{year}}{E_y} \qquad (8.3)$$

Based upon above method, the cost for individual system and finally total cost for the project and energy cost will be calculated.

8.3.1 Micro hydro power plant

The cost involved in case of the MHHP can be divided into civil construction, electrical work, mechanical works, tools, spare parts, transportation cost, and installation, testing, commissioning and contingency [5]. As an example, the Khanikhola MHPP is taken.

Table-civil work

1. Head work (intake/weir/protection)
2. Gravel trap cum spillway
3. Headrace canal
4. Forebay cum distilling basin
5. Anchor blocks
6. Support piers
7. Power house building
8. Machine foundation

The investment cost of the Khanikhola MHPP is Rs. 2,622,600.00. The cost per kW-installed power is Rs. 147,700.00.
Similarly, the cost of some other projects implemented in Nepal are listed below

Table 8.1: The cost of implemented micro hydro power plants in Nepal

No.	Project	Year	kW	Cost (Rs.)	District
1.	Dainekhola MHPP	1998	12	1,481,509.00	
2.	Tikhedhunga MHPP	1997	40	4,977,822.00	
3.	Thulokhola MHPP	2004/05	9	1,421,833.00	Baglung
4.	Kulkulekhola MHHP	2004/05	12	1,792,084.00	Kavre Palanchwok
5.	Surnaya Gud MHHP	2004/05	10	1,452,264.00	Baitai
6.	Khergum MHHP	2004/05	7	3,405,339.00	Lamjung
7.	Kakanikhola MHPP	2004/05	18	2,498,268.00	Okhaldhunga

A suitable project is chosen to make analysis simple. As near to the simulation, Suryana Gud MHPP of 10 kW installed capacity is chosen. Due to devaluation of NRs, around 10% cost from total cost is to be added.

Total cost for 10 kW MHPP = Rs. 1,452,204.00 + 0.1*1,452,204.00
= Rs. 1,597,490.4

Cost to make a reservoir is = Rs. 340,000.00

Total cost for MHPP with a reservoir is Rs. 1,937,490.40

(€1 = Rs.100)

8.3.2 PV System

The cost of PV system can be calculated by getting cost information of different components, which need to be assembled together to form a PV system. The lists of components are

1. PV module
2. Power electronics block (Inverter, Converter)
3. Cables
4. Mechanical Structure

From point of the cost contribution, PV module is the most expensive one. It costs around 70% of the total cost, after that inverter costs around 10-15% and rest for cables, mechanical structure, and installation etc.
Approximately, the cost of the PV system is same in worldwide market. The system costs around $ 4/Wp. So for 4 kWp capacity, the cost of the PV system is around €11000.00 or Rs. 1,088,000.00

8.3.3 Diesel Genset

As explained above, the diesel genset is required to build a reliable isolated grid. The cost of the diesel genset can be calculated based upon an empirical formula [7].

Diesel genset cost is given by

$$Invest_{diesel} = 345.63 \exp - \left(0.039 \frac{P}{kW} \right) \text{ in €/kW} \qquad (8.4)$$

For 10 kW genset, total cost is € 2340.00. (Rs. 234000.00)

Total cost for the components of HPS is

$Invest_{total}$ = cost of MHPP + cost of PV system + cost of diesel genset
= Rs. 1,937,490.00 + 1,088,000.00+ 234,000.00
= Rs. 3,259,490.00
= € 47,933.67

Operation and maintenance (O&M) costs

According to ‘Document of the Word Bank, Project Appraisal Document’, the cost of system administration, management, O&M of HPS is to be calculated as three percent of total project cost. In the targeted HPS, only the PV modules are maintenance free for its lifetime of about 20 years. All other components require like every complex system, repairs, improvements and regular maintenance work [8]. The lifetime of the diesel genset can be taken as 10 years.

The O&M cost includes the cost to run the system for its lifetime. Lifetime is determined at the beginning of the project. It means the expenses for refuelling, maintenance of different energy units, overhaul, replacement of components and administration.

O&M cost of micro hydro

The O&M cost of the MHPP is scaled in the percentage of total investment cost. It is considered as around 4% [5]. So the O&M cost is Rs. 58124,70.

O&M of PV system

In case of PV system, the PV modules are not be replaced during its life time. Inverter is to be replaced once after 10 years. Other maintenance work is just cleaning of the PV modules time to time. The O&M cost of the PV system can be described as

$$PV_{O\&M} = \sum_{i}^{n} fpvPV_{total}(1-r)^{-i} \text{ in} \tag{8.5}$$

Where

$PV_{O\&M}$	=	O&M cost of PV system
PV_{total}	=	Total cost of PV system
f_{PV}	=	O&M cost factor for PV system
n	=	project life time
i	=	year of calculation
r	=	rate of discount

O&M of diesel genset

Lifetime of the diesel genset may vary from 2000 to 4000 operation hours. During this period, maintenance works for example motor oil change, filter replacement etc are to be done time to time as mentioned by the manufacturer. The complete engine also may need to be overhaul. The operation costs include fuel costs, start/stop costs etc. The O&M cost of diesel genset can be expressed as [8]

$$Diesel_{O\&M} = \sum \frac{\left(f_{diesel}N_{ON} + E_{Cf}.F_{-Lit} + f_{st/sp}N_{st/sp}PDR + f_{env}E_{diesel}\right)}{(1+r)^{i}} + Rpl_{diesel} \tag{8.6}$$

Where

$Diesel_{O\&M}$	=	O&M costs of the diesel genset
N_{ON}	=	number of operating hours of the diesel genset per year
f_{evn}	=	environmental cost factor (€/kWh)
f_{diesel}	=	O&M cost factor for the diesel genset (€/h)

EC_f = the unit cost of diesel fuel (€/Lit)
$F_{\_Lit}$ = the consumption of diesel fuel per year (Lit)
$N_{st/sp}$ = number of start/stop cycle per year
$f_{st/sp}$ = the cost factor per start/stop cycle (€/kW/cycle)
E_{diesel} = energy that is annually produced by the diesel engine (kWh)
Rpl_{diesel} = replacement cost of the diesel generator, if any (€)

The fuel consumption can be calculated according to equation (8.6) mentioned above. The start/stop cycle cost is assumed to be the fuel cost for 3 minutes of full power [8].

Use of Homer Software

Per kWh cost for this HPS is calculated using the software Homer that has been developed by NREL. This program provides many combinations of HPS with given energy converters based upon total project cost in the given lifetime. For the targeted HPS, the HOMER software has provided 8 options, which is shown in fig. 8.1. Among these 8 options last 4 options are not possible. Even though the option with 2 kW_P PV system is economic, the 4 kW_P PV system is chosen.

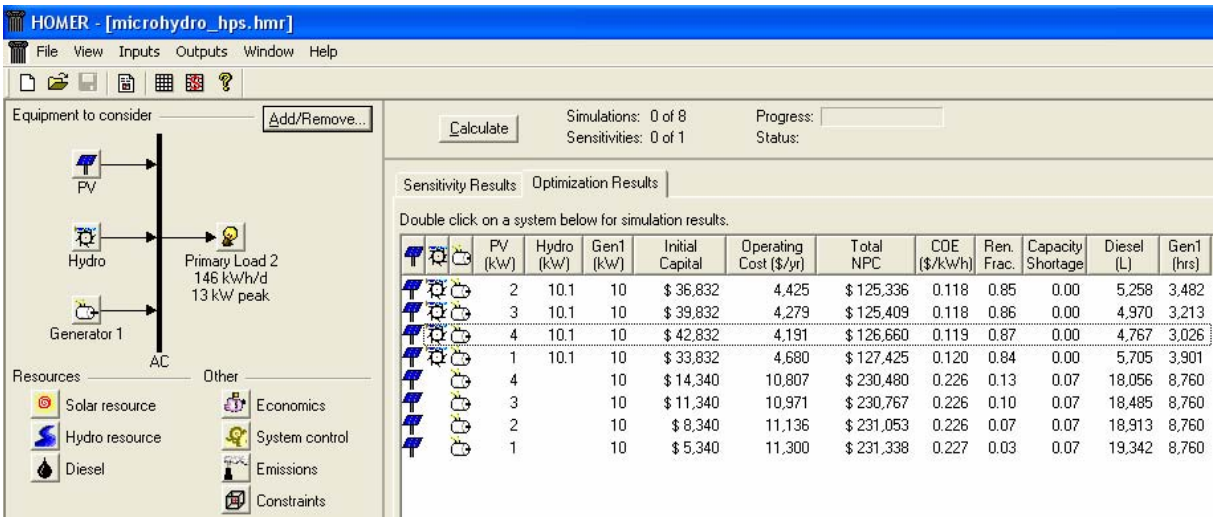

Fig. 8.1: The cost analysis of targeted HPS with different combinations using Homer software

The problem associated with this program is that the reservoir, which is very important component in the considered HPS, cannot be integrated. The total cost of the project at the end of the lifetime is $ 126,660 in which the fuel cost contributes a lot as shown in fig. 8.1. To integrate the effect of the reservoir, the energy balance of every month in the system is calculated and the comparison between the excess energy and the energy from the diesel genset is calculated. This energy scenario is shown in fig. 8.3. From this bar graph, it is clear that the diesel genset only needs to be operated for following months Jan, Feb, Mar, Apr, Dec. Based upon the new energy balance, the actual energy need from the diesel genset is calculated which is 2748 kWh/year. So, the total cost of the project will be drastically reduced. The detail analysis is given in appendix C.

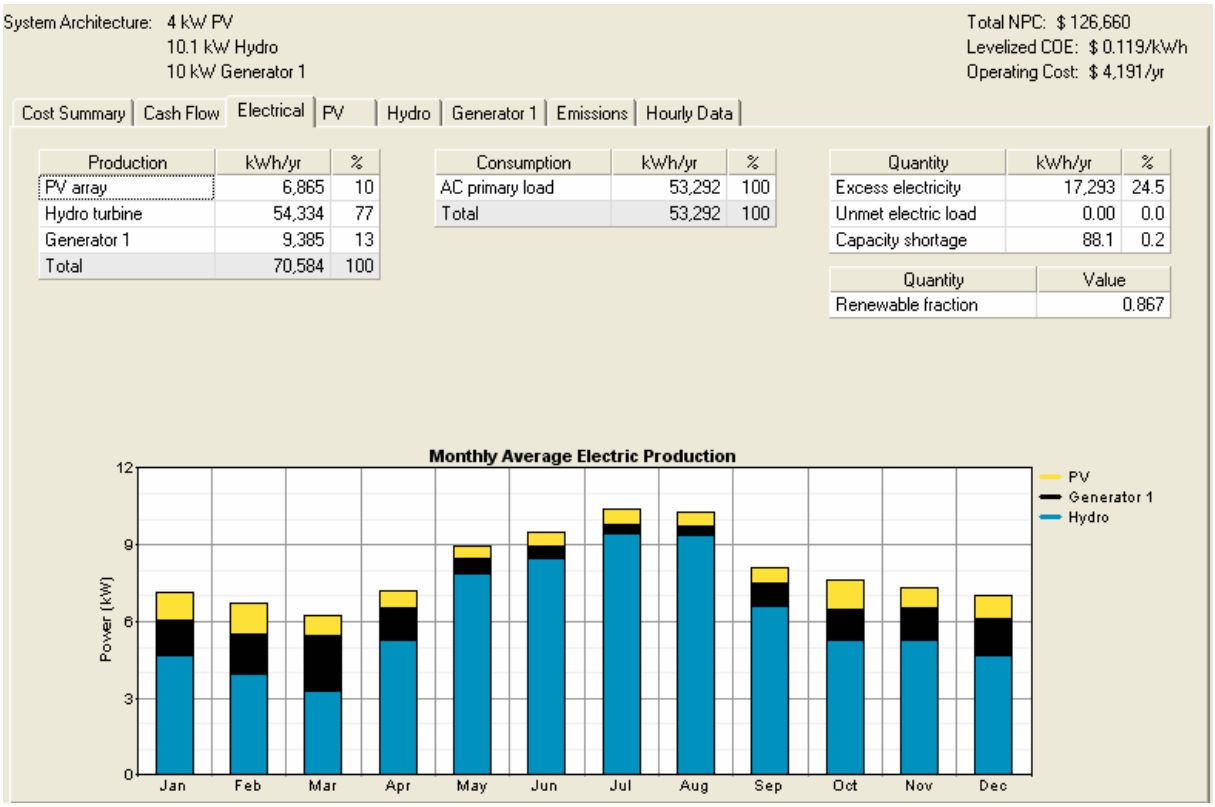

Fig. 8.2: Energy production scenario in the micro hydro based HPS without the reservoir

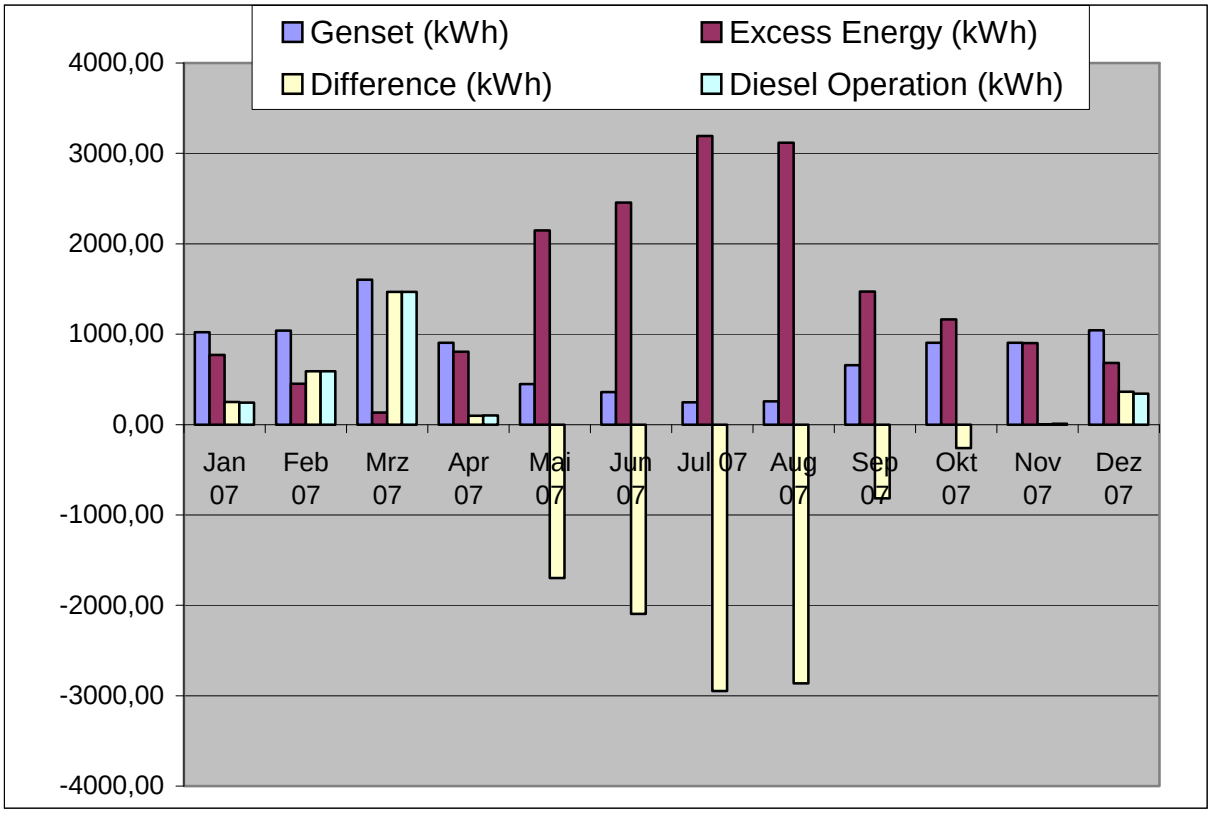

Fig. 8.3: Energy balance scenario in the micro hydro based HPS with the reservoir

9 Conclusion

This research work has mainly concentrated on the development of a hybrid power system and its energy management unit, which guides the individual energy conversion units in such a way that the maximum renewable energy will be utilised to fulfil the load demand as much as possible in priority based as mentioned below.

- *Utilisation of solar energy*
- *Utilisation of water energy*
- *Utilisation of diesel energy*

This research work has been carried out in two parts. The first part is oriented in the development of the mathematical model of HPS, its integration process and EMU using Matlab/Simulink software environment. The second part is oriented in the implementation of EMU in hardware level. Embedded system has been used to achieve this target.

In this research work, a micro-hydro power plant plays main role in terms of the grid formation. It means the grid variables “frequency and voltage” have been formed by the synchronous generator associated in MHPP. PV system and MHPP replenish weak points of each other. Another important change in the layout of HPS is that a water reservoir has been used as an energy storage unit instead of a battery bank. To make the system functional at all the time, a DGS has been integrated. This type of HPS has been developed for the hilly countries where small rivers are available, the sun shines most of the time and loads are quite far from the available grid for example Nepal.

In the first part of the work, the detail modelling of all possible energy converters is carried out. The development of models using respective mathematical equations can be much close to the real system in terms of their behaviours. The synthetic wind velocity profiles, solar irradiation profiles, water flow profiles, charging-discharging current profiles are used to visualise the models characteristics. The parameters are obtained from manufacture’s data, lab measurement etc. The behaviour of the individual models is verified by comparing the results of the simulation models to the measurement results.

A new concept of energy management has been developed to integrate all above-mentioned energy conversion units in the best optimal way in terms of energy utilisation. This concept has been implemented by measuring the isolated grid frequency and comparing it with reference frequency, the total required power is predetermined. It is divided for three connected energy conversion units based upon the water level, irradiation, and temperature etc conditions and it supplies the optimal energy dispatch. This model has been simulated with different loading, meteorological and water level conditions to test all the system functionality.

The results show that the complete integration method and the newly developed energy management unit are functional. A variable load pattern, which is constructed based upon daily load nature in rural areas, has been fed into the model as input. EMU

has guided each energy conversion unit in such a way that the demand power has been supplied and maximum renewable power has been utilised. The starting and stopping of the diesel genset, which based upon the water level in the reservoir and loading condition has been done.
The second part of the research work is carried out to develop the hardware of EMU based upon the simulation model. For this purpose a microcontroller MSP430F449 and C language are chosen. The necessary circuits like the water level sensor, the irradiation and temperature sensor, and user-interfacing keyboard are constructed. The functional code of the EMU is written in the computer language C. The functionality of EMU is tested by two programs in which first one is the loop method and second one is the sensor method. In first option, the program is run is fix number of loops that is defined by the user. The possible events in a real HPS like variable generation from the PV system, the diesel genset turn-on and off, load variation etc are created in the different points of simulation. The developed hardware EMU maintains the load-power equilibrium for all events. In second option, the sensors are integrated to calculate the available power from the PV system and to get the signal for the diesel genset turn-on and off. The power generation from MHPP changes corresponding to the change in the irradiation level or water level etc. The new approach of integration and its hardware implementation clearly shows that the developed system can be applied to build a compact, economic, reliable real HPS.

Further works
The developed EMU provides the reference powers for different energy converters in digital forms. They are displayed in the LCD display. These digital values are to be converted into equivalent analogue signals such that they could be sent to real converter units. Next steps of work to be carried out can be mentioned as follows

1. Development of PI controllers for different purposes for example virtual load determination in the isolated grid
2. Development of further hardware to get reference powers from EMU in form of analogue signals
3. Arrangement of prototype HPS in the lab to test the functionality of EMU.

References

Chapter 1

1. M. Ibrahim: *Decentralized Hybrid Renewable Energy Systems,* Dissertation, 2002, Kassel, Germany
2. R. Saiju, O. Omari, E. Ortjohann: *A Simulation Model for Expandable Hybrid Power Systems, Kasseler Symposium,* 2002, Kassel, Germany
3. ESAP, Nepal: *Micro-hydro year book of Nepal*, 2005, Kathmandu, Nepal
4. DDC, Pyuthan: *Detailed Feasibility Study Report of Khani Khola Micro Hydro Village Electrification Project,* 2004, Pyuthan, Nepal

Chapter 2

1. L. L. Grigsby: *Electric Power Engineering Handbook-Power Systems,* CRC Press, Taylor & Francis Group, Second Edition, 2007, FL 33487-2742,USA
2. S. Drouilhet: *Power Flow Management in a High Penetration Wind-Diesel Hybrid Power System with Short-Term Energy Storage,* Windpower 99, June 20-23, 1999, Burlington, Vermont
3. G. Arnold: Stützung *von Elektrizitätversorgungsnetzen durch Windenergieanlagen und andere erneuerbare Energien,* PhD thesis, 2004, Germany
4. R. Saiju, S. Heier *"Voltage dips compensation by wind farm(s) equipped with power converters as decoupling device "* 11th European conference on power electronics and applications, 11-14 September 2005 – Dresden, Germany

Chapter 3

1. www.apcdproject.org/countryprofile/nepal
2. R. Bhandari, M.B. Gewali: *Renewable Energy Technologies in Nepal,* World Review of Sceince, Technology and Sustainable Development, Vol. 2, No. 1, 2005
3. Electric power in Nepal: *History, Experiences, and Possibilities 2007 IEEE conference on the history of electric power schedule/ program* at NJIT
4. http://www.rzuser.uni-heidelberg.de/~q61/wasserkraft.html
5. http://www.visitnepal.com/nepal_information
6. ESAP, Nepal: *Micro-hydro year book of Nepal*, 2005, Kathmandu, Nepal

Chapter 4

1. AEPC: *Guidelines for Detailed Feasibility Studies of Micro Hydro Projects,* 2004 Nepal Government
2. DDC, Pyuthan: *Detailed Feasibility Study Report of Khani Khola Micro Hydro Village Electrification Project,* 2004, Pyuthan, Nepal
3. Paulo de Carvalho: *Photovoltaik- und windkraftbetriebene Umkehrosmoseanlagen im Inselbetrieb,* Dissertation, 1997, Paderborn, Germany
4. B. Weidemann: Dynamische Verhalten elektrischer Maschinen, 2006, Kassel, Germany
5. G.Schulz, *Regelungstechnik 1*
6. A.Perdana,O.Carlson, J.Persson: *Dynamic Response of Grid-Connected Wind Turbine with Doubly Fed induction generator during Disturbances,* Nordic workshop on power and industrial electronics, 2004, Trondheim, Norway
7. C.J. Winter, R.L. Sizmann, L.L. Vant-Hull*: Solar Power Plants Fundamentals.Technology.Systems.Economics,* 1991, Springer-Verlag, New York, Berlin

8. B. Plangklang: *An Embedded Interactive Monitoring System for PV – Diesel Hybrid Plants in Rural Area,* Dissertation, 2005, Kassel, Germany
9. Report IEA-PVPS T7-06: *2002, Market deployment strategies for PV systems in the built environment,* PVPS 2002
10. G. Bettenwort: *Anforderungen an den Aufbau modularer Photovoltaikanlagen im Netzparallelbetrieb,* Dissertation, VDI Verlag GmbH, 2002
11. S. Heier: *Grid Integration of Wind Energy Conversation,* Second Edition, John Wiley & Sons Ltd, 2006, UK
12. Gerhard Henneberger, *Electrical Machines II, Dynamic Behaviour, Converter Supply and Control,* RWTH, University of Aachen, Germany
13. J. Schumacher: *Digitale Simulation regenerativer elektrischer Energieversorgungssystem, Dissertation,* 1991, Duisburg, Germany
14. M. Ibrahim: *Decentralized Hybrid Renewable Energy Systems,* Dissertation, 2002, Kassel, Germany
15. J. Chiasson and B. Vairamohan: *Estimating the state of charge of a battery*, Electrical and Computer Engineering Department, the university of Tennessee, Knoxville, TN 37996, chiasson@utk.edu
16. find the name
17. M.M.D. Ross: *A Simple but Comprehensive Lead-Acid Battery Model for Hybrid Power System Simulation,* Quebec, Canada
18. *Courtesy of* Icemaster GmbH, Paderborn, Germany
19. Speed droop and Power generation,
20. A.C. Hasen, J.F. Reid, C.E. Goering: *Diesel Engine Simulator as Multimedia Tool,* University of Natal, South Africa, University of Illinois, USA
21. R. Fischer: *Elektrische Maschinen*, Twelve Edition, Hanser, 2004, Germany
22. A. Kremser: *Grundzüge elektrischer Maschinen und Antrieb,* Second Edition, Teubner, 1997, Germany
23. www.awea.org/smallwind/documents/AWEASmallWindMarketStudy2007.pdf
24. R. Saiju: *Developing of control strategies for hybrid power system,* Master Thesis, June 2003, Bolton Institute, University of Applied Science South Westfalia, Soest, Germany
25. R. Saiju, A. Tamzarti, S. Heier: *Performance Analysis of Small Wind Turbine Connected to a Grid through Modelling and Simulation*, 5-8 November 2007, The 33rd Annual Conference of the IEEE Industrial Electronics Society**,** Taipei, Taiwan
26. R. Saiju, S. Heier: Performance Analysis of Lead Acid Battery for Hybrid Power System, IEEE Power

Chapter 5

1. S. Drouilhet: *Power Flow Management in a High Penetration Wind-Diesel Hybrid Power System with Short-Term Energy Storage,* Windpower 99, June 20-23, 1999, Burlington, Vermont
2. R. Saiju, O. Omari, E. Ortjohann: *A Simulation Model for Expandable Hybrid Power Systems, Kasseler Symposium,* 2002, Kassel, Germany
3. R. Saiju: *Developing of Control Strategies for Hybrid Power Systems*, Master Thesis, 2003, Soest, Germany
4. M. Ibrahim: *Decentralized Hybrid Renewable Energy Systems,* Dissertation, 2002, Kassel, Germany
5. S. Heier: *Grid Integration of Wind Energy Conversation,* Second Edition, John Wiley & Sons Ltd, 2006, UK

Chapter 6

1. A. Draper: *Electrical Machines,* Longman Group Limited, Second Edition, 1967, London, New York
2. C.A. Hawa: *Methods for the determination of excitation currents in synchronous, machines,* Technical Report, Department of Electromechanical Design, Svenska Kraftnät, Sweden

Chapter 7

1. Becker, Börcsök, Hofmann: *Mijroprozessortechnik – Architektur, Implementierulg, Schnittstellen*, ADE Verlag, 2003, Germany
2. M. Sturm: *Mikroprozessortechnik – Am Beispiel der MSP430 – Familie*, Hanser Verlag, 2006, Germany
3. L. Biehrl: *Das große MSP430 Praxisbuch , Franzis Verlag, 2004*, Germany
4. Datasheet: *LM117/LM11171 – 800mA Low – Dropout Linear Regulator*
5. Datasheet: *LCD 204B LED – Displaytech Ltd. – LCD Modules 204B Series,*
6. Datasheet: *Positive Voltage Regulator L7800 Series*
7. Datasheet: *Octal Buffer / Line Driver with 3-State Outputs*
8. P. Aikten: B.L Jones: *C in 21 Tagen*, Markt+Technik Verlag, 2000, Germany

Chapter 8

1. V. Quaschning: *Regenerative Energiesysteme Technologie-Berechnung-Simulation*, Carl Hanser Verlag, 1998, Munich, Wien
2. S.P. Gorkhali: *Energy and Economic Welfare (Cost-Benefit Analysis of Micro-Hydro System in Nepal,* IEE Working Papers, Volume 179, Institute of Development Research and Development Policy, 2005, Ruhr University Bochum, Germany
3. Thompson-gorkhali
4. *N.N. Guidelines for Economic analysis of projects*, ADB
5. DDC Pyuthan: *Detailed Feasibility Study Report of Khani Khola Micro Hydro Village Electrification Project – Technical Report,* Volume – I, July 2004, Khalanga, Pyuthan, Nepal khanikhola-Technical report
6. ESAP, Nepal: *Micro-hydro year book of Nepal*, 2005, Kathmandu, Nepal
7. Tom Guemor: *Integrated Analysis of Hybrid Power Systems for Rural Electrification in Developing Countries, Master Thesis,* 2004, Stockholm, Sweden
8. M. Ibrahim: *Decentralized Hybrid Renewable Energy Systems,* Dissertation, 2002, Kassel, Germany

Conference and published papers

1. R. Saiju, S. Heier *"Voltage dips compensation by wind farm(s) equipped with power converters as decoupling device "* 11th European conference on power electronics and applications, 11-14 September 2005 – Dresden, Germany
2. R. Saiju, *" Development and implementation of an isolated grid feeding by renewable energy sources"*, 22-23 September 2005 – National Technical University of Athens, Athens, Greece
3. R. Saiju *"Micro Hydro Based Hybrid Power System"* October 4th and 5th 2006, Risø National Laboratory, Denmark
4. R. Saiju, S. Heier, "*Wind Plant Development and State of the Art of Grid Connected Systems*", 19 *– 25 August 2006-06,* The World Renewable Energy Congress IX and Exhibition, Florence, Italy

5. R. Saiju, A. Tamzarti, S. Heier *"Performance analysis of small wind turbine connected to a grid through modelling and simulation"*, 5-8 November 2007, The 33rd Annual Conference of the IEEE Industrial Electronics Society**,** Taipei, Taiwan
6. R.Saiju, S. Heier " Performance Analysis of Lead Acid Battery Model for Hybrid Power System", 21-24 April, 2008, 2008 IEEE PES Transmission and Distribution Conference and Exposion, Chicago, USA

Nomenclature

A

A	active power droop factor, rotor cross sectional area (m^2)
A_o	investment cost
A_i	O&M cost for each year
AhD_0	initial AHD of the battery (Ah)
AhR	ampere hour remaining in the battery (Ah)
Ah_{nom}	nominal ampere hour of the battery (Ah)
AhD	ampere hour to be discharged (Ah)

B

B	reactive power droop factor

C

C	capacitor connected across asynchronous generator (F)
C	DC link capacitor used in PV system (F)
C_f	unit conversion factor
C_p	performance coefficient of rotor blades
Cu	voltage dependent constant in the battery

D

DK	fit parameter for battery model
$Diesel_{O\&M}$	operation and maintenance cost for diesel genset

E

E	solar irradiation (W/m^2)
e_o	charge of an electron [e=1.6*10-19 As]
E	energy of one photo for given wave length (eV)
E_{new}	new irradiation (W/m^2)
E_{stc}	STC irradiation (W/m^2)
E_{diesel}	annual energy production by diesel genset (kW)
E_c	cost of unit electrical energy
E_y	yearly energy production (kWh)

F

f_{grid}	grid frequency (Hz)
f_{ref}	reference frequency (Hz)
f_{nl}	no load frequency (Hz)
EC_f	cost of the fuel (€/Lit)
F_{-Lit}	yearly fuel consumption by diesel genset (Lit)
$F_{st/sp}$	cost for per start and stop of diesel genset (€/st)
f_{env}	environmental cost fact (€)
f_{diesel}	O&M cost factor for diesel genset (€)
f_{pv}	O&M cost factor for PV system (€)

H

h	plank constant (6.6260755*10-34 Js)
H_g	gross heating value of the fuel (kJ/kg)
h_{it}	indicated thermal efficiency

I

I_d	d-axis current of SG (A)
I_f	field current of SG (A)
I_L	load current of SG (A)
I_q	q-axis current of SG (A)
I_{pv}	Useful PV cell current (A)
I_{ph}	photo cell current (A)
I_D	diode current in PV cell (A)
I_{sc}	PV cell short circuit current (A)
I_{d1}	d axis stator current of ASG (A)
I'_{d2}	d axis rotor current of ASG (A)
I_{q1}	q axis stator current of ASG (A)
I'_{q2}	q axis rotor current of ASG (A)
I_o	saturation current of PV cell (A)
I_c	capacitive current from capacitor (A)
I	magnetising current of asynchronous generator (A)
I_{rec}	reactive current demanded by (A)
I_{recmax}	maximum reactive current demanded by asynchronous generator (A)
I_{mpp}	maximum power point current of PV cell (A)
I_{sc_new}	new short circuit current of PV cell (A)
I_{DC}	DC current in the field winding of SG(A)
I_C	Capacitor current (A)
I	magnetisation current of ASG (A)
I_{rec}	reactive current of ASG (A)
I_{act}	active current of ASG (A)
I_{mr}	main reaction current in the battery (A)
I_{bat}	useful current from or to the battery (A)
I_{gas}	gassing current of the battery (A)
I_{go}	gassing current at no load condition (A)
$Invest_{total}$	total investment cost of the HPS (A)
$Invest_{year}$	yearly total investment cost (A)
$Invest_{diesel}$	investment cost of the diesel genset (A)

J

J_i	moment of inertia of whole system (Kgm^2)

K

K	Boltzmann's constant (8.65*105 eV/K)

L

L_1	Stator inductance of ASG (H)
L'_2	rotor inductance of ASG (H)
L_h	main inductance of asynchronous generator (H)
L_d	d-axis stator inductance of SG (H)
L_q	q-axis stator inductance of SG (H)
L_f	field inductance of SG (H)
L_{fd}	mutual inductance between field and d-axis winding (H)

M

m_f	fuel consumption by diesel genset (Lit/h)

N

n_e	engine speed (rpm)
N_{ON}	number of operating hours of diesel genset per year
$N_{st/sp}$	number of start/stop cycle of diesel genset per year
n	lifetime of HPS in years

P

p	no of pole pairs
P_{mref}	reference power for MHPP (W)
P_{pvref}	reference power for PV system (W)
P_{dref}	reference power for diesel genset (W)
P_m	actual power from MHPP (W)
P_{pv}	actual power from PV system (W)
P_d	actual power from diesel system (W)
$P_{mrefmin}$	minimum reference power for MHPP (W)
P_L	active load (W)
P_{fme}	friction mean effective pressure (W)
P_{load_d}	determined active load (W)
P_{pvav}	available power from PV system (W)
$PV_{O\&M}$	operation and maintenance cost for PV system (W)
PV_{total}	total investment cost for PV system (W)
PDR	diesel engine rated power (W)
P_{wind}	power available from WTG (W)

Q

Q_L	reactive load (VAr)
Q_r	water flow into WR (Lit/s)
Q_t	water flow into the turbine (Lit/s)
Q_r	water flow in the river (Lit/s)
Q_{LV}	the low heat value of the fuel (kWh/l)

R

R_s	stator resistance of SG (Ohm)
R_1	Stator resistance of ASG (Ohm)
R'_2	rotor resistance of ASG (Ohm)
R_f	field winding resistance of SG (Ohm)
Rpl_{diesel}	replacement cost of diesel genset (€)

S

SOC	state of charge of battery
SOC_0	initial SOC of the battery
SG	specific gravity of the battery
SG_{full}	SG of the battery at fully charged condition
SG_{empty}	SG of the battery at fully discharged condition
S	apparent power of ASG (VA)

T

T	temperature (K)
T_c	PV cell temperature (K)
T_{new}	new temperature (K)
T_{stc}	STC temperature of PV cell (K)

T_d	torque produced by diesel engine (Nm)
T_e	electrical torque (Nm)
T_t	mechanical torque (Nm)
T_{zw}	3 phase to 2 phase transformation matrix

V

V_{bat}	battery terminal voltage (V)
V_e	engine displacement (Lit)
V_{grid}	grid voltage (V)
V_{ref}	reference voltage (V)
V_L	line voltage (V)
V_d	d-axis voltage (V)
V_{op}	optimal voltage for PV system (V)
V_q	q-axis voltage (V)
V_{nl}	No load voltage (V)
V_{res}	residual voltage of asynchronous generator (V)
V_{mpp}	maximum power point voltage of PV cell (V)
V_{oc}	open circuit voltage of PV cell (V)
V_{oc_stc}	STC open circuit voltage of PV cell (V)
V	wind velocity (ms^{-1})
V_{q1}	q axis stator voltage of ASG ((V)
V_{d1}	d axis stator voltage of ASG (V)
V_{DC}	DC voltage applied to the field winding of SG (V)

W

W_{ldo}	water level diesel on (m)
WLA	water level actual (m)
WLU	upper water level (m)
WLL	lower water level (m)

Greek Letters

A	current coefficient of PV cell
B	voltage coefficient of PV cell
	correlation factor of PV cell
Δ	torque angle (power angle)
	tip speed ratio
$_D$	efficiency of diesel genset
$_d$	d-axis flux linkage
$_q$	q-axis flux linkage
$_{d2}$	d axis rotor flux linkage of ASG
	power factor angle
$_{d1}$	d axis stator flux linkage of ASG
$_{q1}$	q axis stator flux linkage of ASG
$_{q2}$	q axis rotor flux linkage of ASG
Ω	angular velocity of the generator
	wavelength of the irradiation

Appendixes

Appendix A

1. Microcontroller MSP430F449 based hardware circuit
2. The PCB development based upon the hardware circuit
3. The water reservoir water level measurement circuit
4. The PCB of the reservoir water level measurement circuit

Appendix B

1. The C code software program for the sensor based energy management option

Appendix C

1. The average monthly solar irradiation data (kWh/m^2-day) from a village of Nepal
2. The average monthly water flow data (L/s) from a village of Nepal

Appendix D

1. The detailed cost calculation of the targeted HPS using Homer software from NREL

Appendix A

1. Microcontroller MSP430F449 based hardware circuit

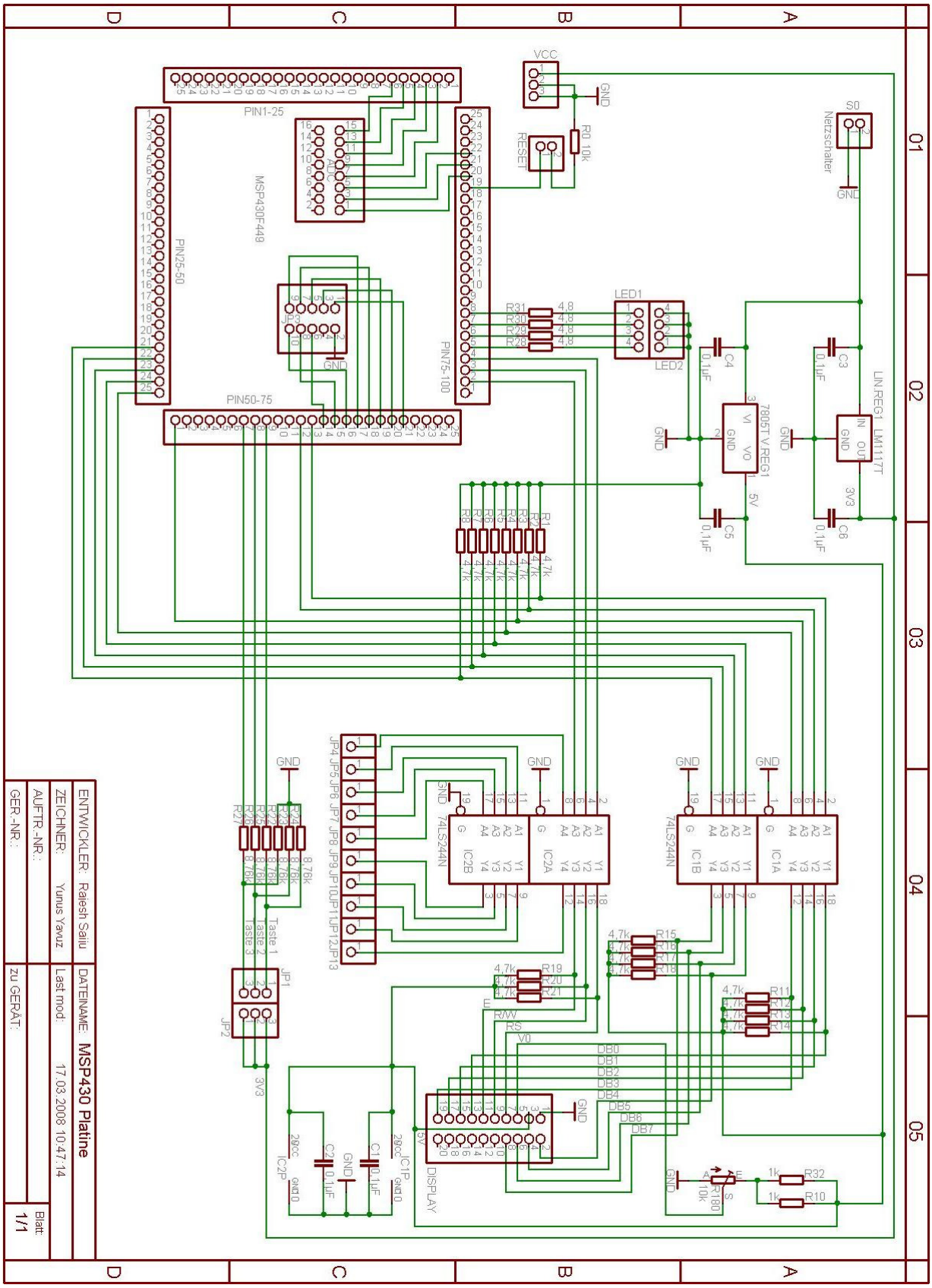

2. The PCB development based upon the hardware circuit

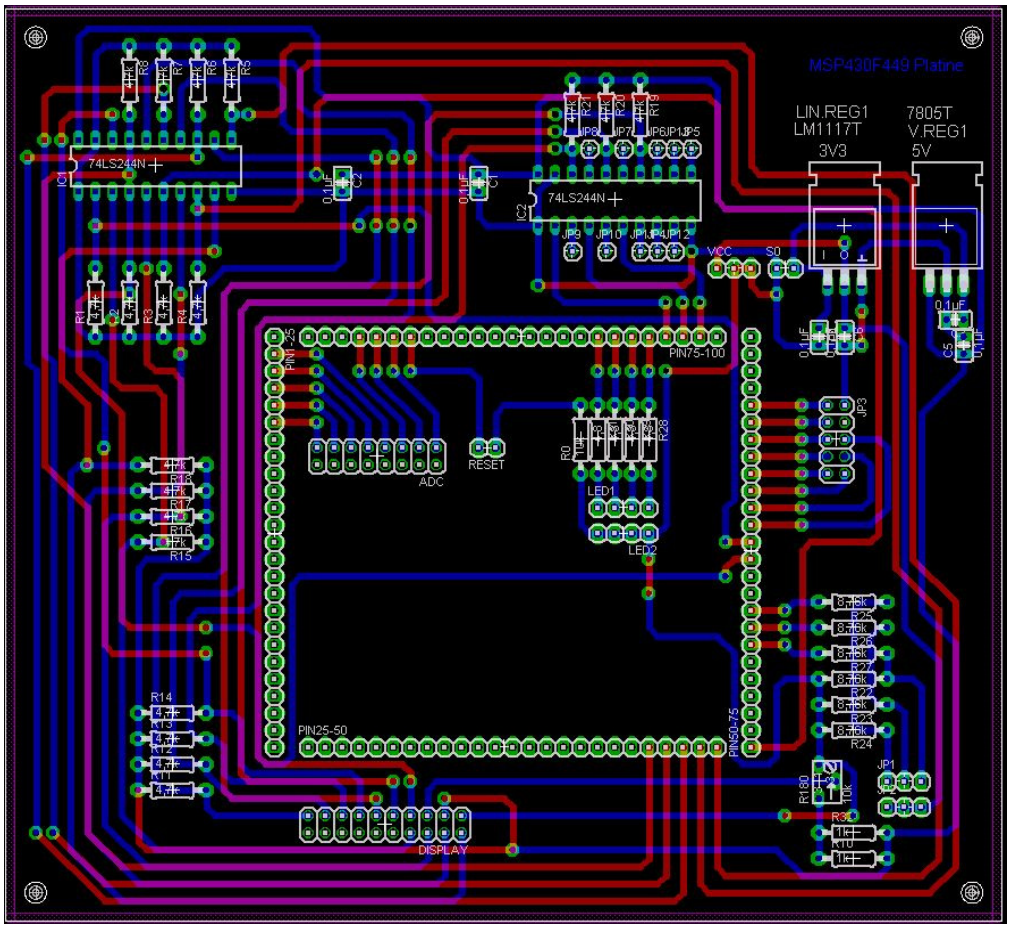

3.The water reservoir water level measurement circuit

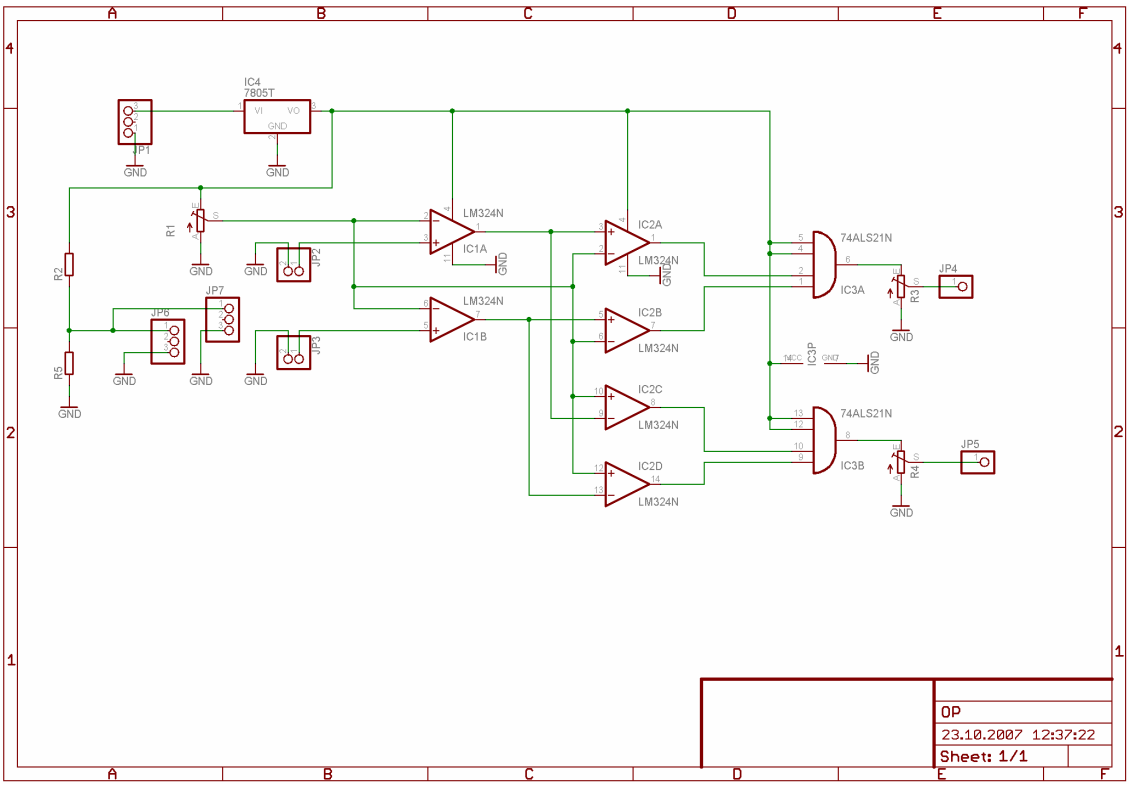

4.The PCB of the reservoir water level measurement circuit

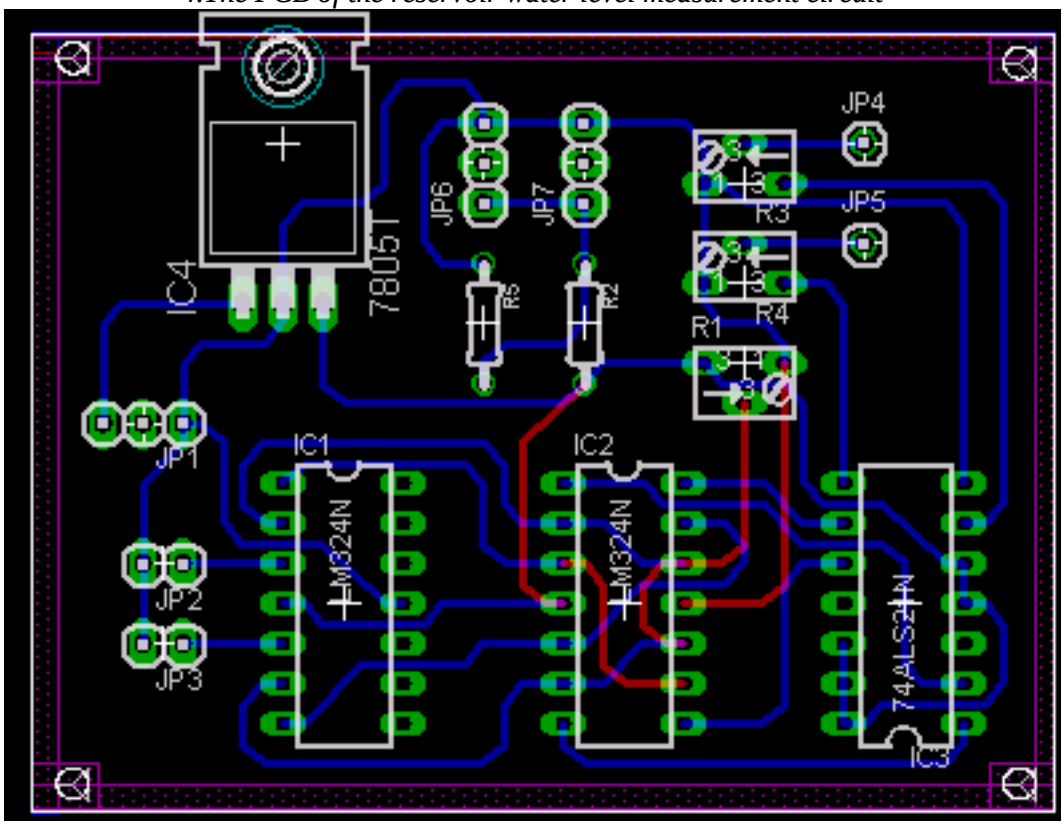

Appendix B

1.The C code software program for the sensor based energy management option

```
/**** HPS Eenergy Manegement Unit****/
/***** Rajesh Saiju  *****/
/** Universität Kassel **/
/****** 06.06.2007 ******/



#include <stdio.h>
#include <stdlib.h>
#include <msp430x44x.h>
#include <string.h>
#include <math.h>

# define PI 3.14159
# define P_MPP_STC 34                   /* Maximum Power [W]          */
# define I_MPP_STC 2.95                 /* MPP current [A]            */
# define I_SC_STC 3.25                  /* Short Circuit Current [A]  */
# define V_MMP_STC 34                   /* MPP voltage [V]            */
# define V_SC_STC 42                    /* Open circuit voltage [V]   */
# define ALPHA 0.0001/3.25              /* Alpha                      */
# define BETA -0.004                    /* Beta                       */
# define E_STC 1000                     /* Irradiation                */
# define T_SC_STC 298.15                /* Temperatur [K=273.15+25]   */

void LCDInit(void);
void LCDClock(void);

void LCDClear(void);
void LCDWrite(void);
void Tastatur(void);
void LCDoutchar(char array);
void LCDoutstring(char *array);
void wait(unsigned int x);

void Display(void);
void Ausgabe(char *text00, char *text01, char *text02, char *text03, char *text04);
void MemorySet(void);

// globale Definitionen
char string[10];
int kontrolle=1;
int i=0;

float zahl;
char *string00={"Please Press Key"};
char *string01={"Pmref ="};
char *string02={"Ppvref="};
char *string03={"Pdref ="};
char *string04={"Ptotal="};
char output00[8];
char output01[8];
char output02[8];
char output03[8];
char output04[8];
```

```
int main(void)
{
  WDTCTL=WDTPW+WDTHOLD;                    // Watchdogtimer turn off
  P1DIR=0xC0;                              // P1.6 und P1.7 as output
  P2DIR=0xFF;                              // Port 2 as output
  P3DIR=0x0F;                              // P3.0 to P3.3 as output und P3.4 to P3.7 as input
  P4DIR=0xFF;                              // Port 4 as output for 8 data bit display
  P5DIR=0x00;                              // Port 5 as inputs

  // Ports as General Purpose I/O

  P1SEL=0x00;
  P2SEL=0x00;
  P3SEL=0x00;
  P5SEL=0x00;
  P4SEL=0x00;
  P1OUT=0x00;                                  // LEDs
  P2OUT=0x00;                                  // initialisation of E, RS and R/W as low level
  P4OUT=0x00;
  P6SEL=0x0F;
  P1IE =0x00;                                  // Turn off Interrupts

  float Ppvref;
  float Pload,Ptotal;
  float Pdref=0;
  float Pmmin=400;
  float Pmref;
  char *text={"-ENERGY MANAGEMENT-"};

  float V_mpp_new;
  float I_pv_new, Ipvav,I_sc_new,V_oc_new;
  float Ppvav,gamma,Io;
  float E_new;
  float T_new;
  int n_s=7, n_p=5;                        // n_s and n_p = no. of PV modules in series and parallel

  // Use of ADC available in MSP430F449

  ADC12CTL0=ADC12ON+SHT0_0+MSC+REFON+REF2_5V;

// ADC12 turn on, n=1, activate the reference of 2,5V

  ADC12CTL1=SHP+CONSEQ_1;                  // Use SHP
  ADC12MCTL0=SREF_1+INCH_0;                // Use of first conversion register for first chanel
  ADC12MCTL1=SREF_1+INCH_1;                // Use of second conversion register for second chanel
  ADC12MCTL2=SREF_1+INCH_2+EOS;            // Use of third conversion register for third chanel
  ADC12CTL0|=ENC;                          // activate conversion
  ADC12MEM0=0x0000;                        // Initialisation of 16 bit internal memories to zero

  ADC12MEM1=0x0000;
  ADC12MEM2=0x0000;

  LCDInit();                                //Initiliasierung mit BF Check
  wait(1000);

  LCDoutstring(text);
  P4OUT=0xC0;
  LCDClock();
  LCDoutstring(string00);

  while(1)
```

```
{
  if(P5IN & 0x80)
     goto start;
  P1OUT=0xA0;
}
start:
// Calculation of available power from PV system

  while(1)
  {

    ADC12CTL0|=ADC12SC;
    wait(10000);
    Pload=ADC12MEM0*2.5;
    E_new=ADC12MEM1*0.3-432;
    T_new=ADC12MEM2*0.0788;

    if(ADC12MEM1<=0x7FF)
    P1OUT=0x80;
    else
    P1OUT=0x40;

    I_sc_new=I_SC_STC*(E_new/E_STC)*(1+ALPHA*(T_new-T_SC_STC));
    U_oc_new=U_SC_STC*(1-BETA*(T_new-T_SC_STC));
    U_mpp_new=U_oc_new*0.8;
    gamma=(U_MMP_STC-U_SC_STC)/(U_SC_STC*log(1-(I_MPP_STC/I_SC_STC)));
    Io=(I_SC_STC-I_MPP_STC)*exp(-U_MMP_STC/(gamma*U_SC_STC));
    I_pv_new=I_sc_new-Io*(exp((U_mpp_new)/(gamma*U_oc_new))-1);
    Ipvav=I_pv_new*n_p;

    Ppvav=U_mpp_new*n_s*Ipvav;
    Ppvref=Ppvav;

// Calculation of reference power for the MHPP, Diesel geset

    Pmref=Pload-Ppvref-Pdref;
    Pdref=Pdref;
    if(Pmref<Pmmin)
           Pmref=Pmmin;
    Ptotal=Pmref+Ppvref+Pdref;
    Display();

              sprintf(output04, "%7.1f", Ptotal);
              sprintf(output01, "%7.1f", Pmref);
         sprintf(output02, "%7.1f", Ppvref);
         sprintf(output03, "%7.1f", Pdref);

         Ausgabe(output00, output01, output02, output03, output04);

         MemorySet();

           if(P5IN & 0x08)                          // Checking the diesel genset turn-on signal
           {
         P1OUT=0x40;                                // Putting red LED on
         if(Pmref>Pmmin)
              {
                Pdref=Pdref+100;                    // Starting of diesel genset and incresing power
                Pmref=Pload-Ppvref-Pdref;
              }
              if(Pmref==Pmmin)
              {
                Pmref=Pmref;
```

```
                Pdref=Pload-Ppvref-Pmmin;
              }
            }

      if (P5IN & 0x04)                                  // Checking the diesel genset turn-off siganl
      {
       P1OUT=0xA0;                                      // Putting yello LED off
            if(Pdref>0)
              {
                Pmref=Pmref+100;
                Pdref=(Pload-Ppvref)-Pmref;             // Decreasing the power from the diesel genset
              }
              if(Pdref<0)
                Pdref=0;
       }
  }

}
//---------------------------------------------------------------------------

void Display(void)
{

  P4OUT=0x80;
  LCDClock();
  LCDoutstring(string04);                               // Pload
  P4OUT=0xC0;                                           // 2. Row
  LCDClock();
  LCDoutstring(string01);                               // Pmref
  P4OUT=0x94;                                           // 3. Row
  LCDClock();
  LCDoutstring(string02);                               // Ppvref
  P4OUT=0xD4;                                           // 4. Row
  LCDClock();
  LCDoutstring(string03);                               // Pdref
}

//---------------------------------------------------------------------------

void Ausgabe(char *text00, char *text01, char *text02, char *text03, char *text04)
{
   char *einheit={" W   "};
   P4OUT=0x87;                                          // 1. Row 8. Column
   LCDClock();
   LCDoutstring(text04);                                // Display: Pload
   LCDoutstring(einheit);
   P4OUT=0xC7;                                          // 2. Row 8. Column
   LCDClock();
   LCDoutstring(text01);                                // Dispaly: Pmref
   LCDoutstring(einheit);
   P4OUT=0x9B;                                          // 3. Row 8. Coulmn
   LCDClock();
   LCDoutstring(text02);                                // Dispaly: Ppvref
   LCDoutstring(einheit);
   P4OUT=0xDB;                                          //4. Row 8. Column
   LCDClock();
   LCDoutstring(text03);                                // Dispaly: Pdref
   LCDoutstring(einheit);

}

//---------------------------------------------------------------------------
```

```
void MemorySet(void)
{
  memset(output01, 0, 8);                                  // Over write die Array with "0"
  memset(output02, 0, 8);
  memset(output03, 0, 8);
  memset(output04, 0, 8);
}

//-------------------------------------------------------------------------

void LCDoutchar(char array)
{
    P4OUT=array;
    LCDWrite();
    wait(300);
}

//-------------------------------------------------------------------------

void LCDoutstring(char *array)
{
    while (*array !=0)
    LCDoutchar(*array++);
}

//-------------------------------------------------------------------------

void LCDInit(void)
{
  wait(1000);
  P4OUT=0x3F;
  LCDClock();
  wait(1750);
  P4OUT=0x3F;
  LCDClock();
  wait(500);
  P4OUT=0x3F;
  LCDClock();
  P4OUT=0x3B;
  LCDClock();
  P4OUT=0x0F;
  LCDClock();
  P4OUT=0x01;
  LCDClock();
  P4OUT=0x06;
  LCDClock();
}

//-------------------------------------------------------------------------

void LCDClock(void)                                        // Display counter
{
  wait(550);
  P2OUT=0x04;                                              // E-Bit first make high
  wait(550);
  P2OUT=0x00;                                               // and now make low
  wait(550);
}

//-------------------------------------------------------------------------
```

```
void wait(unsigned int x)                                  // Wait loop
{
 unsigned int q;
 for(q=0; q<x; q++);
}

//-------------------------------------------------------------------------

void LCDClear(void)
{
  P4OUT=0x01;                                              // Display delete
  LCDClock();
  wait(1000);
}

//-------------------------------------------------------------------------

void LCDWrite(void)                                        // Display write
{
 wait(850);
 P2OUT=0x05;                                               // RS & E activate
 wait(850);
 P2OUT=0x00;
 wait(850);
}

void Tastatur(void)
{
   P3OUT=0x01;                                             // 1. Row of "1"
   if(P3IN & 0x10)
   {                                                       // 1. column
    if(kontrolle==2)
    {
     i=0;
     kontrolle=1;
    }

    P1OUT=0xC0;
    P4OUT=0x31;                                            // Key "1"
    LCDWrite();

    string[i]='1';
    i++;
    wait(60000);
    }
   else
    P1OUT=0x00;

   if(P3IN & 0x20)                                         // 2. Column
   {
    if(kontrolle==2)
    {
     i=0;
     kontrolle=1;
    }

    P1OUT=0xC0;
    P4OUT=0x32;                                            // Key "2"
    LCDWrite();

    string[i]='2';
    i++;
```

```
  wait(60000);
 }
 else
  P1OUT=0x00;

 if(P3IN & 0x40)                                  // 3. Column
 {
  if(kontrolle==2)
  {
   i=0;
   kontrolle=1;
  }

  P1OUT=0xC0;
  P4OUT=0x33;                                     // Key "3"
  LCDWrite();

  string[i]='3';
  i++;
  wait(60000);
 }
 else
  P1OUT=0x00;

 if(P3IN & 0x80)                                  // 4.Coulmn
 {
  if (kontrolle==2)
  {
   i=0;
   kontrolle=1;
  }

  P1OUT=0xC0;
  P4OUT=0x34;                                     // key "4"
  LCDWrite();

  string[i]='4';
  i++;
  wait(60000);
 }
 else
  P1OUT=0x00;

 P3OUT=0x00;                                      // 1. Row of "0"
//*****************************************************************************
 P3OUT=0x02;                                      // 2. Row of "1"
 if(P3IN & 0x10)                                  // 1. Coulmn
 {
  if (kontrolle==2)
  {
   i=0;
   kontrolle=1;
  }

  P1OUT=0xC0;
  P4OUT=0x35;                                     // Key "5"
  LCDWrite();

  string[i]='5';
  i++;
  wait(60000);
 }
```

```
  else
    P1OUT=0x00;

  if(P3IN & 0x20)                                   // 2. Column
  {
    if (kontrolle==2)
    {
      i=0;
      kontrolle=1;
    }

    P1OUT=0xC0;
    P4OUT=0x36;                                     // Key "6"
    LCDWrite();

    string[i]='6';
    i++;
    wait(60000);
  }
  else
    P1OUT=0x00;

  if(P3IN & 0x40)                                   // 3. Column
  {
    if (kontrolle==2)
    {
      i=0;
      kontrolle=1;
    }

    P1OUT=0xC0;
    P4OUT=0x37;                                     // Key "7"
    LCDWrite();

    string[i]='7';
    i++;
    wait(60000);
  }
  else
    P1OUT=0x00;

  if(P3IN & 0x80)                                   // 4. Column
  {
    if (kontrolle==2)
    {
      i=0;
      kontrolle=1;
    }

    P1OUT=0xC0;
    P4OUT=0x38;                                     // Key "8"
    LCDWrite();

    string[i]='8';
    i++;
    wait(60000);
  }
  else
    P1OUT=0x00;

  P3OUT=0x00;                                       // 2. Row of "0"
//*******************************************************************************
```

```
 P3OUT=0x04;                                  // 3. Row of "1"
 if(P3IN & 0x10)                              // 1. Column
{
  if (kontrolle==2)
  {
    i=0;
    kontrolle=1;
  }

  P1OUT=0xC0;
  P4OUT=0x39;                                  // Key "9"
  LCDWrite();

  string[i]='9';
  i++;
  wait(60000);
}
 else
   P1OUT=0x00;

 if(P3IN & 0x20)                              // 2. Column
 {
   if (kontrolle==2)
   {
     i=0;
     kontrolle=1;
   }

   P1OUT=0xC0;
   P4OUT=0x30;                                // Key "0"
   LCDWrite();

   string[i]='0';
   i++;
   wait(60000);
 }
 else
   P1OUT=0x00;

 if(P3IN & 0x40)                              // 3. Column
 {
   if (kontrolle==2)
   {
     i=0;
     kontrolle=1;
   }

   P1OUT=0xC0;
   P4OUT=0x2D;                                // Key "-"
   LCDWrite();

   string[i]='-';
   i++;
   wait(60000);
 }
 else
   P1OUT=0x00;

 if(P3IN & 0x80)                              // 4. Column
 {
   if (kontrolle==2)
   {
```

```
        i=0;
        kontrolle=1;
       }

      P1OUT=0xC0;
      P4OUT=0x2E;                                    // Key "."
      LCDWrite();

      string[i]='.';
      i++;
      wait(60000);
     }
     else
      P1OUT=0x00;
      P3OUT=0x00;                                    // 3. Row of "0"
//*****************************************************************************
      P3OUT=0x08;                                    // 4. Row of "1"
     if(P3IN & 0x10)                                 // 1. Column
     {
      P1OUT=0x80;
      P4OUT=0x10;                                    // "<-"
      LCDClock();
      string[i--];
      wait(60000);
     }
      else
       P1OUT=0x00;

     if(P3IN & 0x20)                                 // 2. Column OK - key
     {

      P1OUT=0xC0;
      LCDClear();
      /*Convert();*/
      wait(6000);
     }
      else
       P1OUT=0x00;

     if(P3IN & 0x40)                                 // 3. Column DEL-key
     {
      P1OUT=0x40;
      P4OUT=0x20;
      LCDWrite();
      wait(60000);
     }
     else
      P1OUT=0x00;

     if(P3IN & 0x80)                                 // 4. Column
     {
      P1OUT=0x80;
      P4OUT=0x14;                                    // "->"
      LCDClock();
      wait(60000);
     }
     else
      P1OUT=0x00;
      P3OUT=0x00;                                    // 4. Row of "0"
//*****************************************************************************
}
```

Appendix C

1.The average monthly solar irradiation data (kWh/m^2-day) from a village of Nepal

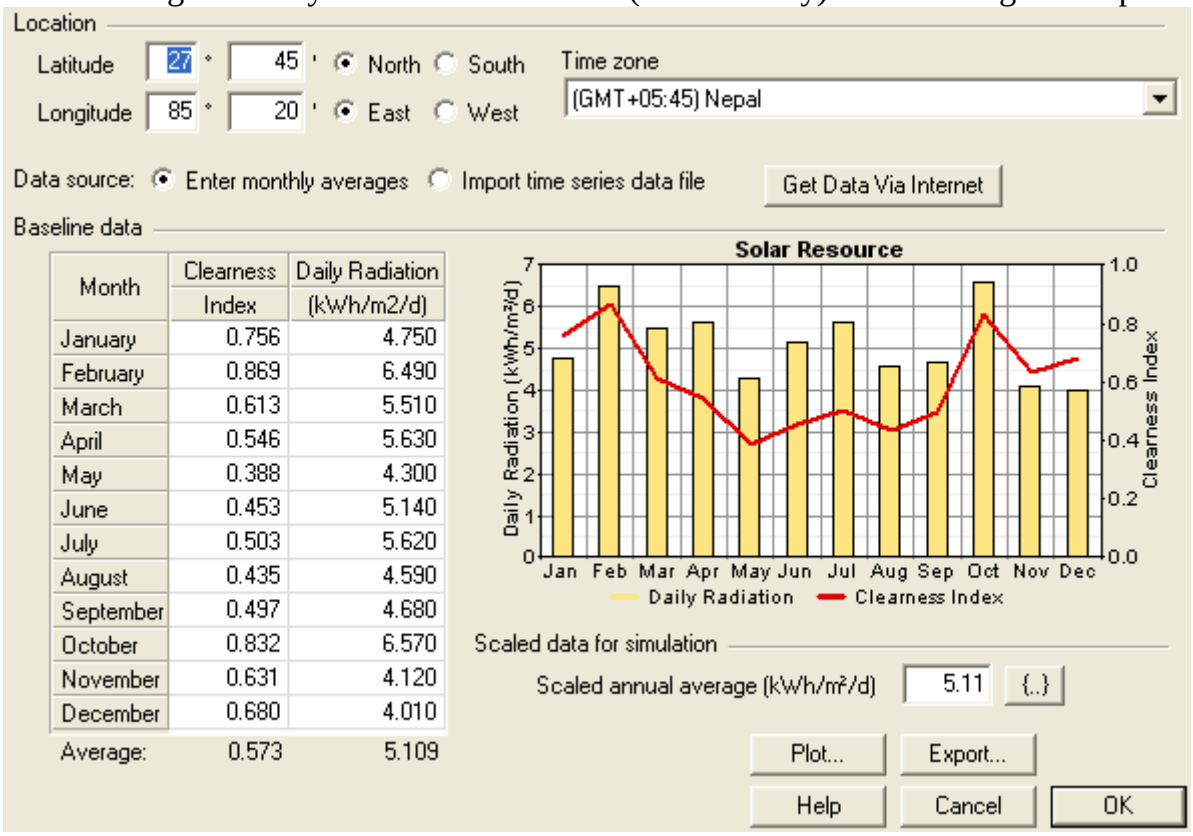

Month	Clearness Index	Daily Radiation (kWh/m2/d)
January	0.756	4.750
February	0.869	6.490
March	0.613	5.510
April	0.546	5.630
May	0.388	4.300
June	0.453	5.140
July	0.503	5.620
August	0.435	4.590
September	0.497	4.680
October	0.832	6.570
November	0.631	4.120
December	0.680	4.010
Average:	0.573	5.109

2. The average monthly water flow data (L/s) from a village of Nepal

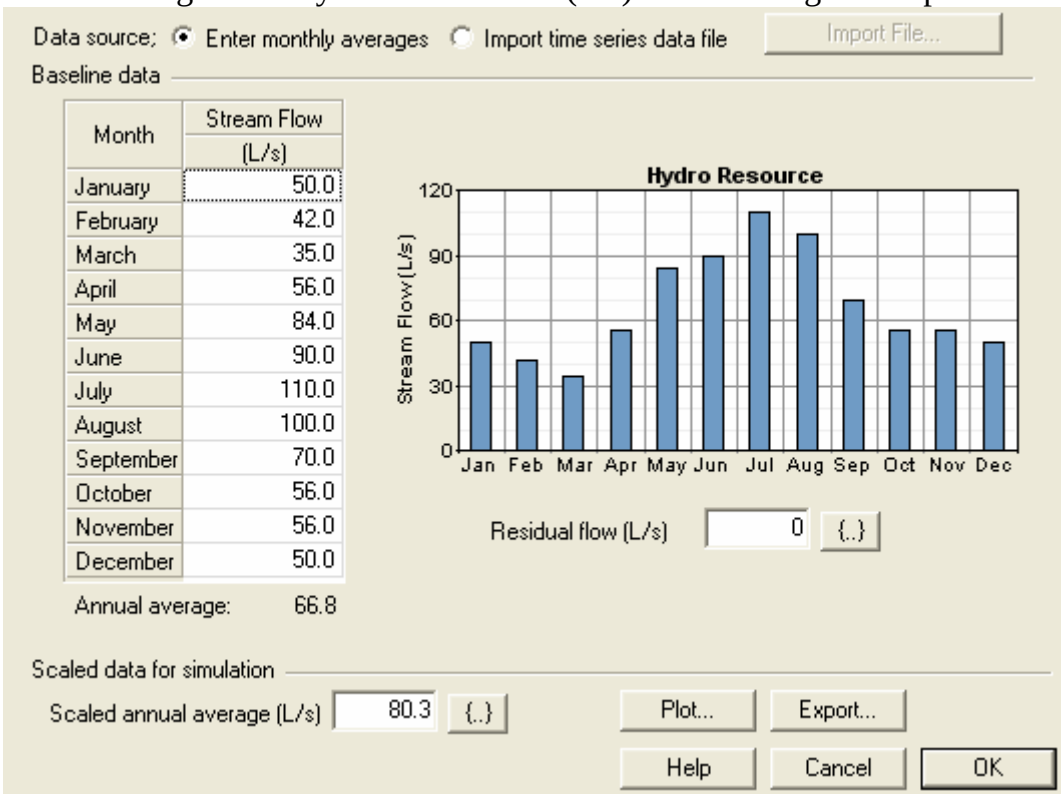

Month	Stream Flow (L/s)
January	50.0
February	42.0
March	35.0
April	56.0
May	84.0
June	90.0
July	110.0
August	100.0
September	70.0
October	56.0
November	56.0
December	50.0
Annual average:	66.8

Appendix D

1. The detailed cost calculation of the targeted HPS using Homer software from NREL

System Report - microhydro_hps.hmr
System architecture

PV Array:	4	kW
Hydro:	10.1	kW
Generator 1:	10	kW

Cost summary

Total net present cost:	$ 126,660
Levelized cost of energy:	0.119 $/kWh

Cost breakdown

Component	Initial Capital ($)	Annualized Capital ($/yr)	Annualized Replacement ($/yr)	Annual O&M ($/yr)	Annual Fuel ($/yr)	Total Annualized ($/yr)
PV Array	12,000	600	0	200	0	800
Hydro	28,492	1,425	0	1,139	0	2,564
Generator 1	2,340	117	166	303	2,384	2,969
Totals	42,832	2,142	166	1,642	2,384	6,333

Annual electric energy production

Component	Production (kWh/yr)	Fraction
PV array	6,865	10%
Hydro turbine	54,334	77%
Generator 1	9,385	13%
Total	70,584	100%

Annual electric energy consumption

Load	Consumption (kWh/yr)	Fraction
AC primary load	53,292	100%
Total	53,292	100%

Variable Value Units

Variable	Value	Units
Renewable fraction:	0.867	
Excess electricity:	17,293	kWh/yr
Unmet load:	0	kWh/yr
Capacity shortage:	88	kWh/yr

PV System

Variable	Value	Units
Average output:	18.8	kWh/d
Minimum output:	0.00	kW
Maximum output:	4.42	kW
Solar penetration:	12.9	%
Capacity factor:	19.6	%
Hours of operation:	4,380	hr/yr

Micro Hydro Power Plant

Variable	Value	Units
Average output:	6.20	kW
Minimum output:	3.29	kW
Maximum output:	9.46	kW
Hydro penetration:	102	%
Capacity factor:	61.3	%
Hours of operation:	8,760	hr/yr

Diesel Genset

Variable	Value	Units
Hours of operation:	3,026	hr/yr
Number of starts:	377	starts/yr
Operational life:	8.26	yr
Average electrical output:	3.10	kW
Minimum electrical output:	0.00	kW
Maximum electrical output:	9.75	kW
Annual fuel consumption:	4,767	L/yr
Specific fuel consumption:	0.508	L/kWh
Average electrical efficiency:	20.0	%

The calculation of actual energy need from the diesel genset is shown in below in the table.

Date	Genset (kWh)	Excess Energy (kWh)	Difference (kWh)	Diesel Operation (kWh)
Jan 07	1022,78	771,848	250,93	244,311
Feb 07	1040,10	450,75	589,35	589,348
Mrz 07	1600,95	134,09	1466,86	1466,857
Apr 07	903,39	805,457	97,93	99,788
Mai 07	447,623	2146,089	-1698,47	0
Jun 07	359,269	2454,368	-2095,10	0
Jul 07	246,98	3193,89	-2946,91	0
Aug 07	255,169	3117,379	-2862,21	0
Sep 07	655,256	1471,764	-816,51	0
Okt 07	904,773	1164,445	-259,67	0
Nov 07	905,271	901,766	3,51	7,255
Dez 07	1043,614	681,176	362,44	341,172
	9385,17	17293,022	-7907,852	2748,731

The fuel consumption for 2748 kWh = 1401 L/yr
The cost of the fuel per year = $ 700 /yr
Total fuel cost for 20 year = $ 14000/yr
Correspondingly the number of starts will also be reduced. So the total project cost at the end of the project is $ 126,660.00 – 47,671.00 + 14,000.00 = $ 92,898.00
Even though the power production from the diesel genset is reduced to 2748 kWh/year, the excess energy (70,584 – 9,385 – 2784 – 53292 = 10,691 kWh) is available. It means the load can be increased so that all energy could be used. If all produced energy is used, the new COE will be reduced as follows,
Total cost of the HPS = $ 92,898.00
Cos of the HPS/yr = $ 4,644.90
Annual energy consumption = 63983 kWh/yr
The new COE = $ 0.0725/kWh